Final Report

EVALUATION OF SUPERPAVE™ CRITERIA FOR VMA AND FINE AGGREGATE ANGULARITY

VOLUME 1 OF 2 VOLUMES
VOIDS IN MINERAL AGGREGATE (VMA)

UF Project No.:	4910-4504-619-12
State Job No.:	99700-3563-119
WPI No.:	0510865
Contract No.:	BB-498

Submitted to:

Florida Department of Transportation
605 Suwannee Street
Tallahassee, FL 32399

by

Principal Investigator: Reynaldo Roque, Professor
Co-Principal Investigators: Bjorn Birgisson, Assistant Professor
Mang Tia, Professor
Researcher: Bensa Nukunya

Department of Civil and Coastal Engineering
College of Engineering
University of Florida
124 Yon Hall
P.O. Box 116580
Gainesville, FL 32611-6580
Tel: (352) 392-537, extension 1458
Fax: (352) 392-3394

UNIVERSITY OF FLORIDA

March 2002

ACKNOWLEDGMENTS

The authors would like to acknowledge and thank the Florida Department of Transportation (FDOT) for providing technical and financial support and materials for this project. Special thanks go to engineers and technicians of the Bituminous Section of the State Materials Office for their contributions in terms of their expert knowledge, experience, and constructive advice throughout the course of this work. Their efforts are sincerely appreciated and clearly made a positive impact on the quality of the research.

TABLE OF CONTENTS

Page

LIST OF TABLES

LIST OF FIGURES

CHAPTER 1
INTRODUCTION

1.1 Problem Statement

Volumetric properties are typically used as mixture design criteria and controls for the durability and performance of HMA mixtures in the field. Volumetric properties include asphalt content, percent air voids, voids in the mineral aggregates (VMA), and the voids filled with asphalt (VFA). Other properties are aggregate surface area and theoretical film thickness. VMA, which is generally considered to be the most important factor for durability, needs to be carefully evaluated since it can disqualify a mixture from being used for road construction.

In the SuperPave™ mixture design system, the minimum VMA is dependent only on nominal maximum aggregate size. Other questions arise as to the type of gradation used in a particular mixture. Since aggregates form the bulk of the mixture, aggregate properties such as gradation, bulk specific gravity and other properties are also important in mixture design. Mixture gradation may vary significantly for the same nominal maximum aggregates size mixtures. A change in gradation could lead to an increase or decrease in surface area, thus affecting the theoretical asphalt film thickness of the mixture if the asphalt content is kept constant. This in turn affects the workability, compaction and cohesion of the mixture.

SuperPave™ criteria specify an uncompacted void content of fine aggregates which is generally referred to as the fine aggregate angularity (FAA), as well as a restricted zone in the fine aggregate region (% passing the #8 sieve size) of the gradation curve. The restricted zone attempts to eliminate excessively dense mixtures which are graded along the maximum density line (MDL) or potentially tender mixtures with excessive amounts

of fine aggregates. Thus, aggregate type, gradation, and volumetric properties were also studied in this research.

1.2 Objectives

The primary objectives of this research were as follows:

- Determine whether existing VMA criteria are viable for controlling mixture durability.
- If necessary, identify other volumetric parameters that may effectively control the performance and durability of HMA mixtures
- Determine whether changes in gradation, which may improve durability, have an adverse effect on either the rutting or fracture resistance of mixtures.
- Determine whether durability requirements should be different for different types of mixtures (e.g., coarse-graded versus fine-graded mixtures).
- If warranted from findings, make appropriate recommendations regarding the use of VMA and other volumetric properties in the SuperPave™ mixture design procedures.

Durability was evaluated by the changes in binder and mixture properties after short-term oven aging (STOA) and long-term oven aging (LTOA).

1.3 Scope

The study addresses the effects of aggregate gradation and resulting volumetric properties on mixture performance. A detailed literature review conducted before this research did not identify any previous research directly relating VMA to durability even though the relationship between VMA and durability is generally accepted and is logical to some extent. Therefore, it was necessary to identify the mixture parameter or proper-

ties that relate most strongly to durability (e.g., VMA or any other volumetric property as it relates to the gradation and absorption by the aggregates, film thickness, permeability and other mixture properties).

The following tests and analyses were performed:

- Mixtures were designed according to the SuperPave™ volumetric mix design method. Initial mixtures included existing FDOT 12.5-mm nominal maximum aggregate size SuperPave™ mixtures. Other 12.5-mm nominal maximum aggregate size SuperPave™ mixtures purposely designed to not pass the VMA criterion were derived from these mixtures.
- Mixtures were produced in the laboratory, aged at STOA for 2 hours (AASHTO PP2-94) and compacted to 7% (± 0.5) air voids. Half of the specimens produced were then aged by LTOA (AASHTO PP2-94). This process involved placing the compacted samples in a force draft oven at 185°F for a period of 5 days and cooled for 16 hours at room temperature. This process was done in order to simulate conditions in the field and thus provide a better measure of expected performance.
- Mixtures were then cut into 2-inch thick specimens before testing. SuperPave™ IDT was used to perform Resilient Modulus (M_R), Creep Compliance and Strength tests from which the following properties were determined: resilient modulus, tensile strength, failure strain, fracture energy density, creep compliance and m-value.
- Binder was extracted and recovered for testing after STOA and LTOA by ASTM standard procedures ASTM D 2712 and ASTM D 5404, respectively.
- Falling head water permeability tests were also conducted to evaluate the effects of void structure and access to oxygen on durability.

1.4 Research Approach

The research approach essentially involved evaluating the effects of changes in mixture gradations that were used to reduce VMA on the performance of mixtures.

1. First a thorough literature review was conducted to unearth previous work pertinent to this research.
2. The effect of mixture volumetric properties on the performance of SuperPave™ mixtures that were designed and produced in the lab were then evaluated.
    - Mixtures with varying volumetric properties such as VMA, film thickness, dust-to-asphalt ratio, surface area and asphalt were considered.
    - Binder age-hardening by measuring properties of binder extracted and recovered from the mixtures after STOA and LTOA.
    - Permeability tests were performed on the various mixtures to evaluate their void structure. The permeability values were used as an indicator of the distribution and size of voids.
    - The following mixture properties were measured after STOA and LTOA:
        – Stiffness: resilient modulus and creep compliance
        – Resistance to cracking: tensile strength, failure strain, fracture energy density and m-value.
        – Mixture durability was evaluated by measuring the changes in stiffness and resistance to cracking after STOA and LTOA. .
        – Resistance to rutting was evaluated by measuring the gyratory shear stress as a function of air void from the Servopac SuperPave™ gyratory machine at 1.25^{o} and 2.5^{o} gyratory angles.
3. The results were then analyzed and recommendations were made.

CHAPTER 2
LITERATURE REVIEW

2.1 Factors Affecting Durability

The term durability is defined as the mixture's resistance to age hardening or water damage. The presence of air voids in a compacted mixture creates the condition for air and/or water to move through the structure of the mixture. The degree of continuity of the flow paths determines the flow rate and hence controls the permeability of asphalt concrete mixtures. An increase or decrease in the permeability can accelerate or decelerate the circulation of air and water through the voids and thus affects the rate of aging of the asphalt mixture.

Aging in the field is generally associated with volatization and oxidation of asphalt binder during the life of the mixture. This process hardens or stiffens the asphalt concrete mixture. There are two types of aging (Bell et al. 1994): short-term aging, which occurs during mixing in the plant and between the time of mixing and final placement and long-term aging which is never-ending process of oxidation, which occurs during the short-term aging time frame, but is the dominant process when the mixture is in service and exposed to the environment. These processes can be simulated in the laboratory by Accelerated Laboratory Testing (ALT) procedures such as those described in AASHTO PP2-94. Short-Term Oven Aging (STOA) at 135^{o}C simulates the short-term aging process, whereas Long-Term Oven Aging (LTOA) at 85^{o} C or 100^{o} C simulates the long-term aging process.

The volume or amount of asphalt binder is critical for durability of mixtures. There should be enough asphalt to provide adequate coating of the aggregates. The gradation and type of the aggregate determines the aggregate’s surface area, and together

with asphalt content and absorption determines the amount of free asphalt available to cover the aggregates. Aggregate gradation is also important for the creation of an interlocking structure such that the movement of air is restricted.

All the above factors are in turn dependent on the compaction of the mixture. Oxidation of asphalt concrete in the field is enhanced by high percent air voids, highly interconnected voids and the amount of free asphalt available to cover the aggregates. Upon aging, the asphalt binder becomes stiffer and more brittle which in turn generally makes the mixture stiffer and stronger, but more brittle. Therefore, to produce a good mixture, a designer must control many factors. The calculated VMA and asphalt binder film thickness are two of the factors currently being considered to control durability. It is currently believed that the VMA is directly linked to the durability of the mixture and an increase or decrease in VMA renders the mixture more or less durable.

2.2 Volumetric Properties of SuperPave™ Asphalt Mixtures

The volumetric properties used in asphalt mix design are shown and explained in this section. It is important to have a good understanding of the volumetric properties currently used in characterizing asphalt mixtures since they are believed to govern binder age-hardening and thus the durability of the mixture as a whole. The important ones are discussed extensively. Below is a summary of some of the important volumetric properties currently used in the SuperPave™ volumetric mix design level I (Asphalt Institute, 1995). Figure 2-1 shows a schematic of the volumetric properties.

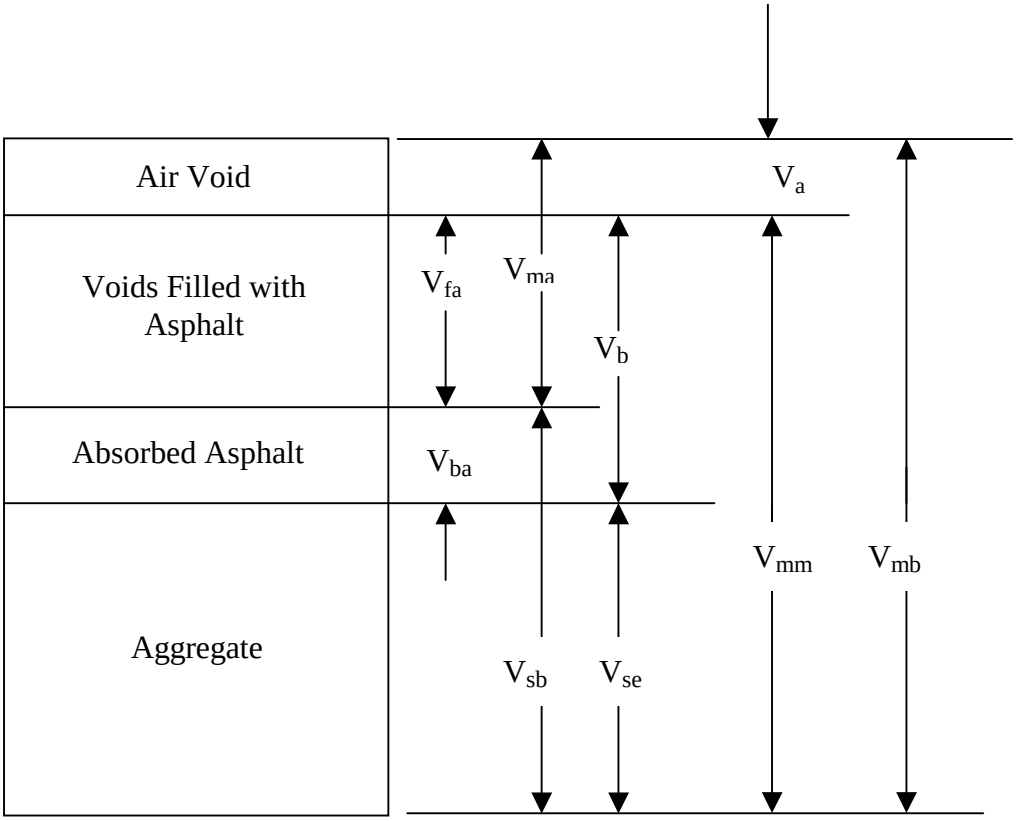

(after Asphalt Institute SuperPave™ Series No.2)

V_{ma} = volume of voids in mineral aggregates
V_{mb} = bulk volume of compacted mix
V_{mm} = voidless volume of pavement mix
V_{fa} = volume of voids filled with asphalt
V_a = volume of air voids
V_b = volume of asphalt
V_{ba} = volume of absorbed asphalt
V_{sb} = volume of mineral aggregate (by bulk specific gravity)
V_{se} = volume of mineral aggregate (by effective specific gravity)

Figure 2-1 Component Diagram of Compacted Sample of HMA

2.2.1 Bulk Specific Gravity

The bulk specific gravity of total aggregate is calculated from the Equation 2-1 when the total aggregate consists of separate aggregate fractions of coarse aggregate, fine aggregate, and mineral filler.

$$G_{sb} = \frac{P_1 + P_2 + ... + P_N}{\frac{P_1}{G_1} + \frac{P_1}{G_2} + ... + \frac{P_N}{G_N}} \quad (2\text{-}1)$$

where

G_{sb} = bulk specific gravity for the total aggregate
P_1, P_2, P_3 = individual percentages by mass of aggregate
G_1, G_2, G_3 = individual bulk specific gravities of aggregate.

The bulk specific gravity of mineral filler is hard to determine accurately so the apparent is generally used.

2.2.2 Effective Specific Gravity

The effective specific gravity of aggregate, G_{se} (Equation 2-2) includes all void spaces in the aggregate particles, except those that absorb asphalt.

$$G_{se} = \frac{P_{mm} - P_b}{\frac{P_{mm}}{G_{mm}} - \frac{P_b}{G_b}} \quad (2\text{-}2)$$

where

G_{se} = effective specific gravity of aggregate
G_{mm} = maximum specific gravity (ASTM D 2041) of paving mixture (no air voids)
P_{mm} = percent by mass of total loose mixture = 100
P_b = asphalt content at which ASTM D 2041 test was performed, percent by total mass of mixture
G_b = specific gravity of asphalt

2.2.3 Asphalt Absorption

Absorption is expressed as a percentage by mass of aggregate rather than as a percentage of total mixture. Absorption (P_{ba}) is determined by Equation 2-3:

$$P_{ba} = 100 * \frac{G_{se} - G_{sb}}{G_{sb} G_{se}} * G_b \quad (2\text{-}3)$$

where

P_{ba} = absorbed asphalt, percent by mass of aggregate and G_{se}, G_{sb} and G_b have their usual meanings.

2.2.4 Effective Asphalt Content

Effective asphalt content P_{be} is the total asphalt content minus the amount of asphalt lost to absorption in the aggregates. It is this portion that remains as a coating on the outside of aggregate particles and it is this that governs the performance of an asphalt paving mixture. It is expressed as in Equation 2-4:

$$P_{be} = P_b - \frac{P_{ba}}{100} * P_s \qquad (2\text{-}4)$$

where

P_{be} = effective asphalt content, percent by total mass of mixture
P_s = aggregate content, percent by total mass of mixture and P_b and P_{ba} have their usual meanings.

2.2.5 Percent VMA in Compacted Paving Mixture

Voids in the mineral aggregate (VMA), as defined earlier, are among the primary factors evaluated in this research. The intergranular void space between aggregates in a compacted mixture, which includes air voids and effective asphalt content, is considered to be very important for the durability of a compacted paving mixture. The voids are calculated from bulk specific gravity of the aggregate and are expressed as a percentage of the bulk volume of the compacted mixture. Thus, the VMA can be calculated by subtracting the volume of the aggregate determined by its bulk specific gravity from the bulk volume of the compacted paving mixture. The calculations are performed as in Equation 2-5, if the mix composition is determined as percent by mass of total mixtures:

$$VMA = 100 - \frac{G_{mb} * P_s}{G_{sb}} \qquad (2\text{-}5)$$

where

VMA = voids in mineral aggregates (percent of bulk volume)
G_{mb} = bulk specific gravity of compacted mixture (ASTM D 1188 or D 2726/AASHTO T 166) and G_{sb} and P_s have their usual meanings.

If the mix composition is determined by percent by mass of aggregate, then calculations are performed as in Equation 2-6:

$$VMA = 100 - \frac{G_{mb}}{G_{sb}} * \frac{100}{100 + P_b} * 100 \quad (2\text{-}6)$$

where the symbols have their usual meanings.

2.2.6 Percent Air Voids in a Compacted Mixture

The air voids in a compacted mixture are the small air spaces between the coated particles. It is determined using Equation 2-7 below:

$$V_a = 100 * \frac{G_{mm} - G_{mb}}{G_{mm}} \quad (2\text{-}7)$$

where

V_a = air voids in compacted mixture, percent of total volume; and G_{mm} and G_{mb} have their usual meanings.

2.2.7 Percent VFA in Compacted Mixture

The percentage of the voids in the mineral aggregate that are filled with asphalt, VFA, not including asphalt absorbed, is determined using Equation 2-8:

$$VFA = 100 * \frac{VMA - V_a}{VMA} \quad (2\text{-}8)$$

where

VFA = voids filled with asphalt; and VMA and V_a have their usual meanings.

2.3 Brief History of Volumetric HMA Design

Mixture designers recognized the role of VMA in mixture design as early as 1901 (Hudson and Davis, 1965). F. J. Warren's application for a patent on bituminous concrete emphasized the importance of minimizing the voids in the mineral aggregates to ensure proper gradation and stability (NCAT, 1991). At this stage, an upper limit of 15% for VMA (McLeod, 1955) was found to be appropriate and no lower limit was considered

at this time. Also, in “The Modern Asphalt Pavement,” Clifford Richardson (1905) recognized the role of the surface area of the aggregates as an important parameter for the design of HMA. The surface area affects the amount of asphalt to be added to the mixture and determines the asphalt film thickness. Coarser mixtures have less surface area so less asphalt is needed to provide the same thickness of coating as in finer mixtures with a larger surface area. However, restrictions placed on the required VMA led to two schools of thought (Hudson and Davis, 1965). One school designed mixtures to achieve maximum density or minimum VMA and then determined the best asphalt content by considering air voids and experience. The second school determined the asphalt content by using computed surface area of aggregates to achieve an optimum film thickness. Designers used air voids, surface area and experience to determine the best asphalt content. This led to the situation where mixture designers produced similar mixtures based mainly on experience or mixtures followed some gradation envelopes or idealized gradations.

The Hubbard-Field mixture design method for sheet asphalt with 100% passing of number 4 sieve size follows the first approach where the optimum asphalt content is determined from mixture and air voids. The stability was determined as the maximum load developed when a 2-inch diameter by 1-inch high specimen is forced through a 1.75-inch diameter orifice. Stability values corresponding to various asphalt contents were plotted and the optimum asphalt content was determined. The maximum stability usually occurred at a minimum air void. After this, the gradation was adjusted to achieve the required air void. The Marshall Method later came to displace this method.

The Hveem (1940) mixture design method follows the second approach, and according to Hveem himself, there was little evidence to show that the void ratio can be used dependably in mixture design, so that binder content cannot be effectively predicted from void volume alone. Hence, in 1942 he concluded that the volume of asphalt is maintained below the volume of voids in the aggregate.

Originally, the Marshall mixture design approach did not have a VMA requirement. Marshall wrote that no limits could be established for VMA for universal application because of the different gradations of aggregates. The Marshall Method stated the following limits: a minimum stability of 500 lb, a maximum flow of 0.020 inch, air voids between 3 and 5% and a VFA between 75% and 85% (Marshall Consulting and Testing Laboratory, 1949). The peak values of all parameters are averaged to determine the design asphalt content (McFadden et al., 1948). However, Marshall did not believe in using VMA, air void and VFA as mixture design parameters.

Specifications in the Marshall mix design method restrict high % AC mixtures (McLeod, 1955). Good performing mixtures were being eliminated in mixture design. The VFA requirement allows mixtures with % AC at 3.76%, which were too low for durability. McLeod (1957) introduced the use of bulk specific gravity and effective asphalt content for volumetric analysis and specified a minimum VMA to ensure at least 4.5% asphalt content and adequate durability, but later argued that requiring minimum VMA and restricting % air void between 3% and 5% was less restrictive than between 75% and 85% VFA (McLeod, 1987). In 1959, McLeod related minimum VMA to nominal maximum aggregate size. However, he warned that it was subject to modification. Others in the field at that time emphasized the importance of film

thickness for durability of asphalt mixtures. It was also believed that VMA is independent of the surface area of the aggregate as two aggregate blends with different surface areas could have different VMAs. Surface area did not indicate the asphalt content required for VMA and increased surface area requires more asphalt.

When McLeod (1956) first introduced VMA requirement, he pointed out that the basic criteria for both the design and analysis of asphalt paving mixtures should be on a volumetric instead of a weight basis. He showed the volumetric relationships between the asphalt binder, air voids between the coated aggregate particles, and the total aggregate in a compacted paving mixture from which the parameter later to be known as VMA was developed. This is essentially the volume of voids between the aggregate particles or simply the voids in mineral aggregates. It was based on specimens obtained from compaction by the Marshall hammer with 75 blows on each side of the specimen. McLeod recommended minimum values such as 15% for VMA, with the volume of air voids (within the VMA) between 3% and 5%, which in turn resulted in minimum of asphalt binder content of 10% by volume, and automatically established a minimum asphalt content of about 4.5% by weight. These calculations were based on aggregate bulk specific gravity of 2.65 and 1.01 for the asphalt binder, and no absorption was considered. Later in 1959, McLeod advocated the use of bulk specific gravity of aggregate for calculating both the VMA and air voids and also considered the absorption of asphalt cement by aggregate in the volumetric analysis. He again recommended minimum values of asphalt content to be 4.5% by weight and air void content of 5% for the mixture. The section below discusses VMA as design criterion and how it found its way into the design specifications of asphalt mixture design.

2.3.1 VMA as a Criterion for Asphalt Mixture Design

The volume of intergranular void space between the particles of a compacted paving mixture that includes the air voids and volume of asphalt not absorbed into the aggregates is called VMA. It consists of two components: the volume of voids filled with asphalt (VFA) and the volume of voids remaining (after compaction) available for thermal expansion of asphalt cement during hot weather. The VMA is thought to depend on the following parameters (Hudson and Davis, 1965): particle arrangement (or degree of compaction), relationship between sizes of aggregate particles in the ratios between percent passing adjacent sieve sizes, the range of sizes between fine and coarse material, aggregate shape, and the amount of air voids within the mixtures.

The VMA of HMA is an important mixture design parameter. It has been linked in the past with its durability. The term durability as used in this research refers to the mixture's resistance to age hardening. The value of the VMA can influence the behavior of asphalt mixtures. High VMA values allow enough asphalt in the mixture to obtain a minimum asphalt binder thickness, which is expected to yield maximum durability without flushing (McLeod, 1971). A mixture with a lower VMA may have a lower asphalt film thickness at a given air void level and end up with less durability. However, at a given air void level, mixtures with excessively high VMA at high asphalt content may lead to stability problems in that the mixture becomes too rich in binder and the binder tends to push the aggregates apart (Coree and Hislop, 1999). In the end, the resulting mixture becomes uneconomical since it contains too much asphalt. But compared to low VMA mixtures, high VMA mixtures have lower stiffness moduli at low temperatures and are believed to be more resistant to age hardening and cracking. They are believed to be less susceptible to variation in asphalt content and fine content

(Kandhal and Koehler, 1985). Such variations can cause mixtures to be too wet or too brittle.

Available literature on asphalt mixture design methods shows that the minimum VMA requirement was not in use until McLeod (1956) introduced it as a criterion. The Asphalt Institute later adopted it in 1962 as a Marshall mixture design requirement. Late in 1994, the Asphalt Institute reintroduced a VFA criterion into the Marshall mix design procedure, changed the design air voids to 4% and added a table for VMA requirement depending on the air voids content and nominal maximum aggregate size (Aschenbrenner and McKean, 1994). It then became a standard mixture design requirement through the Strategic Highway Research Program (SHRP) and was later adopted as a standard in SuperPave™ (Cominsky et al., 1994).

However, VMA requirements deviate from the normal trend of mixture design standards. Foster (1986), after reviewing literature on VMA (including McLeod 1956, 1957, and 1959 and Lefebvre 1957), pointed out that there was no report on actual pavement performance and VMA. He therefore concluded that VMA does not appear to be supported by any field or laboratory data. Also VMA is not a measured parameter, so its determination depends on other laboratory measurements of properties such as specific gravities of aggregates and asphalt, and the bulk specific gravity of compacted mixture. This means that an error in their measurement could lead to the rejection of good mixtures or the acceptance of otherwise poor mixtures based on the VMA criterion alone. Hinrichsen and Heggen (1996) concluded that the VMA criterion is too restrictive as it rules out economic mixtures with acceptable performance properties. This could pose a problem with the increased compactive effort of the SuperPave™ Gyratory

Compactor. The aggregate film thickness and aggregate surface area also should be considered in the mixture design procedures. Kandhal and Chakraborty (1996) recommended that the aggregate film thickness and aggregate surface area be considered as an alternate for mixture design. However, the rationale behind the minimum VMA requirement was to incorporate at least a minimum permissible asphalt content into the mixture in order to ensure its durability by providing an asphalt film thickness of at least eight microns (Kandhal, Foo and Mallick, 1998). Even though VMA has been associated with mixture durability since the turn of the century, it was only in the 1950s that it was recognized as a critical mixture design parameter (Coree and Hislop, 1999). Continued implementation and evaluation of the SuperPave™ system in Florida has led to numerous questions regarding the validity of the existing VMA requirements, which makes it difficult for some aggregate types to be used for road asphalt pavements. There are reports of increased difficulties in meeting the VMA requirement for the SuperPave™ volumetric mixture design; particularly for coarse-graded mixtures. In fact, several researchers including Anderson and Bahia (1997) discussed the difficult nature of this one important parameter and the problems associated with its use in mixture design. The minimum VMA requirement can be difficult to achieve and may lead to the rejection of various otherwise good performing mixtures. Thus, the VMA requirement and other volumetric properties like film thickness need to be critically reviewed to bring out some solutions or better ways of addressing the durability question.

In the SuperPave™ level I mixture design (Asphalt Institute SuperPave™ Series No.2, SP-2), VMA at a design air void content of 4% is a function of nominal maximum aggregate size as shown in Table 2-1. However, mixture volumetric properties are

related to the gradation of aggregates in the mixture. A coarse mixture must have different volumetric criteria than a fine mixture as well as dense and gap graded mixtures of the same nominal maximum sizes. This stems from the fact that the density, or in this case, air voids in the same mass of mixture for different gradations will be different. Therefore, air voids available for asphalt binder will also differ from mixture to mixture, hence VMA and other volumetric properties will vary. Other factors that can affect the VMA include the binder type and fines content. Thus, using the same VMA criteria for all mixtures with the same nominal maximum aggregate size is probably erroneous.

Table 2-1 SuperPave™ Criterion for VMA

Nominal Maximum Aggregate Size (mm)	Minimum VMA (%)
9.5	15
12.5	14
19.0	13
25.0	12
37.5	11

Kandhal, Foo and Mallick (1998) recently studied the effect of aggregate gradation on VMA. Their research involved calculation of the minimum VMA for aggregate gradations using an average film thickness of 8 microns at 4% air voids. Two HMA mixtures with nominal maximum sizes of 19 mm and 12.5 mm were considered with three aggregate gradations: above the restricted zone (ARZ); through the restricted zone (TRZ); and below the restricted zone (BRZ). Their results showed that VMA increased from TRZ to BRZ to ARZ and led to the conclusion that aggregate gradation affects VMA requirement. Their research, however, had some limitations in that it analyzed only sieve sizes around the SuperPave™ restricted zone. Their approach in the calculation of the VMA is not strictly correct because they assumed values for design

asphalt content, specific gravity of asphalt, and aggregates for the VMA calculations. Also, no other properties of the mixture such as shear strength or aggregate properties were documented in their research. Aging effect and durability of the mixture were also not considered.

2.3.2 Film Thickness

As discussed in the previous section, another school of thought indicates that very thin asphalt films or coatings on the aggregate particles are the primary causes of excessive aging of the asphalt binder and contribute to the lack of durability of the HMA mixtures often encountered in the field. Thicker asphalt binder films produce mixtures that are more flexible and durable while thinner films produce mixtures that are more brittle, tend to crack and ravel prematurely, and reduce useful service life. For the same asphalt content, film thickness decreases as the surface area of the aggregate is increased or as the aggregates become finer. This led to the development of another approach to address the VMA criteria. It is known as the rational approach.

In the rational approach, rather than specifying a minimum VMA requirement based on asphalt content, Kandhal and Chakraborty (1996) directly specify a minimum average film thickness to ensure durability of asphalt mixtures for various types of mixtures and quantified the relationship between various asphalt film thickness (ranging from 4 to 13 microns) and the aging characteristics of a dense-graded HMA mixture. This way an optimum average asphalt film thickness desirable for satisfactory mixture durability could be established. They used the SHRP aging procedure to simulate both short- and long-term aging of HMA mixtures and concluded that the optimum film thickness for HMA compacted to 4 to 5% air void content in service should be somewhat lower than 9 to10 microns because the rate of aging would be considerably lower at 4 to

5% air voids than when compacted to 8% air voids. Based on their past research experience, an average film thickness of 8 microns was recommended and used by Kandhal, Foo and Mallick (1998). Some other researchers like Campen et al. (1959) recommended an average film thickness of 6 to 8 microns for dense mixtures. The above also strengthens the point that the VMA criteria as specified in SuperPave™ must be linked to gradation, as film thickness is also a function of aggregate gradation and is interrelated with the volume of voids in a mixture.

2.4 Effect of Aggregate Properties on the Performance of HMA Mixtures

As stated previously, the durability of asphalt mixtures is affected by a number of its properties that affect the VMA and other volumetric properties interacting with each other. Most of the factors that affect the durability of asphalt concrete mixtures like asphalt content and air voids also affect the calculation of VMA, therefore it is not surprising that VMA is linked to its durability. One such property is the type of aggregate used and its properties.

2.4.1 Importance of Aggregate Gradation

Aggregate gradation is one of the important factors affecting the properties of HMA mixtures. The aggregate itself is obviously an important structural component of HMA since it accounts for almost 95% of the mixture by weight. Aggregates are responsible for the shear strength of mixtures, which are bound together by the asphalt binder. Therefore, the aggregate properties must be considered for a comprehensive evaluation of asphalt mixture design. A mixture's gradation typically falls into one of three categories: dense-graded, open-graded, and gap-graded. At the same air void content, dense-graded mixtures require less asphalt and have significantly lower VMA

and film thickness than other gradation types. Changing the gradation alone could lead to an increase or decrease in VMA, surface area, and thus an increase or decrease in asphalt film thickness. Therefore, an important factor for the design of a good mixture and for getting a good estimate of the design asphalt content is the selection of suitable aggregates with emphasis on gradation.

SuperPave™ specifications have certain guidelines for gradations that would possibly lead to a good mixture. There are limits to percent of material retained or passing some selected sieve sizes depending on the nominal maximum aggregate size. There is also a restricted zone, which was added to guide designers against gradations that are close to the maximum density line and reduce the potential for tender mixes. But good mixtures may be obtained by going through the restricted zone. Apart from SuperPave™, there are other gradation types such as that for the Stone Mastic Asphalt (SMA), which also produce good mixtures. Therefore, there is no clear-cut method of selecting an aggregate gradation to produce a good mixture. There is little guidance for blending aggregates so long as the gradation falls within the selected mixture gradation limits where it is assumed to be satisfactory unless proven otherwise by mixture design results. According to Ruth and Birgisson (1999), there are several factors that can be considered to be beneficial in designing high quality mixtures that are not sensitive to variations during production, i.e., preferably a continuously-graded mixture without having an excess or deficiency of aggregates retained on any one sieve and the gradation should generally not be gap-graded.

Although mixture grading that go below the SuperPave™ restricted zone are considered the most desirable from the standpoint of field performance for high traffic,

the minimum VMA is hard to achieve both in the laboratory and the field when these gradations are used. Thus, the implementation of the VMA criterion has caused otherwise good mixtures that have exhibited good performance to be rejected. There is a bias against coarser mixtures with low asphalt, and low fines content, which may be good performing mixtures. This has also led to the total rejection of some aggregates.

Aggregate gradation together with the surface roughness or smoothness, determines the interaction between aggregate and asphalt binder. Several researchers have evaluated the effects of aggregate gradation on fatigue cracking and rutting of asphalt mixtures. Some, such as Epps and Monismith (1969), have concluded that the aggregate gradation has no other significant effect on fatigue resistance than what is explained by asphalt content and air voids and that air void content alone did not explain the effects of air voids on a mixture's fatigue resistance. Harm and Hughes (1989) have also concluded that the asphalt content depends on the aggregate gradation, so that modifications that lead to denser gradation may improve fatigue resistance. Dukatz (1989) concluded that an increase in the amount of fine aggregates, may result in an increase in fracture resistance, which is the result of an increase in stiffness. But it is believed that this also leads to breakdown of the mixture structure as the binder and the mixture tend to become brittle. It is important to note that the amount of fines included in a mixture depends on the amount of coarse aggregates since a coarser structure would allow more fine particles to be incorporated in the mixture.

2.4.2 Fine Aggregates

As stated earlier, particle shape, size, and surface texture play a significant role in the strength and durability of asphalt concrete pavement mixtures. SuperPave™ recommends use of a variety of aggregate tests to ensure desirable aggregate

characteristics or consensus properties to give an acceptable level of performance. Fine aggregates must be tested for Uncompacted Void Content by ASTM C1252-94 standard or Fine Aggregate Angularity, which is influenced by the particle shape, surface texture and gradation. There are other methods used to evaluate these characteristics for fine aggregates as in ASTM D3398 (Standard Test Method for Index of Aggregate Particle Shape and Texture) and the Flow Rate Method (Rex and Robert, 1956; and Jimenez, 1990). Kandhal, Parker and Mallick (1997) have reported that most highway agencies control fine aggregates in HMA mixtures by limiting the use of natural sands and the amount of mineral filler. Currently, the North Carolina Department of Transportation (NCDOT) limits the amount of natural sand to no more than 20% in an HMA mixture (Tayebali, Malpas and Khosla, 1996). Most highway agencies allow 2% to 8% passing the number 200 (75 um) sieve size based on dry analysis. But most of these mixtures are expected to have about 2 to 3% more fines, as a washed gradation will give a higher fine content.

2.4.3 Mineral Filler

Fines or mineral filler affect the design asphalt content of mixtures. Lefebvre (1957) stated that fine fractions and mineral filler are the most critical component of a mixture controlling VMA and the stability. However, it is generally considered good to limit the amount of mineral filler. A high amount of mineral filler may lead to a brittle mixture with low design asphalt content as the filler takes the place of some of the asphalt, while a low amount of mineral filler leads to an increase in asphalt content. Therefore, a balance must be achieved in the use of mineral filler for mixture design. The use of mineral filler or bag house dust can be beneficial to industry and the environment in that the mineral filler and dust can be disposed of in a beneficial way. According to

Tayebali, Malpas and Khosla (1998), mineral filler content of 8% of aggregates is generally accepted as the cut-off level so as not to adversely affect the mixture. They concluded that for a given air void content, increasing the amount of mineral filler decreases the amount of permanent deformation in a repeated load test, which implies that resistance to rutting is enhanced. However, it should be noted that at higher mineral filler content, the asphalt content is reduced considerably, which could have a detrimental effect on the durability of the mixture and characteristics such as resistance to fatigue, thermal cracking and/or raveling.

2.4.4 Specific Gravity, Bulk Density and Maximum Theoretical Density (MTD)

Aggregate properties such as specific gravity, absorption, surface texture, shape and elongation are of great importance as the estimation of percent air void, percent AC and VMA depend on them. Any errors in the determination of bulk density of aggregates or compacted mixes and the MTD from the Rice test will lead to errors in the calculated values mentioned above. The methods used for the determination of density values are outlined in the ASTM standard C127-88 for coarse aggregates and C128–88 for fine aggregates. The determination of the SSD is sometimes tedious and may not be accurate because of its subjective nature. Also, important properties such as particle arrangement, shape, surface texture and absorption of the aggregates also affect the compactibility of the mixture (Kandhal, Khatri and Motter, 1992).

2.4.5 Effect of Mixture Properties on Fracture Resistance

The effect of the gradation of aggregates and the volumetric properties of the mixtures on fracture resistance of mixtures was a key point of this study. It is therefore important to mention a few of the methods available in the literature. In order to do this effectively, a brief literature review of pavement cracking is presented below.

2.4.6 Methods for Evaluating Load Associated Cracking

A lot of methods have been used by researchers to evaluate load-associated cracking in asphalt mixtures. There are at least three main ways to do this. These are the traditional fracture approach, conventional fracture mechanics approach and the visco-elasticity and continuum damage approach.

Fatigue is the process of damage accumulation and eventual failure due to repeated loading at stress levels below a material's strength. The two methods generally used to analyze and design against fatigue are the conventional approach which is based on the analysis of the nominal (average) stresses in the region of the component being analyzed, and the fracture mechanics approach which specifically treats growing cracks using fracture mechanics methods (Dowling, 1993). In recent years, the continuum damage mechanics approach (Kim, Lee and Little, 1997) is gaining ground in the analysis and evaluation of asphalt paving mixtures.

2.4.6.1 Traditional Fatigue Approach

For pavements, the traditional fatigue method is based on load-associated cracks that originate at the bottom of the AC layer and propagate upwards.

Many researchers in the United States have focused mainly on the traditional fatigue method, in which the maximum tensile strain is assumed to occur at the bottom of the AC layer. There are a lot of pavement models that follow this classical approach. However, none of them have been able to relate the asphalt binder properties and aggregate properties like gradation directly to fatigue cracking. According to Monismith (1985), the fatigue behavior of a particular mixture can be defined by Equation 2-9 below:

$$N_f = A\left(\frac{1}{\varepsilon_t}\right)^b\left(\frac{1}{S_{mix}}\right)^c \quad (2\text{-}9)$$

where N_f is the number of load applications to failure, ε_t is the tensile strain, S_{mix} is the mixture stiffness, A is a mixture-related factor based on the asphalt content and degree of compaction of the mixture, and b and c are coefficients determined from strain-controlled laboratory beam fatigue tests at 25^o C. This model indicates that the fatigue life of a mixture depends on the asphalt content, mixture stiffness and compaction effort.

The *Shell Pavement Design Manual* (1978) presents a fatigue relation in Equation 2-10 below for design purposes.

$$N = 4.91*10^{-13}\left(9.86V_b + 1.080\right)^5\left(\frac{1}{\varepsilon}\right)^5\left(\frac{1}{S_{mix}}\right)^{1.8} \quad (2\text{-}10)$$

Where V_b is the percentage of asphalt volume in the mixture, ε is the maximum tensile strain (in/in), and S_{mix} is the dynamic modulus of the mixtures in ksi. This implies that asphalt content is important for predicting fatigue life of pavements. In addition to those discussed above, other strain-based methods have been presented by Illinois DOT (Thompson and Cation, 1986) and by the Asphalt Institute (AI, 1986) which are similar to those discussed above.

Several researchers have also used energy-dependent methods to predict fatigue behavior of asphalt mixtures. This is based on the dissipated energy from cumulative or repeated loads in viscoelastic materials. According to van Dijk (1975), the relation between fatigue and total energy dissipated per volume is given as in Equation 2-11:

$$W_{Nf} = B_f\left(N_f\right)^z \quad (2\text{-}11)$$

where W_{Nf} is the cumulative dissipated strain energy to failure (J/m^3), N_f is the number of load cycles to failure, and B_f and z are experimentally derived mix coefficients.

According the van Dijk et al. (1977), the relationship between the cumulative dissipated energy and the number of cycles depends on the mixture formulation, but is independent of the test methods, temperature and mode of loading. However, Tayebali et al. (1992) disagree and added that the fatigue life of and AC mixture is underestimated by controlled-strain tests and overestimated by controlled-stress tests.

It has not been possible to include all parameters that affect the fatigue failure of asphalt mixtures into these models. Also, these models do not match field observations with laboratory results mainly because fatigue properties of asphalt mixtures depended on the mode of loading and test temperature. Furthermore, these fatigue approach methods do not account for stress concentrations caused by flaws or discontinuities in the asphalt mixtures. In a recent work, Tseng and Lytton (1990), and Harvey and Tsai (1996) demonstrated that the predictive equations had become more complex because the fracture behavior of asphalt mixtures were complex and that no hard-fast rule could guarantee accurate results for all conditions.

2.4.6.2 Fracture Mechanics Approach

Another method used for fatigue analysis is the fracture mechanics method which is based on the "Paris law" and it derivatives. The Paris law states that the rate of crack propagation in AC mixtures can be predicted using the following empirical relation in Equation 2-12:

$$\frac{da}{dN} = A(\Delta K)^n \qquad (2\text{-}12)$$

where *a* is the crack length, ΔK is the difference between the maximum and minimum stress intensity factor during loading, N is the number of load repetitions, and *A* and *n* are parameters depending on the mixture. This method distinguishes three stages of fracture, (1) the initiation phase where hairline or micro cracks develop, (2) the propagation phase where micro cracks develop into macro cracks and crack growth become stable, and (3) the disintegration stage where crack growth becomes unstable and the material fails and collapses completely.

The main assumption in this approach is the presence of cracks or inherent flaws already existing in the material. Therefore, the Paris law could only be used during the propagation stage when crack growth is stable and cannot address crack initiation directly.

Another method is to apply the J integral for fatigue crack growth (Dowling and Begley, 1976) under large-scale yielding conditions where K is no longer valid. The equation governing this is presented in Equation 2-13 below:

$$\frac{da}{dN} = C(\Delta J)^m \tag{2-13}$$

The fracture mechanics approach was developed for brittle or elastic materials such as metals. Asphalt mixtures are viscoelastic, therefore the Paris law cannot be applied directly to asphalt mixtures without modification. Schapery (1984) introduced a theoretical analysis for time dependent fracture of nonlinear viscoelastic materials that was based on his previous work (Schapery, 1973 and 1975). He noted that stress intensity factor should be the primary parameter for characterizing crack initiation and crack growth rate. Since then, other researchers have developed tests that are capable of utilizing the fracture mechanics method. Jacobs et al. (1996) analyzed the crack growth

process in asphalt concrete and validated Schapery's findings. In 1997, Read and Collop evaluated the Indirect Tensile Fatigue Test (ITFT) for fatigue cracking for use on asphalt mixtures and concluded that ITFT was capable of characterizing the fatigue performance of asphalt mixtures.

2.4.6.3 Viscoelastic and Continuum Damage Approach

It has been noted that loading conditions in the laboratory are different than loading in the field, so laboratory tests do not realistically simulate actual traffic conditions in pavements. Kim et al. (1997) modeled damage accumulation under uniaxial tensile cyclic loading and micro damage healing during rest period, using the elastic-viscoelastic correspondence principle and work potential theory. They conclude that this constitutive model could successfully predict damage growth as well as recovery of load conditions with different loading rates and rest periods.

2.4.7 Fatigue Failure Criteria

There are two failure criteria in the conventional fracture approach which are used in asphalt concrete pavements. The first is the number of load applications, N_f (from the initial crack length, a_0 to the critical crack length, a_c (Majidzadeh et al., 1971)). The second one is the fracture energy density. In 1977, Irwin stated that since fracture energy is a function of the initial crack size and the specific surface energy, which is also a scalar invariant that is fundamental to the rate of crack propagation and should be a reliable fatigue failure criterion for pavements. Sedwick (1998) and Zhang (2000) worked on the fracture energy method and concluded that fracture energy was a good indicator for estimating crack resistance of asphalt paving mixtures.

Of all the methods described in this chapter, the fracture energy method was used to predict crack resistance in this research.

CHAPTER 3
MATERIALS AND LABORATORY PROCEDURES

3.1 Introduction

This chapter provides information on the materials used, their properties such as gradation, mixture design procedure and preparation of laboratory specimens. It also summarizes the laboratory procedures for the tests performed and the data analysis procedures. Asphalt type AC30 was used to prepare all the mixtures.

3.2 Materials

3.2.1 Aggregates

Two commonly used aggregates were selected for the research, one very hard aggregate and one softer aggregate. Georgia granite and Miami Oolite blends, which have different shapes and texture, were obtained for the research. Georgia granite is hard, non-porous, angular and has high strength (LA abrasion equals 20%), whereas Miami Oolite (limestone) is softer, more porous, rounded and has relatively lower strength (LA Abrasion equals 33%).

3.2.2 Asphalt Binder

A very important component of HMA mixtures is the asphalt binder used in the preparation of the mixture. The asphalt binder used for this research is AC30, which is commonly used in Florida. It has a viscosity of 3600 poises at 60^{o}C and penetration of 61 at 25^{o} C.

3.3 Material Handling

3.3.1 Material Verification Process

Before the commencement of blending, the aggregates were dried and sieved out to verify the gradations of the whiterock components (i.e., S1A, S1B, screenings and mineral filler) as designated by the FDOT (Table 3-1). The bulk specific gravity (Table 3-1) of the individual components was determined (see Appendix A). All the values obtained agreed with the results from prior FDOT work (Asphalt Institute, 1998). Specific gravity tests were performed again two months after commencement to further verify the measured bulk densities of the aggregates.

Table 3-1 Blend Proportions for Whiterock Mixtures

Mixture	Aggregate (Specific Gravity)				G_{sb} of Mixture
	S1A (2.43)	S1B (2.45)	Scrn (2.53)	Filler (2.69)	
C1	10.20	63.27	25.51	1.02	2.469
C2	35.35	37.37	25.25	2.05	2.465
C3	27.00	39.00	31.00	3.00	2.474
F1	25.51	35.71	35.71	3.06	2.478
F2	44.00	0.00	51.00	5.00	2.489
F3	26.00	36.00	36.00	3.00	2.478

The next stage was to batch out the aggregates and start the volumetric mixture design procedure. Batch weights of dry aggregates were first determined for each mixture gradation and then the aggregates were batched dry to obtain 1000 g of blended aggregate, then a washed sieve analysis was performed to determine the actual amount of dust using ASTM C117-90 standards. Finally, the fine portion was adjusted for excess dust that adheres to the coarser aggregates and the batch weights calculated for a 4500 g sample for testing (see Appendix B).

After this, the F1 and C1 mixtures, which were previously designed by FDOT, were verified by determining the maximum theoretical density of the mixture and the design asphalt content. These two mixtures were considered the reference mixtures.

3.3.2 Determining Aggregate Gradations for Job Mix Formulas

The first part of the research which was done with the oolitic limerock from South Florida was made up of four components; coarse aggregate (S1A), fine aggregate (S1B), screenings and mineral filler. They were blended together in different proportions to produce six HMA mixtures of coarse and fine gradations.

Fine-graded mixtures (above the restricted zone) and coarse-graded mixtures (below the restricted zone) were produced at multiple VMA levels by varying the gradations and proportions for a common set of aggregates and AC30 asphalt cement. Some mixtures were purposely designed to not meet the SuperPave™ VMA requirements, while meeting all other Superpave requirements. Two previously designed SuperPave™ mixtures prepared by FDOT; one coarse-graded (C1) and one fine-graded (F1), were used as the basis for the research. Two more gradations were then produced by changing the coarse portions (larger than sieve number 8 size) of the gradations to produce job mix formulas with substandard VMA. The purpose of this was to test the effect of gradation and VMA on the durability of HMA. Secondly, the fine portion of the gradation curve was changed to produce more gradations of substandard VMA mixtures. This design procedure involved a trial and error process because the VMA could not be predicted directly from the gradation of the mixtures. In all, six mixtures were produced: C1, C2 and C3, for the coarse gradations and F1, F2, and C4/F3 for the fine gradations. The C4/F3 mixture was derived from the fine mixture (F1), but had to be adjusted to fall below the restricted zone to achieve a lower VMA. Thus, it is really a coarse-graded

mixture, so it was given a dual classification. The resulting gradations are shown in Tables 3-1 and Figures 3-1 and 3-2, with C1 and F1 being the two FDOT gradations. Table 3-2 shows the proportions by which aggregates were blended to obtain the various job mix formulae. The mixtures ranged from what could be described as fine uniformly-graded and fine dense-graded to coarse uniformly-graded and coarse gap-graded. Design asphalt contents for all the mixtures were determined such that each mixture had 4 percent air voids at N_{design} = 109 revolutions.

Table 3-2 Gradations for Whiterock Mixtures

Sieve Size	Coarse			Fine		
Seive Size (mm)	C1	C2	C3	F1	F2	C4/F3
25(1")	100.0	100.0	100.0	100.0	100.0	100.0
19(3/4")	100.0	100.0	100.0	100.0	100.0	100.0
12.5(1/2")	97.4	91.1	97.6	95.5	90.8	94.5
9.5(3/8")	90.0	73.5	89.3	85.1	78.0	84.9
4.75(#4)	60.2	47.1	57.4	69.3	61.3	66.5
2.36(#8)	33.1	29.6	36.4	52.7	44.1	36.6
1.18(#16)	20.3	20.2	24.0	34.0	34.7	26.1
0.6(#30)	14.7	14.4	17.7	22.9	23.6	20.5
0.3(#50)	10.8	10.4	12.9	15.3	15.7	13.6
0.15(#100)	7.6	6.7	9.2	9.6	9.1	8.6
0.075(#200)	4.8	4.8	6.3	4.8	6.3	5.8

Other mixtures were then produced and their design asphalt contents determined. All mixtures were prepared from 4500 grams of aggregates and heated in the oven together with the asphalt mixing equipment for at least 3 hours before mixing. The desired amount of asphalt was then added and the resulting samples were mixed at 300° F and subjected to short-term oven aging for two hours at 275° F. The samples were stirred after one hour during aging to allow for uniform mixture exposure to aging. The aging and absorption during this process results in mixture that is more uniform and representative of the mix in the field.

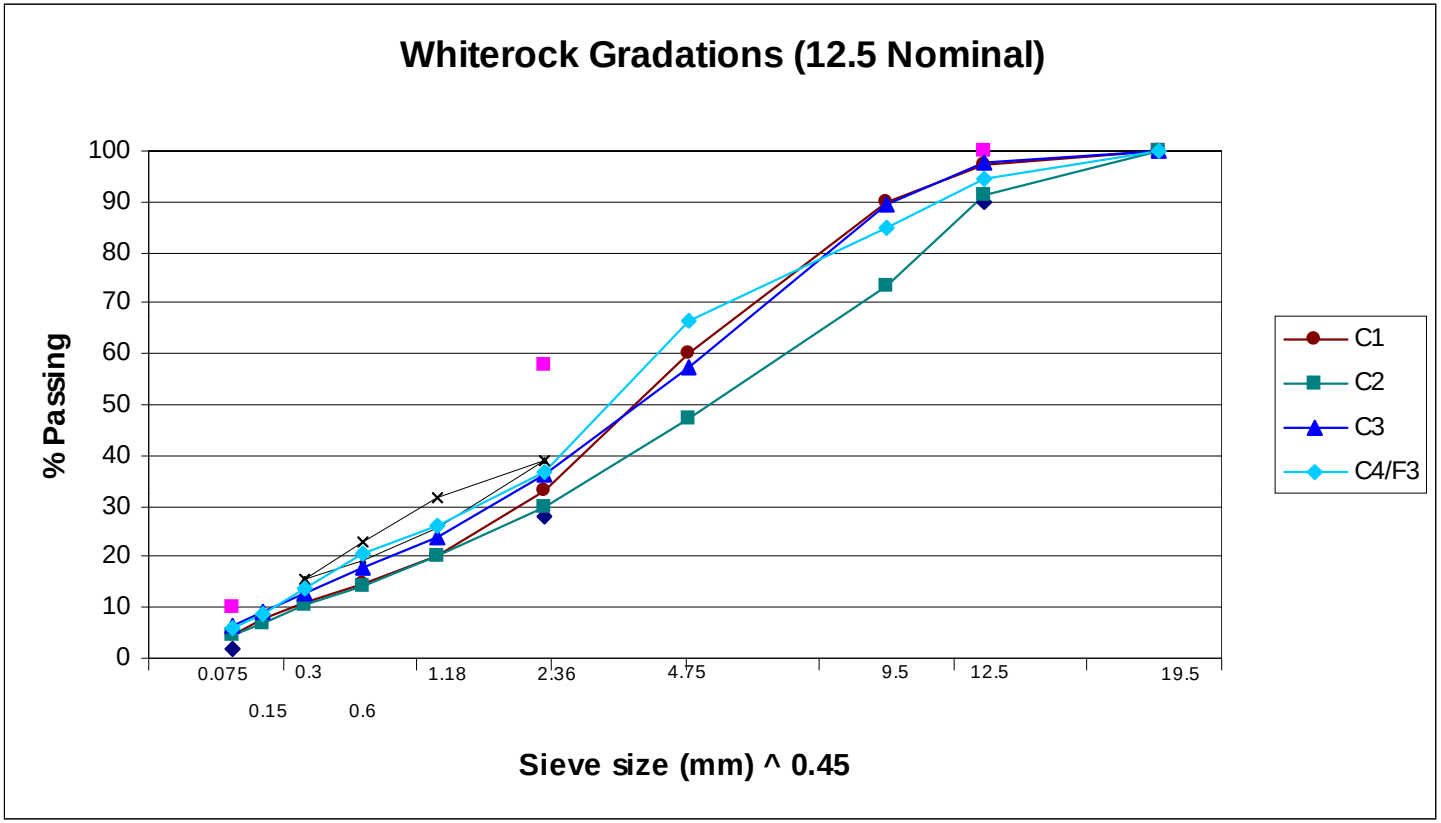

Figure 3-1 Gradation Chart for Coarse Mixtures

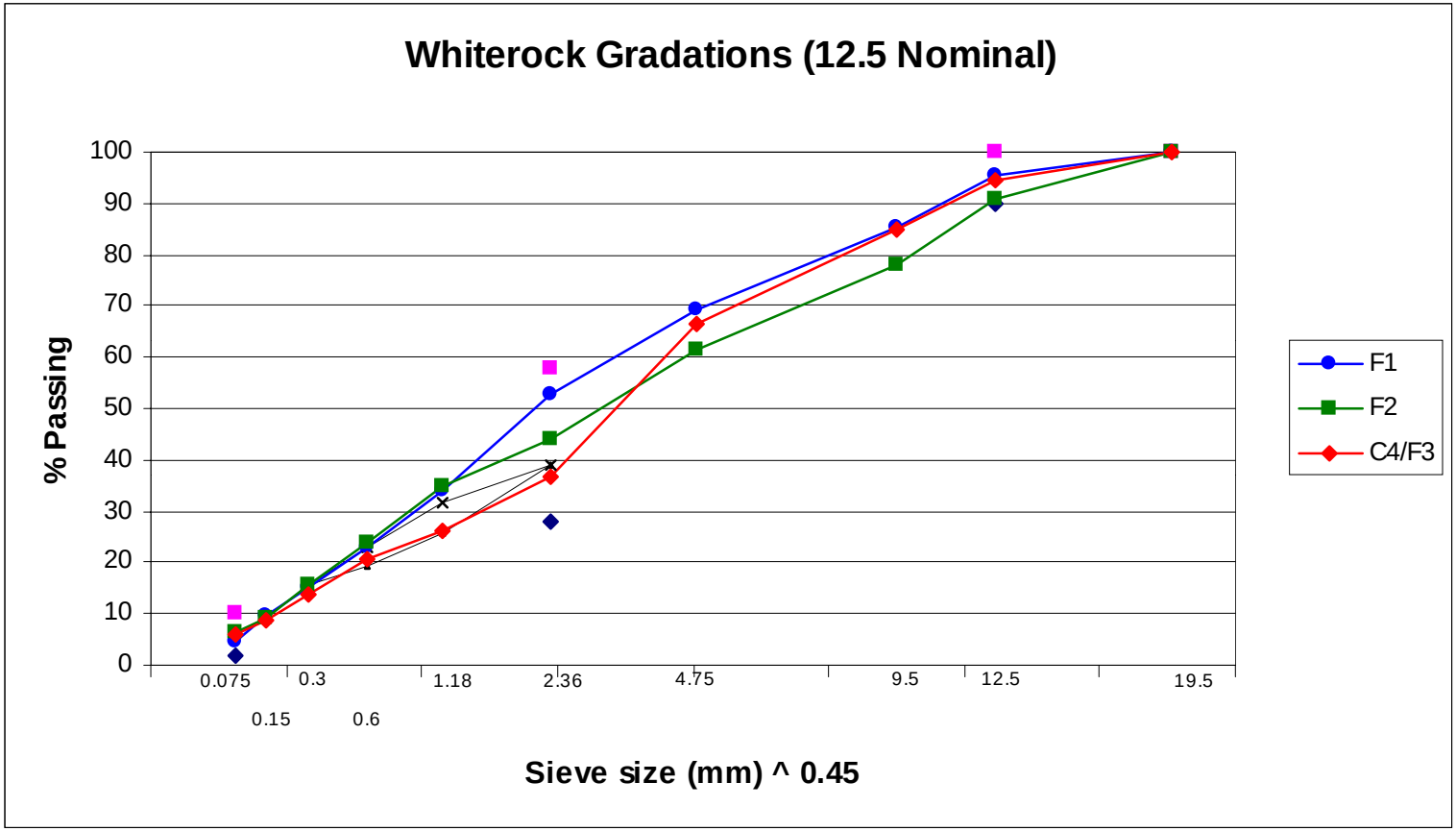

Figure 3-2 Gradation Chart for Fine Mixtures

3.3.3 Mixture Design

The SuperPave™/SHRP design method for compacted asphalt mixtures specifies the number of gyrations to which a sample must be compacted with the SuperPave™ Gyratory compactor. Figure 3-3 shows the Pine Model of the SuperPave™ Gyratory Compactor that was used. The number of gyrations specified for mixture design (Table 3-3) is determined according to volume of traffic and axle loads expected on the road. The air voids/bulk density of the resulting mixture is then calculated based on designated design number of gyrations (N_{des}) at which the air voids of the mixtures is at 4%.

Figure 3-3 Pine SuperPave™ Gyratory Compactor (SGC)

Table 3-3 SuperPave™ Gyratory Compactive Effort

Design ESALS (Millions)	Average Design High Air Temperature <30°C		
	N_{ini}	N_{des}	N_{max}
<0.3	7	68	104
0.3 - 1	7	76	117
1 - 3	7	86	134
3 - 10	8	96	152
10 - 30	8	109	174
30 - 100	9	126	204
>100	9	143	233

(after Asphalt Institute SuperPave™ Series No.2)

Three mixtures at different asphalt contents are produced with about 0.5% difference. This procedure was followed for compaction after which the resulting mixture bulk specific gravity was determined. The same mixing procedure was used for preparing samples for the maximum theoretical density, which was done using the Rice method in AASHTO T 209/ASTM D 2041 standards. In this case, the mixture was left to cool down in the loose state.

The other volumetric properties of the mixture such as air voids (AV), voids in mineral aggregates (VMA), and voids filled with asphalt (VFA), were calculated at these asphalt contents and then each was plotted as a function of asphalt content at $N_{des.}$ The design asphalt content was obtained by interpolating the air void versus asphalt content curve to obtain to asphalt content at 4% air void. The other volumetric properties were then obtained at this design asphalt content.

To verify the design asphalt content, the mixture was produced at the design asphalt content and compacted to N_{des} and the air void was checked. Except for the FDOT mixtures (C1 and F1), all other mixtures were designed to pass all SuperPave™

criteria except VMA. The properties of the mixtures are shown in Table 3-4. The details of all mixtures can be found in Appendix C.

Table 3-4 Mixture Volumetric Properties

		Mixture					
Property	Symbol	C1	C2	C3	C4/F3	F1	F2
Maximum Theoretical Density	Gmm	2.328	2.347	2.349	2.347	2.338	2.375
Specific Gravity of Asphalt	Gb	1.035	1.035	1.035	1.035	1.035	1.035
Bulk Specific Gravity of Compacted Mix	Gmb	2.235	2.255	2.254	2.254	2.244	2.281
Asphalt Content	Pb	6.5	5.8	5.3	5.6	6.3	5.4
Bulk Specific Gravity of Aggregate	Gsb	2.469	2.465	2.474	2.469	2.488	2.489
Effective Specific Gravity of Aggregate	Gse	2.549	2.545	2.528	2.537	2.554	2.565
Asphalt Absorption	Pba	1.3	1.3	0.9	1.1	1.1	1.2
Effective Asphalt Content of Mixture	Pbe	5.3	4.6	4.5	4.5	5.3	4.2
Percent VMA in Compacted Mix	VMA	15.4	13.8	13.6	14.0	15.6	13.2
Percent Air Voids in Compacted Mix	Va	4.0	3.9	4.0	3.9	4.0	3.9
Percent VFA in Compacted Mix	VFA	74.1	71.6	70.2	71.8	74.2	70.1
Dust/Asphalt Ratio	D/A	0.7	0.8	1.2	1.0	0.8	1.2
Surface Area (m^2/kg)	SA	4.9	4.6	5.7	5.6	6.1	6.3
Film Thickness (microns)	FT	11.2	10.1	8.0	8.1	9.0	6.9

Samples for testing were then compacted to 7% air voids, which is the typical air void content immediately after construction. A graph of the number of gyrations vs. density (or air voids) was plotted and the number of gyrations required to compact the samples to 7% air voids was determined by interpolation.

3.4 Mixture Production

3.4.1 Overview

This section presents the methods used in preparing mixtures for testing and how the mixture parameters were determined. As mentioned earlier, the gradation, asphalt content, VMA and the film thickness were different for each mixture. On the other hand, all the mixtures were compacted to the same level, 7% ± 0.5% air voids. A summary for the mixture properties is presented in Table 3-4.

3.4.2 Aggregate Gradation

Six different gradations were used for this study to get an understanding of the effects of gradation on VMA and HMA performance. Three coarse mixtures and three fine mixtures were designed and produced as stated earlier. Mixtures C1and F1 were designed based on gradations provided by FDOT. These gradations were altered in order to have mixtures with differing gradations and properties so that their effects could be determined.

3.4.3 Air Voids, Asphalt Content and Voids in the Mineral Aggregate (VMA)

The percent air voids and VMA depend on the density calculations. By determining the MTD and bulk density, air voids and VMA were calculated for all mixtures as in ASTM D 2041 standards. As stated previously, all mixtures were compacted to predetermined heights using the SGC (Pine) to achieve 7% air voids when cut. The gyratory specimens were cut into 2-inch specimen (which is the sample size used for testing) using a modified Diamond Pacific saw. The gyratory samples were compacted such that when cut, the resulting specimen had an air void content within the range of 6.5% to 7.5%. The air void of the whole sample is about 0.5 % higher than that of the cut samples so the target air void for a whole compacted sample was 7.5%. Details of each individual sample can be found in Appendix D.

3.4.4 Film Thickness and Surface Area

The theoretical film thickness of the asphalt cement was determined for evaluation. The technique used for calculating film thickness used the aggregate gradation, the effective asphalt content and the Hveem method based on the surface area factors (NCAT, 1991). In this method, the surface area is obtained by multiplying the percent passing each sieve size by the surface area factors. The surface area affects the

amount and thickness of the asphalt coating on each aggregate. Theoretical film thickness is then obtained by dividing the effective volume of asphalt by the surface area. Theoretical film thickness for each mixture is also shown in Table 3-4.

3.4.5 Mixture Compaction

Mixtures were then produced at design asphalt content and compacted to a specified number of gyrations in six-inch diameter molds to obtain 7% air void of the compacted sample. It was observed that compacting to a specified number of gyrations produced mixtures with air voids less than 7% in most cases. This can be attributed to the different shapes and sizes of each individual aggregate particle (between mixtures) even though the gradation remains the same. Also, the various sieve sizes used for batching the specimen will give the same weight of aggregate within each range but the actual sizes, shapes and weights of each aggregate may vary.

A more accurate method of producing mixtures at a given air void level is to use heights rather than number of gyrations. There is a relation between height and density (Equation 3-1), thus the SuperPave™ gyratory compactor was set to the required height to produce the 7% air void accurately. This method was also in error even though it was more accurate than the previous method. The error can be attributed to the fact that the gyratory compactor compacts in complete gyrations. Thus, if the height specified required a fraction of a complete gyration, the compactor made a complete gyration, which further compacted the specimen past the required height. In addition, the sample is further compacted when the compactor is self-packing. The resulting specimen is denser than the target density.

$$\frac{h_{N_{max}}}{h_{N_{des}}} = \frac{\rho_{N_{max}}}{\rho_{N_{max}}} \quad (3\text{-}1)$$

It was observed that the SGC compacted gyratory samples to a height of about 0.5 mm below the target height, therefore it was considered when estimating the sample heights.

3.4.6 Mixture Treatment

Before testing, mixtures were treated in two different ways. Half of the specimens remained in the STOA form (no additional aging after the STOA stage) and the other half were oven aged with LTOA method for compacted mixtures. Four 6-inch specimens were produced for each mixture type. Thus for each mixture, two specimens were left in the STOA form and two were oven aged for LTOA. The purpose of this was to evaluate the effect of mixture properties on binder age-hardening after both STOA and LTOA, and then also to test the performance of each mixture after the two aging processes.

3.4.7 Slicing Specimens for Mixture Testing

Indirect Tension Tests (IDT) was conducted for each of the six mixtures. To determine the effects of aging, mixtures were tested after both STOA and LTOA. A minimum of four gyratory compacted specimens (two STOA and two LTOA samples) were used to measure the resilient modulus, creep compliance and indirect tensile strength. A gyratory pill was cut to obtain two 2-inch thick specimens each. Three replicates for each mixture were tested. Appendix D shows the details of the average thickness, the diameter and air void for each specimen used.

3.4.8 Preparing Specimens for Mixture Testing

Four gage points were placed on each face of the cut specimen to perform resilient modulus, creep compliance and tensile strength using the SuperPave™ indirect tensile tests (IDT). This was done using a special gage point placement device. The specimen was placed carefully on the gage placement device making sure that it was perfectly aligned and centered as shown in Figure 3-4. After placing the gage points, a special steel template was used to mark the loading axis of the specimen to ensure that the specimen was aligned perfectly with the loading heads. These were marked on the vertical axis to indicate the direction of traffic flow. After this, the specimen was conditioned in a low relative humidity chamber for approximately forty-eight hours to reduce the effects of excess moisture in the specimen.

Figure 3-4 Gage Points Placement Device

3.5 Mixture Testing

As mentioned earlier, the SuperPave™ IDT was used to perform resilient modulus, creep compliance and tensile strength tests on each mixture at 10^{o} C (50^{o} F) using the testing procedure and data reduction method developed by Roque et al. (1997). After removing the specimens from the humidifier, LVDT's were placed on the gage points (Figure 3-5) after which they were placed in the environmental chamber of the Material Testing System (MTS). Figures 3-6 and 3-7 show the MTS loading frame, the environmental chamber with the sample positioned for testing, and data acquisition system used. The methods used for these tests are discussed below.

Figure 3-5 Setup for Fixing LVDTs onto Specimens

Figure 3-6 Setup Showing Specimen in Environmental Chamber

Figure 3-7 Setup Showing Environmental Chamber and Cooling Unit

3.5.1 Modulus of Elasticity

The dynamic complex modulus and resilient modulus tests have been used for determining the stiffness of asphalt concrete, which is an important property for characterizing a compacted asphalt concrete mixture. The concepts and definitions concerning complex modulus were presented by Papazian (1962) and that for resilient modulus by Seed et al. (1962). Both tests employ the application of repeated loads to a specimen by uniaxial compression and Indirect Tension (IDT) and measuring the displacements and the modulus value calculated as the ratio of stress to recoverable (resilient) strain under these loading conditions. The dynamic complex modulus is determined by applying a dynamic sinusoidal load and the resilient modulus by the application by a loading sequence where the load is applied for 0.1 seconds with a rest period of 0.9 seconds within each loading cycle.

3.5.2 Indirect Tension (IDT) Test

The IDT test is performed by loading a cylindrical specimen with a single or repeated load. It was originally developed by Van der Poel (1954), which is described in detail by Haas (1973). The load acts parallel to and along the vertical diametrical plane as in ASTM D4123 standards. This arrangement develops a relatively uniform tensile stress perpendicular to the direction of the applied load and along the vertical diametrical plane, which results in the specimen failing along the vertical diameter. The equation governing the test is based on the assumption that the HMA is homogeneous, isotropic and elastic (Hadley et al., 1970 and 1972 and Anagnos and Kennedy, 1972). Of course, none of these assumptions are true, but the properties they estimate are useful in evaluating relative properties of HMA mixtures. For plane stress, the governing equations are Equations 3-2 and 3-3.

$$\sigma_x = \frac{2P}{\pi dt} \quad (3\text{-}2)$$

$$\varepsilon_q = x_t \quad (3\text{-}3)$$

where

σ_x = horizontal tensile stress at center of specimen, psi
ε_q = tensile strain at fracture, inches/inch
P = applied load, lb.
d = diameter of specimen, inches
t = thickness of specimen, inches, and
x_t = horizontal deformation across specimen, inches.

The tensile strength and tensile strain at failure are used in calculating the fracture energy, which in turn predicts the fracture resistance of the mixture. It is believed that mixtures that tolerate high strains to failure can resist cracking more than mixtures that cannot tolerate high strains.

3.5.3 Resilient Modulus

The resilient modulus (M_R) is the modulus under repeated loads. It is the most common method for measuring the stiffness modulus of HMA. The test can be conducted in the indirect tensile mode and set up just like the IDT test or it can be run in the compression mode. The difference between resilient modulus and the modulus of elasticity is the mode of load application. The test procedure is in ASTM D 4123 standards. The applied shear is calculated the same way as in the IDT, but the specimen is not loaded to failure, but at stress levels of about 5 to 20% of the tensile strength. Therefore the IDT strength should be estimated prior to performing this test. The load is typically applied for 0.1 second with a rest period of 0.9 second. Hence, the specimen receives one load per 1-second cycle. For plane stress, the equation for computing the M_R values depends on the size of the specimen used.

For a 4-inch diameter specimen, Equation 3-4 is used:

$$\mu = 3.59\frac{H}{V} - 0.27 \tag{3-4}$$

And for a 6-inch diameter specimen, Equation 3-5 is used:

$$\mu = 4.09\frac{H}{V} - 0.27 \tag{3-5}$$

where

u = Poisson's ratio
H = horizontal deformation
V = vertical deformation.

The equation for resilient modulus (M_R) is the same for both 4-inch and 6-inch specimens.

$$M_R = \frac{P}{Ht}(.27 + \mu) \tag{3-6}$$

where

M_R = resilient modulus
P = applied load
H = horizontal deformation (inches)
t = sample thickness (inches), and
μ = Poisson's ratio.

The actual SuperPave™ test and loading methods used for this research can be found in Roque and Buttlar, 1992, Roque et al. (1994) and Buttlar and Roque (1994).

3.5.4 Creep and Permanent Deformation

In the creep test, a static load is applied to HMA specimen and the resulting time-dependent deformation is measured. The creep test in indirect tensile mode has been successfully used to characterize mixtures at low temperatures. The compliance is calculated from this test by dividing the strain by the applied stress as shown in Equation 3-7:

$$D(t) = \frac{\varepsilon_t}{\sigma} \tag{3-7}$$

At any temperature, T, and time of loading, t,
where ε_t = strain at time, t, (inch/inch), and
σ = applied stress, psi.

3.5.5 Methodology for Mixture Tests

The gage points were attached to the samples before samples were placed in an environmental chamber for a minimum of 8 hours to reach temperature stability (see Figure 3-4). The LVDTs were then attached to the gage points and the specimen placed back in the chamber, making sure that the loading head was perfectly aligned with the vertical axis marked on the samples (see Figures 3-5 and 3-6). The experimental set up is shown in Figures 3-7 to 3-9.

Figure 3-8 Material Testing System (MTS) Controller and Data Acquisition System

Figure 3-9 Servopac SuperPave™ Gyratory Compactor (SGC)

Resilient modulus tests were performed at 10^{o} C by applying a peak load resulting in horizontal strains in the range of 200 to 300 micro inches. This load was applied in five full repeated cycles. Each cycle consisted of loading the sample for 0.1 seconds followed by a 0.9-second rest period. After this test, a waiting period of approximately 45 minutes was allowed for the specimen to re-stabilize before a creep test was performed. This was done by applying a constant load on the sample for 1000 seconds. Thirty seconds into the test, the two horizontal deformations were recorded and checked for deformation. The expected deformation was in the range of between 200 to 300 micro inches. Any deformation in excess of this could lead to excessively high strains, which may cause the specimen to enter nonlinear range or fail. A strength test was then

performed on the specimen by applying a constant stroke rate of 50 mm per minute. Once the three tests were completed, the specimen was removed from the environmental chamber and the LVDTs detached from the gage points in preparation for the next specimen.

Testing and data reduction was performed according to the method developed by Roque et al. (1997). This was utilized to determine the resilient modulus, creep compliance, tensile strength, failure strain, fracture energy and the m-value of different mixtures. All tests were conducted at 10° C.

After this, extraction and recovery of the binder was performed on the same test specimens. The SuperPave™ binder tests described earlier were then performed to determine the binder properties.

3.5.6 Shear Characteristics

The compaction characteristics of the mixtures in the SGC were measured in order to evaluate their rutting resistance. The Servopac SuperPave™ Gyratory Compactor was used for this purpose. This equipment, which is manufactured by Industrial Process Controls (IPC) in Australia, is shown in Figure 3-9. The compaction procedure used by the Servopac is similar to the Pine SGC used in the mixture design and preparation stage but it has the added capability of measuring the gyratory shear (resistance to shear) while the mixture is compacting. It can also accommodate variable angle settings such that the mixtures were tested at gyratory angles 1.25 degrees, which is commonly used for compaction during mixture design and at 2.5 degrees. Current research at the University of Florida appears to indicate that the stability parameters for mixtures can be obtained accurately by compacting at 2.5 degrees than at 1.25 degrees.

A 4500-g sample of asphalt concrete was prepared and compacted at 1.25 and 2.5 degrees and gyratory shear was monitored as a function of air voids.

3.5.7 Permeability

The permeability of asphalt concrete mixtures at 7% air voids was determined in order to evaluate the void and aggregate structure of the mixtures. The aging of the binder may be influenced by the ability of air to circulate freely within the mixture. The permeability thus gives an idea as to the continuity of pores or the air voids in the mixture. Some researchers have suggested that rutting of asphalt mixtures is likely to occur due to plastic flow when the air void reduces to less than 3 percent (Brown and Cross, 1989; Huber and Heiman, 1987; and Ford, 1988). However, when air voids are above 7-8 %, the mixture may be permeable to air and water and the rate of binder oxidation may significantly increase (Brown, 1987, Santucci et al., 1985 and Zube, 1962). Two specimens obtained from one gyratory pill were used for the permeability test.

A falling head water permeability test was used. Standard test method FM 5-565 designed by Florida DOT was used. The test method covers the laboratory determination of the water conductivity of a compacted asphalt paving mixture. The method gives a comparison of water permeability between asphalt samples tested in the same manner. The method can be used to test both laboratory compacted cylindrical samples and field core samples. The permeability device is shown in Figure 3-10.

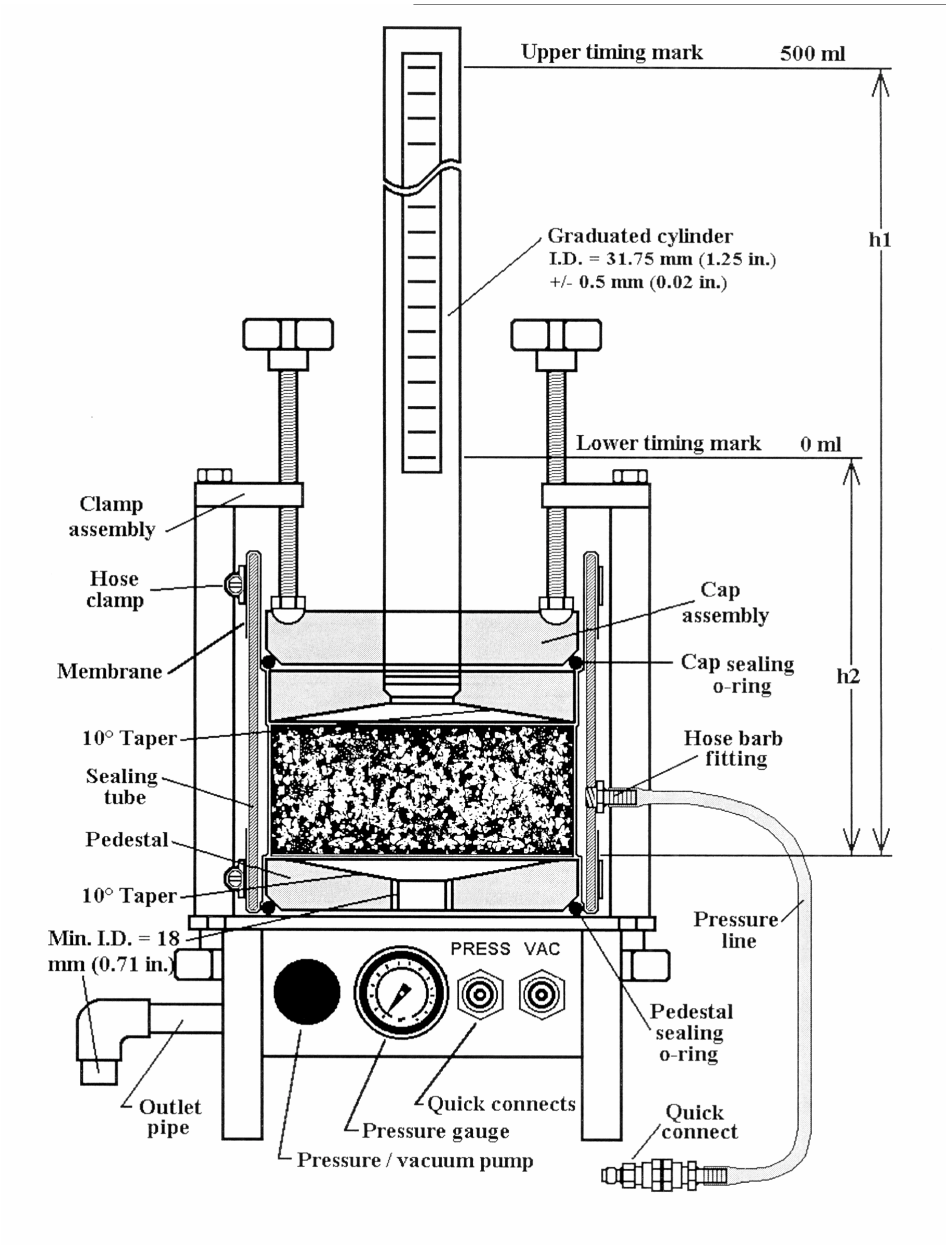

Figure 3-10 Falling Head Permeability Equipment (after FDOT-FM 5-565, 1999)

3.6 Extraction and Recovery of Binder

The binder was extracted from the mixtures to evaluate binder age-hardening. Standard procedures for binder extraction ASTM D 2171–95 and ASTM D 5404–97 for

recovery were used. Trichloroethylene (TCE) solvent was used for the extraction and the Buchi Rotary Evaporator shown in Figure 3-11 was used for the recovery process.

Figure 3-11 Buchi Fractional Distillation Equipment

3.7 Binder Tests

Binder tests were performed to evaluate the effects of short-term and long-term aging on the rheological properties of asphalt binder in relation to film thickness, % AC and VMA. It is essential to identify mixture properties or the range of mixture properties that will minimize the effects of binder hardening. Thus, binder property tests were performed on samples extracted from the tested mixture specimens (both STOA and LTOA). Tests were performed using the penetration device, the Dynamic Shear Rheometer (DSR), and the Brookfield Viscometer.

3.7.1 Penetration

The penetration test was used to determine the relative stiffness of the extracted binder. The test is generally conducted at one standard temperature 77^{o}F (25^{o} C). Although penetration is empirical in nature, the test has been used extensively in the past as an indirect measure of binder stiffness and viscosity. The equipment is shown in Figure 3-12.

Figure 3-12 Penetration Test Equipment

3.7.2 Dynamic Shear Rheometer (DSR)

The Dynamic Shear Rheometer (DSR) was used to characterize the viscous behavior of asphalt binder at high and intermediate temperatures. DSR has been used to evaluate rutting and fatigue resistance. The Brohlin DSR II equipment shown in Figure 3-13 was used. It measures the complex shear modulus (G*) and the phase angle (δ).

The G* consists of two components, G′ or the elastic recoverable part and G″ or the viscous (non-recoverable) part. According to Bahia and Anderson (1995), high G* and low angle delta are desirable for rutting resistance. Complex modulus G* is the total resistance of the binder to deformation when repeatedly sheared. Modulus G*/ cosθ is related to the shear resistance of the binder and G*sin δ which is related to the fatigue resistance of the binder. In the standard test procedure AASHTO TP5, an asphalt binder sample approximately 2-mm thick by 8 mm in diameter, is sheared between two parallel plates. The sample is sheared at low or intermediate temperature by oscillating the top plate at a frequency of 1.59 Hz (10 radians/s).

Figure 3-13 Brohlin DSR II Equipment

3.7.3 Rotational Viscometer (RV)-Brookfield Thermosel Viscometer

The rotational viscometer was used for the determination of the viscosity of the extracted asphalt binder. It is generally used to determine asphalt viscosity at construction temperatures (above 100^{o} C) to ensure that the binder is fluid enough for pumping and mixing (NCAT, 1996). The method is described in ASTM D4402 or AASHTO TP48 "Viscosity Determination of Unfilled Asphalt using the Brookfield Thermosel Apparatus". The apparatus is shown in Figure 3-14.

Figure 3-14 Brookfield Thermosel Viscometer

Approximately 11 grams of preheated binder was used. The asphalt was poured into the sample chamber, which was then placed in the thermos container. The spindle was then lowered into the chamber. The viscometer was turned on once the sample

temperature stabilized at a test temperature of 60^{o}C. A constant torque was applied and the viscosity was obtained as the shear stress divided by the shear strain rate. The viscometer reading was displayed digitally in units of centipoises (cP), whereas the SuperPave™ binder specifications used was in Pa.s. The conversion factor is 1000 cP = 1Pa.s.

CHAPTER 4
BINDER RESULTS AND ANALYSIS

4.1 Introduction

This chapter provides a summary of the testing results for the six different whiterock mixtures (STOA and LTOA). These tests were conducted in order to achieve a clear understanding of mixture behavior in terms of binder age-hardening during preparation, mixing, transportation and compaction. This is one of the objectives discussed in Chapter 1 of this study. Recovered binder properties are summarized in this section.

4.2 Binder Testing Results

The first phase of the research was done with the oolitic limerock made up of four components: coarse aggregate, fine aggregate, screenings and mineral filler. They were blended together in different proportions to produce six HMA mixtures of coarse and fine gradations.

As mentioned earlier, the original FDOT SuperPave™ coarse-graded mixture (C1) and fine-graded mixture (F1) were used as the basis for the research. An additional four gradations were obtained by changing the coarse portions (larger than sieve number 8 size) and keeping the fine portion constant and then changing the fine portions (less than sieve number 8 size) and keeping the coaster portion constant.

The purpose of these changes was to evaluate the effects of mixture properties like VMA, film thickness, asphalt content, aggregate gradation and surface area on the durability (age-hardening rate), fracture resistance, and rutting resistance of mixtures.

All mixtures were subjected to both short-term and long-term oven aging (STOA and LTOA). Permeability tests were performed on all mixtures to get an indication of void structure. The six mixtures were evaluated by determining how the various volumetric properties affected the aging of the binder as measured by changes in different binder properties and the mixture after both STOA and LTOA. The binder was extracted from the same mixtures used for the SuperPave™ IDT tests.

4.2.1 Penetration Test Results

Penetration tests were performed at 25° C for STOA and LTOA samples to measure the consistency of the binder. Tests were performed according to ASTM D5-95. As shown in Table 4-1 and Figure 4-1, the penetration values decreased at a faster rate for the fine mixtures, especially F2 than the coarse mixtures. The test data also indicated a similar binder age-hardening rate for both coarse mixtures (C1 and C2) and a similar rate for both fine mixtures (F1 and F2) at STOA and LTOA conditions. The similarities were observed both in magnitudes of the penetration values as well as the reduction in penetration between STOA and LTOA.

Table 4-1 Penetration Test Results

Mixture	STOA	LTOA	Gain
C1	42.0	39.0	3.0
C2	40.0	36.0	4.0
C3	38.0	32.0	6.0
F1	36.0	28.0	8.0
F2	36.0	26.0	10.0
C4/F3	38.0	32.0	6.0

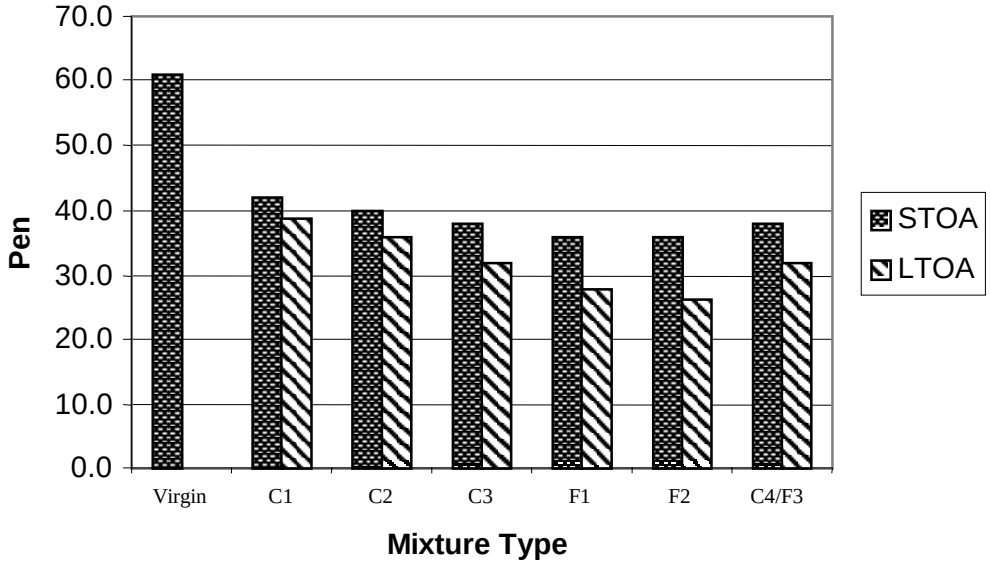

Figure 4-1 Penetration After STOA and LTOA

4.2.2 Dynamic Shear Rheometer

The Dynamic Shear Rheometer (DSR) test was performed on the binder extracted from all mixtures and the results are shown in Table 4-2 and Figure 4-2. Testing temperature of 15°C was selected because it was the lowest temperature at which the binder samples could be tested successfully.

Table 4-2 Dynamic Shear Rheometer (DSR) Test Results for G*

Mixture	STOA	LTOA	Gain
C1	7590700	8257500	666800
C2	7390900	8059000	668100
C3	7858300	9225200	1366900
F1	9720500	11424000	1703500
F2	9760900	11491000	1730100
C4/F3	7796100	9358600	1562500

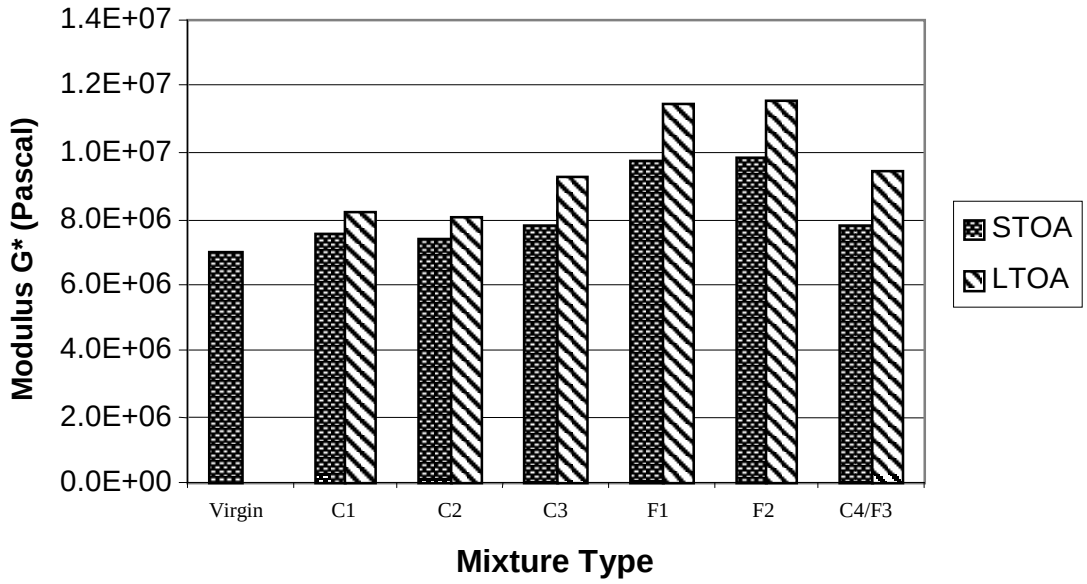

Figure 4-2 Complex Modulus G* After STOA and LTOA

Three tests were performed and averaged. The test was performed according to AASHTO TP-5-93 standards. An asphalt specimen of approximately 2-mm thick by 8 mm in diameter was placed between two parallel plates and sheared by oscillating one of the parallel plates at a frequency of 1.59 Hz (10 radians/s) with respect to the other, which remains stationary. The DSR test results were recorded as shear modulus (G*) and phase angle (δ) which are used to characterize the viscous and the elastic behavior of the asphalt binders (see Table 4-3 and Figure 4-3).

Table 4-3 Results for Phase Angle Delta (δ)

Mixture	STOA	LTOA	Gain
C1	48.4	46.5	1.9
C2	49.9	48.0	1.9
C3	47.9	45.7	2.2
F1	47.5	45.0	2.5
F2	46.2	43.6	2.6
C4/F3	47.9	45.5	2.4

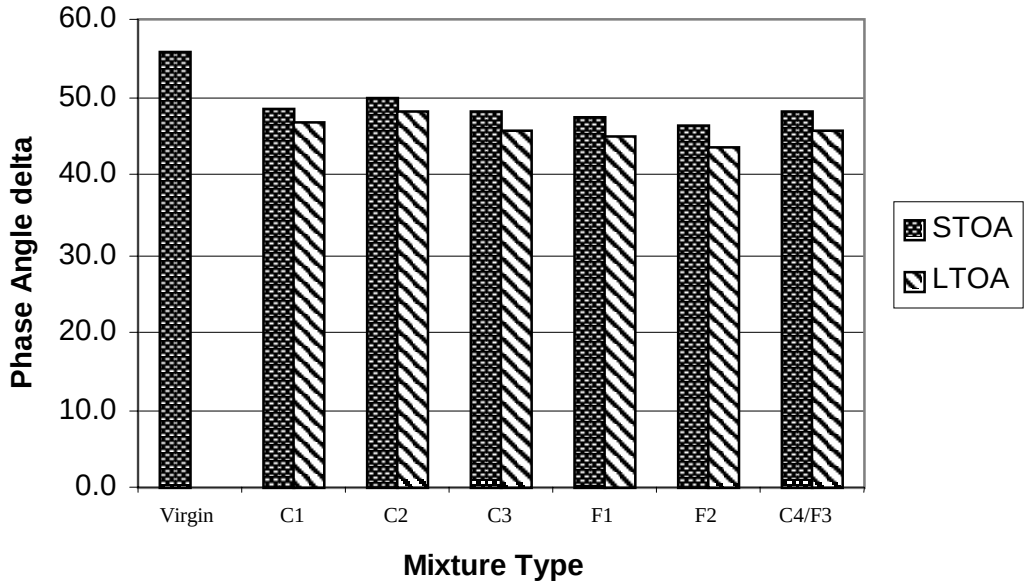

Figure 4-3 Phase Angle Delta After STOA and LTOA

The results from these tests were also used to ascertain the age-hardening rate of the extracted binder which showed the same trends as those observed in the penetration test.

4.2.3 Brookfield Viscosity Test

This test was performed at 60° C, much higher temperature compared to that used for the mixture tests. This test was performed in accordance with ASTM D4402-95 standards, which is the same as SHRP designation B-007 (1993). Both STOA and LTOA results appear to show an increase in the viscosity of the binder after aging. In the case of the fine mixtures, the viscosities increased at a faster rate compared to the coarse (see Table 4-4 and Figure 4-4.)

Table 4-4 Viscosity Results

Mixture	STOA	LTOA	Gain
C1	6435	11107	4672
C2	8706	11750	3044
C3	8064	11860	3796
F1	8965	16953	7988
F2	9650	18048	8398
C4/F3	7139	11721	4582

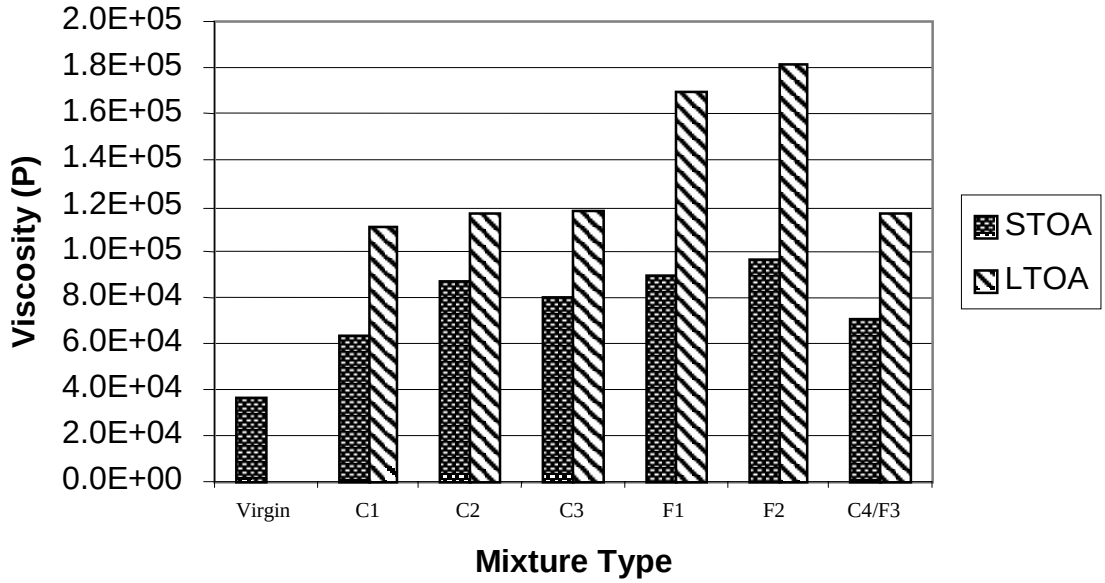

Figure 4-4 Viscosity After STOA and LTOA

4.3 Analysis of Recovered Binder Results

Although the three binder tests (DSR, Penetration and Viscosity) were performed on the mixtures at different temperatures, the same age-hardening trend was observed with each. The DSR results appeared to show that the binder became stiffer for the fine mixtures (F1 and F2) than the coarse mixtures after both STOA and LTOA. The binder stiffness of the coarse mixtures (C1 and C2) did not change much after LTOA.

It is also important to note that the binder stiffness of both coarse mixtures were very similar after aging. A similar age-hardening pattern was observed for both fine mixtures after STOA and LTOA, but G* values were higher than those for the coarse mixtures. From the viscosity and penetration tests, the binder became more resistant to flow after LTOA. The binder data also shows a higher rate of aging for the binder of the fine mixture; which may have been caused by the presence of thin film thickness allowing a faster oxidation rate. The binder data appears to suggest that binder age-hardening in low VMA coarse mixtures was not as high as age-hardening in any of the

fine mixtures. Age-hardening rate did not appear to correlate with low VMA for coarse-graded mixtures. The effects of the mixture parameters on binder age-hardening are summarized below.

4.3.1 Effect of Surface Area (SA) on Binder Aging

Since the mixtures are aged in the loose (uncompacted) form during STOA, aging is expected to be proportional to the amount of exposed surface area of aggregates for a given asphalt content and absorption. Thus, with the same amount of asphalt, a mixture with a higher surface area, which is basically a finer mixture, is expected to age-harden at a faster rate during STOA (see Figure 4-5). Figure 4-6 shows graphs of binder age-hardening rate (measured by binder properties) versus surface area. It appears the binder age-hardening rate increases with increasing surface area for both STOA and LTOA.

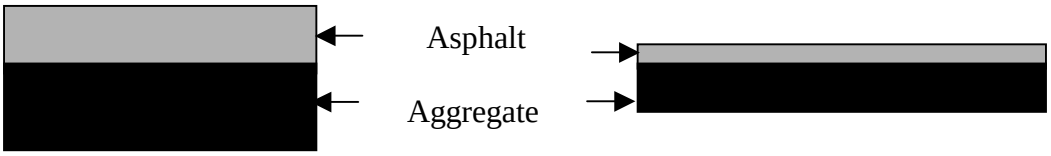

Figure 4-5 Schematic of the Effect of Surface Area on Age-Hardening of Binder

4.3.2 Effect of Film Thickness on Binder Aging

Since binder ages from the surface inwards, a mixture with a low film thickness is expected to age-harden faster than one with a thicker film, irrespective of surface area. However, based on measured binder properties after STOA and LTOA, it is clear that fine mixtures aged more than coarse mixtures irrespective of their film thicknesses (Figures 4-7 and 4-8). Thus, the finest mixtures F1 and F2 aged the most, followed by the mixtures C3 and C4/F3. The coarsest mixtures, C1 and C2 aged the least. Thus, it appears that for the range of film thicknesses evaluated, there was no effect of film

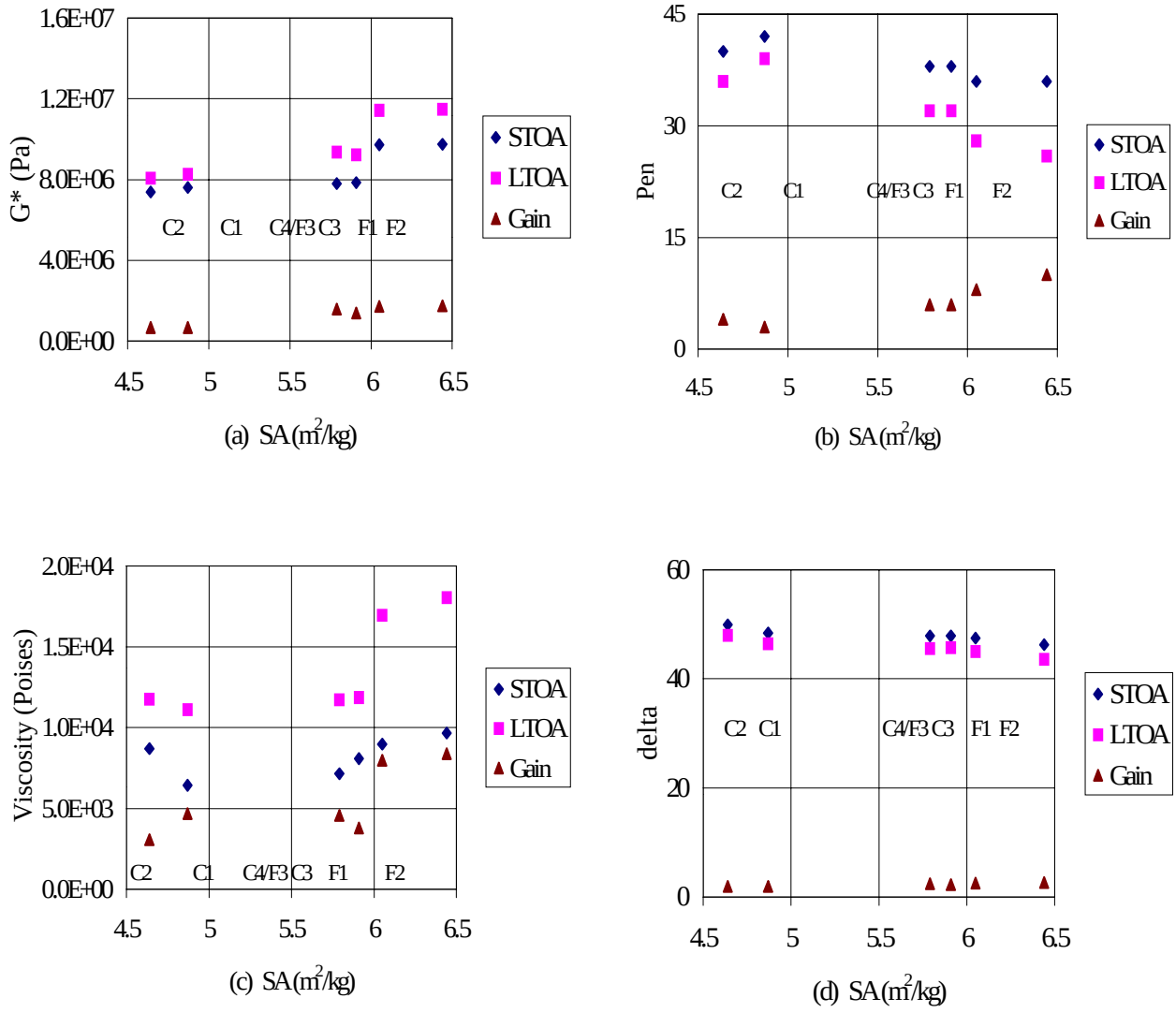

Figure 4-6 Binder Properties Versus Surface Area

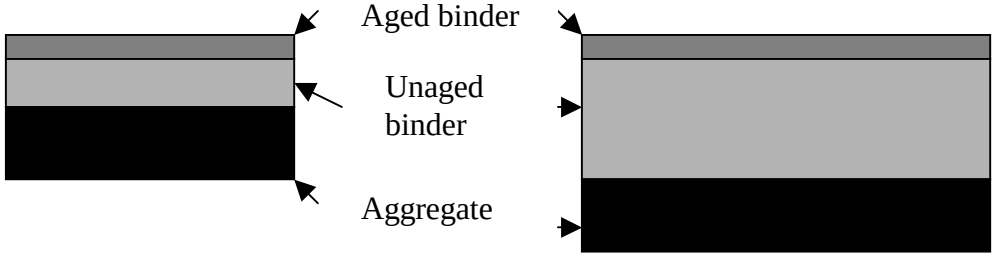

Figure 4-7 Illustration of the Effect of Film Thickness on Age-Hardening of Binder

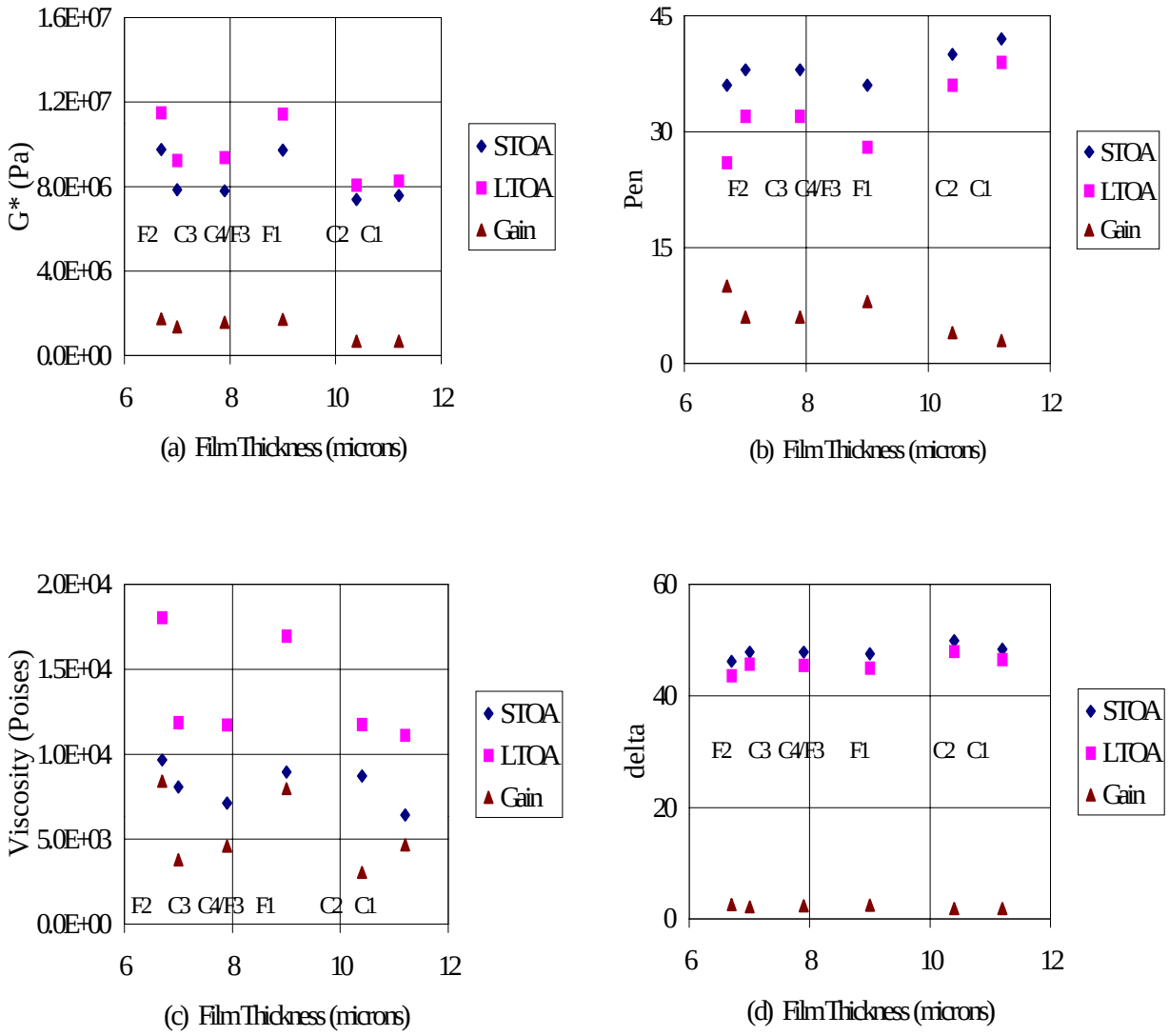

Figure 4-8 Binder Properties Versus Film Thickness

thickness on binder aging after STOA and LTOA. F1 had a high film thickness, higher than those of C3 and C4/F3 but resulted in more aging. In fact, its age-hardening was similar to that of F2, which had the lowest film thickness. In addition, mixtures F1 and F2 had significantly lower permeability as well as lower film thickness. Clearly, there appears to be other factors that affect the rate of age-hardening in mixtures.

Looking at the gain in viscosity or stiffness between STOA and LTOA, it is clear that mixtures that resulted in more binder aging at STOA also resulted in more binder aging during the LTOA process. Thus, the controlling factor during STOA, which is performed with the loose mixture, is also present during LTOA. For the coarse-graded mixtures, there appeared to be a general trend of decrease in aging with increasing film thickness. However, the differences between all coarse mixtures were within a fairly narrow range, and the aging of binders in all coarse mixtures was much less than the aging in fine mixtures.

4.3.3 Effect of Design Asphalt Content on the Aging of Asphalt Binder

There was generally no correlation between design asphalt content and aging of HMA (Figure 4-9). This may be due to the different aggregate structure of coarse and fine mixtures.

4.3.4 Effect of VMA on Binder Aging

No general trend was observed between VMA and binder age-hardening. Binder age-hardening in low VMA fine mixtures was similar to high VMA fine mixtures. Coarse mixtures, no matter what their VMA, resulted in less binder aging than fine mixtures (Figure 4-10). Hence, it is clear that the mixtures evaluated did not require the same amount of VMA for durability even though they are all 12.5-mm nominal maximum aggregate gradations.

4.3.5 Effect of Permeability on Binder Aging

Permeability tests were performed on the compacted mixtures to show how the ease of air flow, circulation and the void structure affect binder aging. In the past, permeability test in asphalt mixtures were an indication of void structure. A higher permeability was considered poor for age hardening due to the possible ease of air flow.

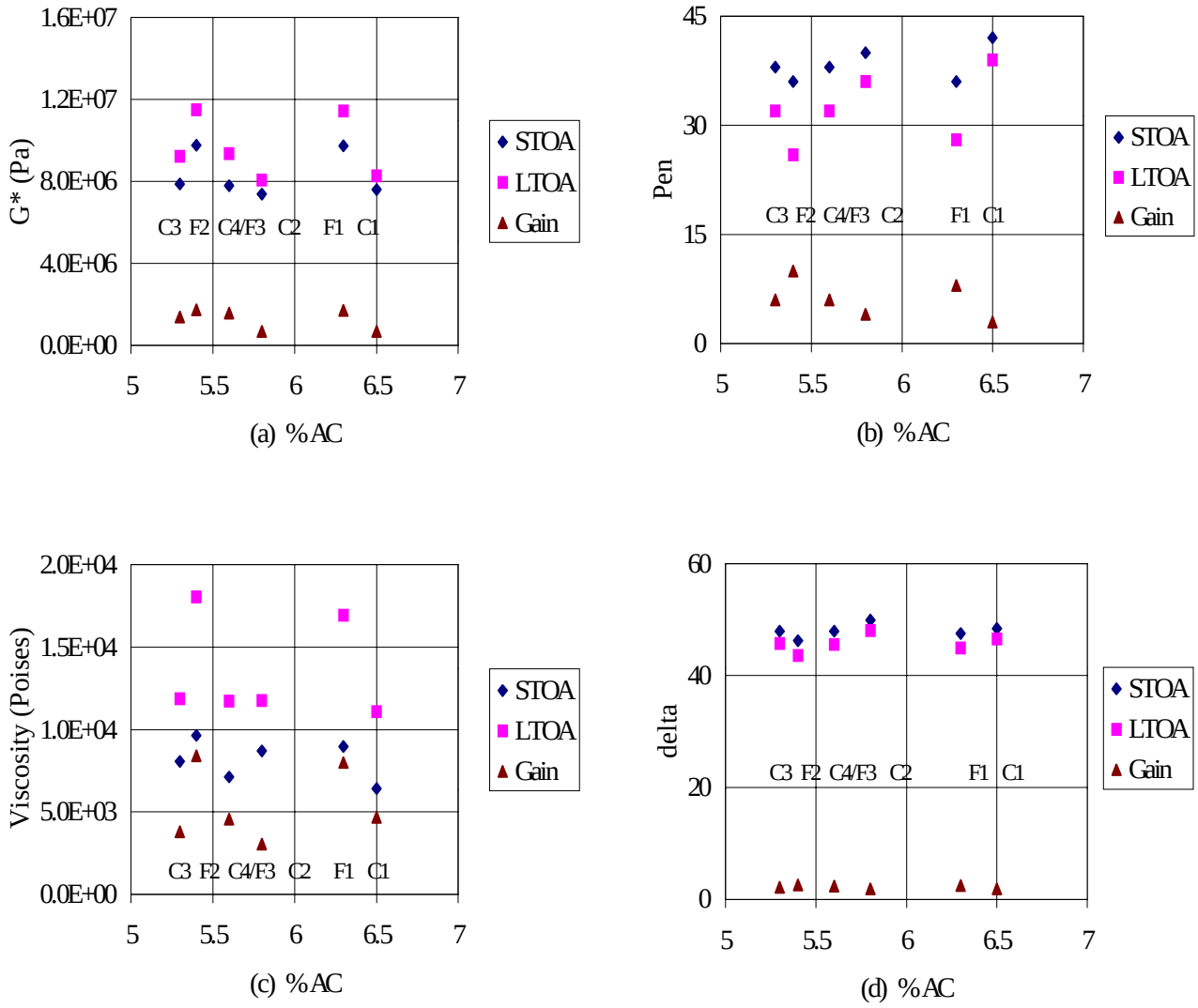

Figure 4-9 Binder Properties Versus % AC

But the permeability results did not show any such correlation with age-hardening (see Table 4-5). Coarse mixtures, which aged less, had higher permeability coefficients. Binder aging in these mixtures did not appear to depend on the rate of air passage through the mixture. The mechanism of aging may not involve a lot of oxygen because it is a surface phenomenon. The observed trend could be attributed to the fact that:

- The range of water permeability values obtained (i.e., 9×10^{-5} to 73×10^{-5} cm/s) was not large enough since all mixtures are essentially dense-graded mixtures.

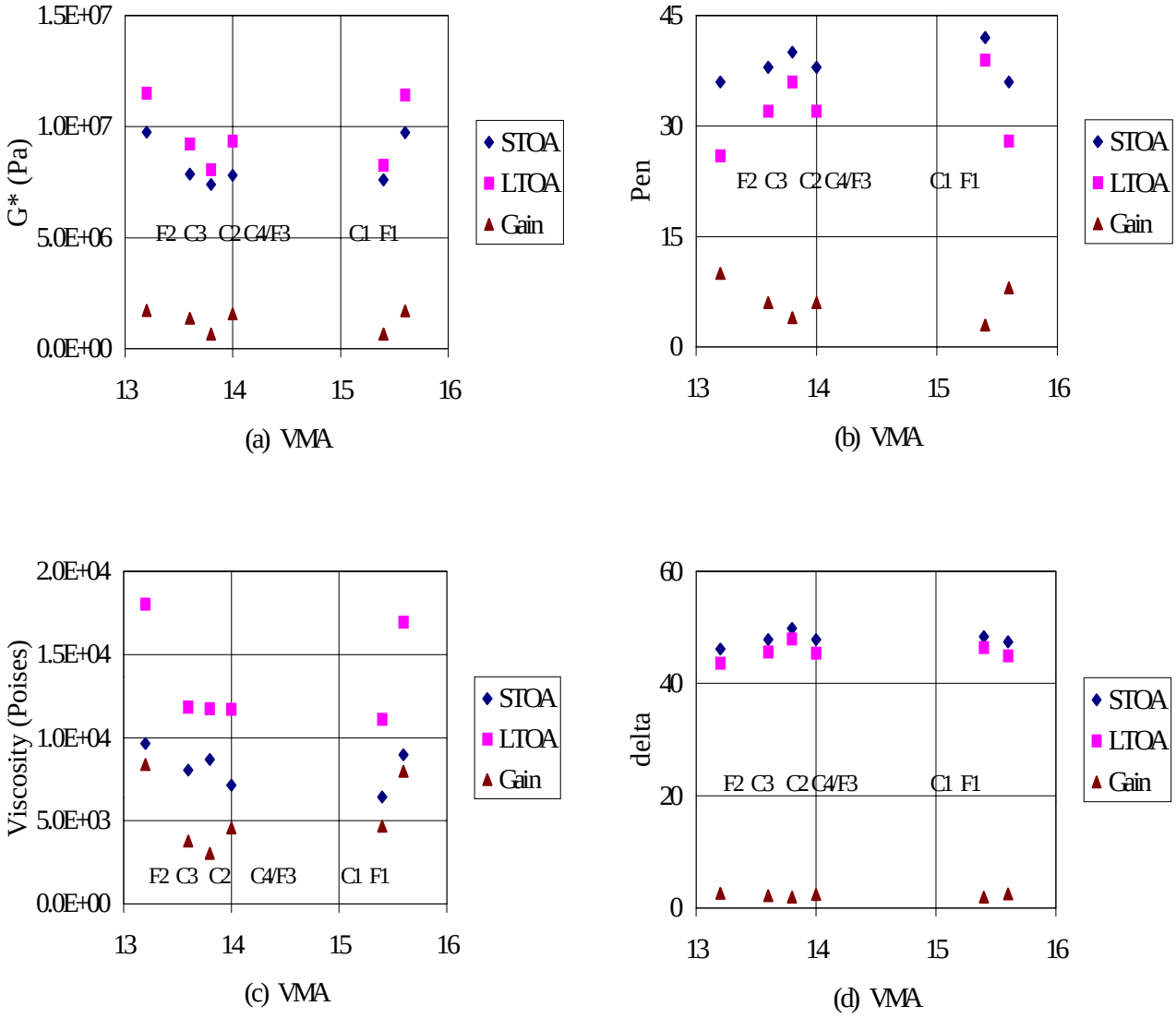

Figure 4-10 Binder Properties Versus VMA

Table 4-5 Permeability Values

Mixture Type	Permeability (10^{-5}cm/s)
C1	72.37
C4/F3	69.63
C3	69.19
C2	24.12
F1	17.81
F2	9.68

- Since aging is a surface phenomenon, only asphalt exposed to air would undergo aging, but that the recovered binder is a blend of aged and unaged binder.
- Only a limited amount of oxygen is required for aging, so no matter how small the flow through the mixture, there is always enough oxygen available for aging.
- The time involved is so long that oxygen is always in abundant supply.

4.3.6 Effect of the Amount of Fine Aggregates on Binder Age-Hardening

Figure 4-11 shows that it is only when mixtures are analyzed by the percent fine aggregates that the aging of the binder is clearly understood. It appears that binder aging was primarily related to the gradation of the fine portion of the mixtures regardless of asphalt content, film thickness or other volumetric properties.

4.4 Volumetric Properties and Binder Hardening

Results indicated that the rate of binder hardening in mixtures was not related to either the VMA or the film thickness of mixtures as currently determined. Figures 4-12 to 4-15 show plots relating binder properties with volumetric properties. It was observed that VMA, film thickness and asphalt content were not capable of predicting the age-hardening rate. Binder hardening was almost entirely controlled by the percentage of fine aggregate in the mixtures where the SuperPave™ restricted zone appeared to provide a proper definition between fine-graded and coarse-graded mixtures for this purpose. A different aggregate structure is developed in mixtures that are graded above and below the restricted zone. Thus, a modified procedure was presented to calculate effective film thickness and effective VMA to reflect the aggregate structure.

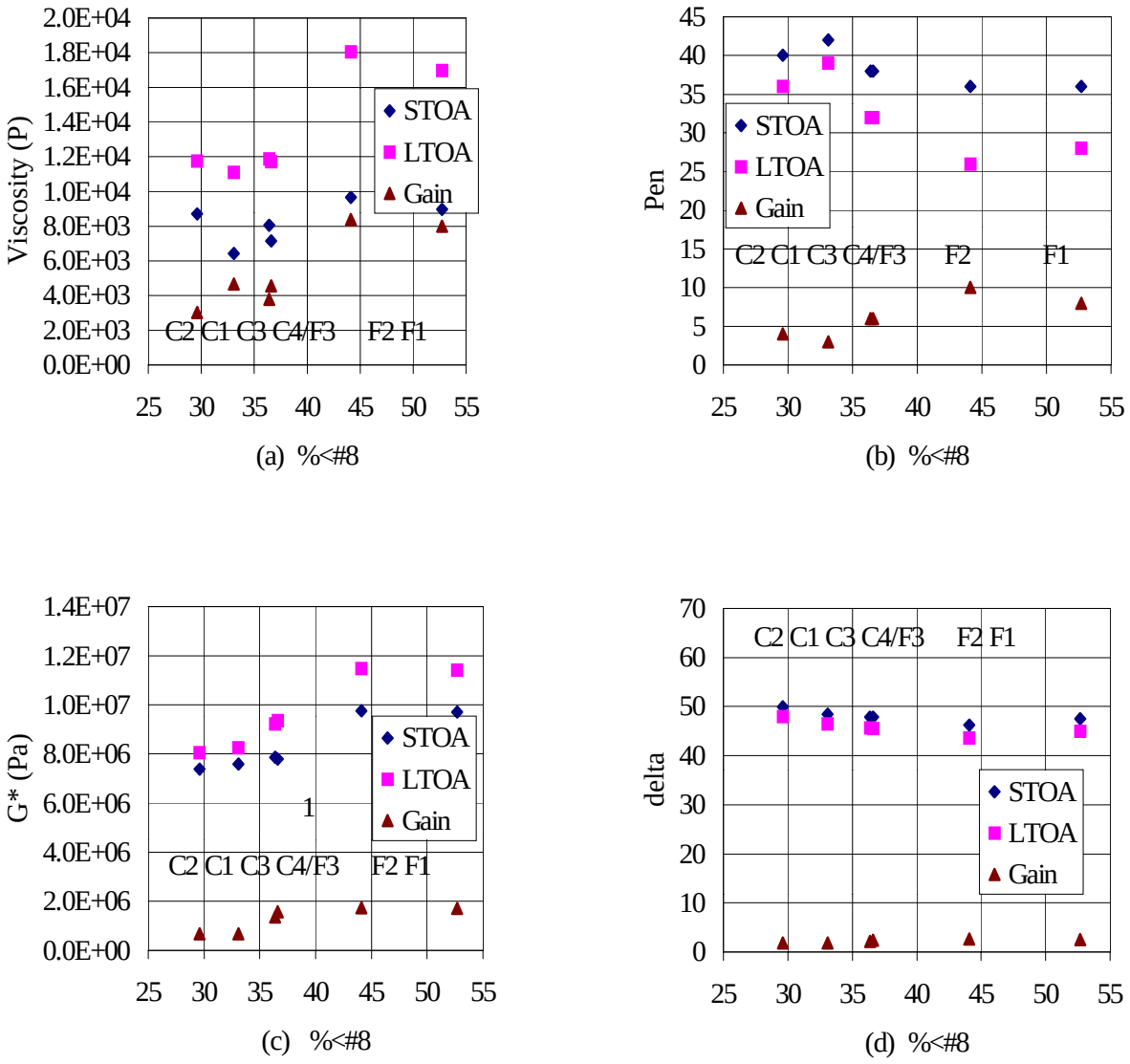

Figure 4-11 Binder Properties Versus % Less Than No. 8 Sieve Size

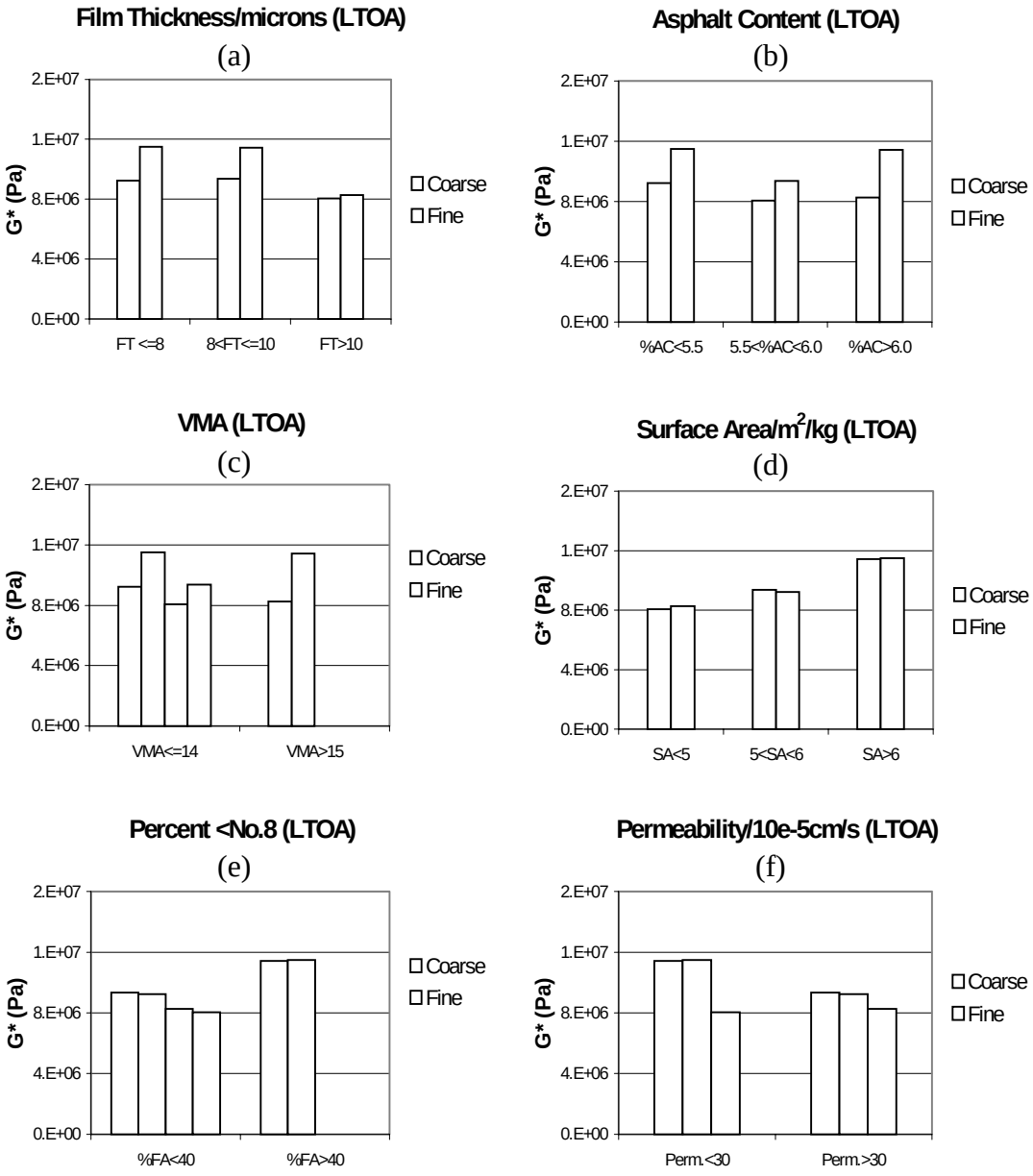

Figure 4-12 G* After LTOA Versus Volumetric Properties and Permeability

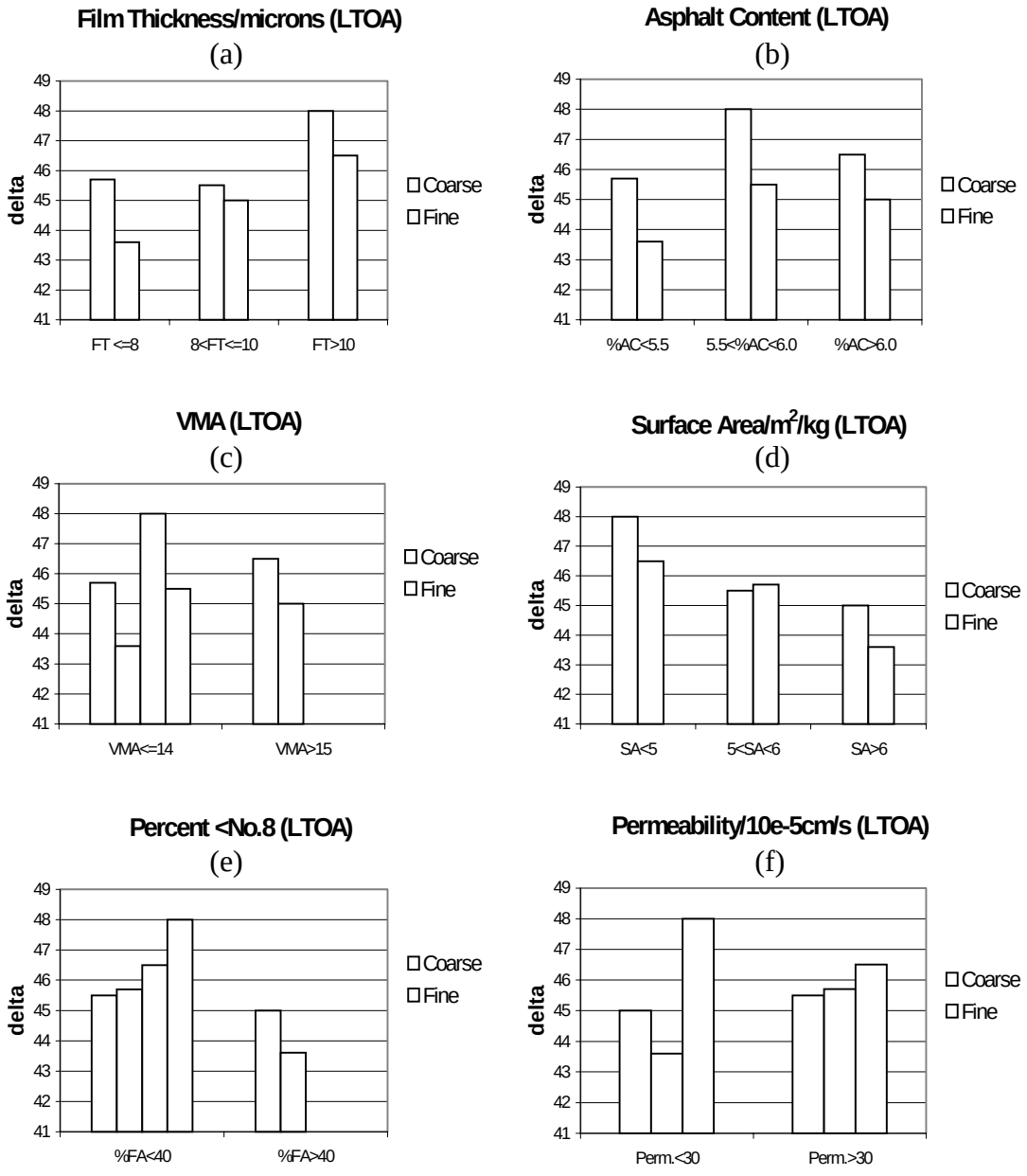

Figure 4-13 Delta After LTOA Versus Volumetric Properties and Permeability

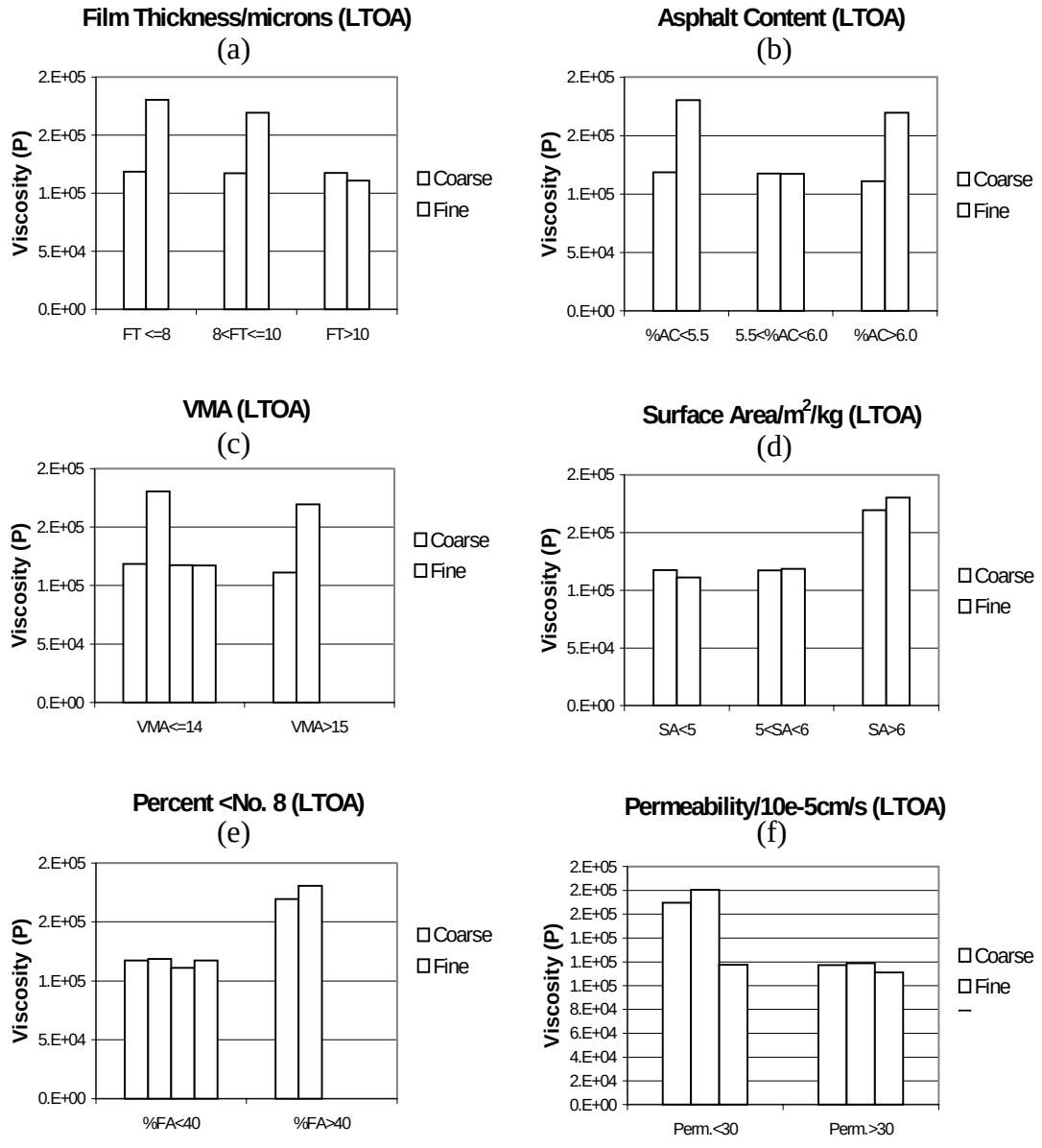

Figure 4-14 Viscosity After LTOA Versus Volumetric Properties and Permeability

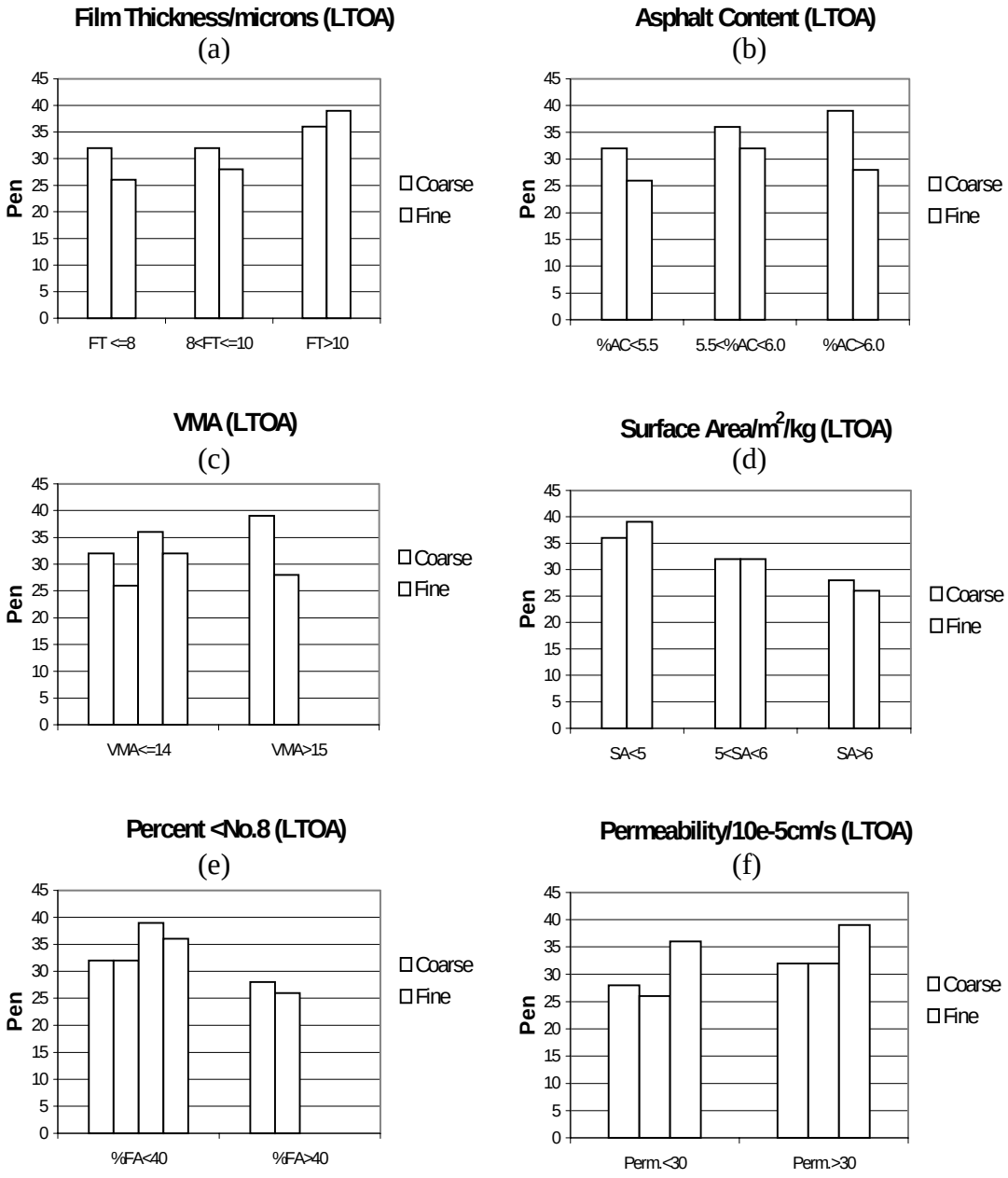

Figure 4-15 Penetration After LTOA Versus Volumetric Properties and Permeability

4.5 Alternative Concept for Calculation of Volumetric Properties

The overall fine aggregate content of the mixture expressed as the percent passing the number 8 sieve, appears to best reflect the age-hardening rate of binders in asphalt mixtures. It appears that mixtures with gradations above the restricted zone resulted in significantly higher rates of binder age hardening than mixtures below the restricted zone. This was found to be true even though the permeability of the mixtures below the restricted zone (i.e., lower fine aggregate content) was greater than mixtures above the restricted zone.

The apparent explanation for this resides in the difference between the resulting aggregate structure of mixtures above and below the restricted zone (see Figure 4-16). Mixtures above the restricted zone, which are commonly referred to as fine-graded mixtures, have more continuous gradations such that the fine-aggregates are an integral part of the aggregate matrix. On the other hand, coarse mixtures (i.e., below the restricted zone) tend to have aggregate structures that are dominated by the coarse aggregate portion (i.e., stone-to-stone contact). In the loose state, the coarse aggregate particles are coated by the mixture made up of asphalt and fine aggregates, and the fine

Coarse Mixtures Fine Mixtures

Figure 4-16 Aggregate Structure for Coarse and Fine Mixtures

aggregates within that matrix have access to all the asphalt within the mixture. Consequently, after compaction, there is aggregate-to-aggregate contact between the coarse aggregates which encapsulates the fine aggregate-asphalt mixture between them. This results in film thicknesses that are much greater than those calculated using conventional calculation procedures that assume that the asphalt is uniformly distributed over all aggregate particles. The results of modified parameters calculated on the basis of this concept, i.e., fine aggregate-asphalt mixture only are presented in Table 4-6.

Table 4-6 Volumetric Properties Based on the New Calculations

Mixtures	%CA	%FA of Total Mix	%AC	VMA	Film thic. (um)	SA (m^2/kg)	Dust/AC Ratio
C1	66.9	30.9	17.4	35.4	39.2	4.20	0.28
C2	70.4	27.9	17.2	35.3	39.3	4.02	0.28
C3	63.6	34.5	13.3	30.4	24.1	5.16	0.47
F1	47.3	49.4	11.3	25.7	19.3	5.36	0.42
F2	55.9	41.7	11.5	25.8	17.1	5.73	0.55
C4/F3	63.4	34.6	13.9	30.6	25.0	5.07	0.42

The values in Table 4-5 were determined from Equations 4-1 to 4-13 below. These equations were based on the new concept that the fine aggregates have access to all the asphalt in the mixture. Thus, the coarse aggregate portions are eliminated creating a new mixture consisting of fine aggregates, asphalt and air voids.

$$P_{Agg} = 100 - Pb \tag{4-1}$$

P_{agg} = percent aggregate by mass of total mixture

$$PC_{Agg} = \frac{100 - \%<\#8}{100} * P_{Agg} \tag{4-2}$$

PC_{agg} = percent coarse aggregate by mass of total mixture

$$PF_{Agg} = \frac{\%<\#8}{100} * P_{Agg} = 100 - PC_{Agg} - Pb \tag{4-3}$$

PF_{agg} = percent fine aggregate by mass of total mixture

$$VMA_C = \frac{V_T - V_{CA}}{V_T} * 100 = 100 - \frac{G_{mb}}{G_{sb}} * \left[100 - \left(Pb + PF_{Agg}\right)\right] \quad (4\text{-}4)$$

$$= 100 - \frac{G_{mb}}{G_{sb}} * \left(100 - PC_{Agg}\right) \quad (4\text{-}5)$$

VMA_C = volume of voids in coarse mineral aggregates

$$Pb_2 = \left(\frac{Pb}{PF_{Agg} + Pb}\right) * 100 \quad (4\text{-}6)$$

Pb_2 = asphalt content based on fine aggregate-asphalt matrix

$$Abse = \frac{Abs}{\%\ <\#8} * 100 \quad (4\text{-}7)$$

Abse = total absorption as a percentage of the fine aggregates

$$Pbe_2 = Pb_2 - \frac{Abse}{100} * (100 - Pb_2) \quad (4\text{-}8)$$

Pbe_2 = effective asphalt content, percent by total mass of mixture based on fine aggregate-asphalt matrix

$$V_b = \frac{W_T * Pb/100}{G_b} \quad (4\text{-}9)$$

V_b = total volume of asphalt (when total volume of mixture, $V_T = 1m^3$, $W_T = G_{mb}$)

$$V_{ba} = \frac{W_T * (1 - Pb) * (Abs/100)}{G_b} \quad (4\text{-}10)$$

V_{ba} = volume of absorbed asphalt

$$V_{be} = V_b - V_{ba} \quad (4\text{-}11)$$

V_{be} = effective volume of asphalt

$$T_f = \frac{V_{be}}{SA * W_T * PF_{Agg}} = \left[\frac{Pb - \left(Abs/100 \right) * P_{Agg}}{SA * PF_{Agg} * G_b} \right] * 1000 \qquad (4\text{-}12)$$

T_f = film thickness

$$VMA_e = \frac{Vol_{AIR} + Vol_{EffAC}}{Vol_{AIR} + Vol_{EffAC} + Vol_{FA}} = \frac{4\% * V_T + V_{be}}{4\% * V_T + V_{be} + \frac{W_T * PF_{Agg}}{G_{sb}}} \qquad (4\text{-}13)$$

VMA_e = volume of voids in mineral aggregates based on fine aggregate-asphalt matrix

Other symbols are:

P_b = asphalt content percent by mass of total mixture
Pb_2 = asphalt content based on fine aggregate-asphalt matrix
Abs = absorption
G_{sb} = bulk specific gravity for the total aggregate
G_{mb} = bulk specific gravity of compacted mixture
G_b = specific gravity of asphalt

Plots relating effective volumetric properties (see Table 4-5) determined from Equations 4-1 to 4-9 to binder age-hardening rate are shown in Figures 4-17 to 4-20. It was observed that this method was suitable for analyzing the age-hardening rate of mixtures. Binder age-hardening decreased with increasing effective film thickness, effective VMA, effective asphalt content and effective surface area. Fine mixtures which had higher amount of fine aggregate portion had lower effective film thickness and VMA resulting in higher binder age-hardening rates, whereas coarse mixtures which had lower amount of fine aggregate portions had higher effective film thickness and VMA resulting in lower binder age-hardening rates. Thus, all effective volumetric properties analyzed correlated well with binder age-hardening rate.

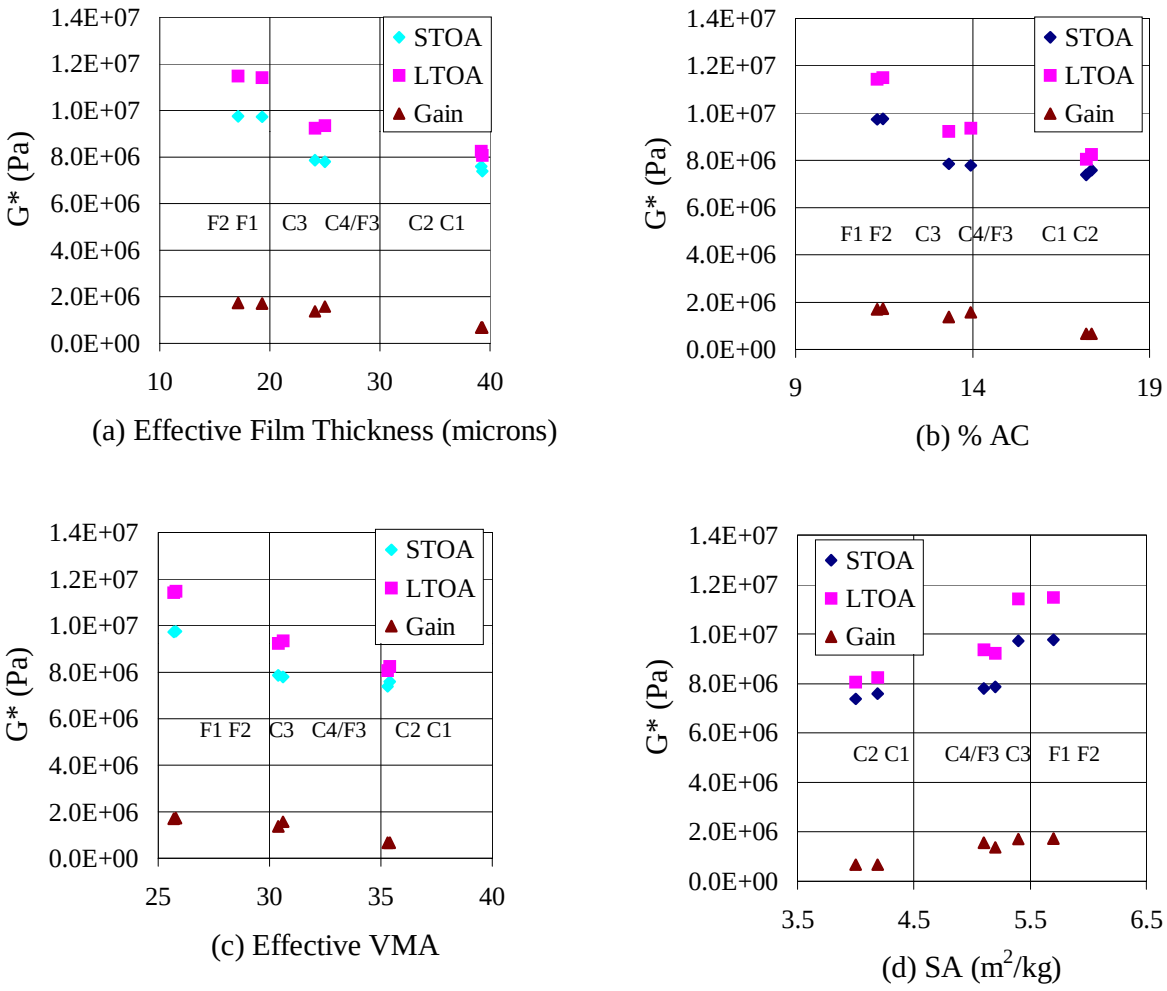

Figure 4-17 G* Versus the Effective Volumetric Properties

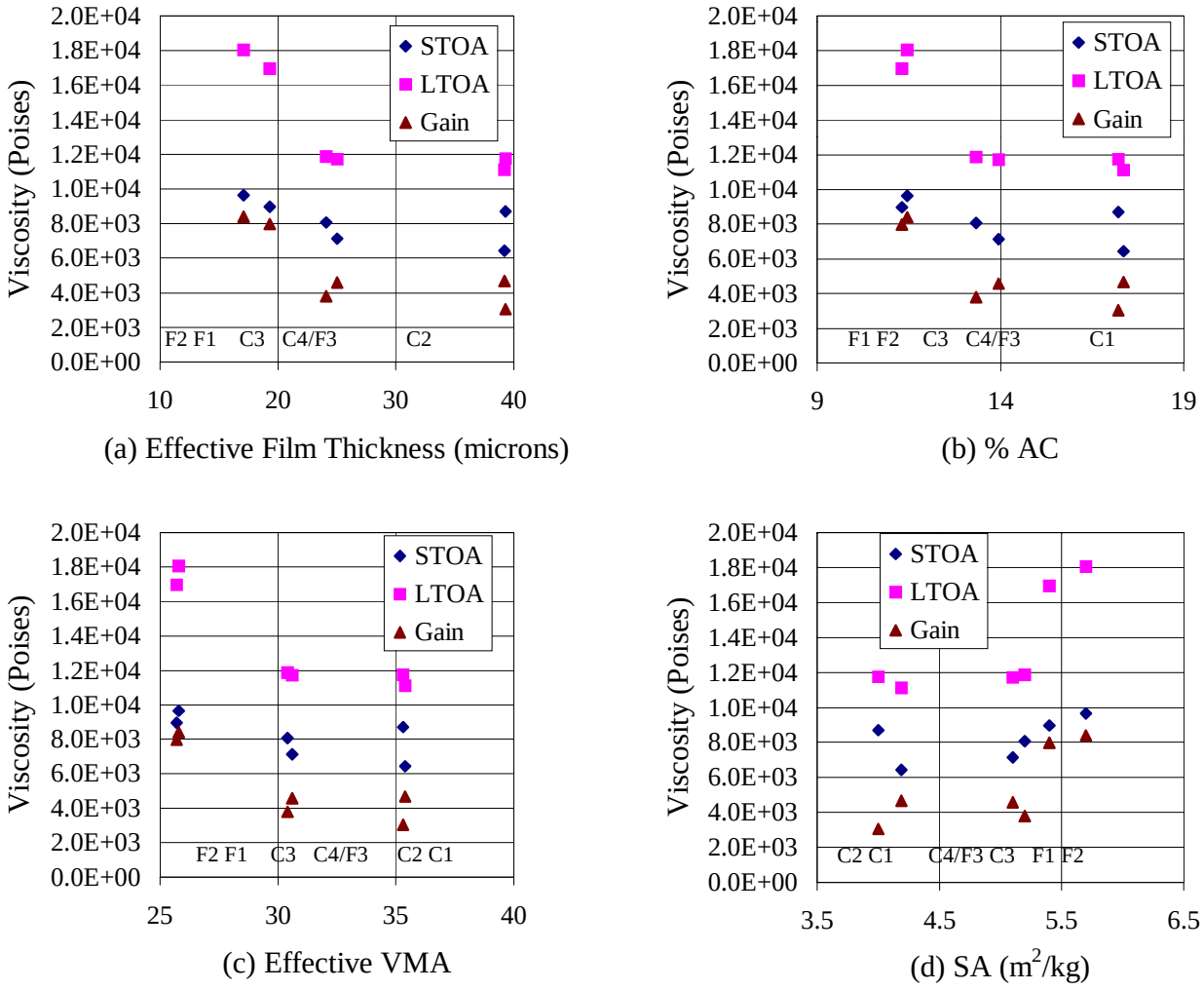

Figure 4-18 Viscosity Versus the Effective Volumetric Properties

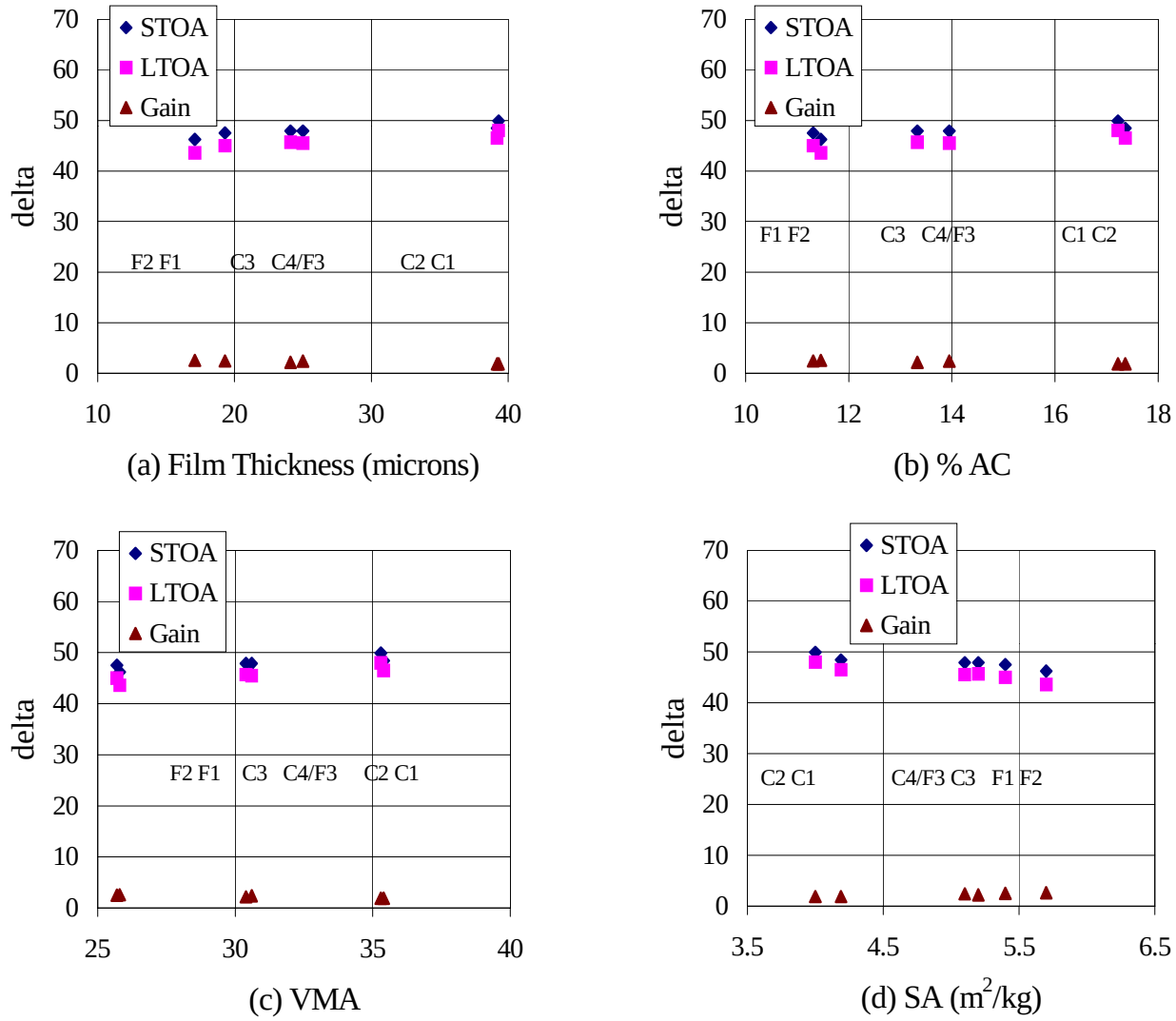

Figure 4-19 Delta Versus the Effective Volumetric Properties

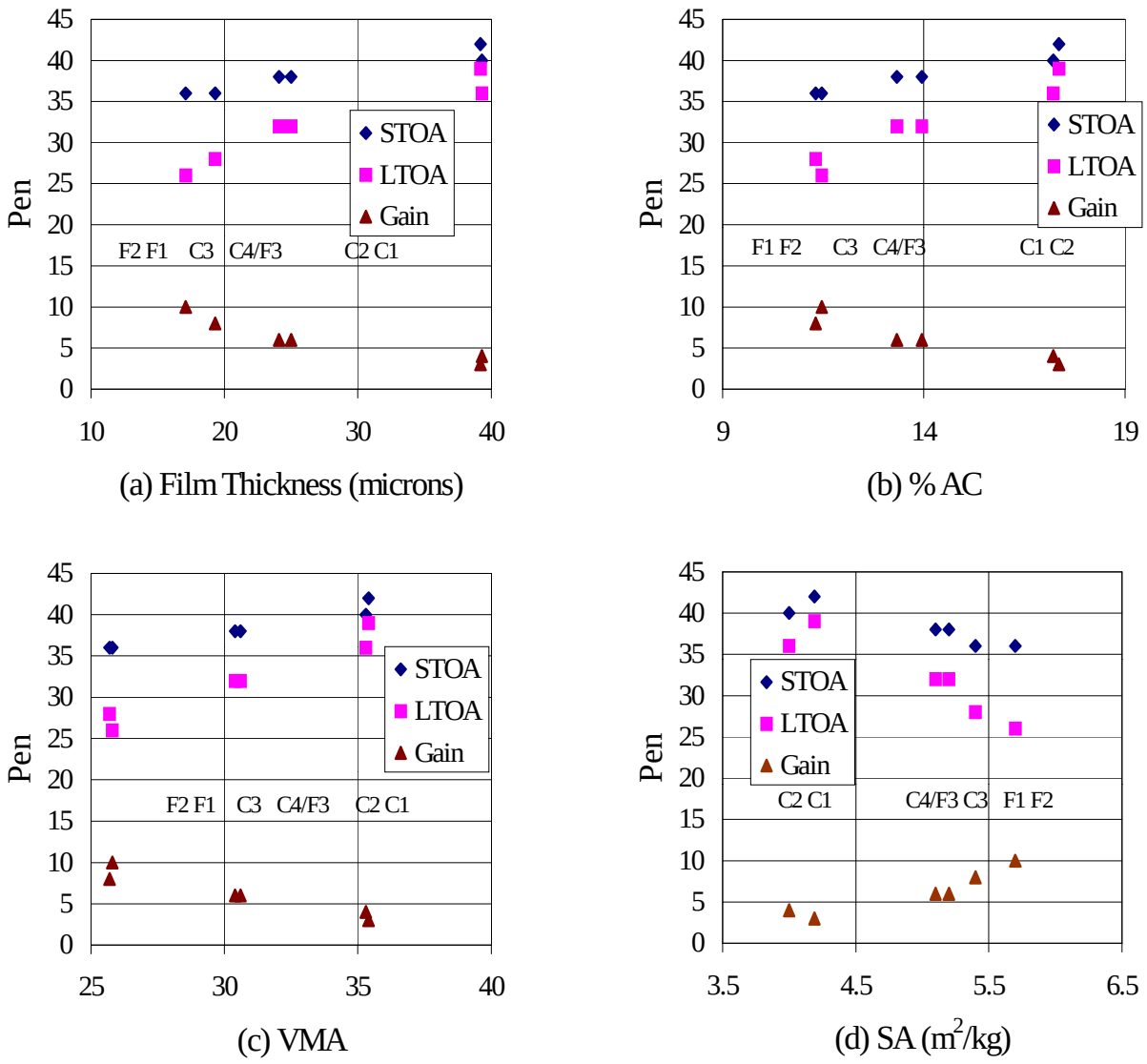

Figure 4-20 Penetration Versus the New Volumetric Properties

4.6 Summary of Binder Test Results

Based on the results of binder age-hardening presented above, it appears that neither VMA nor film thickness, as currently calculated, provide a parameter that adequately reflects the age–hardening rate of binders in asphalt mixtures. A much better trend was observed when the mixtures were analyzed separately as coarse-graded and fine-graded. This implies that restrictions placed on fine mixtures may not be appropriate for coarse mixtures and vice-versa, or perhaps that it would be more appropriate to have different parameters for control of age-hardening in different types of mixtures.

The above results indicate that both coarse- and fine-graded mixtures can be evaluated by using only the fine portion of the mixtures in computing the effective volumetric parameters for the HMA mixtures (see Figures 4-13 through 4-16). This method shows that gradation of the fine part of mixtures is more important for the durability than the average film thickness determined on the basis of the whole mixture.

Thus, by separating out the fine aggregates and the asphalt and computing the volumetric properties, the resulting effective asphalt content, VMA, surface area and the film thicknesses are in much better agreement with the observed aging trends than the ones calculated by the conventional method.

However, binder-hardening rate is not the only factor to be considered in mixture design and evaluation. Other mixture characteristics such as resistance to cracking and rutting must be considered before making any recommendations.

CHAPTER 5
MIXTURE RESULTS AND ANALYSIS

5.1 Introduction

Mixture tests were performed to evaluate the effect of binder age-hardening on mixture performance. As stated earlier, the mixture properties used to evaluate the effects of age-hardening were: fracture energy density; failure strain and tensile strength; resilient modulus; creep compliance; and m-value at 10^{o} C, which were all obtained using the SuperPave™ Indirect Tension (IDT) test. Table 5-1 shows all the results obtained from these tests. Also the effects of volumetric properties such as VMA, film thickness, asphalt content, aggregate gradation and surface area on the durability (age-hardening rate) of the mixtures as a whole was evaluated. Mixture shear resistance was measured with the Servopac SuperPave™ Gyratory Compactor. All mixtures were tested after STOA and LTOA. Permeability tests were also performed on all mixtures to get an indication of the degree of void continuity and interconnection. An evaluation of the effect of

Table 5-1 Mixture Test Results

Mixture	M_R (Gpa)		CreepCompliance(1/GPa)		M-Value	
	STOA	LTOA	STOA	LTOA	STOA	LTOA
C1	7.9	9.6	13.9	4.5	0.80	0.55
C2	7.7	11.9	15.1	2.8	0.77	0.59
C3	11.5	14.2	7.6	2.2	0.66	0.50
F1	9.5	9.9	7.9	4.5	0.66	0.57
F2	8.6	12.9	6.0	1.9	0.56	0.50
C4/F3	12.0	13.9	6.3	1.9	0.58	0.50
Mixture	FractureEnergy(kJ/m^3)		Failure Strain		TensileStrength (MPa)	
	STOA	LTOA	STOA	LTOA	STOA	LTOA
C1	5.8	3.5	4629.8	2224.4	1.6	2.1
C2	4.8	2.9	3771.3	1896.7	1.7	2.1
C3	3.5	2.7	2174.0	1468.3	2.1	2.4
F1	4.2	2.8	2919.6	1833.3	2.1	2.1
F2	5.4	3.2	3714.6	1526.2	1.9	2.6
C4/F3	3.7	1.7	2419.0	1174.7	2.0	2.2

volumetric properties including theoretical film thickness and theoretical VMA on mixture performance properties are presented in the following sections.

5.1.1 Resilient Modulus

As shown in Figure 5-1, resilient modulus values are very similar for C1 and C2 during STOA. The F1 mixture had a slightly higher resilient modulus compared to F2, but overall the gap graded mixtures C3 and C4/F3 had higher resilient moduli.

Among the continuously graded mixtures, F1 and F2 have higher M_R values than C1 and C2. It is known that higher resilient modulus is achieved through higher binder stiffness or good aggregate interlock in a mixture. However, there is no general trend relating volumetric properties, binder age-hardening and M_R. Among the coarse mixtures, it appears that the higher resilient modulus values were obtained from higher binder stiffness as seen in C3 and C4/F3. But C3 and C4/F3 have higher stiffness than F1 and F2 even though the binder in fine mixtures age-hardened more. This appears to suggest that gradation played an important role in the mixture stiffness since the resilient modulus did not change significantly between mixtures with similar gradations, i.e., the two coarse mixtures C1 and C2, gap-graded coarse mixtures C3 and C4/F3 (which have a higher amount of aggregate passing 2.36 mm sieve), and the two fine mixtures F1 and F2. After LTOA aging, the resilient modulus values increased for all mixtures, but some mixtures showed a higher rate of increase than others. As illustrated in Figure 5-1, the resilient modulus of fine mixture F2 which is the low VMA fine mixture, increased more than for all other mixtures.

Thicker asphalt films around the aggregates makes the mixtures less susceptible to aging, thus C1 and C2 have very lower M_R values mainly because of their higher theoretical film thicknesses. However, VMA, theoretical film thickness and asphalt

	C1	C2	C3	C4/F3	F1	F2
VMA	15.4	13.8	13.6	14	15.6	13.2
FT	11.2	10.1	8	8.1	9	6.9
D/A	0.74	0.83	1.18	1.04	0.76	1.16
%FA	33.1	29.6	36.4	36.6	52.7	44.1

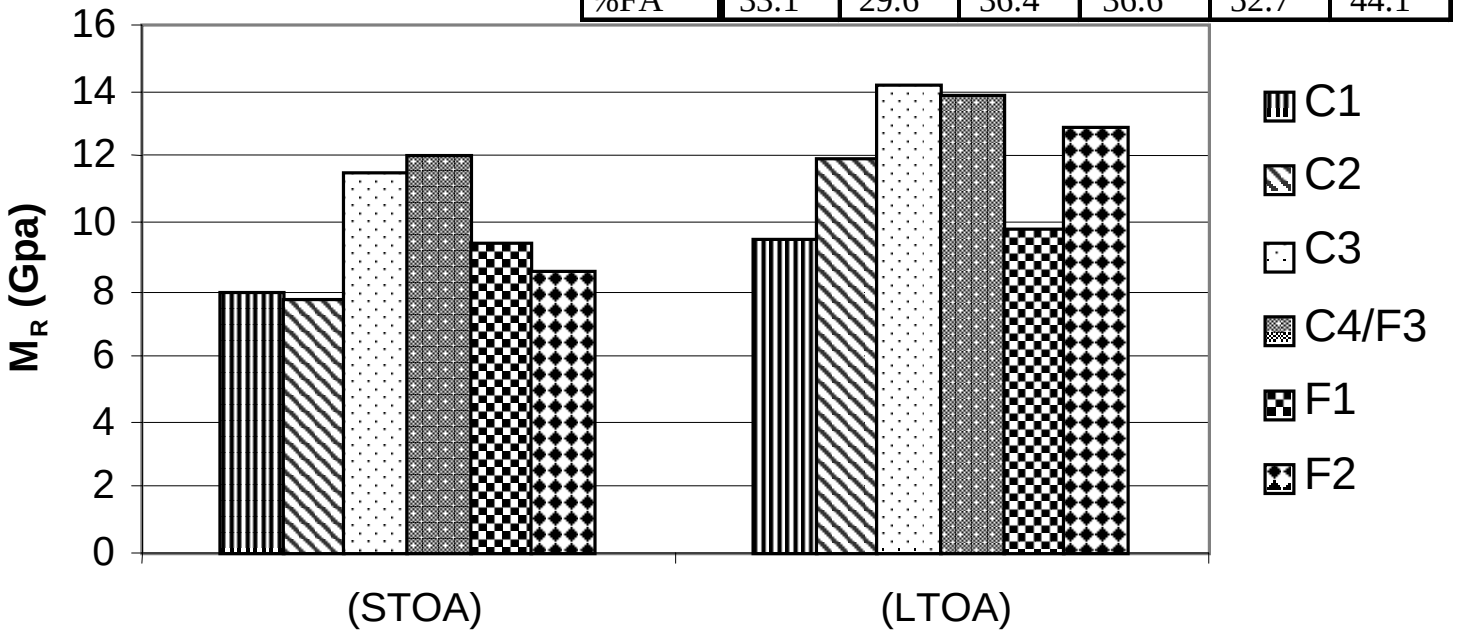

Figure 5-1 M_R and Mixture Volumetric Properties

content do not adequately explain the large differences between the M_R values of mixtures with high theoretical film thickness and VMA and those with lower theoretical film thickness and VMA values. Gradation was another important factor in this case. C3 and C4/F3 exhibited the highest resilient modulus values for both the STOA and LTOA conditions. These are coarse gap-graded mixtures with higher fine aggregate content and lower theoretical film thicknesses than C1 and C2. This gives an indication that M_R may be affected by aggregate gradation and the amount of binder rather than binder stiffness.

5.1.2 Creep Compliance

Creep compliance at longer loading times (e.g., 1000 seconds) is dominated mostly by the binder stiffness since creep is controlled entirely by the properties of the binder. Figure 5-2 shows an expected reduction in creep compliance at 1000 seconds for mixtures, which is consistent with the fact that the binder stiffened with aging. However, there is no consistent trend among all mixtures with respect to binder age-hardening, theoretical film thickness or VMA. It is only when coarse mixtures are evaluated separately from fine mixtures that a consistent trend was observed.

It appears mixtures with high theoretical film thickness have higher creep. However, creep compliance did not appear to be related to VMA. Thus, creep compliance appears to correlate well with the amount and stiffness of the asphalt binder, especially when mixtures are analyzed separately as fine and coarse mixtures.

5.1.3 Tensile Strength

The finer mixtures exhibited a slightly higher tensile strength than the coarser mixtures, but there was not much difference in tensile strength between mixtures. Tensile strength ranged from 1.6 to 2.1 MPa after STOA and 2.1 to 2.6 MPa after LTOA. As indicated in Figure 5-3, tensile strength increased slightly after aging the mixtures.

	C1	C2	C3	C4/F3	F1	F2
VMA	15.4	13.8	13.6	14	15.6	13.2
FT	11.2	10.1	8	8.1	9	6.9
D/A	0.74	0.83	1.18	1.04	0.76	1.16
%FA	33.1	29.6	36.4	36.6	52.7	44.1

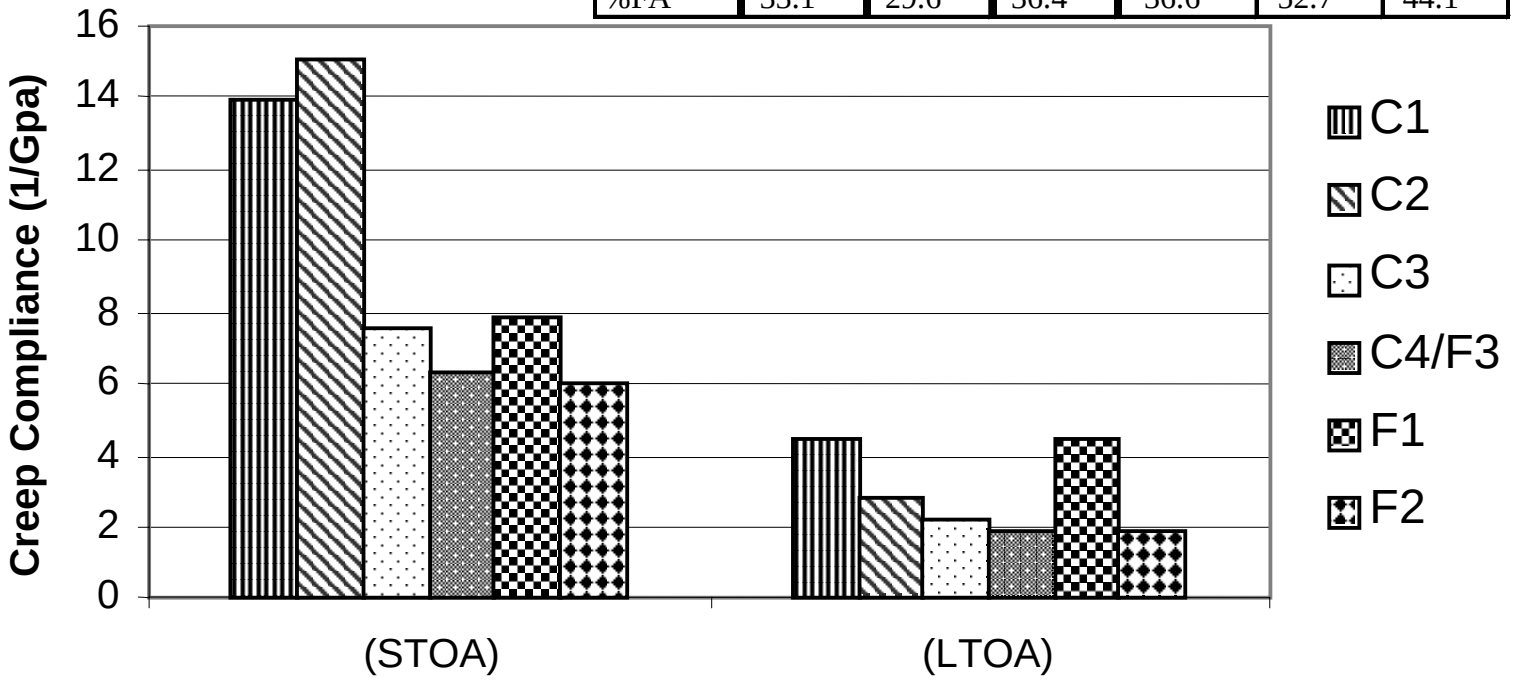

Figure 5-2 Creep Compliance and Mixture Volumetric Properties

	C1	C2	C3	C4/F3	F1	F2
VMA	15.4	13.8	13.6	14	15.6	13.2
FT	11.2	10.1	8	8.1	9	6.9
D/A	0.74	0.83	1.18	1.04	0.76	1.16
%FA	33.1	29.6	36.4	36.6	52.7	44.1

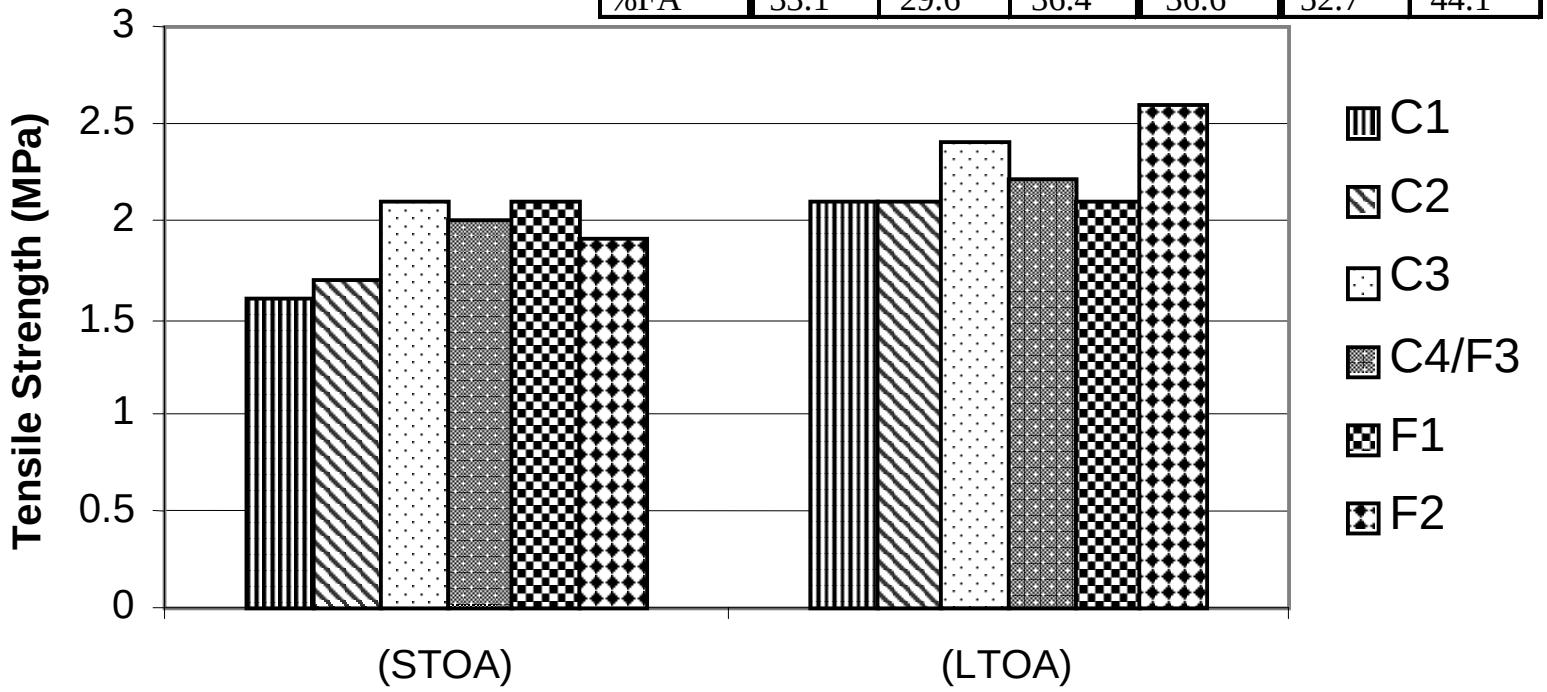

Figure 5-3 Tensile Strength and Mixture Volumetric Properties

Fracture energy depends partly on mixture tensile strength. Although tensile strength is the maximum tensile stress the mixture can tolerate before fracture, mixtures with high tensile strengths tend to be more brittle and may have lower fracture energies.

Apart from C4/F3, which has an unusually high tensile strength of 2.6 MPa after LTOA, all the mixtures had similar strengths both at STOA and LTOA. There was no apparent trend with binder age-hardening and volumetric properties, except when mixtures were separated into three groups of two mixtures of similar gradation (i.e., C1 and C2, C3 and C4/F3, and F1 and F2). It then appeared that higher theoretical film thickness resulted in lower tensile strength. There was no apparent trend between VMA and tensile strength.

5.1.4 Failure Strain

The failure strain value is the horizontal strain when cracking initiates during the tensile strength test where the sample is loaded to failure. The failure strain data shown in Figure 5-4 demonstrates that C1 and F2 have a higher failure strain compared to all the other mixtures. The failure strain was reduced by almost half in all the mixtures after LTOA. F2 exhibited a very large difference between STOA and LTOA values due to its dense gradation and low theoretical film thickness and VMA.

When analyzed separately by groups as discussed previously, it appeared that mixtures with higher theoretical film thickness had higher failure strains. Again, the difference in the VMA values for F2 and some other mixtures is so small that it can be deduced that VMA is not revealing the real picture of what is actually happening in F2 in terms of binder age-hardening.

	C1	C2	C3	C4/F3	F1	F2
VMA	15.4	13.8	13.6	14	15.6	13.2
FT	11.2	10.1	8	8.1	9	6.9
D/A	0.74	0.83	1.18	1.04	0.76	1.16
%FA	33.1	29.6	36.4	36.6	52.7	44.1

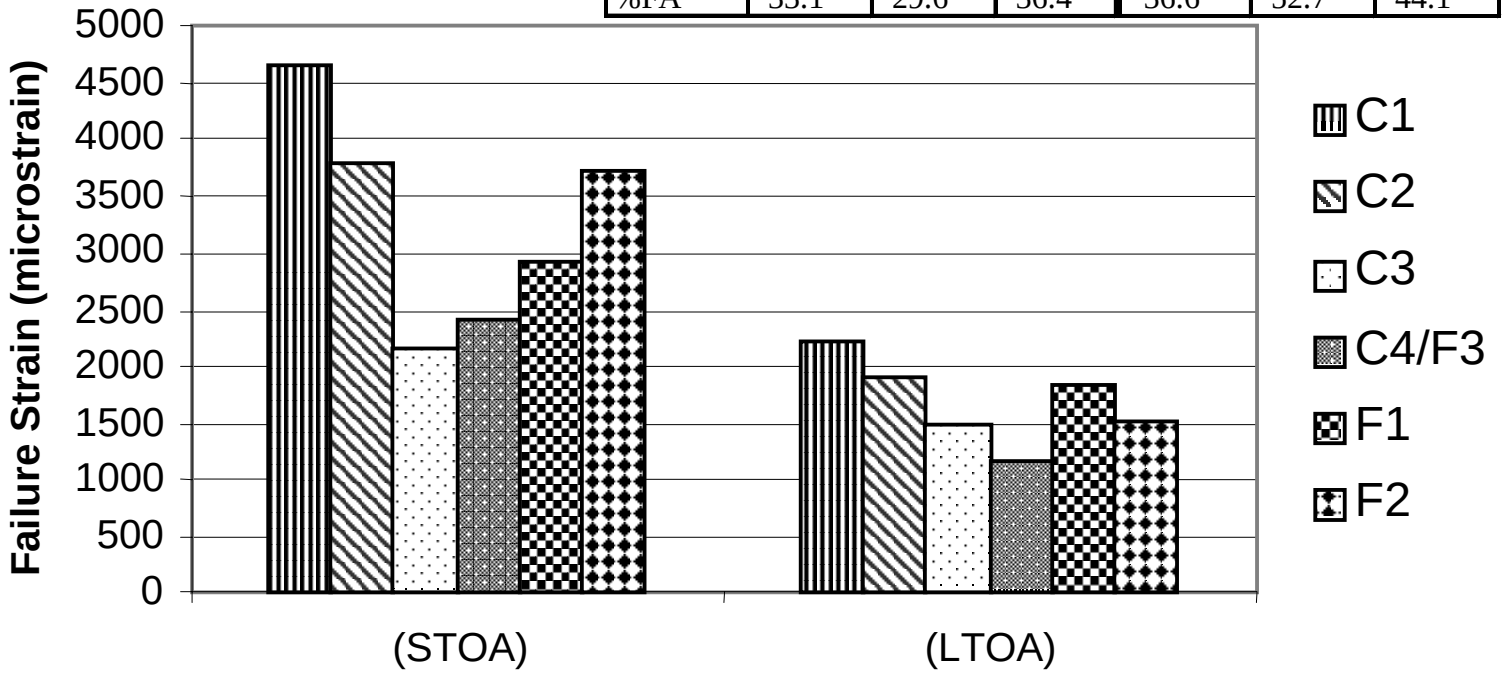

Figure 5-4 Failure Strain and Mixture Volumetric Properties

5.1.5 Fracture Energy Density

Previous studies have indicated that fracture energy density measurements in the lab appeared to be a good indicator of crack performance in the field. The trends in fracture energy are similar to that in failure strain. Mixtures with higher stiffnesses had lower fracture energy densities after both STOA and LTOA. Figure 5-5 shows that mixtures with higher VMA and film thickness also had higher fracture energy densities after STOA and LTOA. Once again F2, which has the lowest film thickness, showed a big difference between its STOA and LTOA values. Therefore, it appears that mixtures with higher stiffness resulted in lower fracture energy density.

A comparison between the two fine mixtures shows that the F1 mixture exhibited a higher resilient modulus and a lower fracture energy density, while both mixtures had similar binder stiffness and the tensile strength. Fracture energy density generally decreases after aging. The findings lend credence to the fact that the trends observed in fracture energy density must be due to the aggregate gradation since trends are clearer when mixtures are analyzed separately as coarse-graded and fine graded mixtures.

5.1.6 m-Value

Current research has led to the belief that lower m-values result in improved fracture resistance. Higher m-value leads to higher micro damage rate but lower fracture energy density (i.e., more brittle).

It appears that mixtures with higher theoretical film thickness had higher m-value. Figure 5-6 shows that coarse mixtures exhibited higher m-values than fine mixtures. Generally, mixtures C1, C2 and F2 have the highest m-values followed by mixtures F1, C3 and C4/F3 (Figure 5-6). By analyzing the coarse-graded mixtures and fine-graded mixtures separately, it appears mixtures with higher theoretical film thickness had higher

	C1	C2	C3	C4/F3	F1	F2
VMA	15.4	13.8	13.6	14	15.6	13.2
FT	11.2	10.1	8	8.1	9	6.9
D/A	0.74	0.83	1.18	1.04	0.76	1.16
%FA	33.1	29.6	36.4	36.6	52.7	44.1

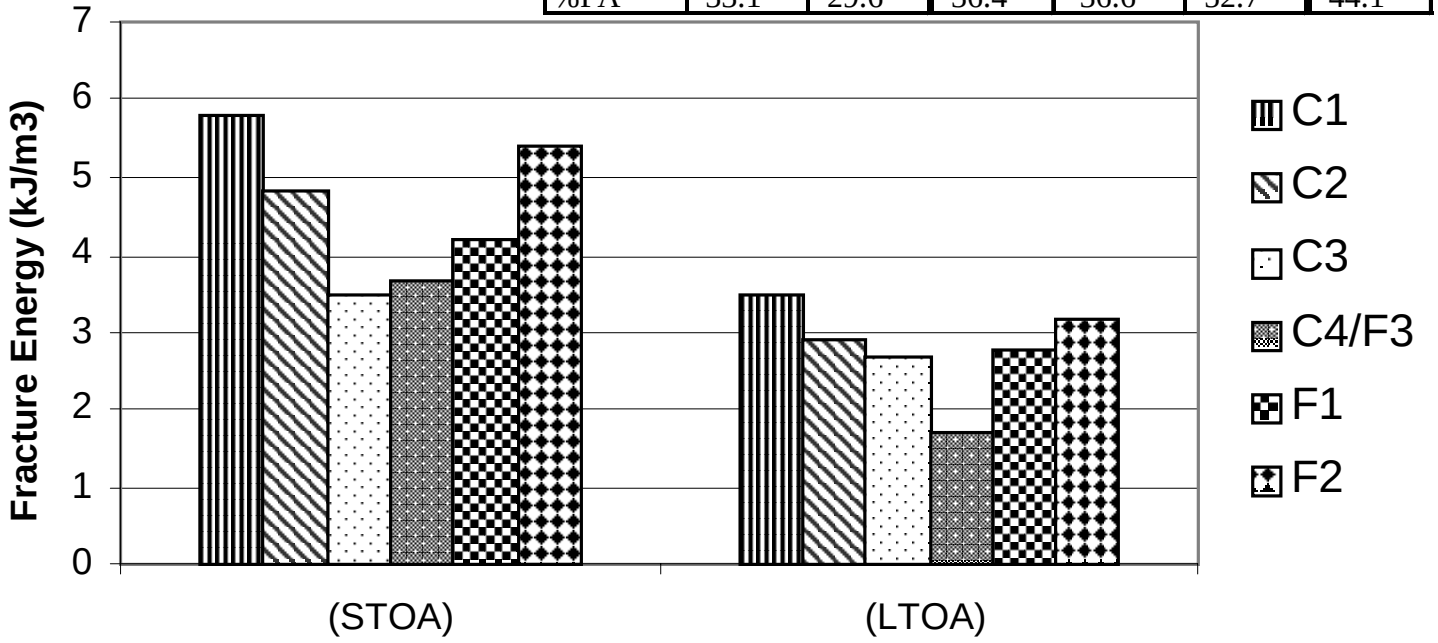

Figure 5.5 Fracture Energy Density and Mixture Volumetric Properties

	C1	C2	C3	C4/F3	F1	F2
VMA	15.4	13.8	13.6	14	15.6	13.2
FT	11.2	10.1	8	8.1	9	6.9
D/A	0.74	0.83	1.18	1.04	0.76	1.16
%FA	33.1	29.6	36.4	36.6	52.7	44.1

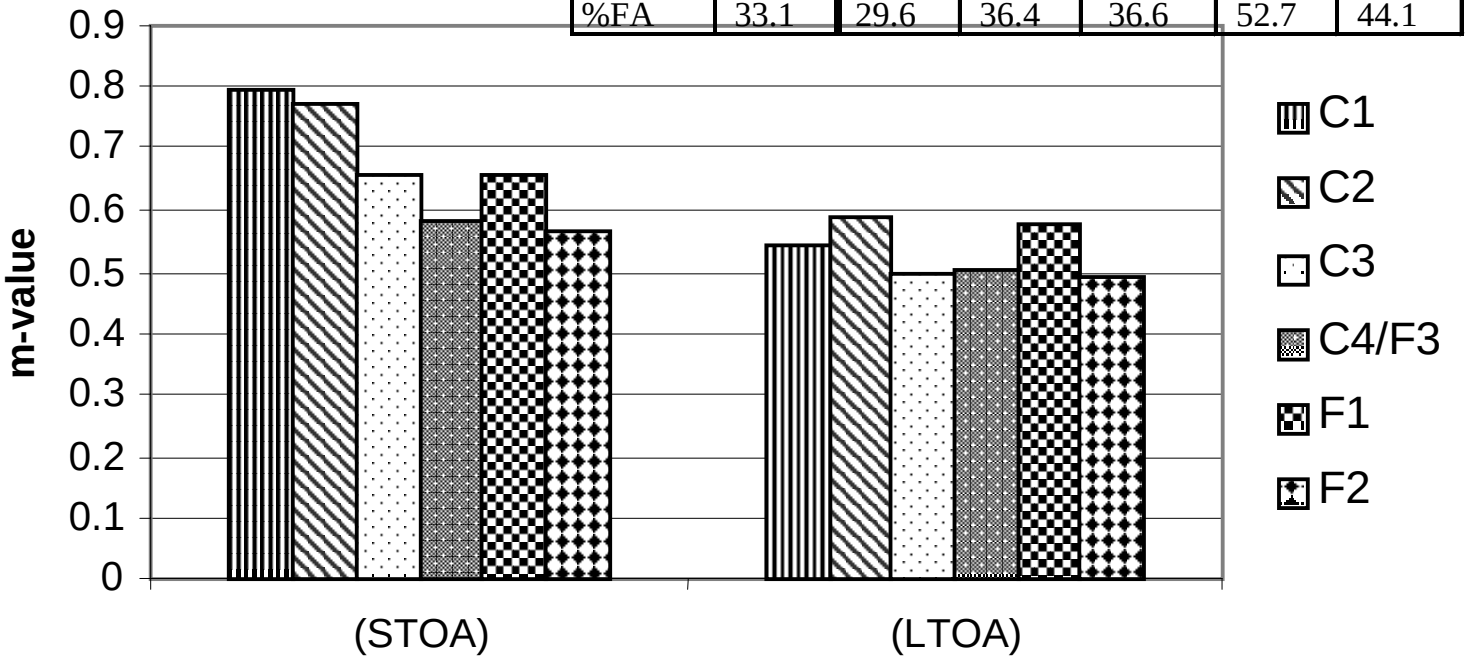

Figure 5.6 m-Value and Mixture Volumetric Properties

m-values with some exceptions. F1 stands out as a fine mixture with a high m-value and the highest VMA of all the mixtures but still has a lower m-value than F2 at STOA. It should be recalled that C2 is the coarsest mixture with an inferior VMA

5.1.7 Permeability

The permeability of mixtures at a given air void content provides an indication of the void structure or interconnection between the voids. Thus, a high permeability denotes larger, more interconnected voids, while a low permeability denotes smaller, more evenly distributed voids with little or no interconnection. The low permeability value for F2 helps explains why it performed so well in fracture even though it had a low film thickness and VMA. However, its low film thickness and VMA are evidenced by its high loss of fracture when aged at LTOA. Permeability values were shown in Table 4.5.

5.2 Summary of Findings

Mixture test results appeared to indicate that low VMA and film thickness identified potential performance problems in fine-graded mixtures, but did not necessarily imply a problem in coarse-graded mixtures. A comparison of mixtures F1 and F2 reveals that even though binder aging was about the same for both mixtures, the lower VMA mixture (F2) became stiffer and more brittle as the mixture was aged. However, the F2 mixture had higher fracture energy than the F1 mixture after both STOA and LTOA. This appeared to be a result of the excellent void structure reflected in the very low permeability of this highly dense graded mixture. The greater stiffening effect for a similar change in binder properties may be explained by the much higher dust-to-asphalt ratio (1.16) of the F2 mixture. The most serious problem with the fine-graded low VMA mixture was the fact that the mixture appeared to become unstable at lower air

void contents. Figures 5-7 and 5-8 show how the shear strength measured during SuperPave™ gyratory compaction dropped significantly when the air void content went below 5 percent. Therefore, it appears that the most important consequence of low VMA or film thickness for this fine-graded mixture was loss of stability and accelerated aging.

The lower VMA and film thickness of the C2 mixture resulted in a slightly stiffer and more brittle mixture than the C1 mixture. However, the differences were relatively small and the C2 mixture still exhibited higher failure strain and fracture energy than the best fine-graded mixture (F1). In addition, as illustrated in Figures 5-7 and 5-8 and Table 5-2, none of the coarse-graded mixtures became unstable at low air voids and all had comparably high shear strengths.

Mixtures C3 and C4/F3 were significantly stiffer and more brittle than the other mixtures. Mixture C4/F3 was particularly poor, even though its VMA was theoretically acceptable at 14 and all other SuperPave™ requirements were met as well. However, both of these mixtures had relatively low film thickness, relatively high dust-to-asphalt ratios (1.18 and 1.04, respectively) and high permeability, which indicate an unfavorable void structure for cracking resistance. It should be noted that these mixtures had the highest percentages of fine aggregates of all four coarse-graded mixtures. In addition, the gradation curves shown in Figure 3-1 show that the C4/F3 mixture and the C3 mixture, to a lesser extent, had a different type of gradation curve than either the C1 or the C2 mixtures. These factors appear to be more important than the VMA or film thickness on the performance of these mixtures.

In all, the binder and mixture test results appear to suggest that coarse and fine mixtures need to be evaluated in different ways. The percent fine aggregates (% FA) in

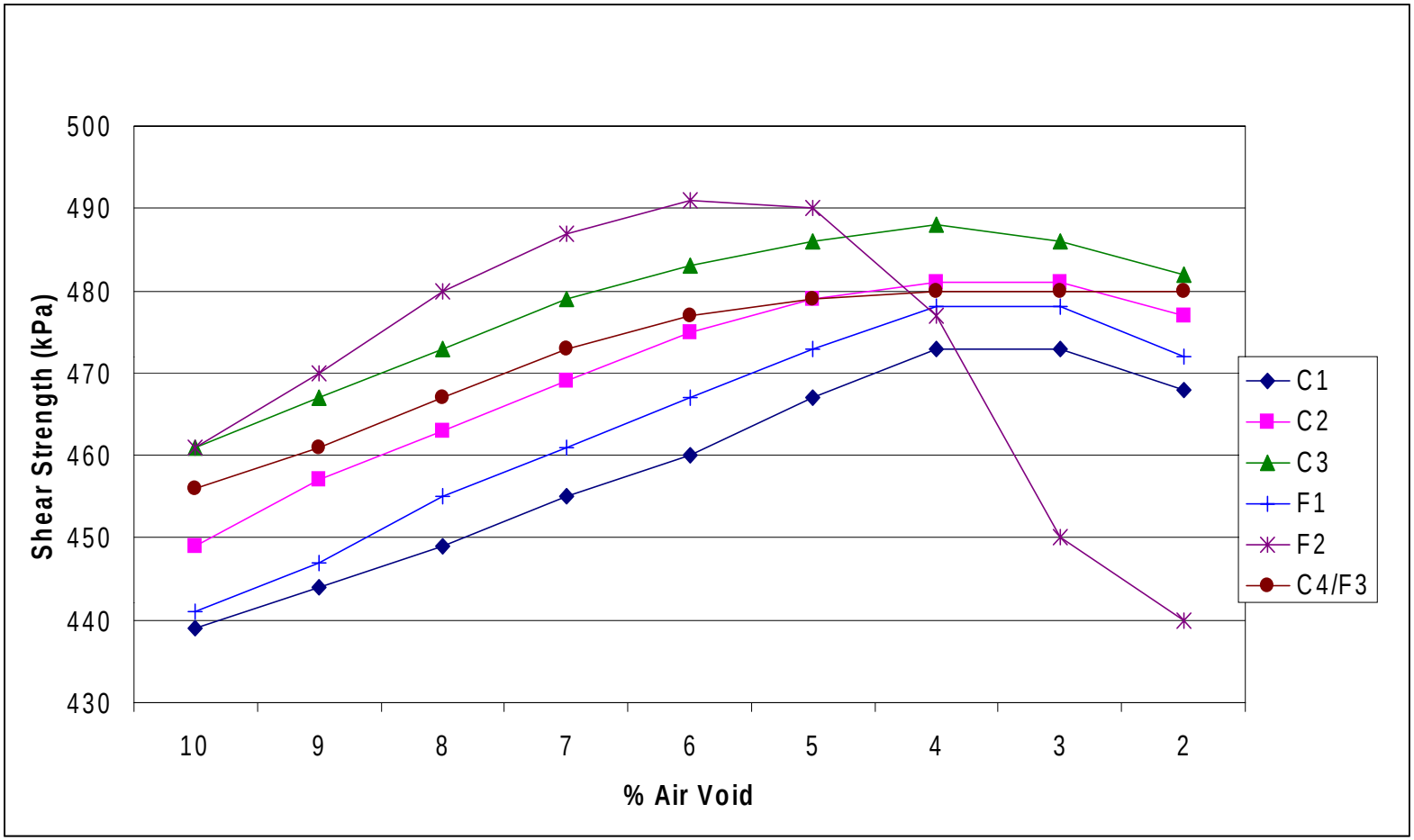

Figure 5-7 Shear Resistance as Measured by the Servopac SuperPave™ Gyratory Compactor (SGC) at 1.25 Degrees

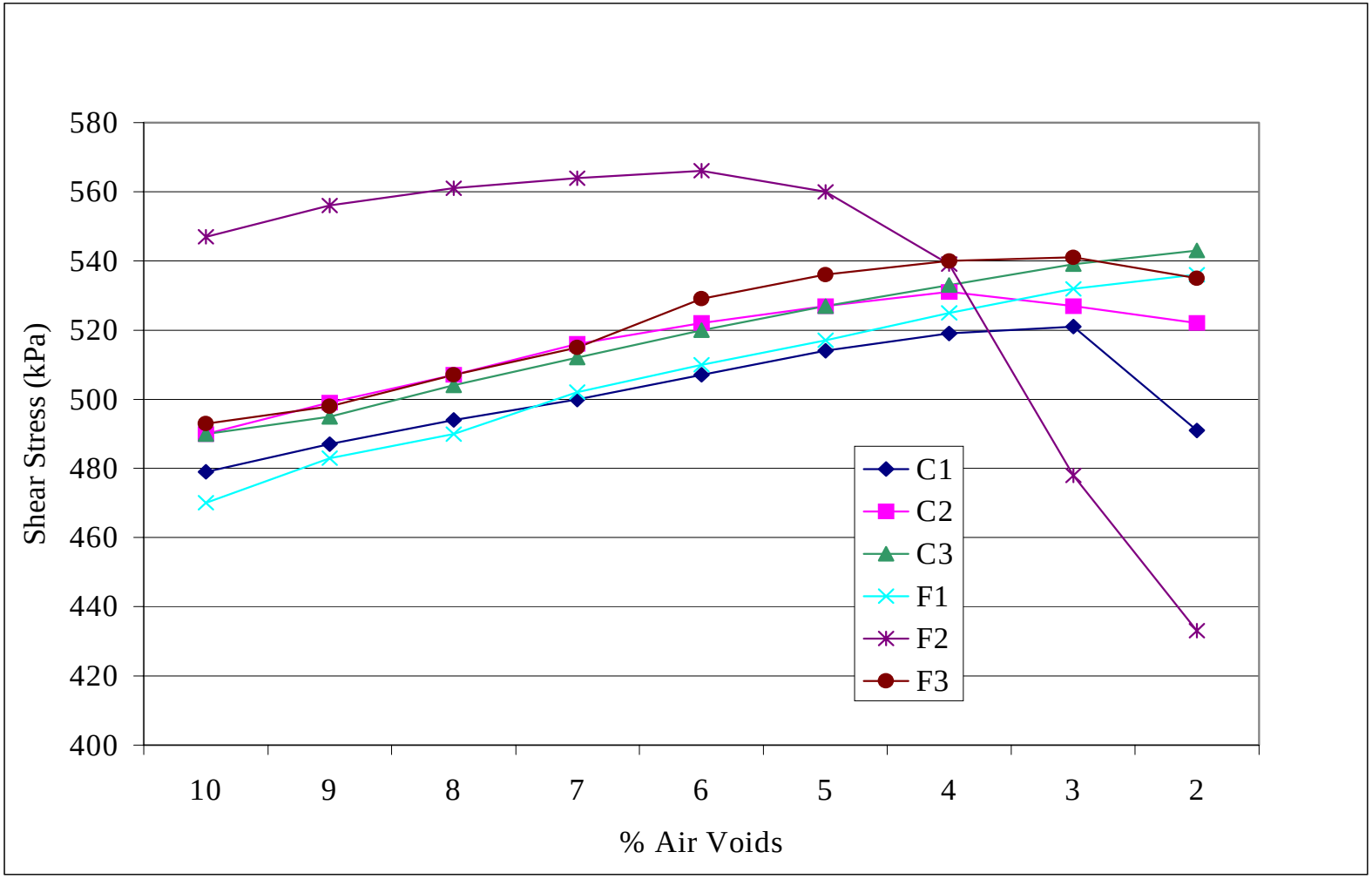

Figure 5-8 Shear Resistance as Measured by the Servopac SuperPave™ Gyratory Compactor (SGC) at 2.5 Degrees

Table 5-2 Summary of Results

		Mixture					
Property	units	**F1**	**F2**	**C1**	**C2**	**C3**	**C4/F3**
VMA		15.6	13.2	15.4	13.8	13.6	14
Film Thickness	microns	9	6.9	11.2	10.1	8	8.1
Dust/Asphalt Ratio	%	0.76	1.16	0.74	0.83	1.18	1.04
% Fine Aggregate	%	52.7	44.1	33.1	29.6	36.4	36.6
Permeability, k	10e-5cm/s	17.8	9.7	72.4	24.1	69.2	69.6
Relative Binder Age Hardening		High	High	Low	Low	Low	Low
G* (LTOA)	MPa	11.4	11.5	8.3	8.1	9.2	9.4
ε_f (STOA)	microstrain	2920	3715	4630	3771	2174	2419
ε_f (LTOA)	microstrain	1833	1526	2224	1897	1468	1175
% Decrease	%	37	59	52	50	32	51
Fracture Energy FE (STOA)	kJ/m^3	4.2	5.4	5.8	4.8	3.5	3.7
Fracture Energy FE (LTOA)	kJ/m^3	2.8	3.2	3.5	2.9	2.7	1.7
% Decrease	%	33	41	40	40	23	54
Resilient Modulus, M_R (STOA)	Gpa	9.5	8.6	7.9	7.7	11.5	12
Resilient Modulus, M_R (LTOA)	Gpa	9.9	12.9	9.6	11.9	14.2	13.9
% Increase	%	4	50	22	55	23	16
m-value (STOA)		0.6560	0.5649	0.7961	0.7729	0.6563	0.5817
m-value (LTOA)		0.5726	0.4955	0.5480	0.5856	0.4977	0.5039
% Decrease	%	13	12	31	24	24	13
Creep Compliance, D_{1000} (STOA)	1/Gpa	7.9	6	13.9	15.1	7.6	6.3
Creep Compliance, D_{1000} (LTOA)	1/Gpa	4.5	1.9	4.5	2.8	2.2	1.9
% Decrease	%	43	68	68	81	71	70
Tensile Strength, S_t (STOA)	MPa	2.1	1.9	1.6	1.7	2.1	2
Tensile Strength, S_t (LTOA)	MPa	2.1	2.6	2.1	2.1	2.4	2.2
% Increase	%	0	37	31	24	14	10
Gyratory Shear, G_s @ 3% Air Void (1.25^o)	kPa	477	450	473	482	486	480
% Max G_s	%	100	93	100	100	100	100
Gyratory Shear, G_s @ 3% Air Void (2.5^o)	kPa	530	480	520	523	540	540
% Max G_s	%	100	85	100	100	100	100

the mixture appears to play a critical role on the rate of binder age-hardening. Fine graded SuperPave™ mixtures (higher % FA, above the SuperPave™ restricted zone) result in much higher binder age-hardening than coarse-graded mixtures (lower % FA, below the SuperPave™ restricted zone), regardless of VMA, film thickness, permeability, or any other volumetric parameter. It appears that key differences in aggregate structure exist between mixtures above and below the restricted zone that affect the effective film thickness and permeability (void structure) of the mixtures. Therefore, it may be helpful

to examine the effects of volumetric changes (e.g., VMA) on mixture properties separately for fine-graded and coarse-graded mixtures.

5.2.1 Fine-Graded Mixtures

The VMA of the standard SuperPave™ fine-graded mixture was reduced in two ways. It was found that lower VMA could only be achieved by producing a very dense-graded mixture either by increasing the amount of coarse aggregate to make it denser, or by reducing the amount of fine aggregates to make it denser. Attempts to densify by reducing the fine aggregates reduced the VMA to 14, but the fine aggregate had to be graded below the restricted zone, which made it a fourth coarse-graded mixture (C4), as well as the third modified fine-graded-mixture (F3). Hence, the designation C4/F3. This resulted in a discontinuous gradation curve. Comparing the age-hardening and mixture properties of these two F1 derivatives to F1 in Table 5-2, it can be seen that the dense F2 had low film thickness, high dust-to-asphalt ratio and very low permeability, which implied a better void structure. Thus, cracking was not a problem as measured by the fracture energy density even though film thickness was low. However, the mixture F2 became unstable at low air voids in gyratory shear.

Mixture C4/F3 also had a lower VMA, lower film thickness, increased dust-to-asphalt ratio and much higher permeability, implying a poor void structure. The poor void structure combined with the low film thickness led to lower fracture energy density. However, the mixture had very high resistance to shear. Thus, reduction in VMA for the fine-graded mixtures resulted in poor consequences, but for different reasons, and different failure mechanisms.

5.2.2 Coarse Mixtures

The VMA of the standard SuperPave™ coarse-graded was also reduced in two ways. Increasing the coarse aggregates resulted a denser mixture C2, which had a lower film thickness, slightly higher dust-asphalt-ratio, and a lower permeability, which implied a better void structure. However, its lower VMA and film thickness did not appear to adversely affect its rutting and cracking performance. In addition, its binder age-hardening and mixture properties were similar to that of C1, even though the mixture was slightly stiffer. All the same, these two mixtures had the lowest resistance to shear. This may be attributed their high asphalt content as shown by their effective film thickness and effective VMA values.

Densifying by increasing the amount of fine aggregates resulted in low VMA mixture C3. The result was lower film thickness, increased dust-to-asphalt ratio and high permeability. Thus, it also had a poor void structure coupled with low film thickness. However, its fracture energy was comparable to that of F1, which was the best fine-graded mixture. C3 was similar to C4/F3 in binder aging, but its fracture resistance was somewhat better. It appears that the discontinuous grading of the C4/F3 mixture, which had 29.9% material between the number 4 and number 8 sieves resulted in an unfavorable aggregate structure, which may result in poor fracture resistance. It should be noted that the C4/F3 mixture met all SuperPave™ requirements including VMA, while C2 and C3 mixtures did not. However these mixtures performed very well in shear. Since their fracture resistance was comparable to that of the best fine mixtures, they can be considered as good performance mixtures with a reasonable fracture resistance and superior rutting performance than their C1 and C2 counterparts.

Even with these above conclusions, it is clear that there is a lot more going on within these mixtures than meets the eye. For example, some of the mixture properties do not seem to correlate with the volumetric properties or binder aging. Some have to split into coarse and fine categories for the relationships to come out. This observed phenomenon can be attributed the aggregate gradation or aggregate structure, the different degrees of aging of binder or simply experimental error.

More tests must therefore be performed using different material, aggregates and gradations. Performing more experiments and having more data points is expected to clear up some of the discrepancies that existed in the results and arrive at a more concrete conclusion.

Definitely, a mixture with good gradation could resist both rutting and cracking. But still a good binder is needed in order to control age-hardening of the whole mixture during its lifetime. The results show that even mixtures with gradations or aggregate structures that resist binder aging must also lose some of their fracture resistant characteristics after aging. Thus, mixture design must focus on more than just the volumetric properties since a good mixture must have a good gradation, aggregate structure and aging resistant binder. This gives enough reason to further research effects of aggregate gradation and aggregate type. The next section of this research focuses on new mixtures that were designed with emphasis on aggregate type and gradation instead the volumetric properties such as VMA and film thickness.

CHAPTER 6
FURTHER TESTING OF DIFFERENT AGGREGATE TYPES AND GRADATIONS

6.1 Introduction

Based on the conclusions presented in Chapter 5, it was evident that additional research was needed to address the question of gradation and aggregate type. Therefore, more mixtures were designed with whiterock materials, while another set of mixtures was designed with Georgia granite aggregates to evaluate the effect of aggregate type and gradation. The granite mixtures were 9.5-mm nominal sieve size gradations. The additional experiments were designed to clear up some of the remaining uncertainties so that clearer conclusions and recommendations could be made.

The investigation focused on the effects of gradation, aggregate type and binder age-hardening on mixture performance. Research presented in earlier chapters indicated that the influence of gradation on binder age-hardening was clearly understood. Therefore, additional work focused on effects of extreme gradations (e.g., gap-grading and very dense-grading), and using different aggregate types with varying properties. The basis for expanding the research study was to:

- Evaluate the SuperPave™ restricted zone as a guideline to separate fine-graded and coarse-graded mixtures.
- Further evaluate the effects of aggregate type and gradation (i.e., continuous, gap-graded or mixtures with little or too much material retained on any one sieve size) on mixture response and performance.
- Evaluate the effects of volumetric properties and their effects on the behavior and performance of SuperPave™ asphalt paving mixtures such as resistance to fatigue cracking and rutting.
- Provide recommendations with regards to whether coarse-graded and fine-graded mixtures need to be designed and analyzed separately and whether these mixtures react differently to change in binder properties.

6.2 Research Plan for Further Testing

As discussed earlier, this phase of the research was done by testing new mixtures. The mixtures used are described in the following paragraphs under the following headings.

6.2.1 Coarse-Graded Mixtures

Among the coarse mixtures, it was observed, as in C3, that changing the gradation of C1 by a small increase in the amount of fines decreased the effective VMA and effective film thickness by about 10 percent. But the values were still greater that for the fine mixtures. However, changing the gradation on the coarse side only changed the effective VMA and the effective film thickness values a little. This was not so for the mixture properties. The fracture energy dropped when the mixture became more open-graded and when the fines content was increased slightly. However, aggregate structures may have been similar since an extreme open-graded mixture was not investigated previously.

Thus, the following change was made for a new open-graded coarse mixture C5 (see Figure 6-1 and Table 6-1) along the following lines.

- Dramatic change in the gradation of the coarse aggregate portion of mixture C1
- Use open-grading, i.e., little (15%) material between 2.36 mm and 4.75-mm sieve sizes and 45 % material between 4.75 mm and 9.5 mm
- Maintain low percent fine aggregate as in C1.

That was done to throw more light on the effects of gradation on the behavior of coarse mixtures.

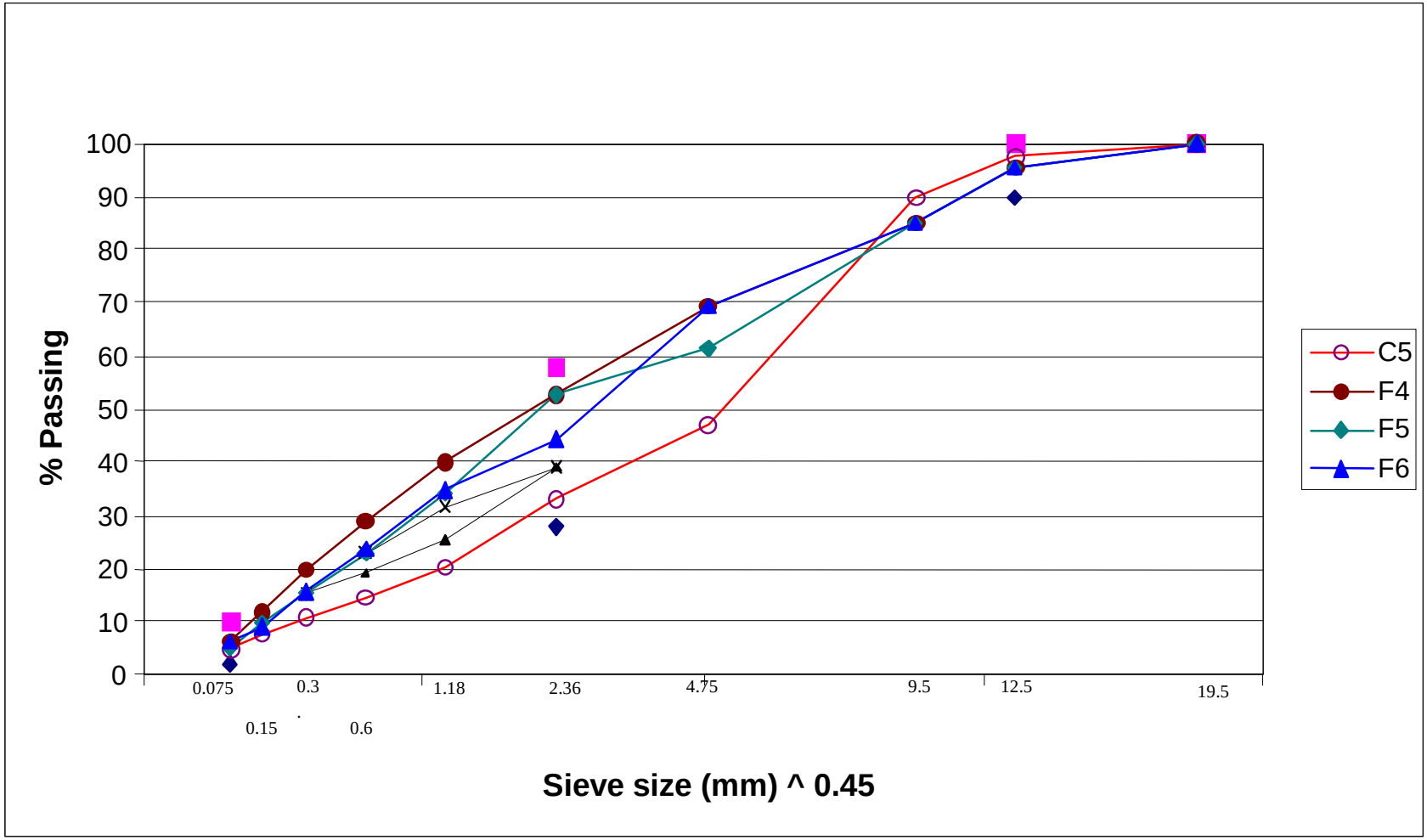

Figure 6-1 Gradations for New Whiterock Mixtures

Table 6-1 Gradations for New Whiterock and Georgia Ruby Granite Mixtures

Sieve Size mm	C5	F4	F5	F6	GAC1	GAC2	GAF1
25(1")	100.0	100.0	100.0	100.0	100.0	100.0	100.0
19(3/4")	100.0	100.0	100.0	100.0	100.0	100.0	100.0
12.5(1/2")	97.4	95.5	95.5	95.5	100.0	100.0	100.0
9.5(3/8")	89.9	85.1	85.1	85.1	99.2	99.3	99.9
4.75(#4)	47.1	69.3	61.3	69.3	54.8	57.9	86.5
2.36(#8)	33.1	52.7	52.7	44.1	32.2	34.3	63.2
1.18(#16)	20.3	40.0	34.0	34.7	18.5	20.4	43.0
0.6(#30)	14.7	29.0	22.9	23.6	14.5	15.6	30.3
0.3(#50)	10.8	20.0	15.3	15.7	9.8	10.3	22.1
0.15(#100)	7.6	12.0	9.6	9.1	6.6	6.8	9.8
0.075(#200)	4.8	6.3	4.8	6.3	3.3	3.4	4.5

6.2.2 Fine-Graded Mixtures

The result of open-grading of fine mixtures was not investigated previously. The only open-graded fine mixture was C4/F3, which was obtained by decreasing the amount of fines in the F1 mixture and grading below the restricted zone. However, C4/F3 was essentially a coarse mixture (below the restricted zone), therefore there was the need to further investigate open-graded fine mixtures without grading below the restricted zone. Changing the coarse part of F1 mixture led to a low VMA mixture F2 which became unstable in shear at low air void contents. The result of gap grading and the high fine aggregate content in mixtures needed further studying of the effects these changes may have on fine mixtures. Therefore, the following changes were made to arrive at new fine-graded mixtures F4, F5 and F6 (see Figure 6-1 and Table 6-1).

- Increase fine aggregate amount on sieves smaller than 2.36 mm (#8) of F1 to get a very dense-graded mixture F4.
- Gap-grading of mixture F1 by reducing material retained on 2.36-mm sieve to less than 10% (17% in F1) and increasing material retained on 4.75-mm sieve from 15% in F1 to 25%. This resulted in a more open-graded mixture F5 (see Figure 6-1 and Table 6-1).

- Gap grading of mixture F1 by reducing material retained on 1.18-mm sieve to less than 10% (20% in F1) and increasing material retained on 2.38-mm sieve from 17% in F1 to 27%. This resulted in a more open-graded mixture F6 (see Figure 6-1 and Table 6-1).

6.3 Aggregate Type Analysis

Next, was to follow with selected changes in aggregate type with more emphasis on the fine portion. Fine aggregates have been identified as a potential source for unique mixture behavior. This stems from the fact that fine aggregates, depending on their FAA or shear strength (from direct shear tests) significantly affect the volumetric properties and performance of the mixtures. It is therefore important to investigate the effects of these fine aggregates on binder aging and fracture resistance.

Georgia Ruby granite mixtures were designed and produced for this purpose. GAC2 is a purely granite (#89 stone and W-10 screens) mixture, while GAC1 is a combination of granite and whiterock comprising #89 stone (Granite) and Anderson screens (whiterock). There is also a fine-graded mixture GAF1 comprising #89 stone, W-10 screens and Anderson screens. These mixtures were used to verify the effect of aggregate type on binder age-hardening and performance. The gradation for these mixtures is shown in Table 6-1 and Figure 6-2.

6.4 Results

The procedure for design and production of these mixtures was the same as those for the mixtures analyzed previously in Chapter 3. The mixtures in this section were analyzed together with all the other mixtures to give a clearer picture and understanding of all the results obtained in the entire research. The design properties of these mixtures, together with the previous ones in Tables 6-1, are shown in Table 6-2.

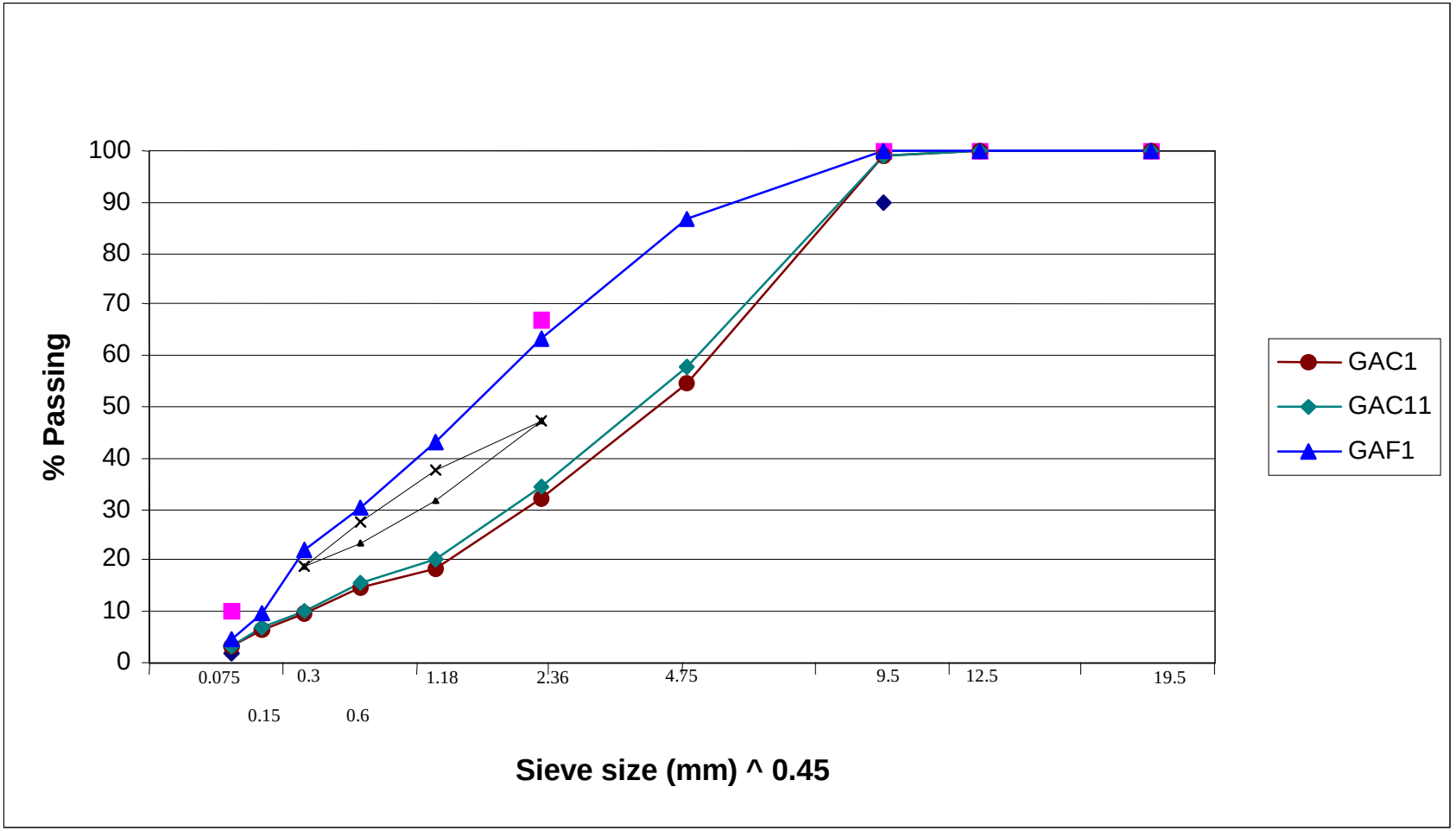

Figure 6-2 Gradations for 9.5-mm Granite Mixture

Table 6-2 Effective Volumetric Properties of All Mixtures

Mixture	%CA	%FA of Total Mix	%AC	VMA	Film thic. (um)	SA (m^2/kg)	Dust/AC Ratio
C1	66.9	30.9	17.4	35.4	39.2	4.20	0.28
C2	70.4	27.9	17.2	35.3	39.3	4.02	0.28
C3	63.6	34.5	13.3	30.4	24.1	5.16	0.47
C5	66.9	31.0	16.9	34.2	36.3	4.20	0.28
F1	47.3	49.4	11.3	25.7	19.3	5.36	0.42
F2	55.9	41.7	11.5	25.8	17.1	5.73	0.55
C4/F3	63.4	34.6	13.9	30.6	25.0	5.07	0.42
F4	47.3	49.7	10.3	23.4	13.2	6.69	0.61
F5	47.3	49.2	12.0	26.7	20.7	5.34	0.40
F6	36.8	41.4	12.8	28.8	20.9	5.76	0.49
GAC1	67.8	29.9	19.4	34.7	45.7	3.28	0.16
GAC2	65.7	32.3	15.0	34.4	44.9	3.43	0.22
GAF1	36.8	58.2	12.0	22.8	14.5	6.13	0.38

6.4.1 Binder Results for Whiterock Mixtures

Mixtures together with their effective volumetric properties are shown in Table 6-2 and their theoretical volumetric properties are shown in Table 6-3. The binder test results of all the mixtures are shown in Table 6-4. Plots showing the effective volumetric

Table 6-3 Properties of All Mixtures

Mixture	Gsb	MTD	%AC	VMA	Film thic. (um)	SA (m^2/kg)	Dust/AC Ratio
C1	2.469	2.3279	6.5	15.4	11.2	4.87	0.74
C2	2.465	2.3466	5.8	13.8	10.1	4.64	0.83
C3	2.474	2.3486	5.3	13.6	8.0	5.68	1.18
C5	2.467	2.3418	6.3	14.6	10.5	4.81	0.76
F1	2.478	2.3378	6.3	15.6	9.0	6.05	0.76
F2	2.489	2.3752	5.4	13.2	6.9	6.31	1.16
C4/F3	2.478	2.3466	5.6	14.0	8.1	5.64	1.04
F4	2.491	2.3677	5.7	14.0	6.3	7.40	1.11
F5	2.485	2.3264	6.7	16.2	9.7	6.02	0.72
F6	2.489	2.3412	6.1	15.4	8.2	6.48	0.97
GAC1	2.496	2.4254	7.1	13.3	11.3	3.93	0.38
GAC2	2.705	2.5225	5.7	15.7	12.6	4.09	0.58
GAF1	2.540	2.4134	7.9	16.0	8.1	6.91	0.57

Table 6-4 Binder Test Results

	STOA				LTOA				Gain			
Mixture	Pen	Viscosity (Poise)	G* (Pa)	Delta	Pen	Viscosity (Poise)	G* (Pa)	Delta	Pen	Viscosity (Poise)	G* (Pa)	Delta
C1	42	6435	7590700	48.4	39	11107	8257500	46.5	3	4672	666800	1.9
C2	40	8706	7390900	49.9	36	11750	8059000	48.0	4	3044	668100	1.9
C3	38	8064	7858300	47.9	32	11860	9225200	45.7	6	3796	1366900	2.2
C5	39	7520	7714000	48.0	33	11738	9099600	44.8	6	4217	1385600	3.2
F1	36	8965	9720500	47.5	28	16953	11424000	45.0	8	7988	1703500	2.5
F2	36	9650	9760900	46.2	26	18048	11491000	43.6	10	8398	1730100	2.6
C4/F3	38	7139	7796100	47.9	32	11721	9358600	45.5	6	4582	1562500	2.4
F4	34	9506	10928800	44.8	25	19204	11528900	43.3	9	9698	600100	1.5
F5	36	9769	9469900	46.3	29	13307	11269900	44.2	7	3538	1800000	2.1
F6	37	8926	9371200	47.4	30	12922	10942300	44.9	7	3995	1571100	2.5
GAC1	44	6136	6242000	52.4	39	11022	8134700	47.0	5	4886	1892700	5.4
GAC2	39	8873	7317500	50.4	34	12100	8944000	45.3	5	3227	1626500	5.1
GAF1	38	9206	7479500	50.1	33	13781	9052800	44.4	5	4575	1573300	5.7

properties and binder age-hardening are shown in Figures 6-3 to 6-6. The results show the relationships between the effective volumetric properties and the binder age hardening as measured by the penetration test, DSR and the viscosity test. Once again, the theoretical VMA and film thickness values did not relate to the binder age-hardening rates of asphalt mixtures, but the effective volumetric properties based on the fine aggregate portion of the mixtures (% < #8 sieve size) appeared to relate well to the binder age-hardening.

The model in Equation 6-1 was fitted to the binder data to identify a relation between mixture volumetric properties (e.g., VMA and film thickness and surface area) on binder age hardening using Microsoft Excel. This was only done for the ten limestone mixtures to limit variability in aggregate type. The traditional volumetric properties were used as the predictor variables in the first case, whereas the effective volumetric parameters were used in the second case.

$$Y = B_O x^{B_1} + \mathrm{E} \tag{6.1}$$

where Y = response variable (i.e., G*, viscosity, penetration or delta), x = predictor variable (i.e., VMA, film thickness or surface area), B_o and B_1 = unknown constant parameters and E is the error term. This provided a tool for using the volumetric properties to predict binder age-hardening by identifying the best model to fit the data. After trying a number of models, it was identified that the power model (Equation 6.1) provided the best fit for the data. Figures 6-7 to 6-24 show the trend lines of the fitted data. The actual measured raw lab data shown in Tables 6-5 to 6-8 were used. There were three replicates for G* and viscosity and five replicates for penetration.

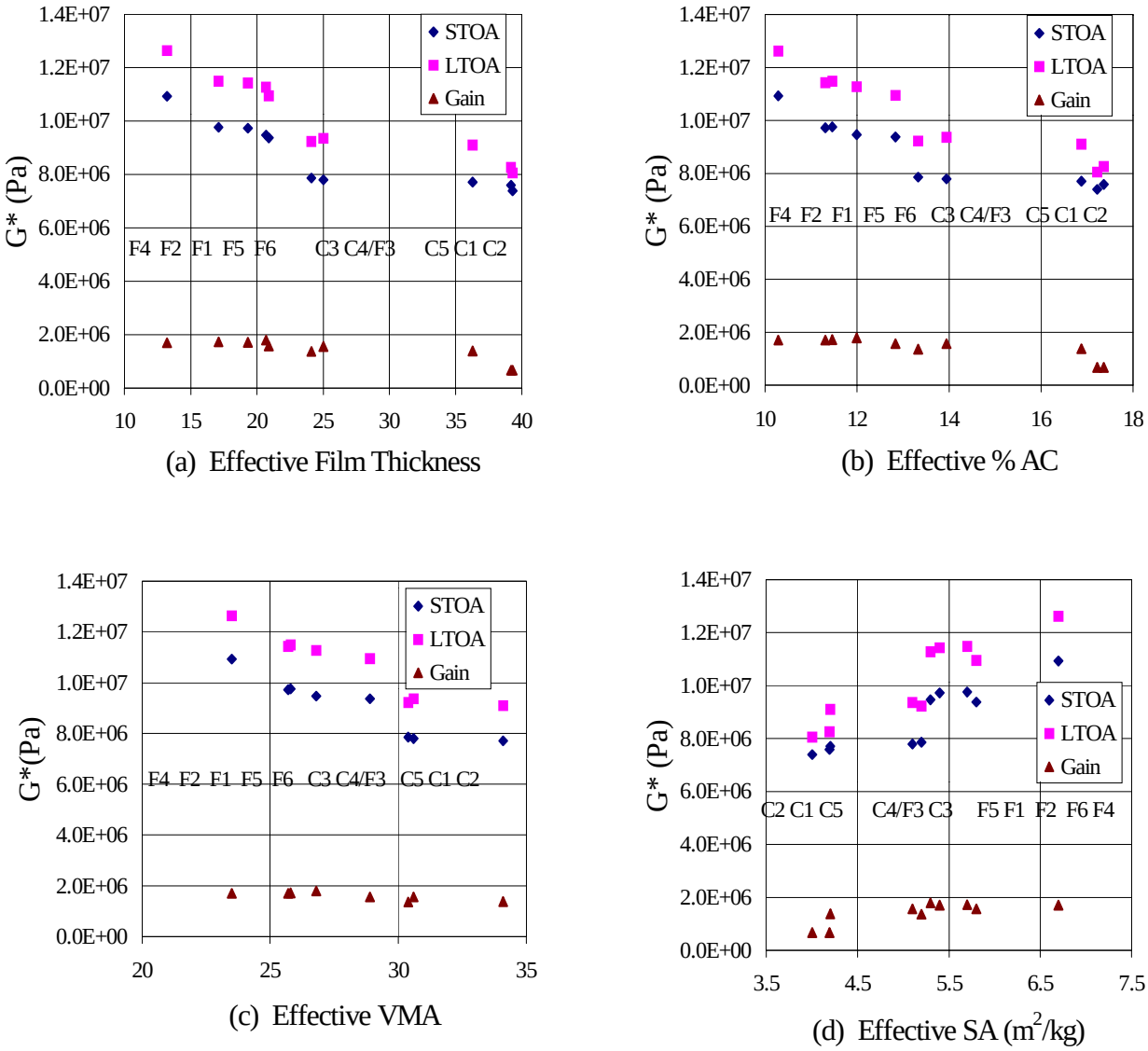

Figure 6-3 G* versus Effective Volumetric Properties

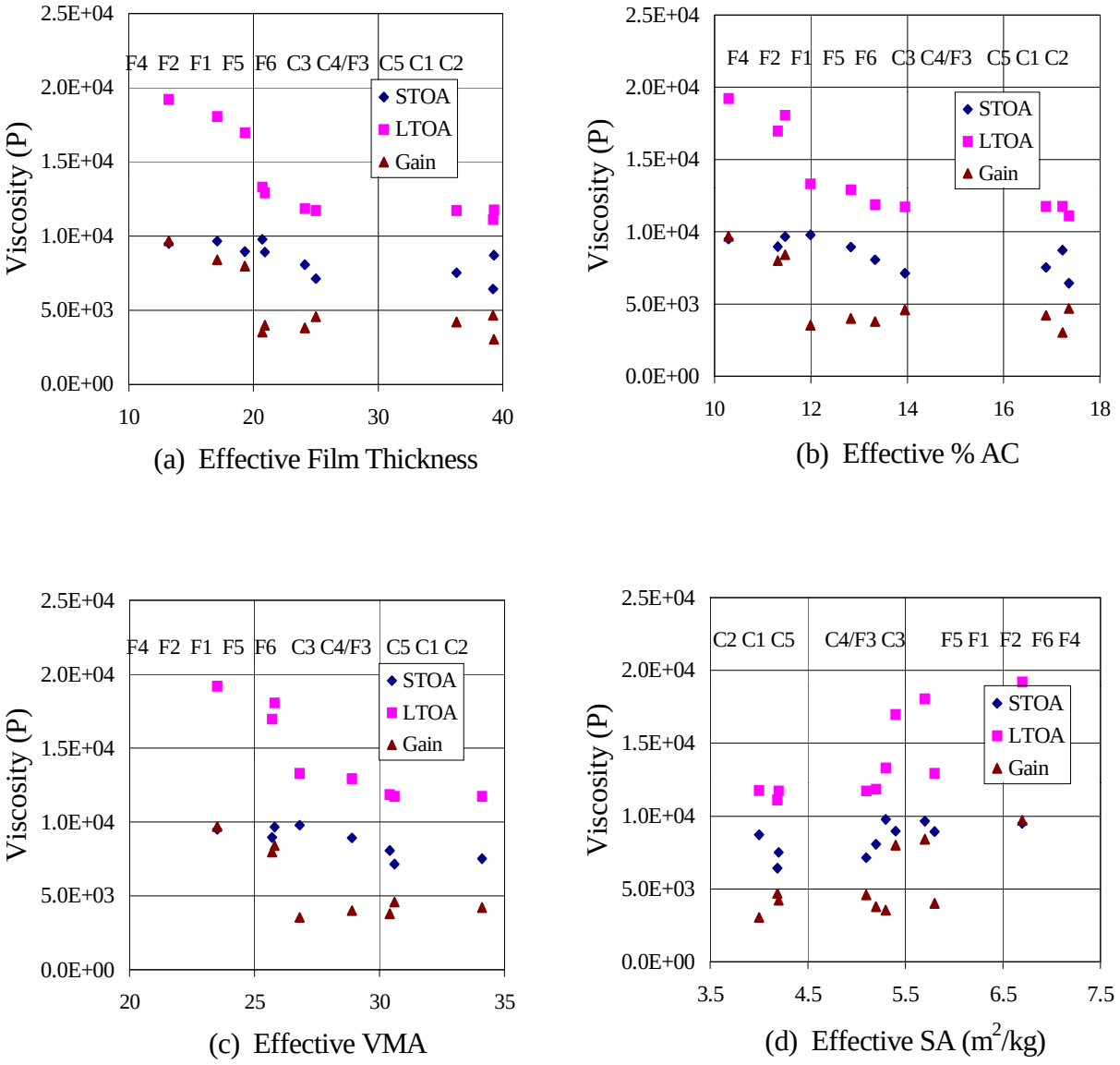

Figure 6-4 Viscosity Versus Effective Volumetric Properties

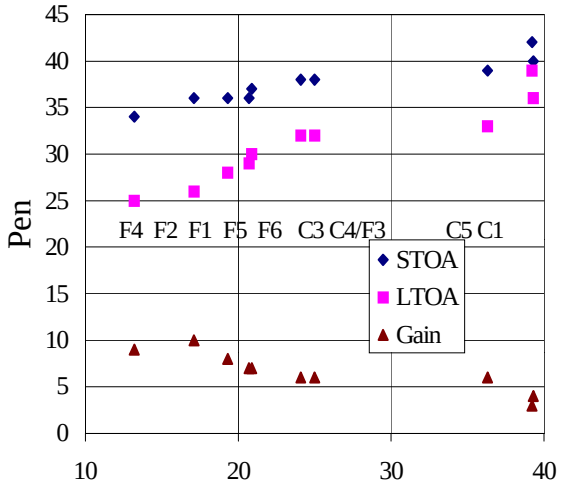

(a) Effective Film Thickness

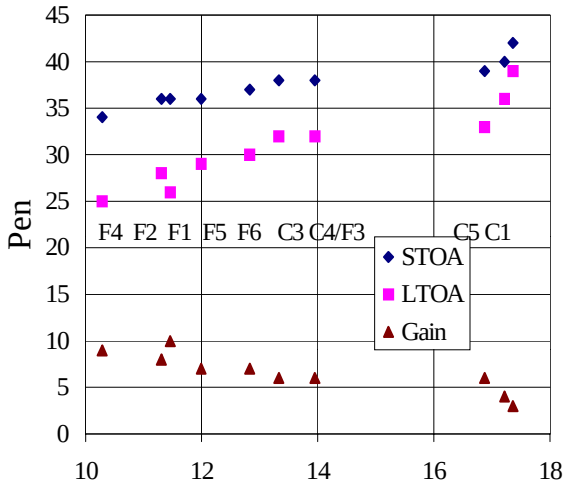

(b) Effective % AC

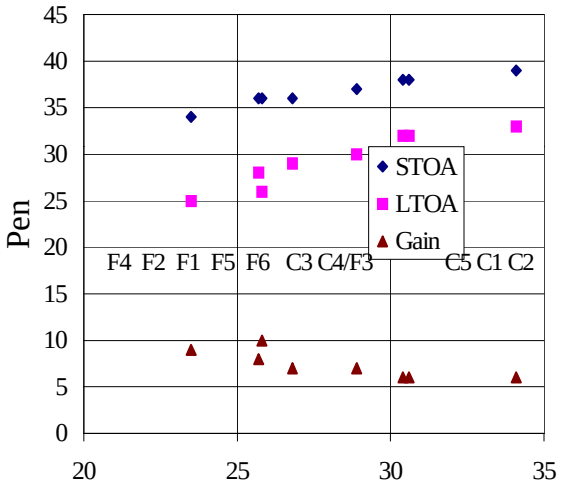

(c) Effective VMA

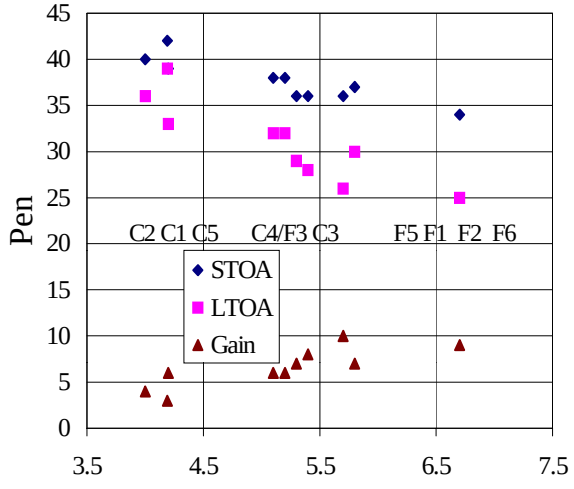

(d) Effective SA (m^2/kg)

Figure 6-5 Penetration Versus Effective Volumetric Properties

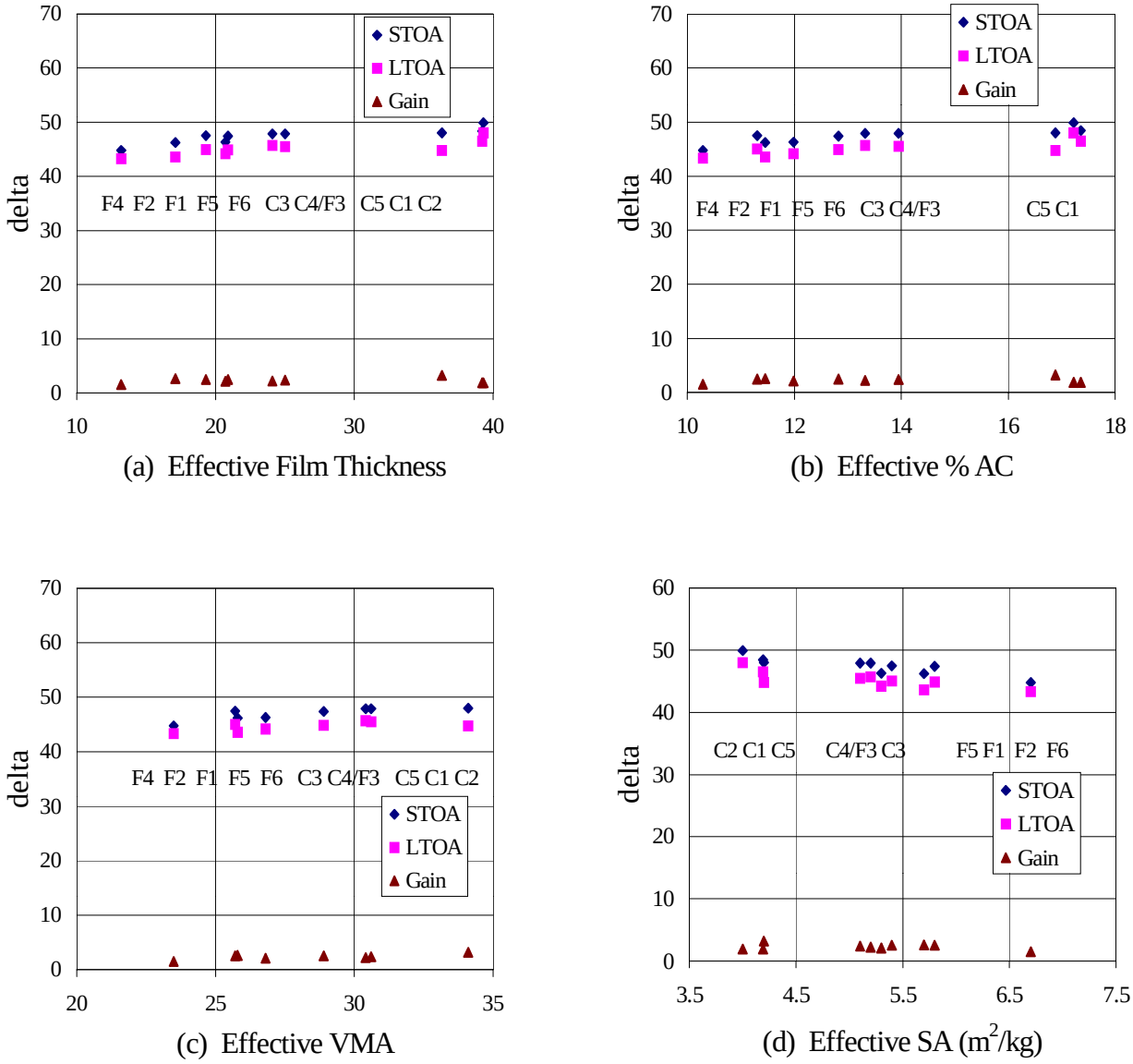

Figure 6-6 Delta Versus Effective Volumetric Properties

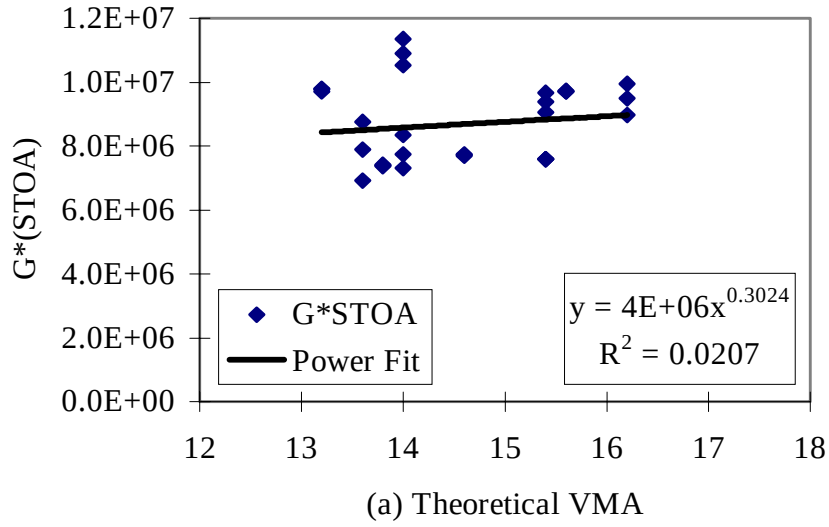

(a) Theoretical VMA

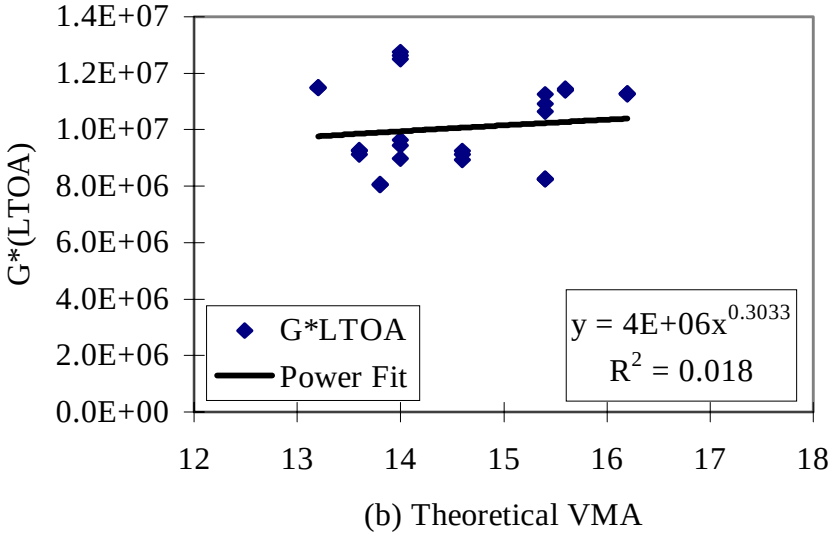

(b) Theoretical VMA

Figure 6-7 Effect of Theoretical VMA on G* After Short- and Long-Term Oven Aging

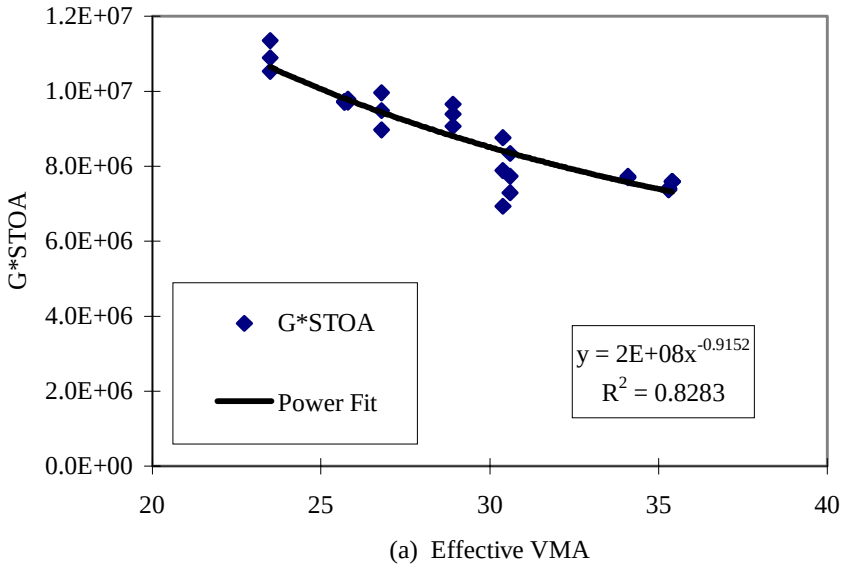

(a) Effective VMA

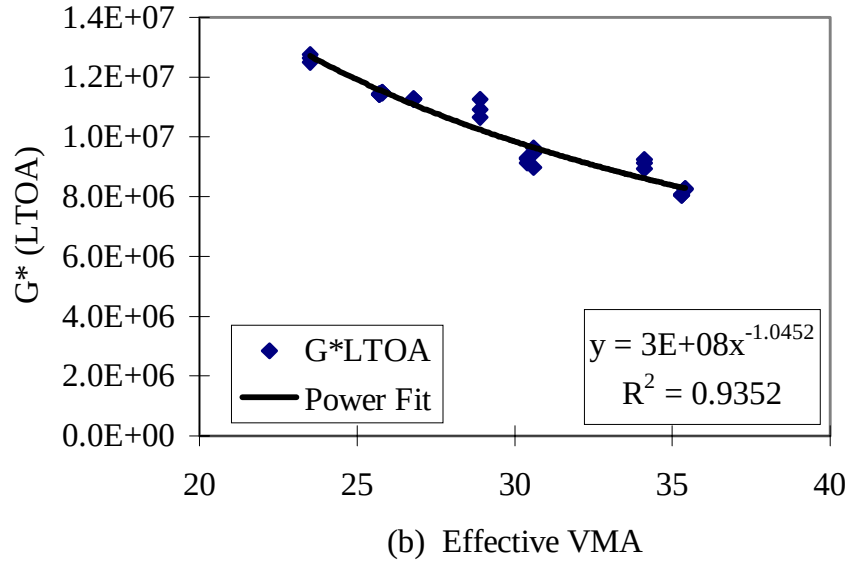

(b) Effective VMA

Figure 6-8 Effect of Effective VMA on G* After Short- and Long-Term Oven Aging

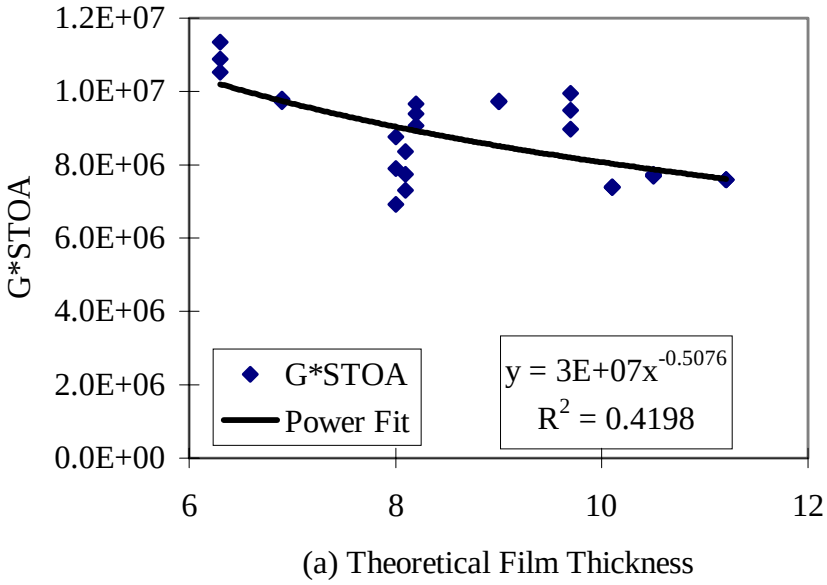

(a) Theoretical Film Thickness

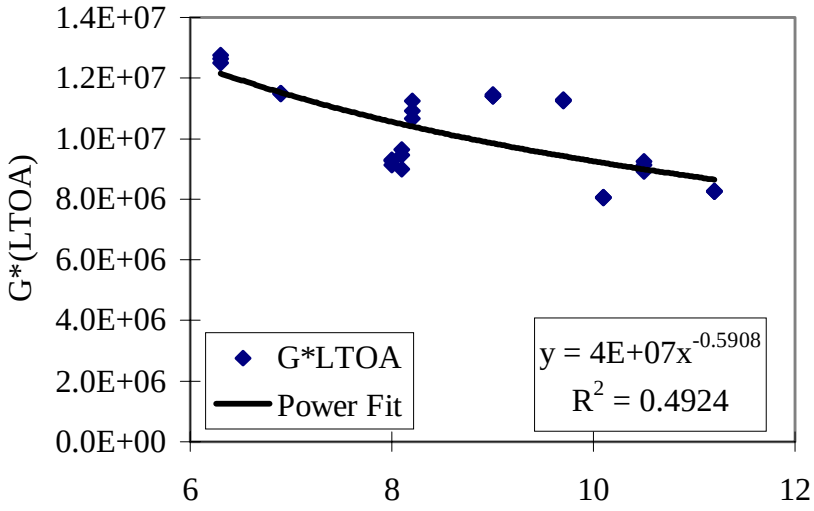

(b) Theoretical Film Thickness

Figure 6-9 Effect of Theoretical Film Thickness on G* after Short- and Long-Term Oven Aging

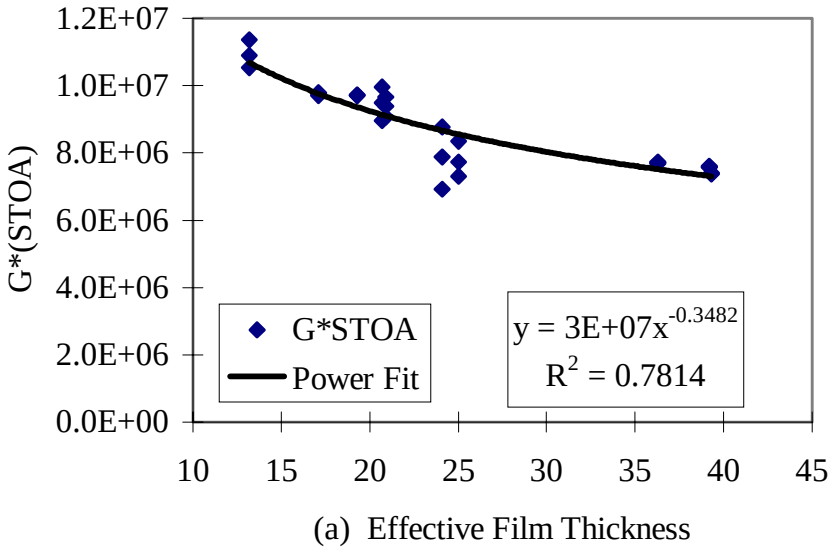

(a) Effective Film Thickness

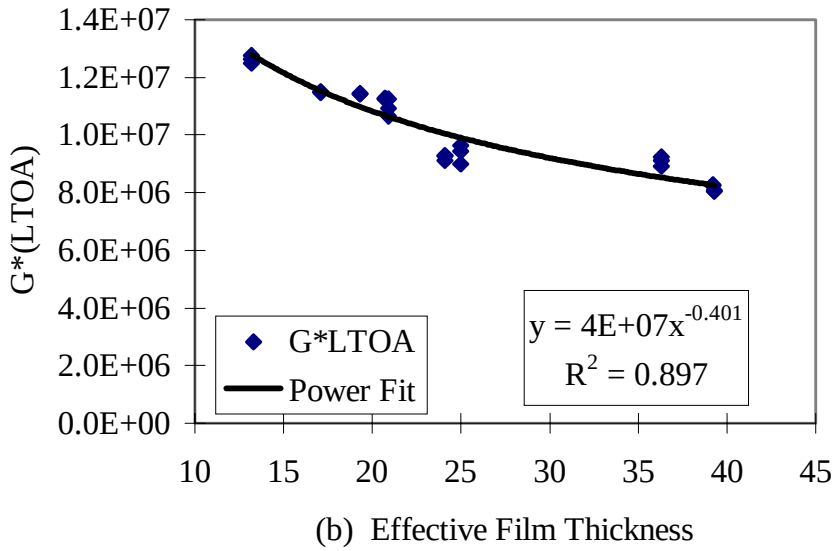

(b) Effective Film Thickness

Figure 6-10 Effect of Effective Film Thickness on G* After Short- and Long-Term Oven Aging

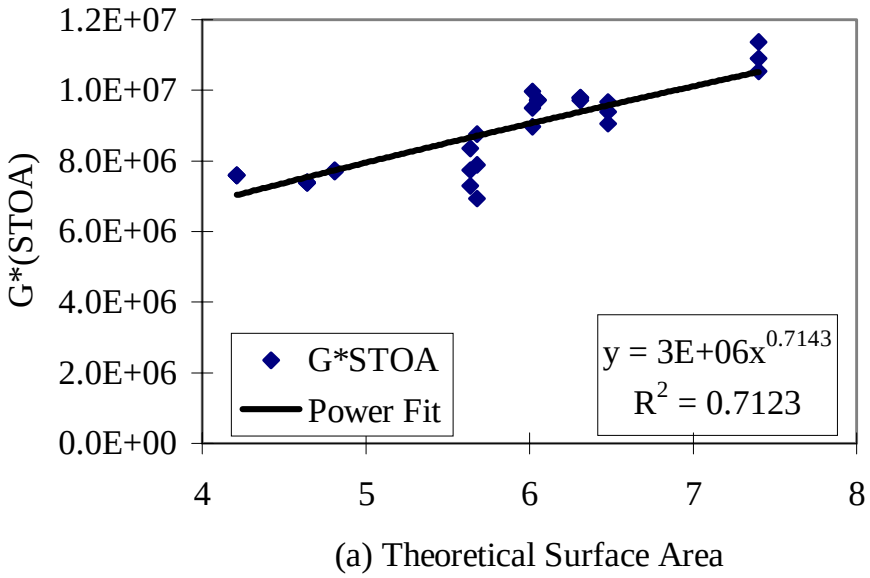

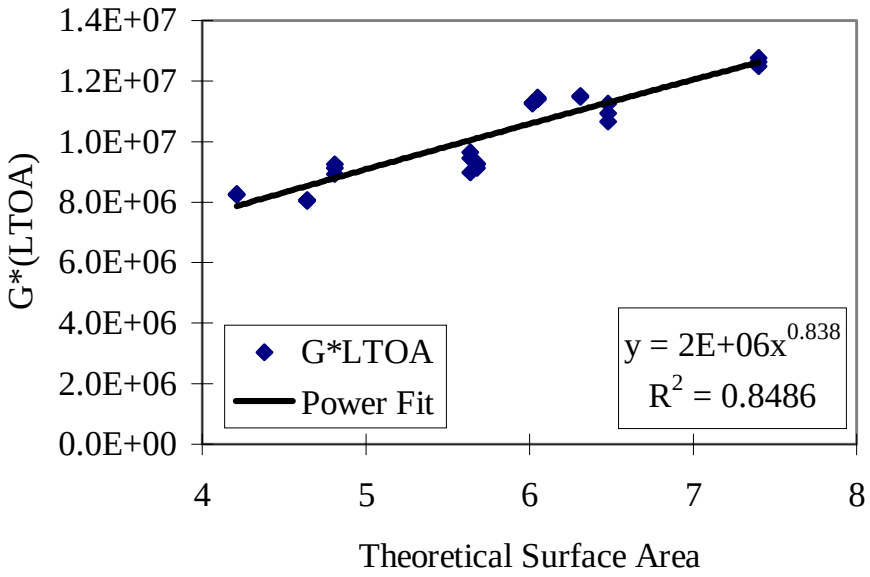

Figure 6-11 Effect of Theoretical Surface Area on G* After Short- and Long-Term Oven Aging

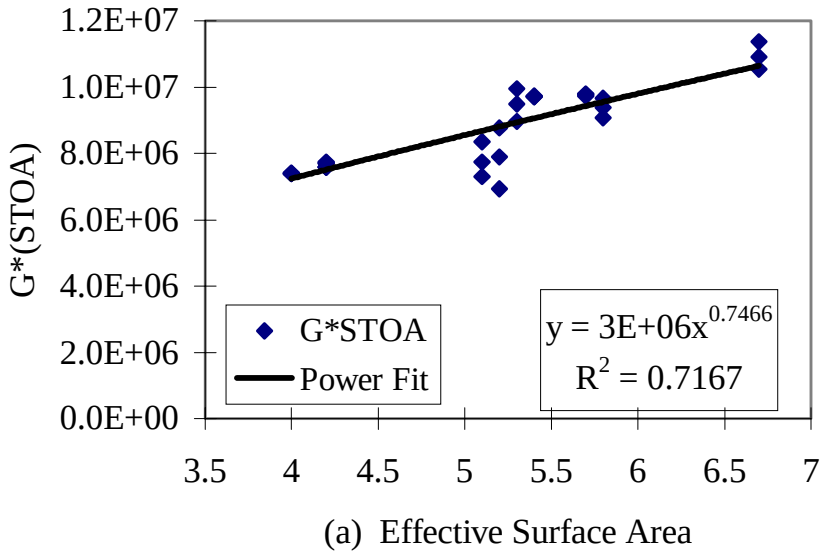

(a) Effective Surface Area

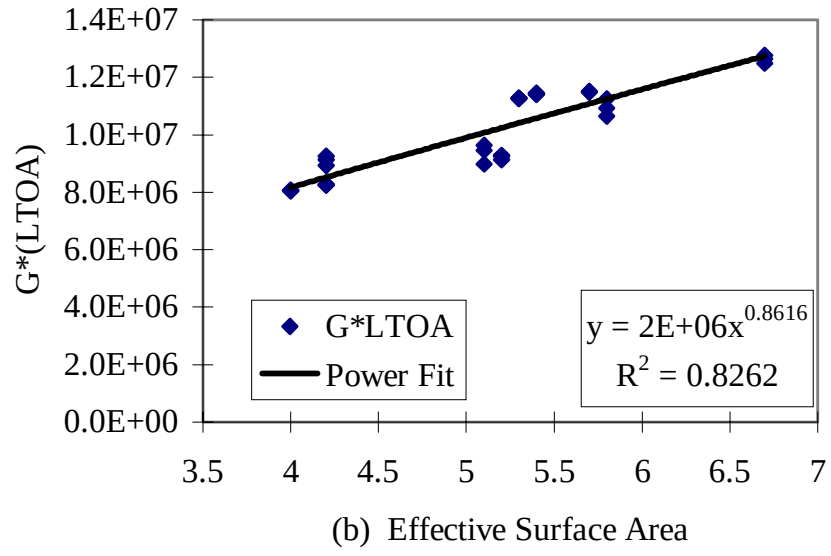

(b) Effective Surface Area

Figure 6-12 Effect of Effective Surface Area on G* After Short- and Long-Term Oven Aging

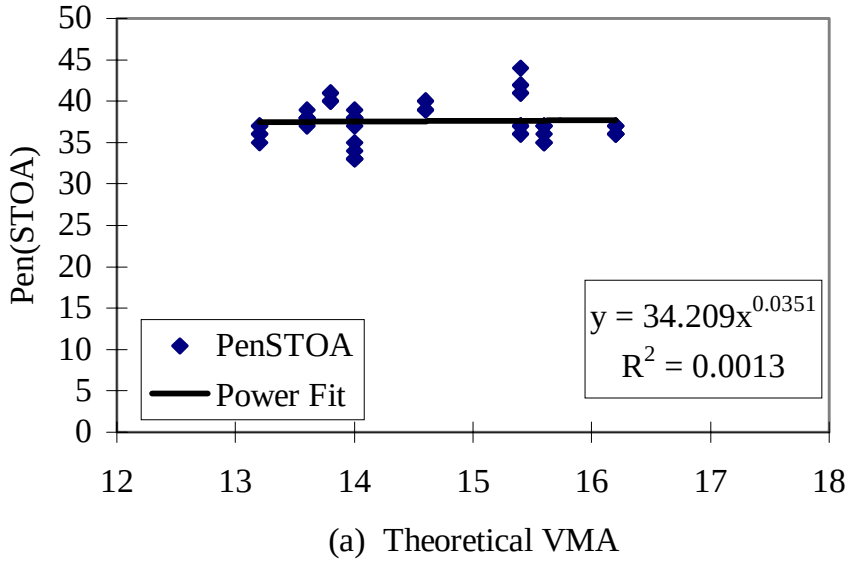

(a) Theoretical VMA

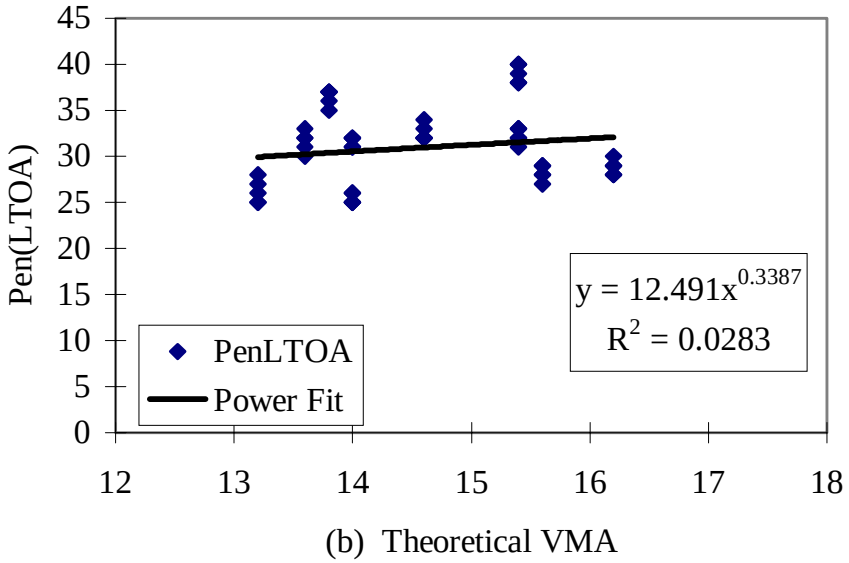

(b) Theoretical VMA

Figure 6-13 Effect of Theoretical VMA on Penetration After Short- and Long-Term Oven Aging

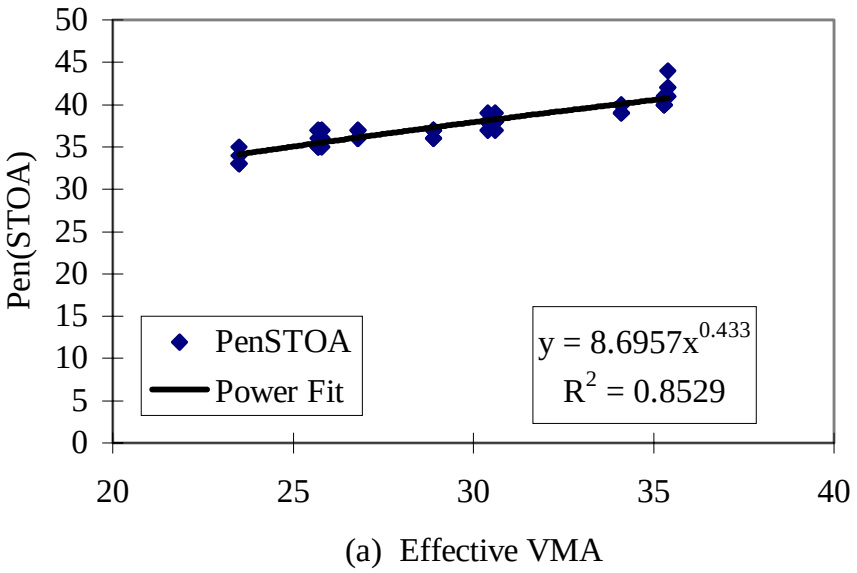

(a) Effective VMA

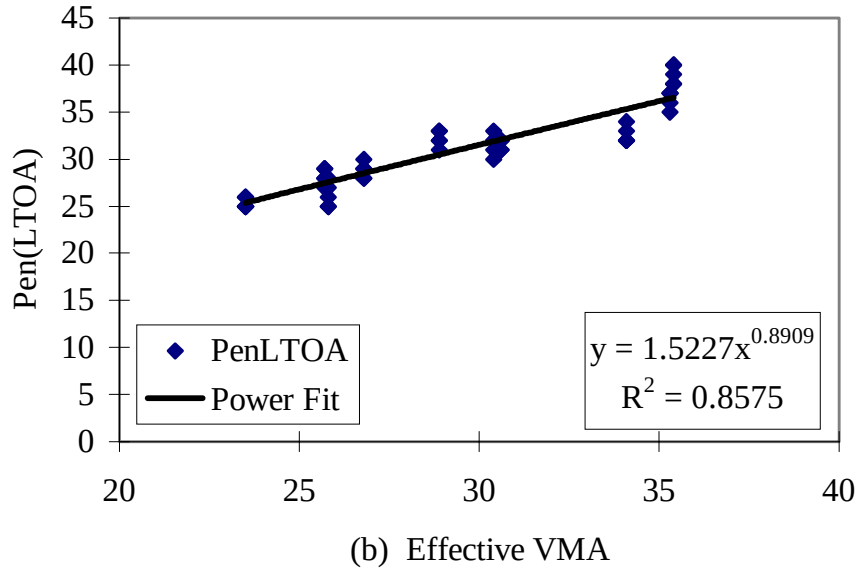

(b) Effective VMA

Figure 6-14 Effect of Effective VMA on Penetration After Short- and Long-Term Oven Aging

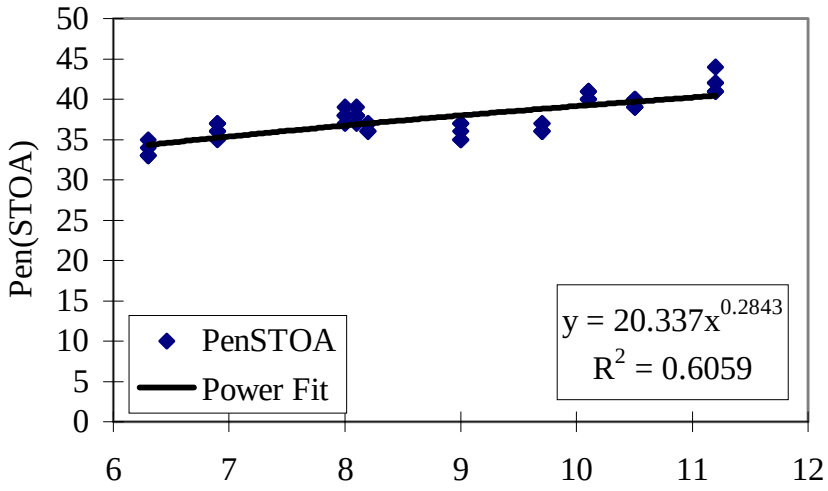

(a) Theoretical Film Thickness

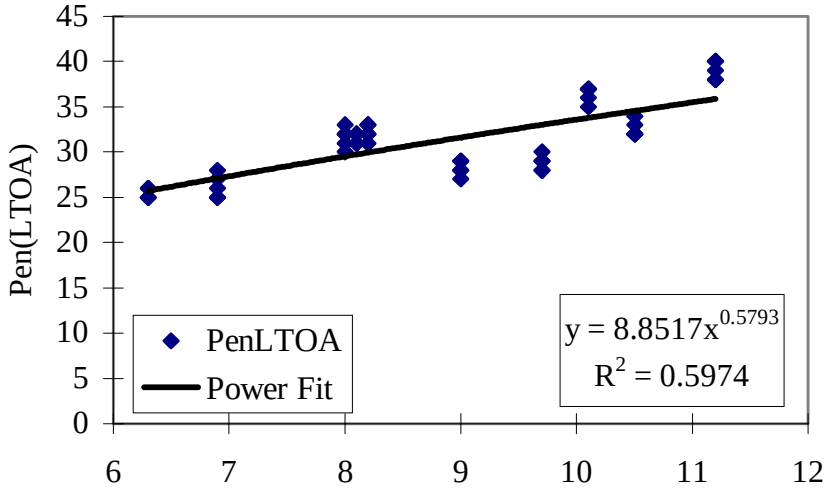

(b) Theoretical Film Thickness

Figure 6-15 Effect of Theoretical Film Thickness on Penetration After Short- and Long-Term Oven Aging

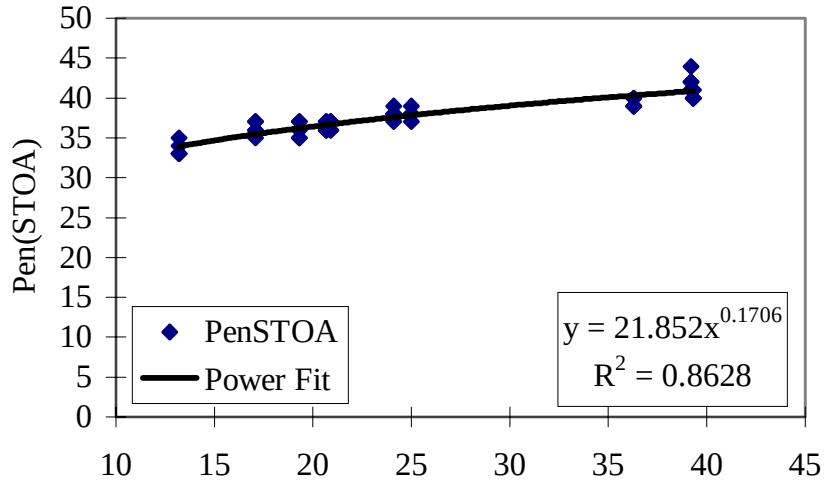

(a) Effective Film Thickness

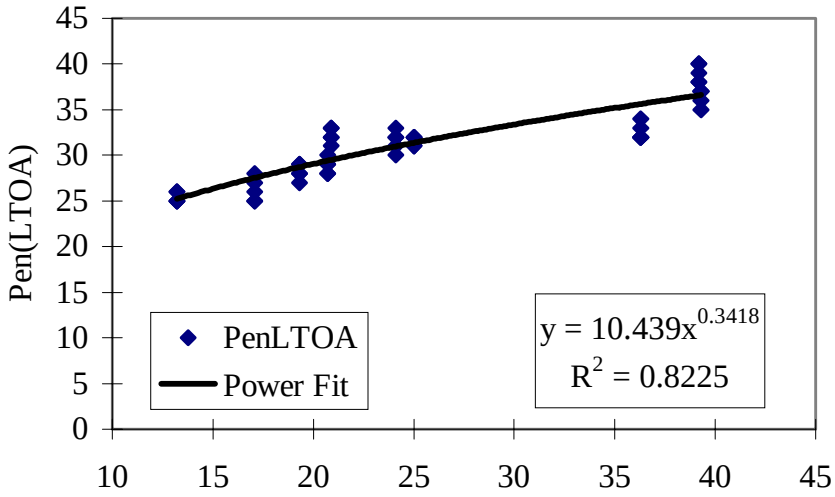

(b) Effective Film Thickness

Figure 6-16 Effect of Effective Film Thickness on Penetration after Short- and Long-Term Oven Aging

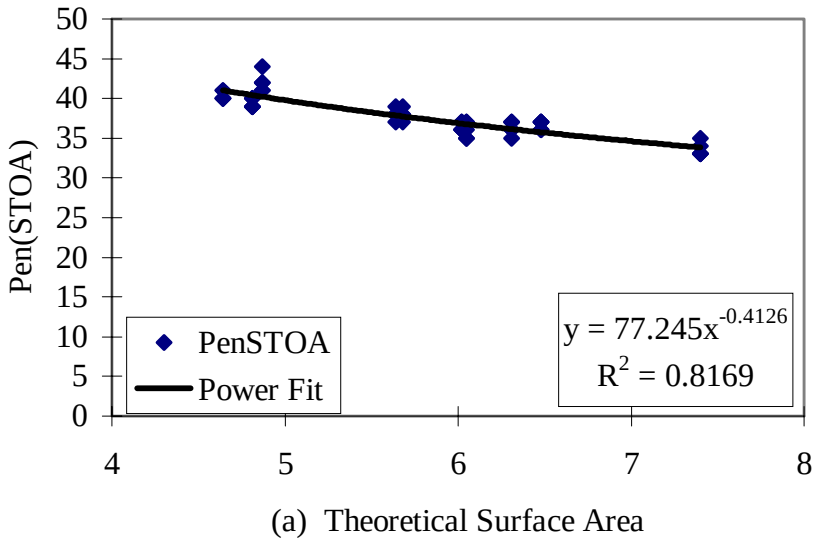

(a) Theoretical Surface Area

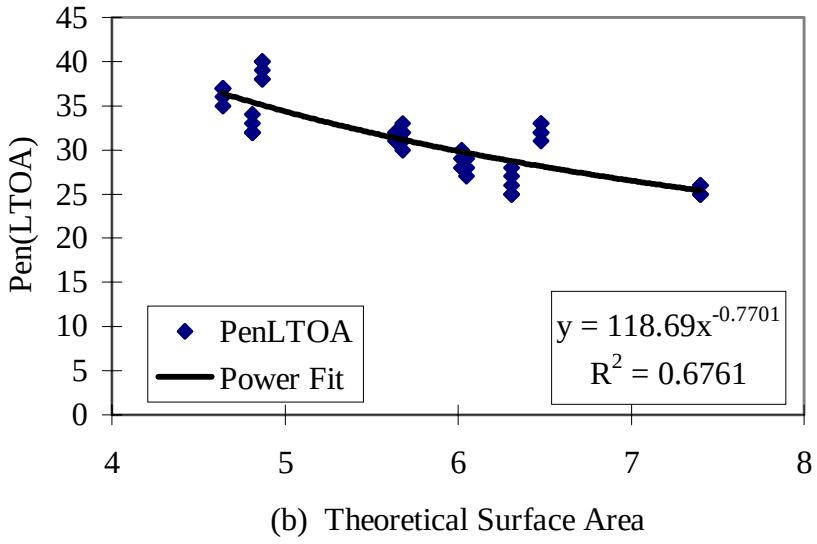

(b) Theoretical Surface Area

Figure 6-17 Effect of Theoretical Surface Area on Penetration After Short- and Long-Term Oven Aging

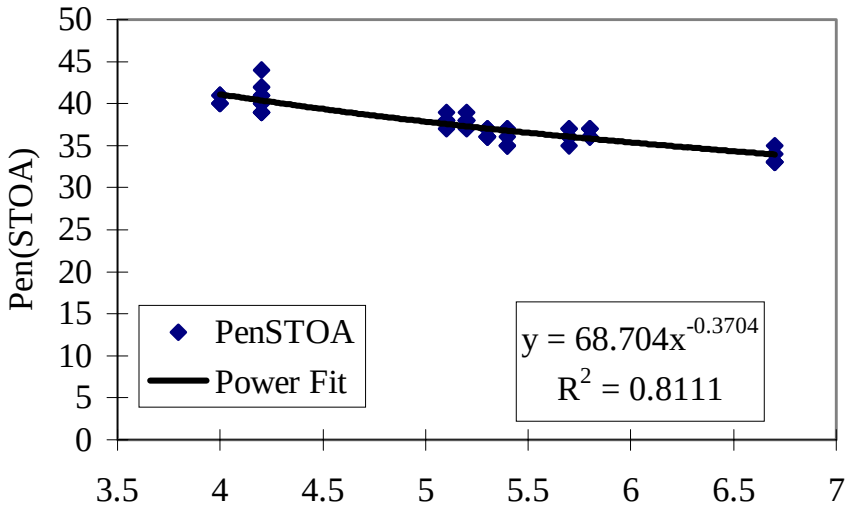

(a) Effective Surface Area

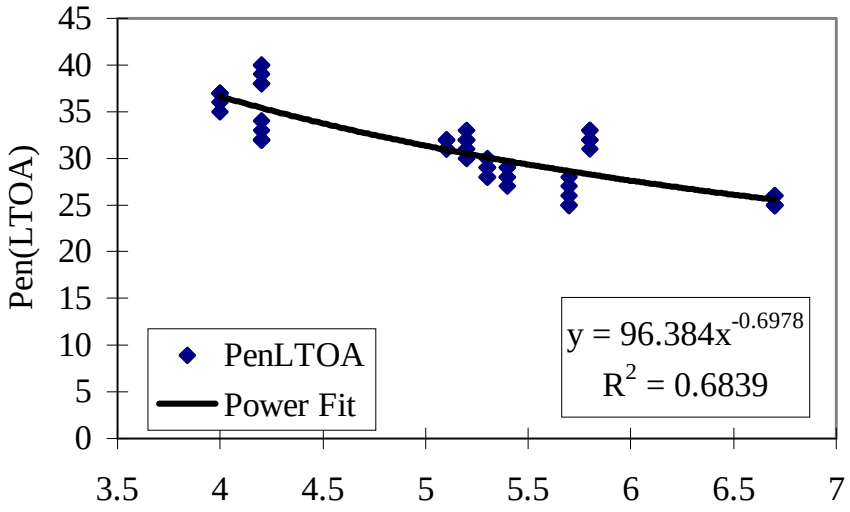

(b) Effective Surface Area

Figure 6-18 Effect of Effective Surface Area on Penetration After Short- and Long-Term Oven Aging

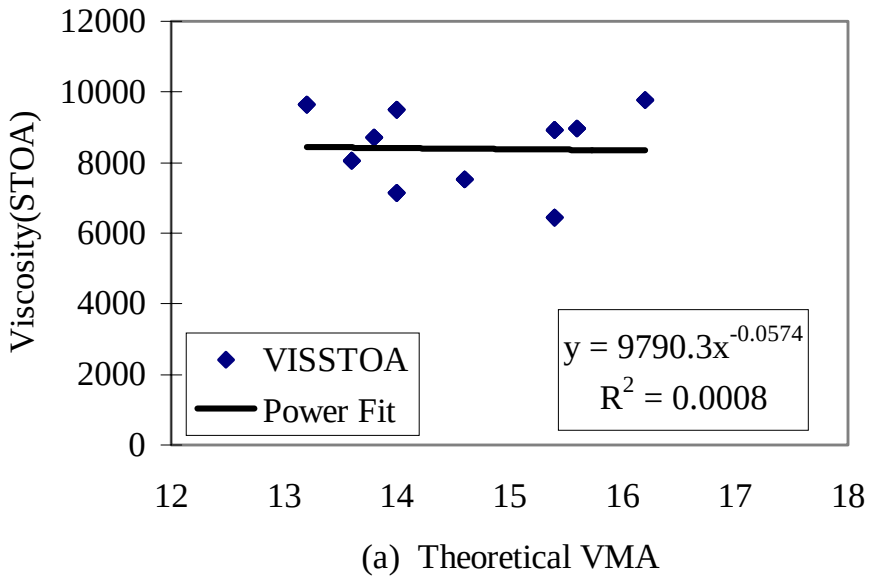

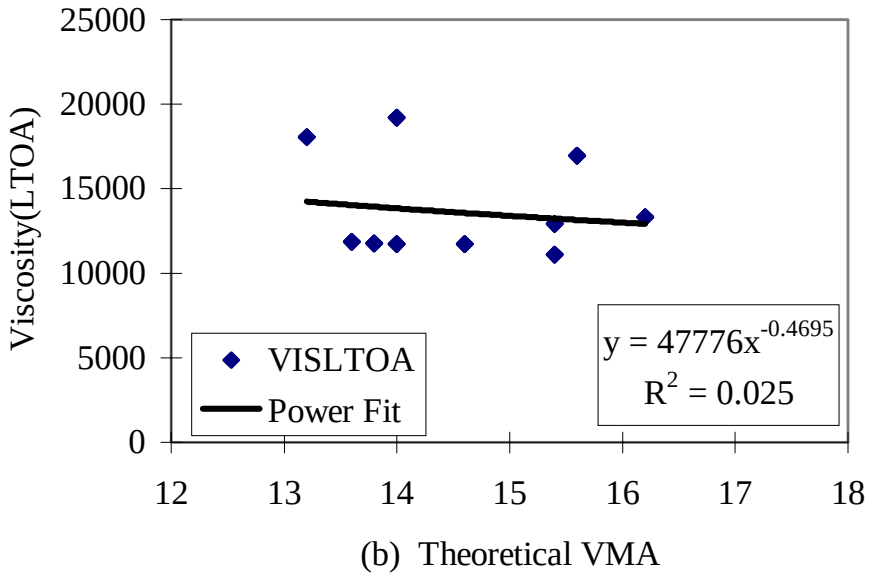

Figure 6-19 Effect of Theoretical VMA on Viscosity After Short- and Long-Term Oven Aging

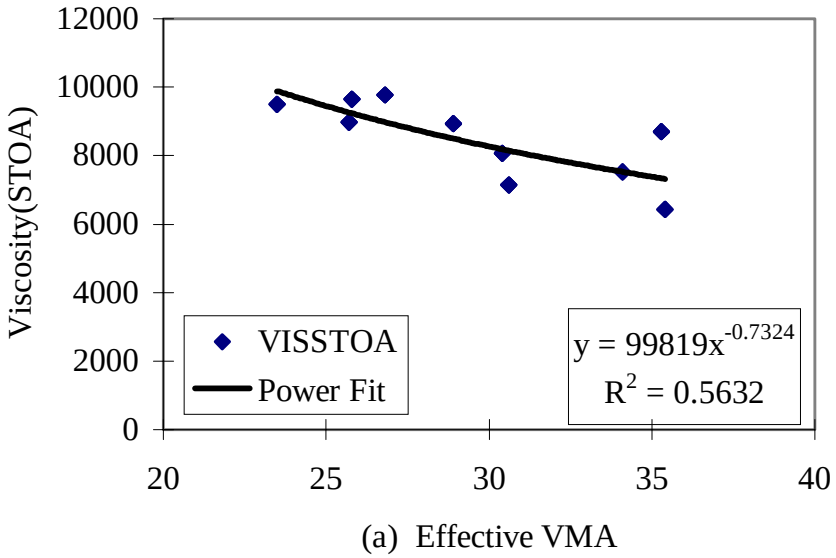

(a) Effective VMA

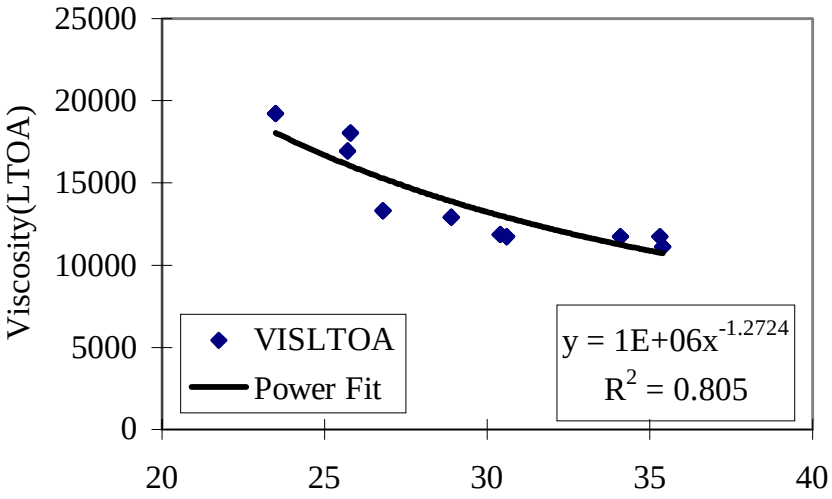

(b) Effective VMA

Figure 6-20 Effect of Effective VMA on Viscosity After Short- and Long-Term Oven Aging

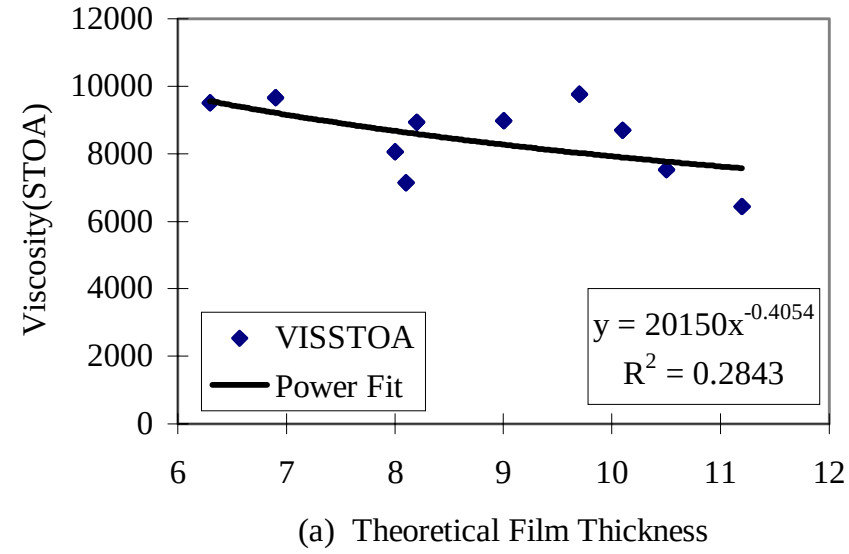

(a) Theoretical Film Thickness

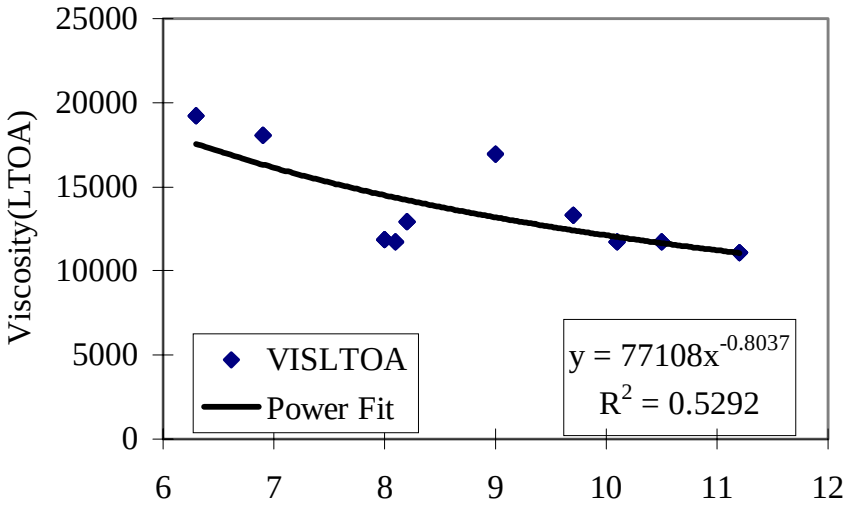

(b) Theoretical Film Thickness

Figure 6-21 Effect of Theoretical Film Thickness on Viscosity After Short- and Long-Term Oven Aging

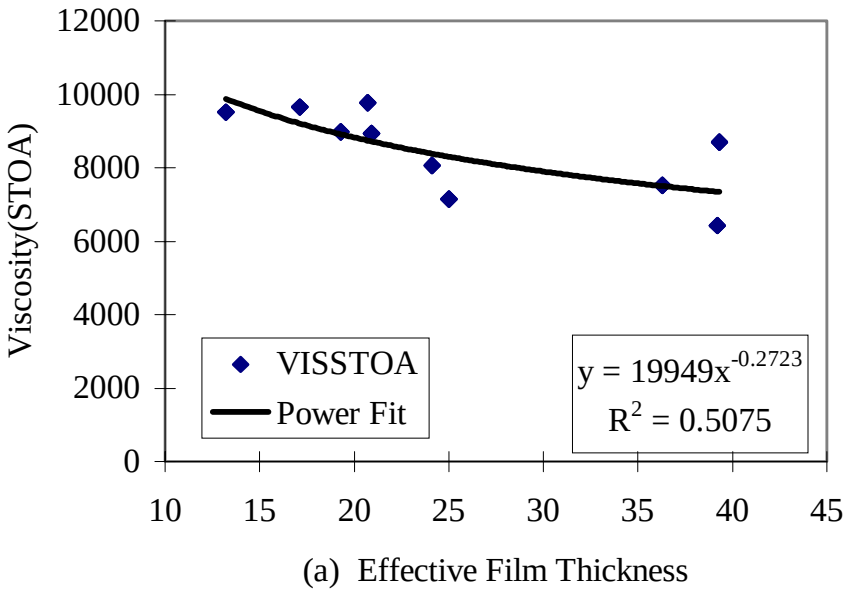

(a) Effective Film Thickness

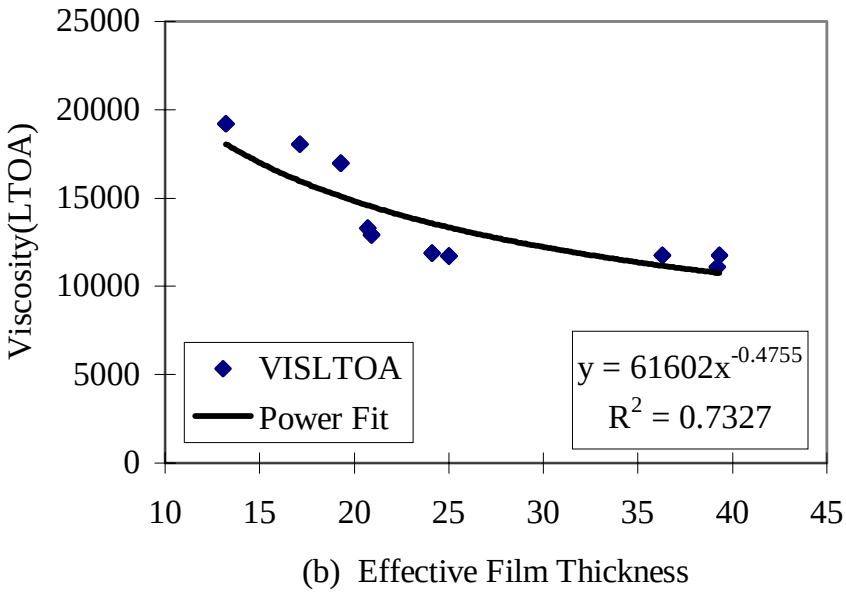

(b) Effective Film Thickness

Figure 6-22 Effect of Effective Film Thickness on Viscosity After Short- and Long-Term Oven Aging

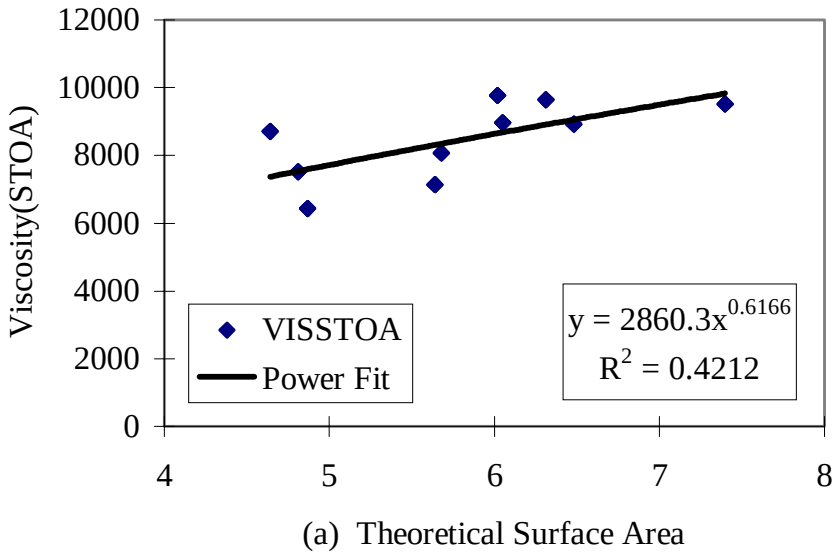

(a) Theoretical Surface Area

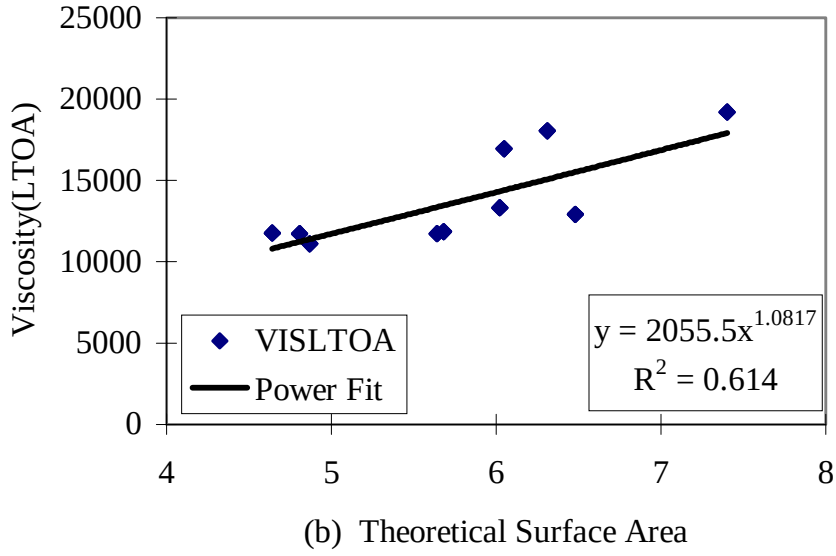

(b) Theoretical Surface Area

Figure 6-23 Effect of Theoretical Surface Area on Penetration After Short- and Long-Term Oven Aging

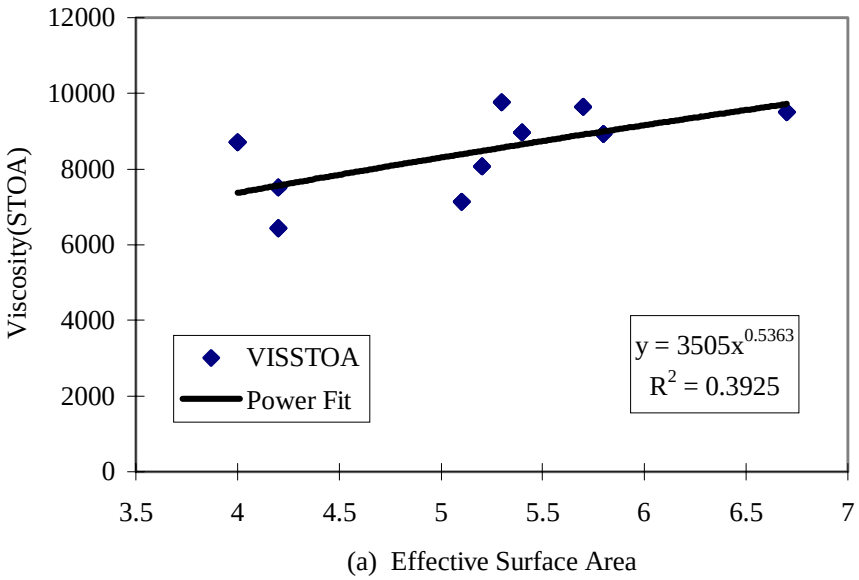

(a) Effective Surface Area

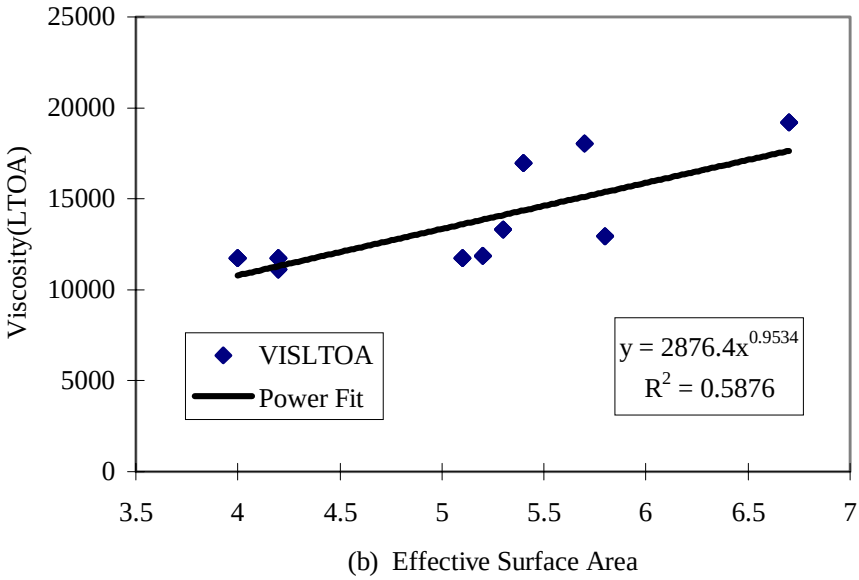

(b) Effective Surface Area

Figure 6-24 Effect of Effective Surface Area on Viscosity After Short- and Long-Term Oven Aging

Table 6-5 Theoretical Volumetric Properties Used for Regression Analysis (Penetration)

Mixture	Theoretical VMA	Theoretical Surface Area	Theoretical Film Thickness	Penetration STOA	Penetration LTOA	Mixture	Theoretical VMA	Theoretical Surface Area	Theoretical Film Thickness	Penetration STOA	Penetration LTOA
	15.4	4.9	11.2	41	38		15.6	6.1	9.0	35	28
	15.4	4.9	11.2	44	40		15.6	6.1	9.0	36	29
C1	15.4	4.9	11.2	41	40	F1	15.6	6.1	9.0	37	27
	15.4	4.9	11.2	42	39		15.6	6.1	9.0	35	28
	15.4	4.9	11.2	42	38		15.6	6.1	9.0	37	29
	13.8	4.6	10.1	41	37		13.2	6.3	6.9	35	27
	13.8	4.6	10.1	40	35		13.2	6.3	6.9	36	26
C2	13.8	4.6	10.1	40	37	F2	13.2	6.3	6.9	37	28
	13.8	4.6	10.1	40	37		13.2	6.3	6.9	36	25
	13.8	4.6	10.1	41	36		13.2	6.3	6.9	37	25
	13.6	5.7	8.0	38	31		14.0	7.4	6.3	35	26
	13.6	5.7	8.0	38	30		14.0	7.4	6.3	34	25
C3	13.6	5.7	8.0	37	32	F4	14.0	7.4	6.3	33	25
	13.6	5.7	8.0	39	32		14.0	7.4	6.3	33	25
	13.6	5.7	8.0	38	33		14.0	7.4	6.3	33	26
	14.0	5.6	8.1	38	32		16.2	6.0	9.7	36	28
	14.0	5.6	8.1	38	31		16.2	6.0	9.7	36	29
C4/F3	14.0	5.6	8.1	37	32	F5	16.2	6.0	9.7	36	30
	14.0	5.6	8.1	39	31		16.2	6.0	9.7	37	29
	14.0	5.6	8.1	38	32		16.2	6.0	9.7	37	28
	14.6	4.8	10.5	39	32		15.4	6.5	8.2	36	32
	14.6	4.8	10.5	39	34		15.4	6.5	8.2	37	31
C5	14.6	4.8	10.5	40	33	F6	15.4	6.5	8.2	37	33
	14.6	4.8	10.5	40	32		15.4	6.5	8.2	37	32
	14.6	4.8	10.5	39	32		15.4	6.5	8.2	36	33

Table 6-6 Effective Volumetric Properties Used for Regression Analysis (Penetration)

Mixture	Effective VMA	Effective Surface Area	Effective Film Thickness	Penetration STOA	Penetration LTOA	Mixture	Effective VMA	Effective Surface Area	Effective Film Thickness	Penetration STOA	Penetration LTOA
	35.4	4.2	39.2	41	38		25.7	5.4	19.3	35	28
	35.4	4.2	39.2	44	40		25.7	5.4	19.3	36	29
C1	35.4	4.2	39.2	41	40	F1	25.7	5.4	19.3	37	27
	35.4	4.2	39.2	42	39		25.7	5.4	19.3	35	28
	35.4	4.2	39.2	42	38		25.7	5.4	19.3	37	29
	35.3	4.0	39.3	41	37		25.8	5.7	17.1	35	27
	35.3	4.0	39.3	40	35		25.8	5.7	17.1	36	26
C2	35.3	4.0	39.3	40	37	F2	25.8	5.7	17.1	37	28
	35.3	4.0	39.3	40	37		25.8	5.7	17.1	36	25
	35.3	4.0	39.3	41	36		25.8	5.7	17.1	37	25
	30.4	5.2	24.1	38	31		23.5	6.7	13.2	35	26
	30.4	5.2	24.1	38	30		23.5	6.7	13.2	34	25
C3	30.4	5.2	24.1	37	32	F4	23.5	6.7	13.2	33	25
	30.4	5.2	24.1	39	32		23.5	6.7	13.2	33	25
	30.4	5.2	24.1	38	33		23.5	6.7	13.2	33	26
	30.6	5.1	25.0	38	32		26.8	5.3	20.7	36	28
	30.6	5.1	25.0	38	31		26.8	5.3	20.7	36	29
C4/F3	30.6	5.1	25.0	37	32	F5	26.8	5.3	20.7	36	30
	30.6	5.1	25.0	39	31		26.8	5.3	20.7	37	29
	30.6	5.1	25.0	38	32		26.8	5.3	20.7	37	28
	34.1	4.2	36.3	39	32		28.9	5.8	20.9	36	32
	34.1	4.2	36.3	39	34		28.9	5.8	20.9	37	31
C5	34.1	4.2	36.3	40	33	F6	28.9	5.8	20.9	37	33
	34.1	4.2	36.3	40	32		28.9	5.8	20.9	37	32
	34.1	4.2	36.3	39	32		28.9	5.8	20.9	36	33

Table 6-7 Theoretical Volumetric Properties Used for Regression Analysis (G* and Viscosity)

Mixture	Theoretical VMA	Theoretical Surface Area	Theoretical Film Thickness	G* STOA	G* LTOA	Viscosity STOA	Viscosity LTOA
	15.4	4.9	11.2	7.5866E+06	8.2483E+06	6435	11107
C1	15.4	4.9	11.2	7.5923E+06	8.2593E+06	6435	11107
	15.4	4.9	11.2	7.5932E+06	8.2649E+06	6435	11107
	15.6	6.1	9.0	9.7145E+06	1.1414E+07	8965	16953
F1	15.6	6.1	9.0	9.7319E+06	1.1443E+07	8965	16953
	15.6	6.1	9.0	9.7151E+06	1.1415E+07	8965	16953
	13.6	5.7	8.0	6.9239E+06	9.2632E+06	8064	11860
C3	13.6	5.7	8.0	8.7615E+06	9.1256E+06	8064	11860
	13.6	5.7	8.0	7.8895E+06	9.2869E+06	8064	11860
	14.0	5.6	8.1	7.7353E+06	9.6385E+06	7139	11721
C4/F3	14.0	5.6	8.1	8.3510E+06	8.9848E+06	7139	11721
	14.0	5.6	8.1	7.3020E+06	9.4524E+06	7139	11721
	13.8	4.6	10.1	7.3876E+06	8.0473E+06	8706	11750
C2	13.8	4.6	10.1	7.3772E+06	8.0587E+06	8706	11750
	13.8	4.6	10.1	7.4079E+06	8.0710E+06	8706	11750
	13.2	6.3	6.9	9.7898E+06	1.1502E+07	9650	18048
F2	13.2	6.3	6.9	9.7159E+06	1.1473E+07	9650	18048
	13.2	6.3	6.9	9.7771E+06	1.1498E+07	9650	18048
	14.6	4.8	10.5	7.7102E+06	9.1216E+06	7520	11738
C5	14.6	4.8	10.5	7.7356E+06	9.2523E+06	7520	11738
	14.6	4.8	10.5	7.6962E+06	8.9250E+06	7520	11738
	14.0	7.4	6.3	1.0897E+07	1.2636E+07	9506	19204
F4	14.0	7.4	6.3	1.0533E+07	1.2755E+07	9506	19204
	14.0	7.4	6.3	1.1357E+07	1.2496E+07	9506	19204
	16.2	6.0	9.7	9.4883E+06	1.1272E+07	9769	13307
F5	16.2	6.0	9.7	8.9652E+06	1.1285E+07	9769	13307
	16.2	6.0	9.7	9.9562E+06	1.1252E+07	9769	13307
F6	15.4	6.5	8.2	9.3873E+06	1.0921E+07	8926	12922
	15.4	6.5	8.2	9.0610E+06	1.1252E+07	8926	12922
	15.4	6.5	8.2	9.6652E+06	1.0653E+07	8926	12922

Table 6-8 Effective Volumetric Properties Used for Regression Analysis (G* and Viscosity)

Mixture	Effective VMA	Effective Surface Area	Effective Film Thickness	G* STOA	G* LTOA	Viscosity STOA	Viscosity LTOA
	35.4	4.2	39.2	7.5866E+06	8.2483E+06	6435	11107
C1	35.4	4.2	39.2	7.5923E+06	8.2593E+06	6435	11107
	35.4	4.2	39.2	7.5932E+06	8.2649E+06	6435	11107
	25.7	5.4	19.3	9.7145E+06	1.1414E+07	8965	16953
F1	25.7	5.4	19.3	9.7319E+06	1.1443E+07	8965	16953
	25.7	5.4	19.3	9.7151E+06	1.1415E+07	8965	16953
	30.4	5.2	24.1	6.9239E+06	9.2632E+06	8064	11860
C3	30.4	5.2	24.1	8.7615E+06	9.1256E+06	8064	11860
	30.4	5.2	24.1	7.8895E+06	9.2869E+06	8064	11860
	30.6	5.1	25.0	7.7353E+06	9.6385E+06	7139	11721
C4/F3	30.6	5.1	25.0	8.3510E+06	8.9848E+06	7139	11721
	30.6	5.1	25.0	7.3020E+06	9.4524E+06	7139	11721
	35.3	4.0	39.3	7.3876E+06	8.0473E+06	8706	11750
C2	35.3	4.0	39.3	7.3772E+06	8.0587E+06	8706	11750
	35.3	4.0	39.3	7.4079E+06	8.0710E+06	8706	11750
	25.8	5.7	17.1	9.7898E+06	1.1502E+07	9650	18048
F2	25.8	5.7	17.1	9.7159E+06	1.1473E+07	9650	18048
	25.8	5.7	17.1	9.7771E+06	1.1498E+07	9650	18048
	34.1	4.2	36.3	7.7102E+06	9.1216E+06	7520	11738
C5	34.1	4.2	36.3	7.7356E+06	9.2523E+06	7520	11738
	34.1	4.2	36.3	7.6962E+06	8.9250E+06	7520	11738
	23.5	6.7	13.2	1.0897E+07	1.2636E+07	9506	19204
F4	23.5	6.7	13.2	1.0533E+07	1.2755E+07	9506	19204
	23.5	6.7	13.2	1.1357E+07	1.2496E+07	9506	19204
	26.8	5.3	20.7	9.4883E+06	1.1272E+07	9769	13307
F5	26.8	5.3	20.7	8.9652E+06	1.1285E+07	9769	13307
	26.8	5.3	20.7	9.9562E+06	1.1252E+07	9769	13307
F6	28.9	5.8	20.9	9.3873E+06	1.0921E+07	8926	12922
	28.9	5.8	20.9	9.0610E+06	1.1252E+07	8926	12922
	28.9	5.8	20.9	9.6652E+06	1.0653E+07	8926	12922

The correlation coefficient R^2 was also obtained from the Microsoft Excel output. Currently, SuperPave™ specifications were based on the belief that binder age-hardening rate depended on the traditional volumetric properties, but were important parameters. It was observed that the R^2 values for the effective parameters were higher than those for the theoretical volumetric parameters. This shows that the effective volumetric properties are better tools for predicting binder age-hardening than the traditional theoretical values.

In addition to the regression analysis, the mixtures were grouped into levels as shown in Tables 6-9 and 6-10. This grouping was done such that mixtures could be designated as high, medium or low in terms of VMA, film thickness and surface area. The values for binder age-hardening in Table 6.11 were obtained by normalizing the extracted binder properties in relation to C1 (i.e., C1 =1) and then categorized as high, medium or low age-hardening. For these categories high is designated level 1, medium is level 2 and low is level 3. The comparisons presented in Figure 6-25 clearly show that the effective parameters result in better correlations than the conventional parameters.

6.4.1.1 Observations

It was observed that:

1. Both theoretical and effective surface area values are capable of predicting binder age hardening in mixtures. However, surface area does not directly indicate the amount of binder available for aggregate coating in a mixture. Surface area is also not a good indicator of gradation.

2. Effective volumetric parameters can be used for predicting the binder age-hardening rate for mixtures and thus can be used as a measure of durability, whereas the traditional volumetric parameters cannot be used for predicting the binder age-hardening rate.

Table 6-9 Groups of Theoretical Volumetric Properties

Volumetric Property	Properties of Mixtures					
	VMA		FT		SA	
Catergory	Range	Mixtures	Range	Mixtures	Range	Mixtures
1 (High)	>15	C1 C5 F1 F5 F6	>9	C1 C2 C5 F5 F6	>6	F1 F2 F4 F5 F6
2 (Medium)	14-15	C4/F3 F4	7-9	F1 C3 C4/F3	5-6	C3 C4/F3
3 (Low)	<14	C2 C3 F2	<7	F2 F4	<5	C1 C2 C5

Table 6-10 Groups for Effective Volumetric Properties

Volumetric Property	Properties of Mixtures					
	VMA		FT		SA	
Catergory	Range	Mixtures	Range	Mixtures	Range	Mixtures
1 (High)	>34	C1 C2 C5	>32	C1 C2 C5	>5.3	F1 F2 F4 F5 F6
2 (Medium)	30-34	C3 C4/F3	22-32	C3 C4/F3	4.3-5.3	C3 C4/F3
3 (Low)	<22	F1 F2 F4 F5 F6	<22	F1 F2 F4 F5 F6	<4.3	C1 C2 C5

Table 6-11 Normalized Binder Data (C1 = 1)

	STOA				LTOA					
Mixture	Pen	Viscosity (Poise)	G* (Pa)	Delta	Pen	Viscosity (Poise)	G* (Pa)	Delta	Average	Age Hardening
C1	1.00	1.00	1.00	1.00	1.00	1.00	1.00	1.00	1.00	LOW
C2	1.05	1.35	0.97	0.97	1.08	1.06	0.98	0.97	1.05	LOW
C3	1.11	1.25	1.04	1.01	1.22	1.07	1.12	1.02	1.10	MED
C5	1.08	1.17	1.02	1.01	1.18	1.06	1.10	1.04	1.08	LOW
F1	1.17	1.39	1.28	1.02	1.39	1.53	1.38	1.03	1.27	HIGH
F2	1.17	1.50	1.29	1.05	1.50	1.62	1.39	1.07	1.32	HIGH
C4/F3	1.11	1.11	1.03	1.01	1.22	1.06	1.13	1.02	1.09	MED
F4	1.24	1.48	1.44	1.08	1.56	1.73	1.40	1.07	1.37	HIGH
F5	1.17	1.52	1.25	1.05	1.34	1.20	1.36	1.05	1.24	HIGH
F6	1.14	1.39	1.23	1.02	1.30	1.16	1.33	1.04	1.20	HIGH

		Binder Age-Hardening		
		High (>1.15)	Medium (1.09-1.15)	Low (<1.09)
Theoretical Film Thickness (micron)	High (>9)	F5 F6		C1 C2 C5
	Medium (7-9)	F1	C4/F3 C3	
	Low (<7)	F2 F4		

		Binder Age-Hardening		
		High (>1.15)	Medium (1.09-1.15)	Low (<1.09)
Theoretical VMA (%)	High (>15)	F1 F5 F6		C1 C5
	Medium (14-15)	F4	C4/F3	
	Low (<14)	F2	C3	C2

		Binder Age-Hardening		
		High (>1.15)	Medium (1.09-1.15)	Low (<1.09)
Effcetive Film Thickness (micron)	High (>32)			C1 C2 C5
	Medium (22-32)		C4/F3 C3	
	Low (<22)	F1 F2 F4 F5 F6		

		Binder Age-Hardening		
		High (>1.15)	Medium (1.09-1.15)	Low (<1.09)
Effective VMA (%)	High (>34)			C1 C2 C5
	Medium (30-34)		C4/F3 C3	
	Low (<30)	F1 F2 F4 F5 F6		

Figure 6-25 Levels for Volumetric Properties and Binder Age-Hardening

6.4.2 Mixture Results

The mixture results are shown in Table 6-12. When all the mixtures were plotted on the same graph as in Figures 6-26 to 6-31, there was a visible trend to the effect that mixtures with higher effective film thickness and effective VMA had higher strain tolerance, lower stiffness, higher fracture energy density and higher creep compliance. This shows that there was good correlation between effective volumetric properties and mixture behavior and led to a better understanding of the effect of the aggregate structures on the performance of asphalt mixtures. This was true for all mixtures except for the gap-graded mixtures C5, F5 and F6, which were more brittle and had lower resistance to fracture, but higher rutting resistance. It should be emphasized that the brittle nature of gap-graded mixtures is not a result of higher binder age-hardening, but appeared to result primarily from gap-grading in the coarse range. Binder age-hardening in these mixtures was actually reduced by allowing more asphalt to be incorporated into the mastic of the mixture resulting in thicker films of asphalt on the aggregates. These gap-graded mixtures required a greater compactive effort during mixture production (Table 6-13) to get to the test air void content of 7%. However, it is clear from figures that both tensile strength and M_R at the STOA and LTOA levels of aging, increased with decreasing values for the effective film thickness and effective VMA and increase with increasing dust-to-asphalt ratio. This means that the fine mixtures with very low effective film thickness and VMA were more affected by aging. This does not seem to be a problem with coarse mixtures because their effective volumetric properties (VMA and film thickness) were always higher than those of the fine mixtures. Even low effective film thickness and effective VMA values for coarse mixtures were higher than

Table 6-12 Mixture Properties

Mixture	Mr (Gpa)		CreepCompliance(1/Gpa)		M-Value	
	STOA	LTOA	STOA	LTOA	STOA	LTOA
C1	7.9	9.6	13.9	4.5	0.80	0.55
C2	7.7	11.9	15.1	2.8	0.77	0.59
C3	11.5	14.2	7.6	2.2	0.66	0.50
C5	9.7	11.4	4.1	1.2	0.58	0.51
F1	9.5	9.9	7.9	4.5	0.66	0.57
F2	8.6	12.9	6.0	1.9	0.56	0.50
C4/F3	12.0	13.9	6.3	1.9	0.58	0.50
F4	10.4	12.4	4.6	0.9	0.58	0.42
F5	8.3	9.7	6.0	2.0	0.54	0.57
F6	8.0	10.5	6.0	2.0	0.55	0.56
GAC1	7.6	10.7	6.1	3.0	0.62	0.52
GAC11	6.9	9.0	8.6	4.2	0.55	0.57
GAF1	7.1	8.4	6.5	2.8	0.55	0.47

Mixture	FractureEnergy(kJ/m^3)		Failure Strain		TensileStrength (MPa)	
	STOA	LTOA	STOA	LTOA	STOA	LTOA
C1	5.8	3.5	4629.8	2224.4	1.6	2.1
C2	4.8	2.9	3771.3	1896.7	1.7	2.1
C3	3.5	2.7	2174.0	1468.3	2.1	2.4
C5	2.5	2.1	1808.4	1413.9	1.8	1.8
F1	4.2	2.8	2919.6	1833.3	2.1	2.1
F2	5.4	3.2	3714.6	1526.2	1.9	2.6
C4/F3	3.7	1.7	2419.0	1174.7	2.0	2.2
F4	3.1	2.0	2235.1	1225.1	1.9	2.1
F5	3.2	2.3	2400.1	1626.7	1.8	1.8
F6	3.0	2.5	2424.5	1646.8	1.7	2.1
GAC1	3.9	2.6	2810.0	1875.7	1.7	1.8
GAC11	5.8	5.8	4171.7	3402.2	1.8	2.1
GAF1	8.4	4.6	5128.5	2685.4	2.0	2.2

	C1	C2	C5	C4/F3	C3	F6	F5	F1	F2	F4
VMA	15.4	13.8	14.6	14.0	13.6	15.4	16.2	15.6	13.2	14.0
FT	11.2	10.1	10.5	8.1	8	8.2	9.7	9	6.9	6.3
VMAe	34.4	33.5	32.3	28.6	28.4	27.5	27.9	24.6	23.8	21.8
FTe	39.1	39.1	36.2	24.9	24.1	20.8	20.7	19.3	17.1	14.5

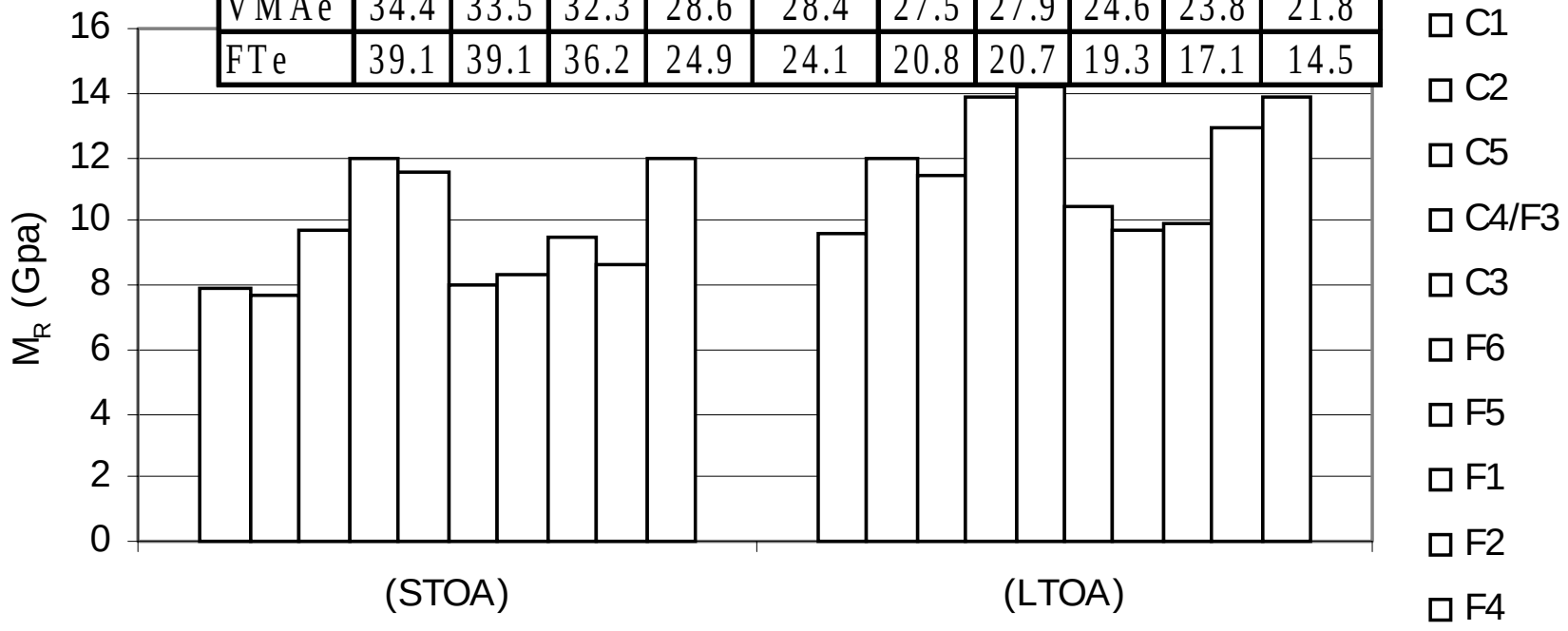

Figure 6-26 Resilient Modulus and Mixture Volumetric Properties

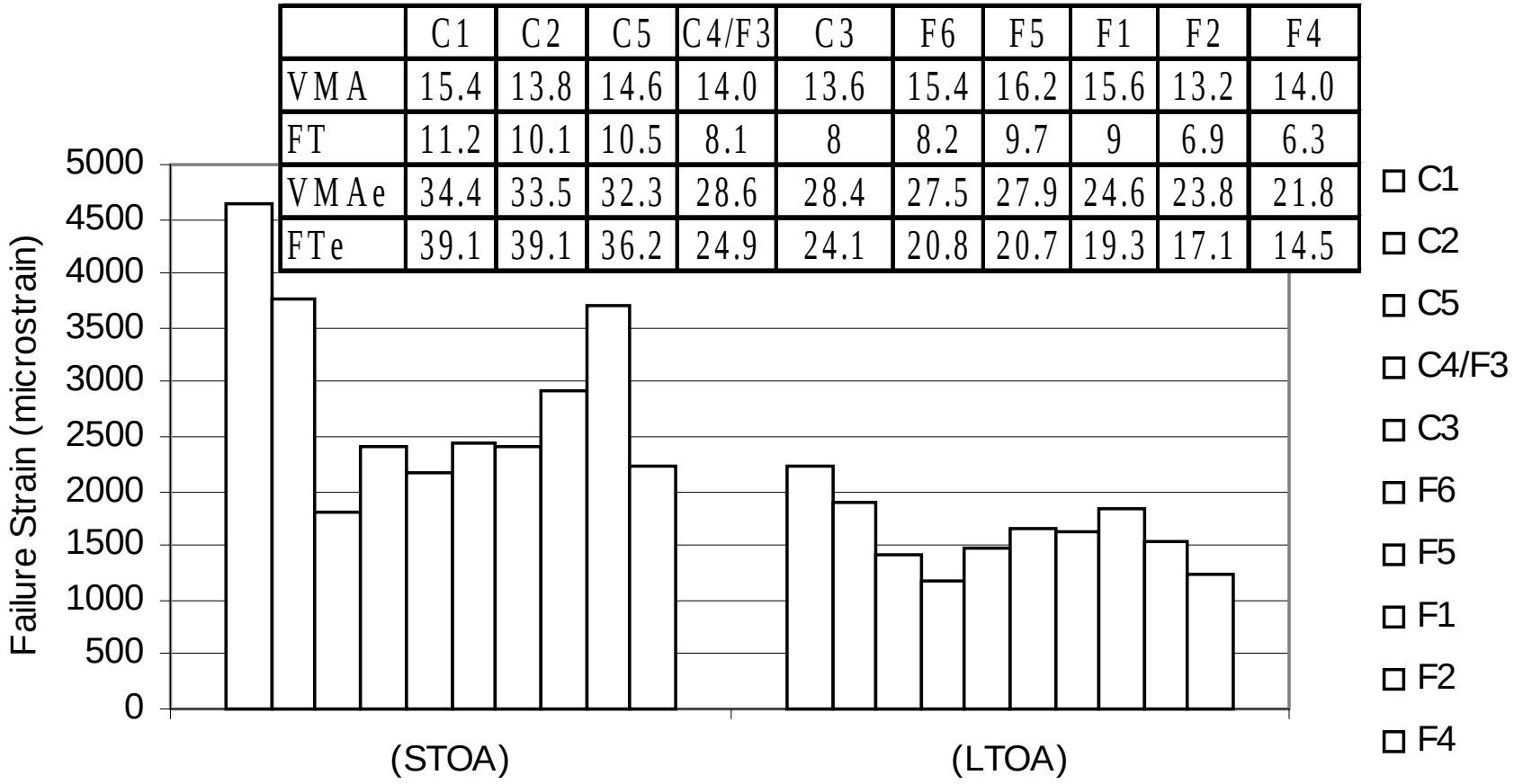

Figure 6-27 Failure Strain and Mixture Volumetric Properties

	C1	C2	C5	C4/F3	C3	F6	F5	F1	F2	F4
VMA	15.4	13.8	14.6	14.0	13.6	15.4	16.2	15.6	13.2	14.0
FT	11.2	10.1	10.5	8.1	8	8.2	9.7	9	6.9	6.3
VMAe	34.4	33.5	32.3	28.6	28.4	27.5	27.9	24.6	23.8	21.8
FTe	39.1	39.1	36.2	24.9	24.1	20.8	20.7	19.3	17.1	14.5

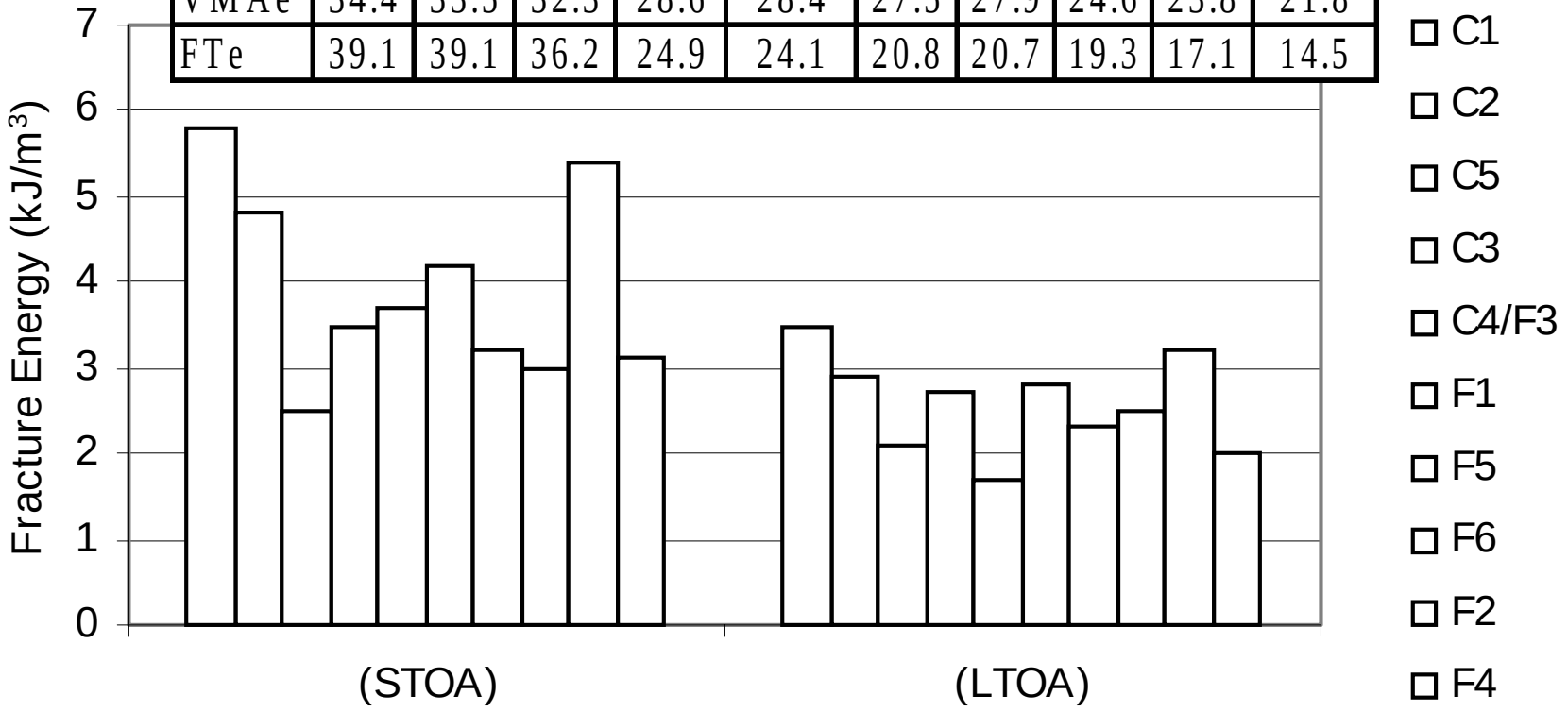

Figure 6-28 Fracture Energy and Mixture Volumetric Properties

	C1	C2	C5	C4/F3	C3	F6	F5	F1	F2	F4
VMA	15.4	13.8	14.6	14.0	13.6	15.4	16.2	15.6	13.2	14.0
FT	11.2	10.1	10.5	8.1	8	8.2	9.7	9	6.9	6.3
VMAe	34.4	33.5	32.3	28.6	28.4	27.5	27.9	24.6	23.8	21.8
FTe	39.1	39.1	36.2	24.9	24.1	20.8	20.7	19.3	17.1	14.5

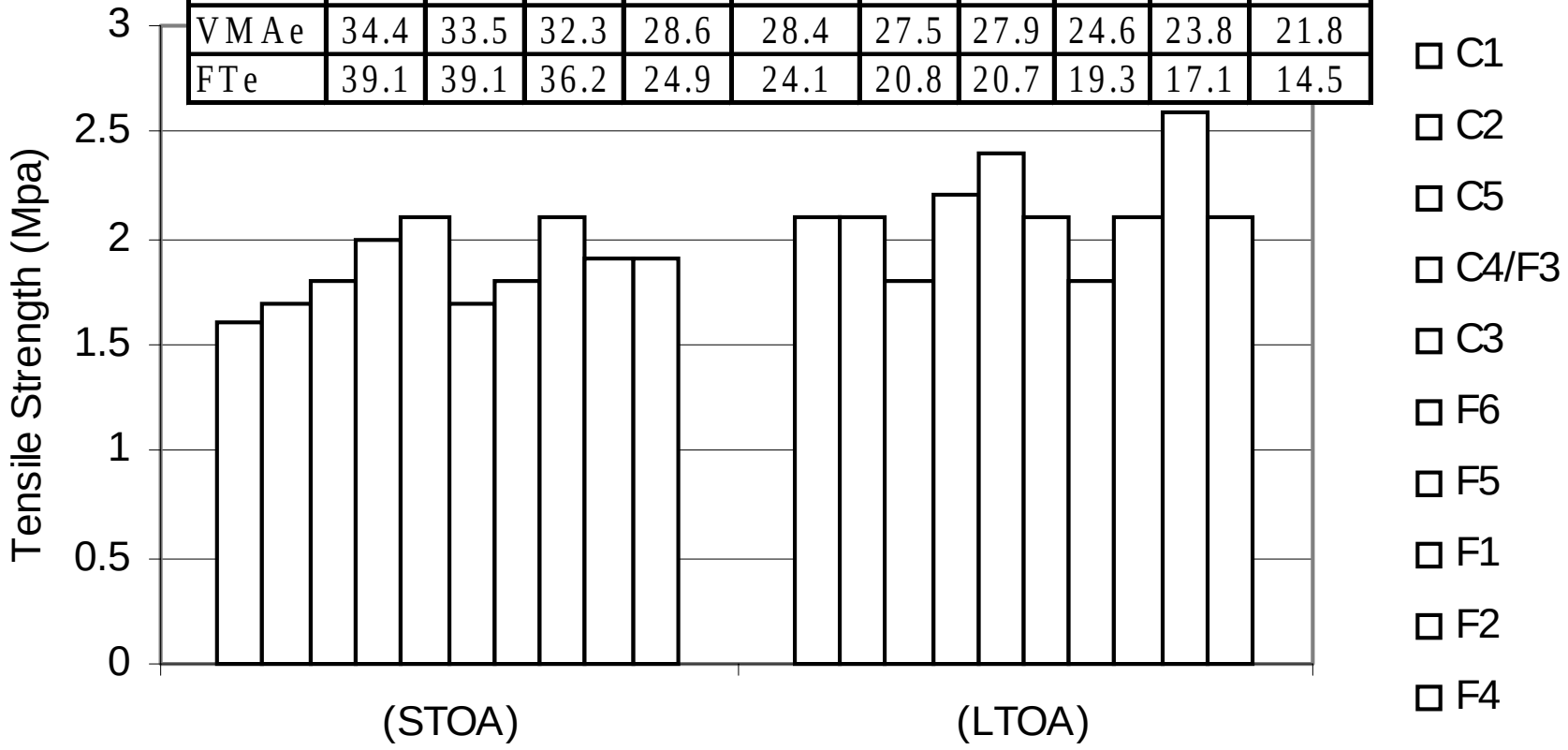

Figure 6-29 Tensile Strength and Mixture Volumetric Properties

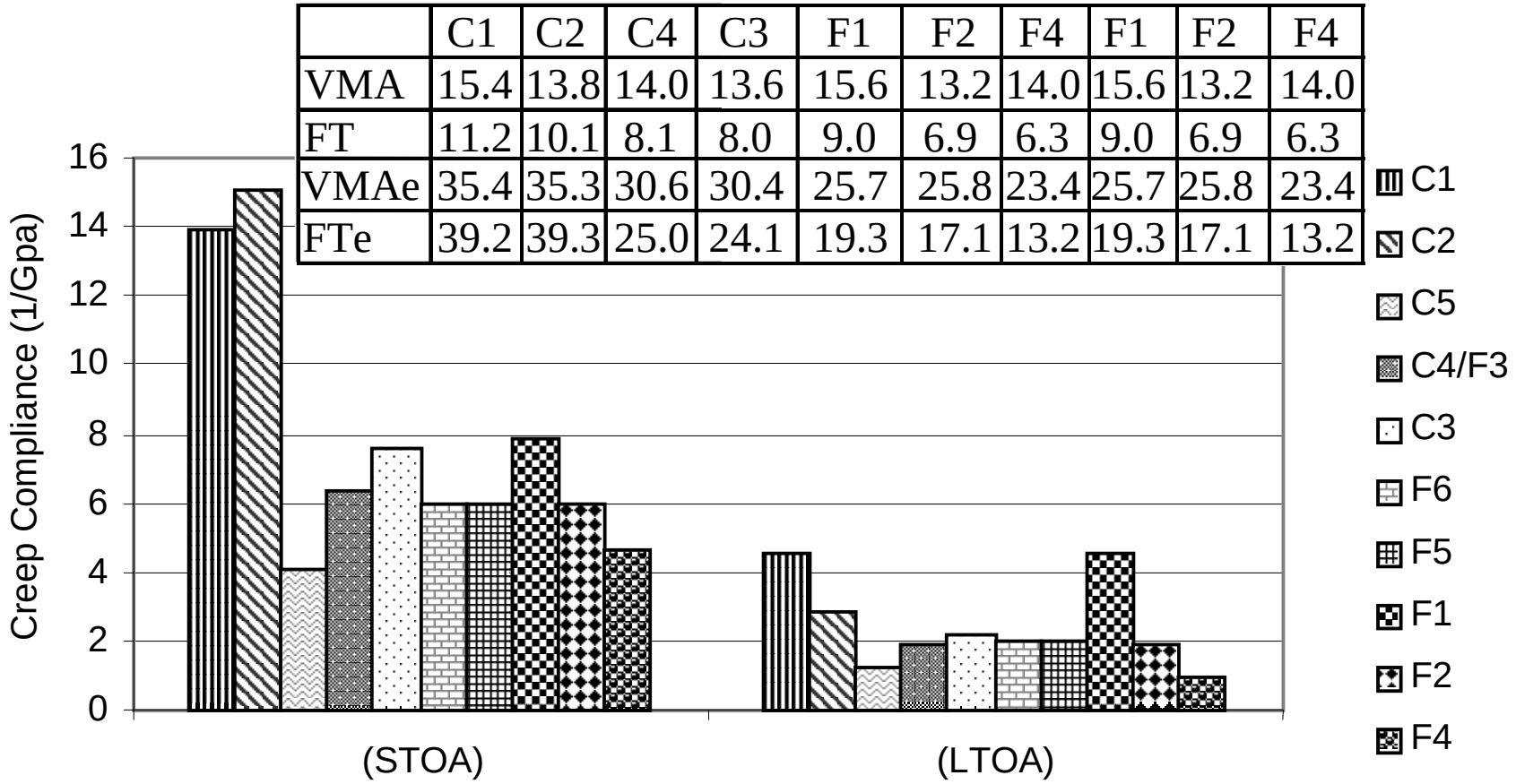

Figure 6-30 Creep Compliance and Mixture Volumetric Properties

	C1	C2	C5	C4/F3	C3	F6	F5	F1	F2	F4
VMA	15.4	13.8	14.6	14.0	13.6	15.4	16.2	15.6	13.2	14.0
FT	11.2	10.1	10.5	8.1	8	8.2	9.7	9	6.9	6.3
VMAe	34.4	33.5	32.3	28.6	28.4	27.5	27.9	24.6	23.8	21.8
FTe	39.1	39.1	36.2	24.9	24.1	20.8	20.7	19.3	17.1	14.5

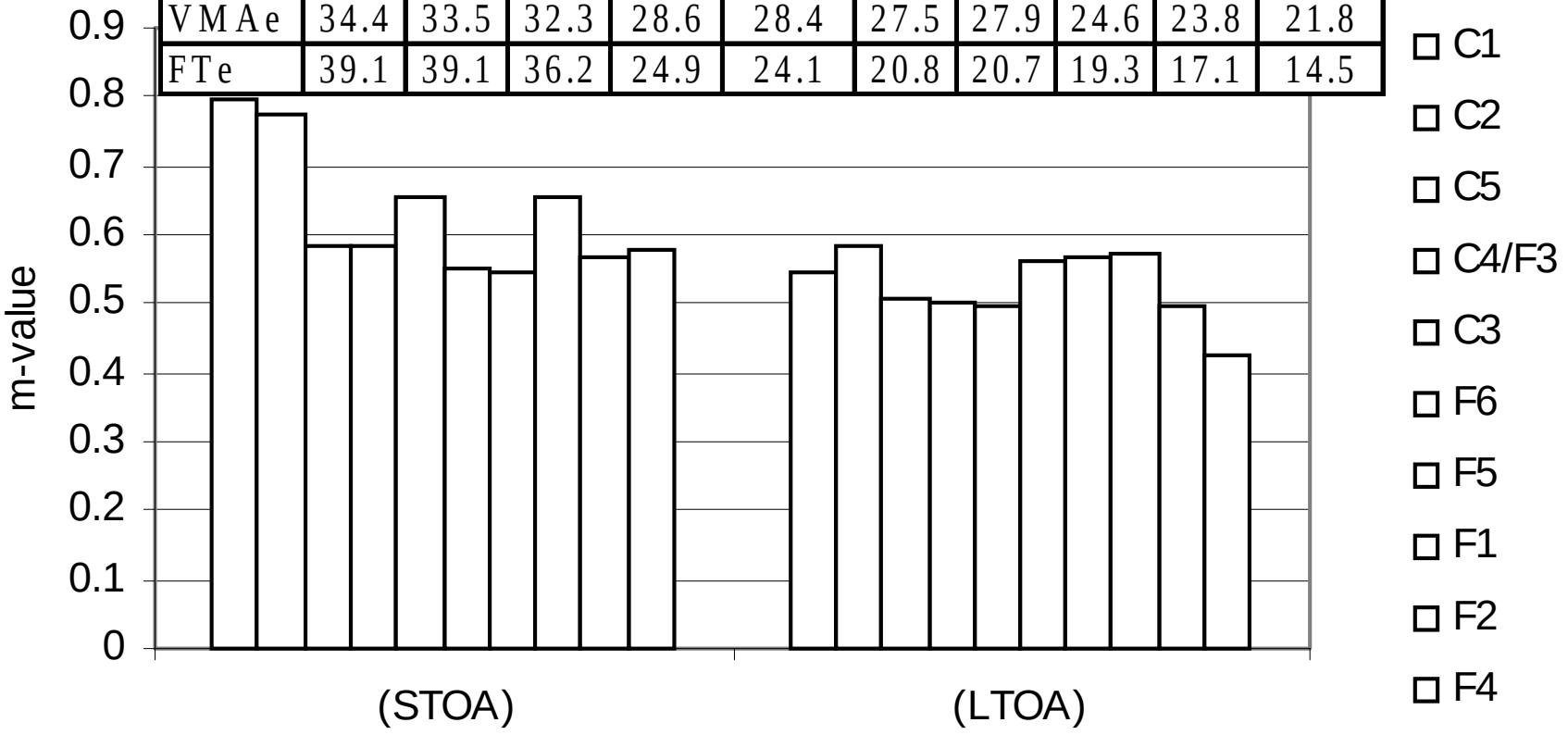

Figure 6-31 m-Value and Mixture Volumetric Properties

Table 6-13 Number of Gyrations and Mixture Height at 7% Air Void

Mixture Type	No. of Gyrations	Height (mm)
C1	45.8	130.0
C2	34.7	129.4
C3	33.4	127.9
C4/F3	40.3	128.1
C5	60.5	129.1
F1	32.0	127.6
F2	22.1	125.4
F4	53.5	125.3
F5	41.5	129.3
F6	48.0	127.5
GAC1	48.5	124.6
GAC2	64.0	118.5
GAF1	41.8	124.6

those of the best fine mixtures. The failure strain, fracture energy density, creep compliance and m-value increased with increasing effective film thickness.

Therefore, the effective volumetric properties of mixtures were capable of determining the effective amount of binder in asphalt mixtures. Volumetric properties that depict the amount of binder rather than its stiffness appeared to control mixture properties such as tensile strength, M_R, m-value fracture energy, shear resistance and creep compliance.

The other exception to this trend was mixture F2. The peculiarity of this mixture can be seen from the fact that its effective asphalt content was as high as that for F1, which is a good performing mixture, and had a very low permeability (about half that of F1). These factors, coupled with its high tensile strength should make the F2 mixture more resistant to fatigue failure. However, the fracture energy density of the F2 mixture

decreased much more during aging than that of the F21 mixture. This appeared to indicate that the F2 mixture was affected by its low film thickness.

6.5 Binder Results – Georgia Granite Mixtures

Three additional mixtures were produced to analyze the effect of aggregate type on binder age-hardening and performance. These were 9.5-mm nominal maximum aggregate sized mixtures as compared to the 12.5-mm nominal mixtures used for the limestone mixtures. They were also blended with at least two different aggregate type materials by combining Georgia granite coarse aggregates with either Georgia granite screens or Anderson screens (very porous whiterock) or both. GAC2 is a pure granite blend comprised of granite coarse aggregate and granite screenings. GAC1, which has the same gradation as GAC2 is a combination of granite coarse aggregate and Anderson screens while GAF1 is a combination of all three. Because of their different absorptive nature, their recovered binder properties did not follow the trends observed in the other mixtures. There were slight deviations from the previously observed trends. But their fatigue and shear performance followed the same trend with effective parameters as the previous whiterock mixtures. When dealing with mixtures blended from different aggregate types with varying degrees of absorption (e.g., porous versus nonporous), the absorption of these aggregates become significant and may affect the measured binder age-hardening rates of the recovered binder. Figures 6-32 to 6-35 show the aging rates of the granite mixtures as compared with their effective film thickness and VMA. Because of its low absorption and higher unit weight, GAC2 had higher theoretical film thickness and VMA than GAC1, even though its design asphalt content was lower than GAC1. However, GAC2 had slightly lower effective film thickness and effective VMA than

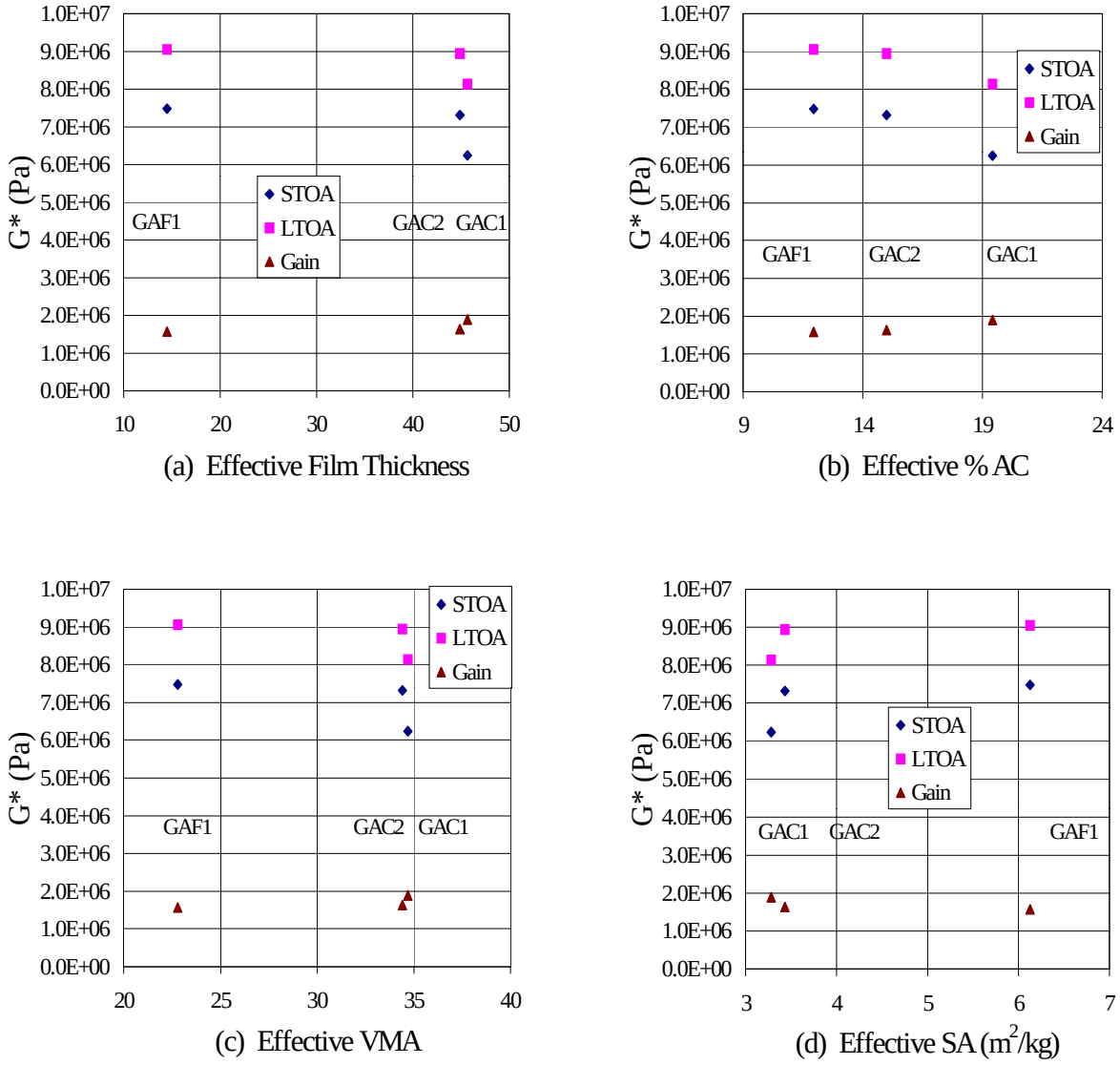

Figure 6-32 Modulus G* Versus Effective Volumetric Properties (Granite Mixtures)

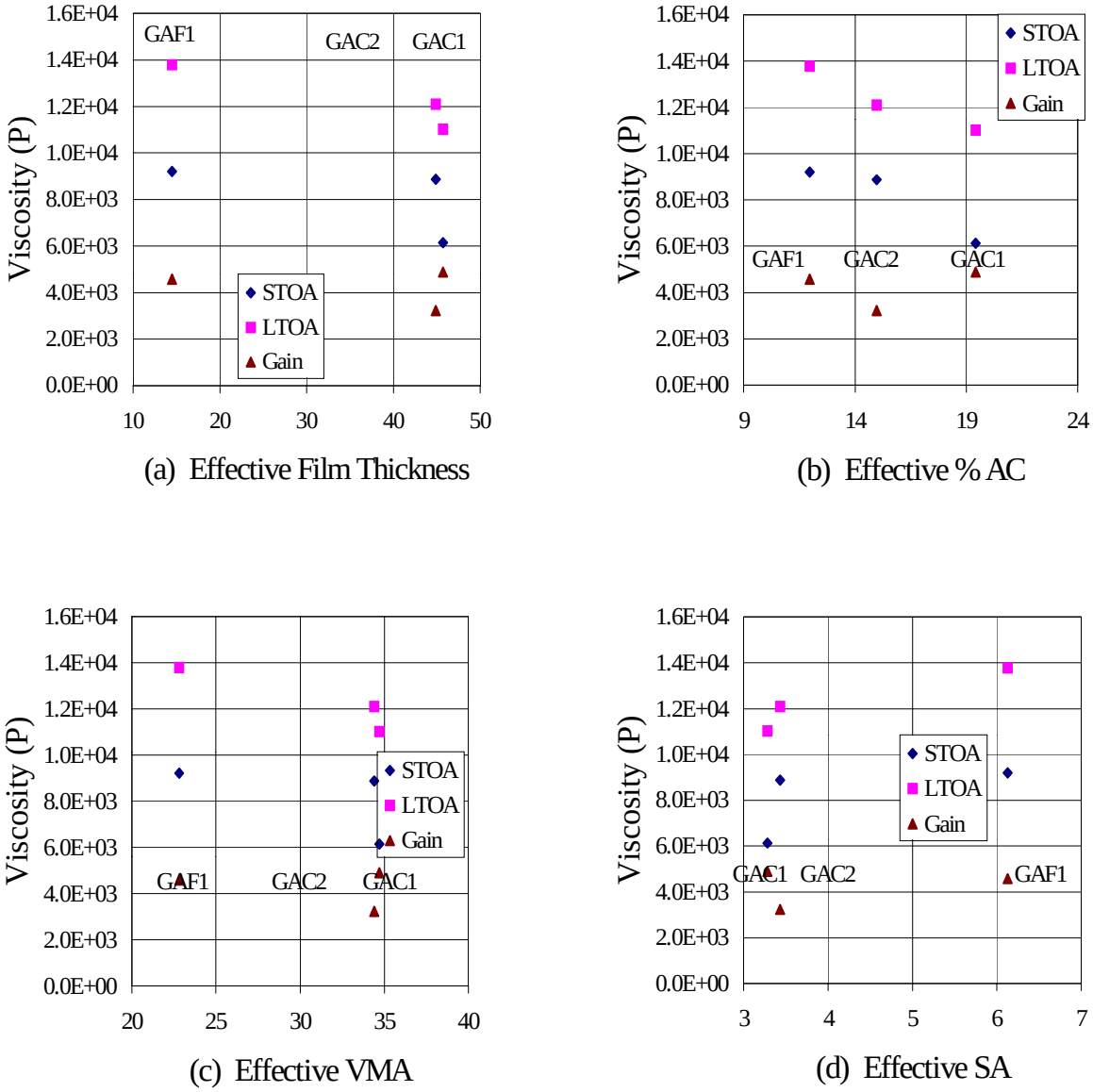

Figure 6-33 Viscosity Versus Effective Volumetric Properties (Granite Mixtures)

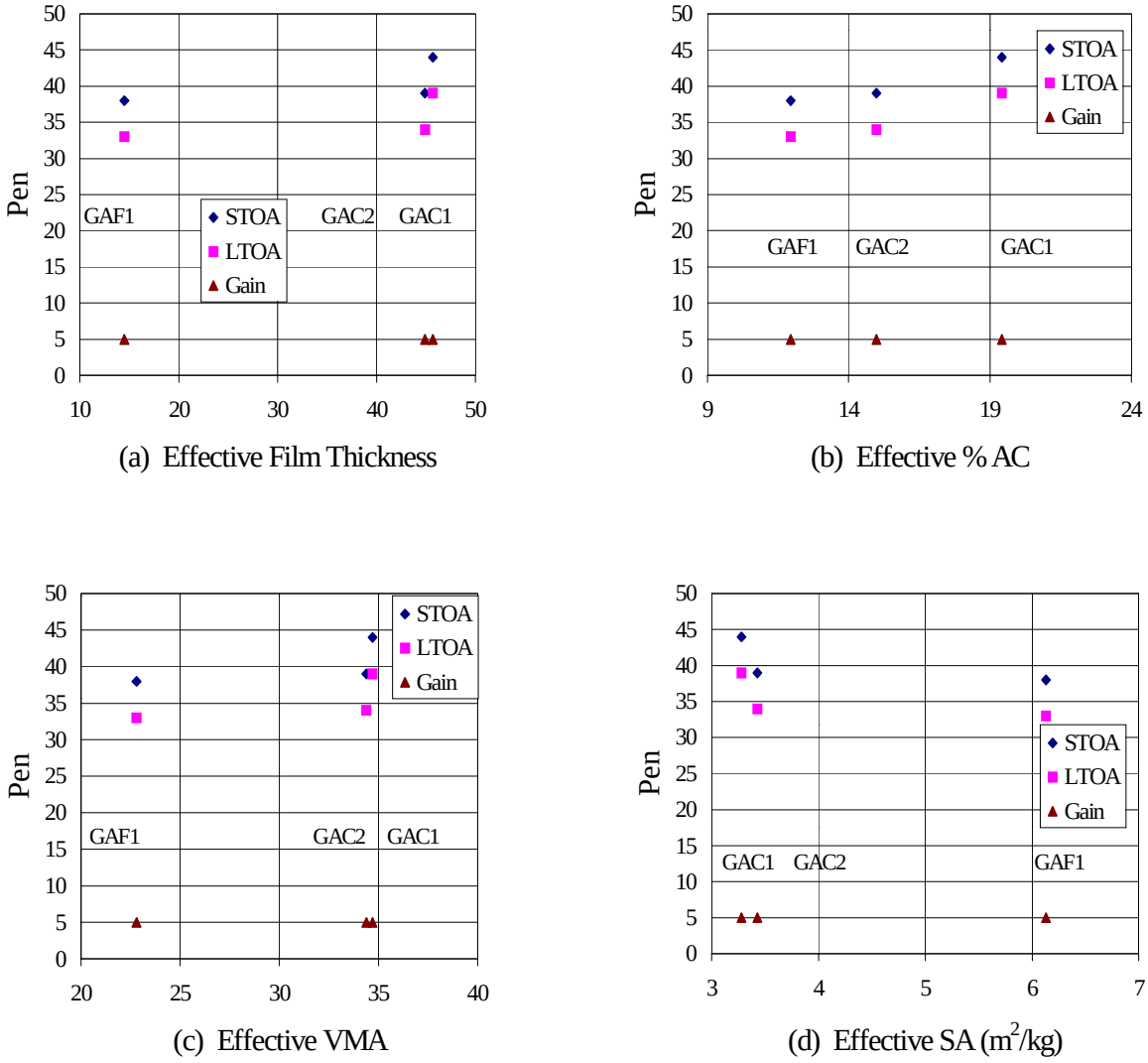

Figure 6-34 Penetration Versus Effective Volumetric Properties (Granite Mixtures)

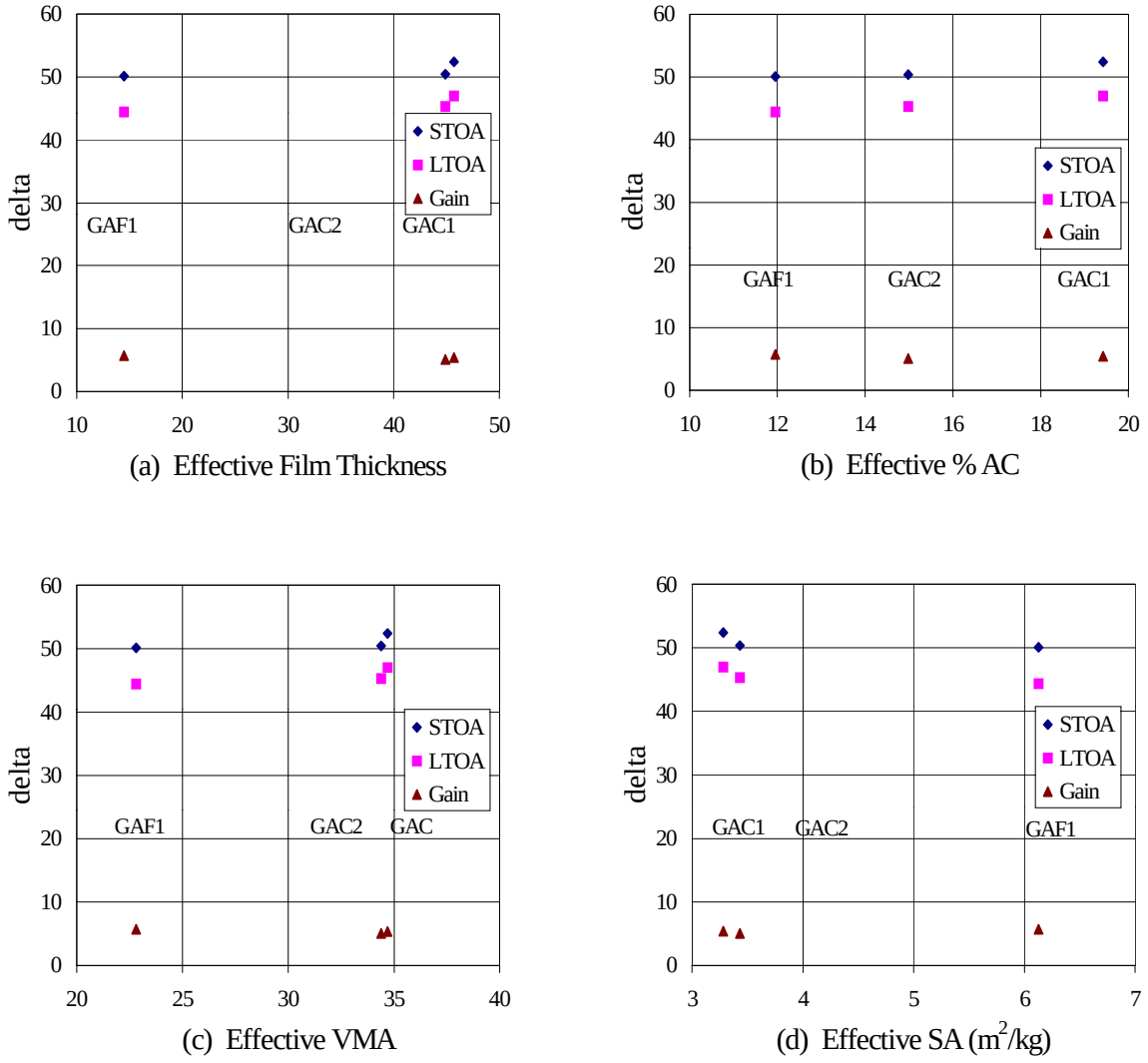

Figure 6-35 Delta Versus Effective Volumetric Properties (Granite Mixtures)

GAC1. This led to higher failure strain, higher fracture energy density, creep compliance and lower stiffness of GAC2 than GAC1. GAC2 therefore had a higher tensile strength than GAC1. This situation is explained in Figure 6-36.

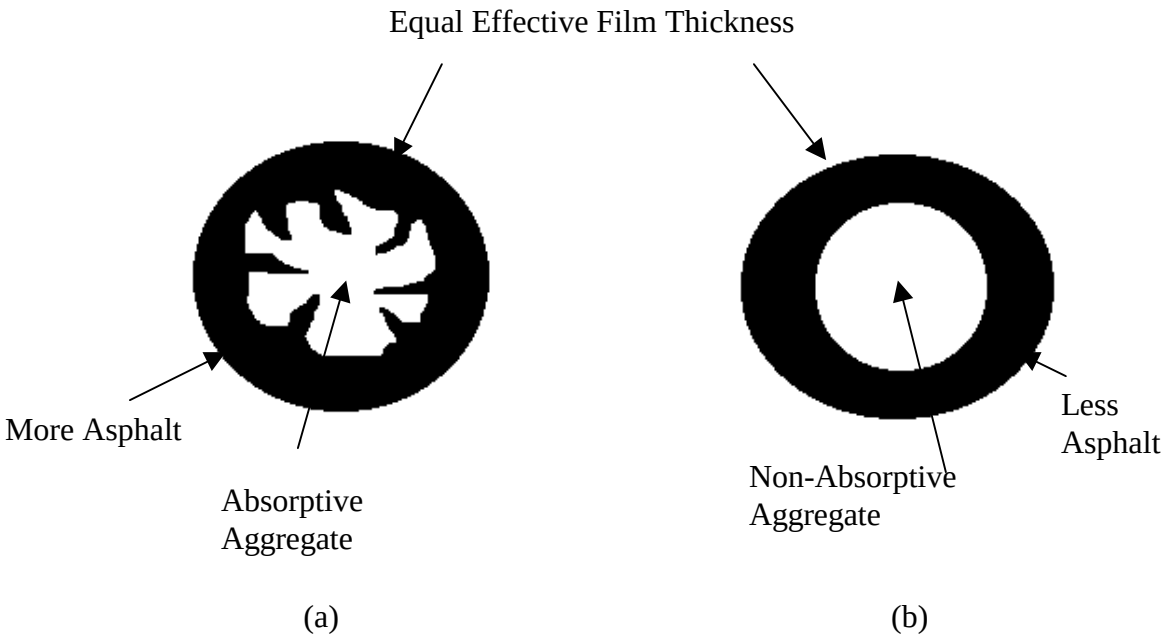

Figure 6-36 Schematic of Asphalt Film on Absorptive and Non-Absorptive Aggregates

GAC1 is made up of absorptive aggregate in Figure 6-36. GAC2 is the non-absorptive aggregate. GAC1 has lower theoretical VMA, film thickness and asphalt content than GAC1. GAC1 also has slightly higher effective parameters than GAC2. However when extracted binder properties were measured, binder from GAC2 was much stiffer than that of GAC1, because the extracted binder is a blend of both aged and unaged binder and GAC1 binder contained more absorbed binder. This implies that extracted binder contains more than the part of the binder which constitutes the effective film thickness and effective VMA, i.e., the part of the binder which is important for mixture performance. This phenomenon also explains why the stiffness of the binder

from GAF1, which is also a high absorptive aggregate, is not as high as is expected, but its properties change after age hardening because of its lower effective film thickness and VMA.

The effect of lower effective film thickness and VMA on age-hardening rate was more pronounced in the behavior of the fine mixture GAF1.

6.6 Findings

In conclusion, it could be stated that:

- Analysis of more mixtures confirmed previous results obtained in Chapters 4 and 5 in that there was no relationship between binder age-hardening rate and volumetric properties of the mixtures as they are calculated now. Rather there was a good correlation between binder age-hardening and effective film thickness and effective VMA.
- No clear relationship was observed between the mixture properties and the effective film thickness and effective VMA when all mixtures were analyzed together. However, there is good correlation when mixtures were analyzed separately as coarse-graded and fine-graded mixtures. Also, mixtures with lower effective film thickness age-hardened more than mixtures with higher effective film thickness. This showed that aging was accelerated at lower effective VMA and effective film thicknesses.
- Aging of asphalt is a diffusion process. Thus, aging is a surface phenomenon where asphalt is oxidized by the absorption of oxygen into the surface of the asphalt bounding the voids where aging starts. When the asphalt is extracted, the properties of the recovered binder are an average of the aged and unaged binder (including the

absorbed binder which may not have aged at all). The degree of aging measured by tests on the recovered binder are therefore an average value of the recovered asphalt blend. This may explain why the mixture behavior does not correlate well with the stiffness of the recovered binder measurements in mixtures containing aggregate blends with different degrees of absorption.

- Gradation is an important parameter for controlling mixture behavior. Gap-graded and open-graded mixtures tend to have inferior performance in relation to other continuous or dense-graded mixtures. The amount of binder within the mastic as measured by the effective asphalt content, effective film thickness and effective VMA also controls binder stiffness as well as mixture behavior.

CHAPTER 7
CLOSURE

7.1 Summary of Findings

This study provided some insight into the effects of changes in mixture volumetrics on specific mixture properties. Perhaps the clearest message from this research is to emphasize the importance of evaluating gradation and of performing physical tests, in addition to using volumetric criteria, when other reliable assessments of mixture performance are required to supplement volumetric mixture design.

The existing SuperPave™ VMA criterion, which is based solely on the nominal maximum sieve size did not relate to mixture aging and performance. The future of mixture durability and performance prediction for analyzing mixture behavior lies with the use of effective volumetric properties such as VMA and film thickness which are based on the percent passing the No. 8 sieve size. The existing methods for analyzing mixture durability is unacceptable for coarse mixtures especially after it has been shown in this research that the durability or resistance to age hardening of a mixture is influenced by the amount of the fine aggregates in the mixture.

The results from this research also show that the high minimum VMA requirement for coarse mixtures may result excessive asphalt, which may result in premature rutting. The findings are summarized below.

1. The maximum density line appears to separate coarse-graded mixtures from fine-graded mixtures.
2. Within the limits tested, percent fine aggregates (FA) appeared to control binder hardening, which was independent of theoretical film thickness and permeability.

3. Coarse-graded mixtures develop structures, which appear to encapsulate pockets of fine aggregates and asphalt mastic. This makes the theoretical film thickness concept used today irrelevant for coarse-graded mixtures. Similarly, VMA loses its meaning with respect to durability in this case.
4. Effective film thickness and VMA provide appropriate substitutes for evaluating mixture durability, but requirements may differ for coarse-graded and fine-graded mixtures.
5. Mixture properties such as resistance to shear and fracture tend to be more sensitive to the effective amount of binder as measured by the effective volumetric properties rather that the binder age hardening.
6. Low theoretical VMA or film thickness in coarse mixtures does not necessarily result in low effective VMA and film thickness. Also, high theoretical VMA and film thickness for fine mixtures does not necessarily result in higher effective values.
7. The effect of low effective film thickness and effective VMA on mixture performance are more pronounced in the fine mixtures than the coarse mixtures. Thus, fine mixtures with low film thickness and VMA lose their flexibility and become more brittle during aging.
8. Effect of gradation, which is obviously related to aggregate structure, has a significant influence on mixture fracture resistance and other performance indices like shear resistance, stiffness, failure strain and creep compliance.
9. The effective volumetric properties appear to be an effective tool for evaluating and controlling binder age hardening and mixture properties irrespective of the aggregate type used.

7.2 Conclusions

The current SuperPave™ VMA criterion at the design number of gyrations (N_{des}) at 4 % air voids may be adequate for the design of fine mixtures but not for coarse mixtures. From the analysis of the data, it can be concluded that the current minimum VMA restriction forces too much asphalt to be used in designing coarse mixtures. It allows mix designers to gap-grade coarse mixtures in order to meet the VMA criterion. High creep values and low shear resistance for high VMA coarse mixtures confirm these analyses. It would be very difficult to assign each gradation type its own design parameters. However, separate design parameters can be considered for fine and coarse categories of mixtures. Based on the findings above, the following conclusions were drawn:

- Within the limits of permeability of the mixtures studied, it appears binder age hardening does not depend on the permeability or degree of air circulation of asphalt mixtures. It neither depends on the void interconnection or voids structure of the mixtures so long as the air voids content remains the same.
- Binder age-hardening, as measured by the properties of the extracted binder alone, may not give an accurate picture of the stiffness of the asphalt film around the aggregate particles, especially when absorptive aggregates are used.
- VMA and film thickness as they are currently calculated do not control binder age-hardening, mixture durability and performance.

- Binder age-hardening and durability are controlled by the effective volumetric properties of mixtures calculated from formulas based on the fine aggregate portion of mixtures defined as percent aggregates passing the #8 sieve size.
- Mixtures with higher effective film thickness, VMA and effective asphalt content. have low stiffness and are more susceptible to rutting. This implies coarse mixtures that have high theoretical film thickness and VMA tend to have lower shear resistance. Thus, high minimum VMA requirement for SuperPave™ coarse mixtures is rather too restrictive and leads to soft SuperPave™ coarse mixtures.
- Coarse graded mixtures and fine-graded mixtures must not have the same design restrictions. They must be designed separately with different specifications.
- Mixture performance properties depend on the effective volumetric properties and may apply to mixtures of all aggregate types.

7.3 Recommendations

The following recommendations are provided for consideration:

- The current VMA criterion for SuperPave™ mixtures may be discontinued for coarse mixtures, especially when addressing their durability. However, it must be been done with caution in order to prevent mix designers from using inferior aggregates in their blends.
- The current VMA criterion together with film thickness could be used for analyzing and comparing fine mixtures.
- Any new SuperPave™ criteria for durability should be different for coarse and fine mixtures.

- Mixtures may be analyzed using the new concept described in this research since it has been tested extensively to confirm its viability in predicting binder age-hardening and mixture performance.
- There is the need to identify a system to select better gradations that will have a potential to yield much adequate and better mixtures. Additional gradation guidelines for fracture energy and rutting in asphalt mixtures may be in order. Development of a performance-based test for mixtures is desirable.

APPENDIX A
AGGREGATE PROPERTIES

Table A1: Coarse Aggregate Results

Aggregate Type	Percent By Mass (FDOT)	Percent By Mass (UF)	Bulk Specific Gravity (FDOT)	Bulk Specific Gravity (UF)
S1A Stone	10%	10.20%	2.441	2.4252
S1B Stone	62%	63.27%	2.442	2.4509
Stone Screenings	25%	25.51%	2.534	2.527
Mineral Filler	3%	1.02%	2.71	2.69
Combined Gradation	100%	100%	2.496	2.469

Table A2: Fine Aggregate Results

Aggregate Type	Percent By Mass (FDOT)	Percent By Mass (UF)	Bulk Specific Gravity (FDOT)	Bulk Specific Gravity (UF)
S1A Stone	20.0%	20.30%	2.441	2.4252
S1B Stone	25.0%	25.37%	2.442	2.4509
Stone Screenings	52.5%	53.29%	2.534	2.527
Mineral Filler	2.5%	1.03%	2.71	2.69
Combined Gradation	100%	100%	2.496	2.488

Table A3: Coarse Aggregate Specific Gravity

	SIA (1)	**SIA (2)**	**SIB (1)**	**SIB (2)**	**GA-185#89 (1)**	**GA-185#89 (1)**
Dry Weight in air (g)	2301.9	2136	2115.7	1910.2	1636	1665
Wet weight + sieve (g)	2462.5	2366.6	2364	2227.5	2106.6	2126.6
Weight of sieve (g)	1063.1	1063.1	1085	1085	1063.1	1063.1
Sat. weight in water (g)	1399.4	1303.5	1279	1142.5	1043.5	1063.5
SSD weight (g)	2348.7	2184.1	2142.1	1922	1646.2	1680.8
Bulk specific gravity	2.425	2.426	2.451	2.451	2.714	2.697
Average bulk specific gravity (g)	**2.4252**		**2.4509**		**2.7058**	
bulk sp. Gravity (SSD)	2.474	2.480	2.482	2.466	2.731	2.723
apparent sp. Gravity	2.551	2.566	2.529	2.488	2.761	2.768
absorption (%)	2.033	2.252	1.248	0.618	0.623	0.949

Table A4: Fine Aggregate Specific gravity

Screens	Asph. Scrn Whiterock	Asph. Scrn Whiterock	GA-185 W10-SCR	GA-185 W10-SCR	Anderson And. SCR	Anderson And. SCR
Wt + wt. Of flask	2519	2210.7	1752.8	1930.7	1882.1	1835.6
Wt. + wt of flask + water	4234.7	3948.8	3749.4	3852.7	3776.3	3767.7
wt. Of flask + water	3322.6	3243	3208.3	3231.7	3236	3198.9
wt. Of flask	1040.5	1078	907.5	961.8	990.5	900.2
Dry wt.	1478.5	1132.7	845.3	968.9	891.6	935.4
Wet wt.	3194.2	2870.8	2841.9	2890.9	2785.8	2867.5
SSD wt.	1499.2	1152.5	854.0	978.8	942.5	987.8
bulk sp. Gravity	2.5183	2.5357	2.7018	2.7077	2.2168	2.2325
Average bulk specific gravity	**2.5270**		**2.7047**		**2.2246**	
apparent sp. Gravity (SSD)	2.6103	2.6533	2.7788	2.7850	2.5380	2.5516
absorption	1.4001	1.7480	1.0252	1.0252	5.7088	5.6019
bulk sp. Gravity (SSD)	2.5536	2.5800	2.7295	2.7354	2.3434	2.3575

Table A5: Aggregate Pit Numbers

Aggregate Type	Pit Number	FDOT Code
SIA Stone	87-339	41
SIB Stone	87-340	54
Screenings	87-341	20

Table A6: Washed Gradation Results (Whiterock)

	S1A			S1B			Screens		
Sieve Size	Weight Retained	Weight Passing	% passing	Weight Retained	Weight Passing	% passing	Weight Retained	Weight Passing	% passing
25(1")	0.0	1733.6	100.0	0.0	1589.2	100.0	0.0	1592.9	100.0
19(3/4")	0.0	1733.6	100.0	0.0	1589.2	100.0	0.0	1592.9	100.0
12.5(1/2")	372.6	1361.0	78.5	1589.2	1589.2	100.0	0.0	1592.9	100.0
9.5(3/8")	822.0	539.0	31.1	140.3	1448.9	91.2	0.0	1592.9	100.0
4.75(#4)	462.3	76.7	4.4	775.7	673.2	42.4	0.8	1592.9	100.0
2.36(#8)	33.1	43.6	2.5	481.4	191.8	12.1	195.1	1397.8	87.8
1.18(#16)	7.9	35.7	2.1	108.9	82.9	5.2	376.3	1021.5	64.1
0.6(#30)	2.2	33.5	1.9	23.1	59.8	3.8	278.3	743.2	46.7
0.3(#50)	2.5	31.0	1.8	9.8	50.0	3.1	281.6	461.6	29.0
0.15(#100)	4.8	26.2	1.5	9.8	40.2	2.5	323.9	137.7	8.6
0.075(#200)	6.3	19.9	1.1	11.0	29.2	1.8	109.9	27.8	1.7
<0.075(<200)	19.9			29.2			27.0		
Total Wt. (g)	1733.6			1589.2			1592.9		

Table A7: Washed Gradation Results (Granite)

GA 185	#89 Stone			W-10-Screens			Anderson Screens		
Sieve Size	Weight Retained	Weight Passing	% passing	Weight Retained	Weight Passing	% passing	Weight Retained	Weight Passing	% passing
25(1")	0.0	1688.7	100.0	0.0	1206.5	100.0	0.0	1243.0	100.0
19(3/4")	0.0	1688.7	100.0	0.0	1206.5	100.0	0.0	1243.0	100.0
12.5(1/2")	0.0	1688.7	100.0	0.0	1206.5	100.0	0.0	1243.0	100.0
9.5(3/8")	158.8	1529.9	90.6	0.0	1206.5	100.0	0.0	1243.0	100.0
4.75(#4)	1166.5	363.4	21.5	10.0	1196.5	99.2	117.7	1125.3	90.5
2.36(#8)	344.6	18.8	1.1	230.4	966.1	80.1	231.2	894.1	71.9
1.18(#16)	8.4	10.4	0.6	310.3	655.8	54.4	243.6	650.5	52.3
0.6(#30)	0.9	9.5	0.6	210.6	445.2	36.9	174.0	476.5	38.3
0.3(#50)	0.4	9.1	0.5	174.0	271.2	22.5	167.1	309.4	24.9
0.15(#100)	0.6	8.5	0.5	145.3	125.9	10.4	183.0	126.4	10.2
0.075(#200)	1.4	7.1	0.4	68.7	57.2	4.7	75.2	51.2	4.1
<0.075(<200)	7.1			57.2			51.2		
Total Wt. (g)	1688.7			1206.5			1243.0		

APPENDIX B
GRADATIONS

Table B1: Verification of FDOT Job Mix Formula

Sieve Size	Coarse 1			Fine 1		
mm	UF	DOT	AI	UF	DOT	AI
25(1")	100.0	100.0	100.0	100.0	100.0	100.0
19(3/4")	100.0	100.0	100.0	100.0	100.0	100.0
12.5(1/2")	97.4	98.3	97.5	95.5	96.6	94.9
9.5(3/8")	90.0	91.5	89.4	85.1	86.6	84.6
4.75(#4)	60.2	58.3	56.9	69.3	68.6	67.7
2.36(#8)	33.1	30.5	31.6	52.7	52.4	50.8
1.18(#16)	20.3	20.8	21.3	34.0	34.5	34.2
0.6(#30)	14.7	15.1	15.3	22.9	23.6	22.5
0.3(#50)	10.8	11.0	11.3	15.3	15.2	14.4
0.15(#100)	7.6	6.5	7.3	9.6	7.5	7.4
0.075(#200)	4.8	4.4	5.2	4.8	4.4	4.5

Table B3: Coarse Whiterock Gradation

Sieve Size	Coarse				
mm	C1	C2	C3	C4/F3	C5
25(1")	100.0	100.0	100.0	100.0	100.0
19(3/4")	100.0	100.0	100.0	100.0	100.0
12.5(1/2")	97.4	91.1	97.6	94.5	97.4
9.5(3/8")	90.0	73.5	89.3	84.9	89.9
4.75(#4)	60.2	47.1	57.4	66.5	47.1
2.36(#8)	33.1	29.6	36.4	36.6	33.1
1.18(#16)	20.3	20.2	24.0	26.1	20.3
0.6(#30)	14.7	14.4	17.7	20.5	14.7
0.3(#50)	10.8	10.4	12.9	13.6	10.8
0.15(#100)	7.6	6.7	9.2	8.6	7.6
0.075(#200)	4.8	4.8	6.3	5.8	4.8

Table B4: Fine Whiterock Gradations

Sieve Size	Fine					
mm	F1	F2	C4/F3	F4	F5	F6
25(1")	100.0	100.0	100.0	100.0	100.0	100.0
19(3/4")	100.0	100.0	100.0	100.0	100.0	100.0
12.5(1/2")	95.5	90.8	94.5	95.5	95.5	95.5
9.5(3/8")	85.1	78.0	84.9	85.1	85.1	85.1
4.75(#4)	69.3	61.3	66.5	69.3	61.3	69.3
2.36(#8)	52.7	44.1	36.6	52.7	52.7	44.1
1.18(#16)	34.0	34.7	26.1	40.0	34.0	34.7
0.6(#30)	22.9	23.6	20.5	29.0	22.9	23.6
0.3(#50)	15.3	15.7	13.6	20.0	15.3	15.7
0.15(#100)	9.6	9.1	8.6	12.0	9.6	9.1
0.075(#200)	4.8	6.3	5.8	6.3	4.8	6.3

Table B5: Granite Gradations

Sieve Size	GA Mixtures		
mm	C1	C11	F1
25(1")	100.0	100.0	100.0
19(3/4")	100.0	100.0	100.0
12.5(1/2")	100.0	100.0	100.0
9.5(3/8")	99.2	99.3	99.9
4.75(#4)	54.8	57.9	86.5
2.36(#8)	32.2	34.3	63.2
1.18(#16)	18.5	20.4	43.0
0.6(#30)	14.5	15.6	30.3
0.3(#50)	9.8	10.3	22.1
0.15(#100)	6.6	6.8	9.8
0.075(#200)	3.3	3.4	4.5

Table B6: Batch Weights for C1

sieve size mm	s1a	s1b	scr	filler
12.5	116	459	3306	4454
9.5	318	630	3306	4454
4.75	429	2011	3306	4454
2.36	445	2987	3472	4454
1.18	449	3127	3804	4454
600	450	3149	4054	4454
300	451	3158	4230	4454
150	452	3192	4376	4454
75	454	3226	4424	4459
<75	459	3306	4454	4500

Table B7: Batch Weights for C2

sieve size mm	s1a	s1b	scr	filler
12.5(1/2)	403	1591	3273	4409
9.5(3/8)	1103	1692	3273	4409
4.75(#4)	1486	2508	3273	4409
2.36(#8)	1543	3084	3438	4409
1.18(#16)	1556	3167	3766	4409
600(#30)	1559	3180	4014	4409
300(#50)	1562	3185	4188	4409
150(#100)	1567	3206	4332	4409
75(#200)	1573	3226	4380	4418
<75(#200)	1591	3273	4409	4500

Table B8: Batch Weights for C3

sieve size mm	s1a	s1b	scr	filler
12.5(1/2)	122	1215	2970	4365
9.5(3/8)	358	1320	2970	4365
4.75(#4)	1018	2171	2970	4365
2.36(#8)	1179	2773	3172	4365
1.18(#16)	1188	2859	3575	4365
600(#30)	1191	2873	3880	4365
300(#50)	1193	2879	4093	4365
150(#100)	1197	2900	4270	4365
75(#200)	1215	2921	4329	4379
<75(#200)	1215	2970	4365	4500

Table B9: Batch Weights for C5

sieve size mm	whiterock
12.5(1/2)	119
9.5(3/8)	462
4.75(#4)	2417
2.36(#8)	3057
1.18(#16)	3642
600(#30)	3898
300(#50)	4076
150(#100)	4223
75(#200)	4351
<75(#200)	4500

Table B10: Batch Weights for F1

sieve size mm	s1a	s1b	scr	filler
12.5(1/2)	231	914	2056	4454
9.5(3/8)	633	983	2056	4454
4.75(#4)	853	1536	2056	4454
2.36(#8)	886	1928	2404	4454
1.18(#16)	893	1984	3097	4454
600(#30)	895	1993	3619	4454
300(#50)	897	1997	3986	4454
150(#100)	900	2010	4291	4454
75(#200)	903	2024	4392	4459
<75(#200)	914	2056	4454	4500

Table B11: Batch Weights for F2

sieve size mm	s1a	s1b	scr	filler
12.5(1/2)	416	1980	1980	4275
9.5(3/8)	990	1980	1980	4275
4.75(#4)	1742	1980	1980	4275
2.36(#8)	1940	1980	2554	4275
1.18(#16)	1940	1980	2976	4275
600(#30)	1940	1980	3476	4275
300(#50)	1944	1980	3827	4275
150(#100)	1950	1980	4119	4275
75(#200)	1958	1980	4266	4298
<75(#200)	1980	1980	4275	4500

Table B12: Batch Weights for C4/F3

sieve size mm	s1a	s1b	scr	filler
12.5(1/2)	122	1215	2970	4365
9.5(3/8)	358	1320	2970	4365
4.75(#4)	1018	2171	2970	4365
2.36(#8)	1179	2773	3172	4365
1.18(#16)	1188	2859	3575	4365
600(#30)	1191	2873	3880	4365
300(#50)	1193	2879	4093	4365
150(#100)	1197	2900	4270	4365
75(#200)	1215	2921	4329	4379
<75(#200)	1215	2970	4365	4500

Table B13: Batch Weights for F4

sieve size mm	whiterock
12.5(1/2)	210
9.5(3/8)	696
4.75(#4)	1433
2.36(#8)	2208
1.18(#16)	2801
600(#30)	3314
300(#50)	3734
150(#100)	4108
75(#200)	4374
<75(#200)	4500

Table B14: Batch Weights for F5

sieve size mm	whiterock
12.5(1/2)	209
9.5(3/8)	693
4.75(#4)	1801
2.36(#8)	2200
1.18(#16)	3069
600(#30)	3585
300(#50)	3939
150(#100)	4204
75(#200)	4427
<75(#200)	4500

Table B15: Batch Weights for F6

sieve size mm	whiterock
12.5(1/2)	47
9.5(3/8)	154
4.75(#4)	318
2.36(#8)	579
1.18(#16)	676
600(#30)	791
300(#50)	873
150(#100)	941
75(#200)	971
<75(#200)	1000

Table B16: Batch Weights for GAC1

sieve size mm	#89 stone	W-10-SCR	And. SCR
12.5(1/2)	0	2722	2722
9.5(3/8)	11	2722	2722
4.75(#4)	1981	2722	2894
2.36(#8)	2692	2722	3232
1.18(#16)	2705	2722	3587
600(#30)	2705	2722	3841
300(#50)	2705	2722	4084
150(#100)	2705	2722	4351
75(#200)	2705	2722	4462
<75(#200)	2722	2722	4500

Table B17: Batch Weights for GAC2

sieve size mm	#89 stone	W-10-SCR	And. SCR
12.5(1/2)	0	2700	4500
9.5(3/8)	27	2700	4500
4.75(#4)	1917	2736	4500
2.36(#8)	2511	3204	4500
1.18(#16)	2646	3636	4500
600(#30)	2646	3906	4500
300(#50)	2646	4122	4500
150(#100)	2646	4302	4500
75(#200)	2673	4403	4500
<75(#200)	2700	4500	4500

Table B18: Batch Weights for GAF1

sieve size mm	#89 stone	W-10-SCR	And. SCR
12.5(1/2)	0	684	3150
9.5(3/8)	3	684	3150
4.75(#4)	498	704	3280
2.36(#8)	676	1303	3535
1.18(#16)	680	1933	3803
600(#30)	680	2324	3994
300(#50)	680	2550	4178
150(#100)	680	2931	4379
75(#200)	680	3054	4462
<75(#200)	684	3150	4500

APPENDIX C
MIXTURE DESIGN DATA

Table C1: Mixture Design Properties for C1

Property	Symbol	Blend			Design	Superpave Criteria
	AC%	6.2	6.7	7.2	6.5	
Maximum Theoretical Specific Gravity	Gmm	2.3343	2.3236	2.3143	2.3279	
Asphalt Specific Gravity	Gb	1.035	1.035	1.035	1.035	
Bulk Specific Gravity of Compacted Mix	Gmb	2.2276	2.2421	2.2492	2.2349	
Asphalt Content	Pb	6.2	6.7	7.2	6.5	
Bulk Specific Gravity of Aggregate	Gsb	2.469	2.469	2.469	2.469	
Effective Specific Gravity of Aggregate	Gse	2.546	2.552	2.560	2.549	
Asphalt Absorption	Pba	1.260	1.359	1.487	1.320	
% Gmm @ N_{ini}		83.6	84.6	85.0	85.0	89% Maximum
% Gmm @ N_{max}		97.4	98.4	98.8	98.8	98% Maximum
Effective Asphalt Content of Mixture	Pbe	5.018	5.432	5.820	5.266	
Percent VMA in Compacted Mix	VMA	15.371	15.274	15.461	15.365	14% Minimum
Percent Air Voids in Compacted Mix	Va	4.571	3.507	2.813	3.995	4%
Percent VFA in Compacted Mix	VFA	70.263	77.037	81.807	74.000	65% to 75%
Dust to Asphalt Ratio	D/A	1.0	1.0	0.9	1.0	0.6% to 1.2%

Table C2: Mixture Design Properties for C2

Property	Symbol	Blend			Design	Superpave Criteria
	AC%	5.2	5.7	6.2	5.8	
Maximum Theoretical Specific Gravity	Gmm	2.3743	2.3511	2.3288	2.3466	
Asphalt Specific Gravity	Gb	1.035	1.035	1.035	1.035	
Bulk Specific Gravity of Compacted Mix	Gmb	2.2356	2.2531	2.2589	2.2545	
Asphalt Content	Pb	5.2	5.7	6.2	5.8	
Bulk Specific Gravity of Aggregate	Gsb	2.465	2.465	2.465	2.465	
Effective Specific Gravity of Aggregate	Gse	2.556	2.547	2.539	2.545	
Asphalt Absorption	Pba	1.490	1.349	1.217	1.323	
% Gmm @ N_{ini}		83.3	84.8	85.2	84.7	89% Maximum
% Gmm @ N_{max}		95.8	97.5	98.8	97.7	98% Maximum
Effective Asphalt Content of Mixture	Pbe	3.787	4.427	5.059	4.554	
Percent VMA in Compacted Mix	VMA	14.022	13.806	14.043	13.844	14% Minimum
Percent Air Voids in Compacted Mix	Va	5.842	4.168	3.002	3.925	4%
Percent VFA in Compacted Mix	VFA	58.340	69.809	78.626	71.650	65% to 75%
Dust to Asphalt Ratio	D/A	1.3	1.1	0.9	1.0	0.6% to 1.2%

Table C3: Mixture Design Properties for C3

Property	Symbol	Blend			Design	Superpave Criteria
	AC%	5.5	6	6.5	5.3	
Maximum Theoretical Specific Gravity	Gmm	2.3497	2.3441	2.3361	2.3486	
Asphalt Specific Gravity	Gb	1.035	1.035	1.035	1.035	
Bulk Specific Gravity of Compacted Mix	Gmb	2.2617	2.2723	2.2824	2.2535	
Asphalt Content	Pb	5.5	6	6.5	5.3	
Bulk Specific Gravity of Aggregate	Gsb	2.474	2.474	2.474	2.474	
Effective Specific Gravity of Aggregate	Gse	2.537	2.550	2.560	2.528	
Asphalt Absorption	Pba	1.043	1.246	1.402	0.897	
% Gmm @ N_{ini}		84.8	85.2	85.1	84.2	89% Maximum
% Gmm @ N_{max}		98	98.7	99.1	97.5	98% Maximum
Effective Asphalt Content of Mixture	Pbe	4.514	4.828	5.189	4.451	
Percent VMA in Compacted Mix	VMA	13.609	13.664	13.741	13.740	14% Minimum
Percent Air Voids in Compacted Mix	Va	3.745	3.063	2.299	4.049	4%
Percent VFA in Compacted Mix	VFA	72.481	77.583	83.271	70.530	65% to 75%
Dust to Asphalt Ratio	D/A	1.2	1.1	1.0	1.2	0.6% to 1.2%

Table C4: Mixture Design Properties for C5

Property	Symbol	Blend			Design	Superpave Criteria
	AC%	6	6.3	6.5	6.3	
Maximum Theoretical Specific Gravity	Gmm	2.3477	2.3418	2.3379	2.3418	
Asphalt Specific Gravity	Gb	1.035	1.035	1.035	1.035	
Bulk Specific Gravity of Compacted Mix	Gmb	2.2203	2.2472	2.2669	2.2472	
Asphalt Content	Pb	6	6.3	6.5	6.3	
Bulk Specific Gravity of Aggregate	Gsb	2.467	2.467	2.467	2.467	
Effective Specific Gravity of Aggregate	Gse	2.555	2.559	2.562	2.559	
Asphalt Absorption	Pba	1.437	1.509	1.558	1.509	
% Gmm @ N_{ini}		83.1	84.2	85	84.2	89% Maximum
% Gmm @ N_{max}		96.5	97.8	98.8	97.8	98% Maximum
Effective Asphalt Content of Mixture	Pbe	4.649	4.886	5.044	4.886	
Percent VMA in Compacted Mix	VMA	15.400	14.648	14.084	14.648	14% Minimum
Percent Air Voids in Compacted Mix	Va	5.427	4.040	3.037	4.040	4%
Percent VFA in Compacted Mix	VFA	64.762	72.423	78.437	72.423	65% to 75%
Dust to Asphalt Ratio	D/A	1.0	1.0	1.0	1.0	0.6% to 1.2%

Table C5: Mixture Design Properties for F1

Property	Symbol	Blend			Design	Superpave Criteria
	AC%	5.5	6	6.5	6.3	
Maximum Theoretical Specific Gravity	Gmm	2.3595	2.3472	2.3315	2.3378	
Asphalt Specific Gravity	Gb	1.035	1.035	1.035	1.035	
Bulk Specific Gravity of Compacted Mix	Gmb	2.2072	2.2393	2.2433	2.2436	
Asphalt Content	Pb	5.5	6	6.5	6.3	
Bulk Specific Gravity of Aggregate	Gsb	2.488	2.488	2.488	2.488	
Effective Specific Gravity of Aggregate	Gse	2.549	2.554	2.554	2.554	
Asphalt Absorption	Pba	1.002	1.073	1.073	1.074	
% Gmm @ N_{ini}		84.6	86.0	86.6	86.3	89% Maximum
% Gmm @ N_{max}		94.8	96.8	97.7	97.4	98% Maximum
Effective Asphalt Content of Mixture	Pbe	4.554	4.991	5.496	5.293	
Percent VMA in Compacted Mix	VMA	16.165	15.396	15.696	15.504	14% Minimum
Percent Air Voids in Compacted Mix	Va	6.455	4.597	3.783	4.029	4%
Percent VFA in Compacted Mix	VFA	60.071	70.142	75.898	74.011	65% to 75%
Dust to Asphalt Ratio	D/A	1.1	1.0	0.9	0.9	0.6% to 1.2%

Table C6: Mixture Design Properties for F2

Property	Symbol	Blend			Design	Superpave Criteria
	AC%	5.5	6	6.5	5.4	
Maximum Theoretical Specific Gravity	Gmm	2.371	2.3545	2.338	2.3752	
Asphalt Specific Gravity	Gb	1.035	1.035	1.035	1.035	
Bulk Specific Gravity of Compacted Mix	Gmb	2.2892	2.3277	2.3248	2.2814	
Asphalt Content	Pb	5.5	6	6.5	5.4	
Bulk Specific Gravity of Aggregate	Gsb	2.489	2.489	2.489	2.489	
Effective Specific Gravity of Aggregate	Gse	2.564	2.563	2.562	2.565	
Asphalt Absorption	Pba	1.210	1.202	1.189	1.229	
% Gmm @ N_{ini}		87.9	90.2	91	87.5	89% Maximum
% Gmm @ N_{max}		97.6	99.7	100	97.4	98% Maximum
Effective Asphalt Content of Mixture	Pbe	4.357	4.870	5.389	4.238	
Percent VMA in Compacted Mix	VMA	13.086	12.092	12.668	13.290	14% Minimum
Percent Air Voids in Compacted Mix	Va	3.450	1.138	0.565	3.949	4%
Percent VFA in Compacted Mix	VFA	73.635	90.587	95.543	70.286	65% to 75%
Dust to Asphalt Ratio	D/A	1.5	1.5	1.2	1.5	0.6% to 1.2%

Table C7: Mixture Design Properties for C4/F3

Property	Symbol	Blend			Design	Superpave Criteria
	AC%	5.5	5.8	6	5.6	
Maximum Theoretical Specific Gravity	Gmm	2.3488	2.3448	2.3421	2.3466	
Asphalt Specific Gravity	Gb	1.035	1.035	1.035	1.035	
Bulk Specific Gravity of Compacted Mix	Gmb	2.2402	2.2644	2.2649	2.2541	
Asphalt Content	Pb	5.5	5.8	6	5.6	
Bulk Specific Gravity of Aggregate	Gsb	2.478	2.478	2.478	2.478	
Effective Specific Gravity of Aggregate	Gse	2.536	2.543	2.547	2.537	
Asphalt Absorption	Pba	0.958	1.067	1.139	0.977	
% Gmm @ N_{ini}		84.2	85.6	85.6	84.7	89% Maximum
% Gmm @ N_{max}		96.5	98.2	98.3	97.2	98% Maximum
Effective Asphalt Content of Mixture	Pbe	4.595	4.795	4.930	4.678	
Percent VMA in Compacted Mix	VMA	14.569	13.920	14.084	14.130	14% Minimum
Percent Air Voids in Compacted Mix	Va	4.624	3.429	3.296	3.942	4%
Percent VFA in Compacted Mix	VFA	68.263	75.367	76.596	72.102	65% to 75%
Dust to Asphalt Ratio	D/A	1.3	1.2	1.2	1.2	0.6% to 1.2%

Table C8: Mixture Design Properties for F4

Property	Symbol	Blend			Design	Superpave Criteria
	AC%	5.5	5.7	6	5.7	
Maximum Theoretical Specific Gravity	Gmm	2.3748	2.3677	2.3571	2.3677	
Asphalt Specific Gravity	Gb	1.035	1.035	1.035	1.035	
Bulk Specific Gravity of Compacted Mix	Gmb	2.2404	2.2724	2.3149	2.2724	
Asphalt Content	Pb	5.5	5.7	6	5.7	
Bulk Specific Gravity of Aggregate	Gsb	2.491	2.491	2.491	2.491	
Effective Specific Gravity of Aggregate	Gse	2.568	2.568	2.566	2.568	
Asphalt Absorption	Pba	1.251	1.239	1.220	1.239	
% Gmm @ N_{ini}		86.9	88.5	89.4	88.5	89% Maximum
% Gmm @ N_{max}		95.4	97	99.3	97	98% Maximum
Effective Asphalt Content of Mixture	Pbe	4.318	4.532	4.853	4.532	
Percent VMA in Compacted Mix	VMA	15.007	13.975	12.645	13.975	14% Minimum
Percent Air Voids in Compacted Mix	Va	5.659	4.025	1.790	4.025	4%
Percent VFA in Compacted Mix	VFA	62.288	71.199	85.842	71.199	65% to 75%
Dust to Asphalt Ratio	D/A	1.4	1.3	1.2	1.3	0.6% to 1.2%

Table C9: Mixture Design Properties for F5

Property	Symbol	Blend			Design	Superpave Criteria
	AC%	6	6.5	6.7	6.7	
Maximum Theoretical Specific Gravity	Gmm	2.3429	2.3311	2.3264	2.3264	
Asphalt Specific Gravity	Gb	1.035	1.035	1.035	1.035	
Bulk Specific Gravity of Compacted Mix	Gmb	2.2063	2.2257	2.2325	2.2325	
Asphalt Content	Pb	6	6.5	6.7	6.7	
Bulk Specific Gravity of Aggregate	Gsb	2.485	2.485	2.485	2.485	
Effective Specific Gravity of Aggregate	Gse	2.548	2.553	2.555	2.555	
Asphalt Absorption	Pba	1.037	1.116	1.147	1.147	
% Gmm @ N_{ini}		85.5	86.5	86.8	86.8	89% Maximum
% Gmm @ N_{max}		95.5	96.8	97.4	97.4	98% Maximum
Effective Asphalt Content of Mixture	Pbe	5.025	5.457	5.630	5.630	
Percent VMA in Compacted Mix	VMA	16.542	16.256	16.180	16.180	14% Minimum
Percent Air Voids in Compacted Mix	Va	5.830	4.521	4.036	4.036	4%
Percent VFA in Compacted Mix	VFA	64.755	72.186	75.054	75.054	65% to 75%
Dust to Asphalt Ratio	D/A	0.9	0.9	0.8	0.8	0.6% to 1.2%

Table C10: Mixture Design Properties for F6

Property	Symbol	Blend			Design	Superpave Criteria
	AC%	5.5	6	6.1	6.1	
Maximum Theoretical Specific Gravity	Gmm	2.3557	2.3436	2.3412	2.3412	
Asphalt Specific Gravity	Gb	1.035	1.035	1.035	1.035	
Bulk Specific Gravity of Compacted Mix	Gmb	2.2114	2.2415	2.2436	2.2436	
Asphalt Content	Pb	5.5	6	6.1	6.1	
Bulk Specific Gravity of Aggregate	Gsb	2.489	2.489	2.489	2.489	
Effective Specific Gravity of Aggregate	Gse	2.545	2.549	2.550	2.550	
Asphalt Absorption	Pba	0.910	0.984	0.999	0.999	
% Gmm @ N_{ini}		85.5	86.2	86.7	86.7	89% Maximum
% Gmm @ N_{max}		95.1	97.1	97.7	97.7	98% Maximum
Effective Asphalt Content of Mixture	Pbe	4.640	5.075	5.162	5.162	
Percent VMA in Compacted Mix	VMA	16.040	15.347	15.358	15.358	14% Minimum
Percent Air Voids in Compacted Mix	Va	6.126	4.357	4.169	4.169	4%
Percent VFA in Compacted Mix	VFA	61.810	71.613	72.856	72.856	65% to 75%
Dust to Asphalt Ratio	D/A	1.3	1.2	1.1	1.1	0.6% to 1.2%

Table C11: Mixture Design Properties for GAC1

Property	Symbol	Blend			Design	Superpave Criteria
	AC%	6	6.5	7.1	7.1	
Maximum Theoretical Specific Gravity	Gmm	2.4764	2.4532	2.4254	2.4254	
Asphalt Specific Gravity	Gb	1.035	1.035	1.035	1.035	
Bulk Specific Gravity of Compacted Mix	Gmb	2.2965	2.3064	2.3301	2.3301	
Asphalt Content	Pb	6	6.5	7.1	7.1	
Bulk Specific Gravity of Aggregate	Gsb	2.496	2.496	2.496	2.496	
Effective Specific Gravity of Aggregate	Gse	2.718	2.711	2.703	2.703	
Asphalt Absorption	Pba	3.387	3.295	3.174	3.174	
% Gmm @ N_{ini}		81.7	82.4	83.9	83.9	89% Maximum
% Gmm @ N_{max}		94.5	95.8	97.9	97.9	98% Maximum
Effective Asphalt Content of Mixture	Pbe	2.816	3.419	4.151	4.151	
Percent VMA in Compacted Mix	VMA	13.513	13.602	13.275	13.275	15% Minimum
Percent Air Voids in Compacted Mix	Va	7.265	5.984	3.929	3.929	4%
Percent VFA in Compacted Mix	VFA	46.241	56.008	70.401	70.401	65% to 75%
Dust to Asphalt Ratio	D/A	1.1	0.9	0.8	0.8	0.6% to 1.2%

Table C12: Mixture Design Properties for GAC2

Property	Symbol	Blend			Design	Superpave Criteria
	AC%	5.4	5.5	6.5	5.7	
Maximum Theoretical Specific Gravity	Gmm	2.536	2.5315	2.487	2.5225	
Asphalt Specific Gravity	Gb	1.035	1.035	1.035	1.035	
Bulk Specific Gravity of Compacted Mix	Gmb	2.3896	2.4072	2.472	2.4193	
Asphalt Content	Pb	5.4	5.5	6.5	5.7	
Bulk Specific Gravity of Aggregate	Gsb	2.705	2.705	2.705	2.705	
Effective Specific Gravity of Aggregate	Gse	2.765	2.764	2.756	2.762	
Asphalt Absorption	Pba	0.829	0.818	0.705	0.796	
% Gmm @ N_{ini}		84.3	84.4	87.4	85.9	89% Maximum
% Gmm @ N_{max}		95.4	95.7	99.4	97.6	98% Maximum
Effective Asphalt Content of Mixture	Pbe	4.616	4.727	5.841	4.949	
Percent VMA in Compacted Mix	VMA	16.430	15.904	14.554	15.660	15% Minimum
Percent Air Voids in Compacted Mix	Va	5.773	4.910	0.603	4.091	4%
Percent VFA in Compacted Mix	VFA	64.864	69.126	95.856	73.875	65% to 75%
Dust to Asphalt Ratio	D/A	0.7	0.7	0.6	0.6	0.6% to 1.2%

Table C13: Mixture Design Properties for GAF1

Property	Symbol	Blend			Design	Superpave Criteria
	AC%	7.0	7.5	7.9	7.9	
Maximum Theoretical Specific Gravity	Gmm	2.435	2.423	2.4134	2.4134	
Asphalt Specific Gravity	Gb	1.035	1.035	1.035	1.035	
Bulk Specific Gravity of Compacted Mix	Gmb	2.275	2.3015	2.3173	2.3173	
Asphalt Content	Pb	7	7.5	7.9	7.9	
Bulk Specific Gravity of Aggregate	Gsb	2.540	2.540	2.540	2.540	
Effective Specific Gravity of Aggregate	Gse	2.711	2.719	2.725	2.725	
Asphalt Absorption	Pba	2.570	2.677	2.762	2.762	
% Gmm @ N_{ini}		84.9	86.2	87.1	87.1	89% Maximum
% Gmm @ N_{max}		94.6	96.2	97.4	97.4	98% Maximum
Effective Asphalt Content of Mixture	Pbe	4.609	5.024	5.357	5.357	
Percent VMA in Compacted Mix	VMA	16.703	16.186	15.975	15.975	15% Minimum
Percent Air Voids in Compacted Mix	Va	6.571	5.014	3.982	3.982	4%
Percent VFA in Compacted Mix	VFA	60.660	69.019	75.074	75.074	65% to 75%
Dust to Asphalt Ratio	D/A	1.0	1.0	0.9	0.9	0.6% to 1.2%

Table C14: Summary of Mixture Properties

	Gsb	MTD	%AC	VMA	Film thic. (um)	SA (m^2/kg)	Dust/AC Ratio
C1	2.469	2.3279	6.5	15.4	11.2	4.87	0.74
C2	2.465	2.3466	5.8	13.8	10.1	4.64	0.83
C3	2.474	2.3486	5.3	13.6	8.0	5.68	1.18
C5	2.467	2.3418	6.3	14.6	10.5	4.81	0.76
F1	2.478	2.3378	6.3	15.6	9.0	6.05	0.76
F2	2.489	2.3752	5.4	13.2	6.9	6.31	1.16
C4/F3	2.478	2.3466	5.6	14.0	8.1	5.64	1.04
F4	2.491	2.3677	5.7	14.0	6.3	7.40	1.11
F5	2.485	2.3264	6.7	16.2	9.7	6.02	0.72
F6	2.489	2.3412	6.1	15.4	8.2	6.48	0.97
GAC1	2.496	2.4254	7.1	13.3	11.3	3.93	0.38
GAC2	2.705	2.5225	5.7	15.7	12.6	4.09	0.58
GAF1	2.54	2.4134	7.9	16.0	8.1	6.91	0.57

Table C15: Summary of Mixture Effective Properties

	%CA	%FA of Total Mix	%AC	VMA	Film thic. (um)	SA (m^2/kg)	Dust/AC Ratio
C1	66.9	30.95	17.36	35.4	39.2	4.20	0.28
C2	70.4	27.88	17.22	35.3	39.3	4.02	0.28
C3	63.6	34.47	13.33	30.4	24.1	5.16	0.47
C5	66.9	31.01	16.88	34.2	36.3	4.20	0.28
F1	47.3	49.38	11.31	25.7	19.3	5.36	0.42
F2	55.9	41.72	11.46	25.8	17.1	5.73	0.55
C4/F3	63.4	34.55	13.95	30.6	25.0	5.07	0.42
F4	47.3	49.70	10.29	23.4	13.2	6.69	0.61
F5	47.3	49.17	11.99	26.7	20.7	5.34	0.40
F6	36.8	41.44	12.83	28.8	20.9	5.76	0.49
GAC1	67.8	29.88	19.42	34.7	45.7	3.28	0.16
GAC2	65.7	32.34	14.98	34.4	44.9	3.43	0.22
GAF1	36.8	58.21	11.95	22.8	14.5	6.13	0.38

Table C16: Mixture Summary Report for Varying %AC

Mixture Type	All Mixtures
Asphalt Grade	AC-30
Design ESALs (millions)	10
Design Temperature (Celsius)	38
N inirial	8
N design	109
N maximum	174
Nominal Sieve Size (whiterock)	12.5
Nominal Sieve Size (Granite)	9.5
Compaction Temperature ^{o}C	100
Aging Temperature ^{o}C	150
Mold Size (mm)	150

APPENDIX D
DATA FOR TESTED SAMPLES

Table D1: Test Specimen Information - Coarse Whiterock

STOA				
Mixture Type	Specimen Name*	Average Thickness (inches)	Average Diameter (Inches)	Percent Air Void
C1	C1-14-T	2.05	5.910	6.96
	C1-14-B	2.07	5.906	7.27
	C1-13-B	2.11	5.950	7.54
C2	C2-10-T	2.11	5.870	6.95
	C2-10-B	2.11	5.872	7.10
	C2-9-T	2.07	5.910	6.98
C3	C3-1-B	2.16	5.915	6.89
	C3-2-T	2.08	5.899	6.84
	C3-2-B	2.03	5.907	7.00
C4/F3	F3-4-T	2.08	5.897	7.23
	F3-4-B	2.15	5.898	7.23
	F3-1-T	2.09	5.897	6.87
C5	C5-1-T	2.13	5.925	7.19
	C5-2-T	1.98	5.915	7.37
	C5-2-B	2.07	5.910	7.20
LTOA				
Mixture Type	Specimen Name*	Average Thickness (inches)	Average Diameter (Inches)	Percent Air Void
C1	C1-10-T	2.126	5.908	6.44
	C1-1-B	2.02	5.906	6.60
	C1-1-T	2.008	5.910	7.26
C2	C2-1-B	2.01	5.905	7.11
	C2-1-T	2.04	5.905	6.60
	C2-2-B	2.03	5.910	7.34
C3	C3-3-T	1.9769	5.902	7.00
	C3-3-B	2.0636	5.902	7.45
	C3-4-T	2.0336	5.904	6.73
C4/F3	F3-3-T	2.00	5.900	7.13
	F3-2-B	2.07	5.931	7.42
	F3-2-T	2.09	5.932	7.61
C5	C5-3-T	2.09	5.924	7.82
	C5-3-B	2.02	5.918	7.35
	C5-4-B	2.07	5.913	7.24

* First Character C1 indicates mixture type C1
Second Character C1-14 indicates C1 mixture number 14
Third Character C1-14-T/B indicates C1 Mixture 14 top or bottom

Table D2: Test Specimen Information - Fine Whiterock

STOA				
Mixture Type	Specimen Name*	Average Thickness (inches)	Average Diameter (Inches)	Percent Air Void
F1	F1-5-T	2.00	5.875	6.63
	F1-5-B	2.10	5.870	6.51
	F1-6-T	2.07	5.873	6.57
F2	F2-3-T	2.05	5.871	7.10
	F2-3-B	2.05	5.870	7.20
	F2-4-T	2.05	5.873	6.90
F4	F4-1-T	1.98	5.906	7.11
	F4-1-B	1.99	5.899	7.14
	F4-2-B	2.17	5.903	7.34
F5	F5-1-T	2.05	5.914	6.60
	F5-2-T	2.03	5.905	6.51
	F5-2-B	2.09	5.906	7.11
F6	F6-1-T	2.02	5.912	6.80
	F6-1-B	2.15	5.912	6.92
	F6-2-T	1.99	5.911	6.54
LTOA				
Mixture Type	Specimen Name*	Average Thickness (inches)	Average Diameter (Inches)	Percent Air Void
F1	F1-A-T	2.00	5.907	6.55
	F1-1-B	2.01	5.908	7.95
	F1-2-T	2.03	5.910	7.04
F2	F2-9-T	2.00	5.906	6.89
	F2-9-B	2.01	5.908	6.77
	F2-7-T	2.00	5.910	6.51
F4	F4-3-T	2.02	5.910	7.30
	F4-3-B	2.08	5.906	7.41
	F4-4-B	1.97	5.906	7.15
F5	F5-3-T	2.07	5.916	7.09
	F5-3-B	2.17	5.911	7.11
	F5-4-B	2.03	5.911	7.05
F6	F6-3-T	1.99	5.912	6.88
	F6-3-B	2.06	5.906	7.02
	F6-4-B	2.02	5.911	6.95

* First Character C1 indicates mixture type C1
Second Character C1-14 indicates C1 mixture number 14
Third Character C1-14-T/B indicates C1 Mixture 14 top or bottom

Table D3: Test Specimen Information – Granite

STOA				
Mixture Type	Specimen Name*	Average Thickness (inches)	Average Diameter (Inches)	Percent Air Void
GAC1	GAC1-2-T	2.00	5.904	6.88
	GAC1-2-B	1.99	5.904	7.07
	GAC1-3-T	2.02	5.902	6.83
GAC2	GAC2-2-T	1.94	5.905	7.50
	GAC2-2-B	1.74	5.916	7.26
	GAC2-3-B	2.01	5.904	6.74
GAF1	GAF1-2-T	2.12	5.896	6.71
	GAF1-3-T	2.11	5.908	6.56
	GAF1-3-B	1.95	5.901	6.59
LTOA				
Mixture Type	Specimen Name*	Average Thickness (inches)	Average Diameter (Inches)	Percent Air Void
GAC1	GAC1-4-B	1.94	5.899	6.96
	GAC1-5-T	2.01	5.911	7.10
	GAC1-5-B	1.96	5.901	7.06
GAC2	GAC2-4-T	2.03	5.918	7.26
	GAC2-5-T	1.82	5.917	7.35
	GAC2-5-B	1.98	5.914	7.97
GAF1	GAF1-4-B	2.07	5.900	6.59
	GAF1-5-T	2.05	5.904	6.57
	GAF1-5-B	2.05	5.899	6.68

* First Character C1 indicates mixture type C1
Second Character C1-14 indicates C1 mixture number 14
Third Character C1-14-T/B indicates C1 Mixture 14 top or bottom

Table D4: Mixture Compaction Data for ITLT Tested Specimens

Mixture Type		C1							
Tests Performed		MR, Creep, Strength and Permeability							
Asphalt Content	AC%	6.5	6.5	6.5	6.5	6.5	6.5	6.5	6.5
Maximum Theoretical Density	Gmm	2.3279	2.3279	2.3279	2.3279	2.3279	2.3279	2.3279	2.3279
Asphalt Specific Gravity	Ap. Gr. Asp	1.035	1.035	1.035	1.035	1.035	1.035	1.035	1.035
Bulk Specific Gravity of Compacted Mix	Gmb	2.1750	2.1743	2.1590	2.1578	2.1562	2.1531	2.1668	2.1562
	Pb	6.5	6.5	6.5	6.5	6.5	6.5	6.5	6.5
Specimen Number		**1/t**	**1/b**	**10/t**	**10/b**	**13/t**	**13/b**	**14/t**	**14/b**

Analyzing a Compacted Paving Mixture

A. Bulk Specific Gravity of Aggregates

	Aggregate	S1A	SIB	SCRN	FILLER
Individual % by mass	P	10.204	63.265	25.51	1.021
individual specific Gravity	G	2.4252	2.4509	2.527	2.69

A. Bulk Specific Gravity of Aggregate									
	Gsb	2.469	2.469	2.469	2.469	2.469	2.469	2.469	2.469
B. Effective Specific Gravity of Aggregate									
	Gse	2.549	2.549	2.549	2.549	2.549	2.549	2.549	2.549
C. Maximum Specific Gravity of Mixtures with Different Asphalt Contents									
D. Asphalt Absorption									
	Pba	1.313	1.313	1.313	1.313	1.313	1.313	1.313	1.313
E. Effective Asphalt Content of Mixture									
	Pbe	5.273	5.273	5.273	5.273	5.273	5.273	5.273	5.273
F. Percent VMA in Compacted Mix									
	VMA	17.648	17.675	18.254	18.300	18.360	18.478	17.959	18.360
G. Percent Air Voids in Compacted Mix									
	Va	**6.568**	**6.598**	**7.255**	**7.307**	**7.376**	**7.509**	**6.920**	**7.376**
H. Percent VFA in Compacted Mix									
	VFA	62.783	62.669	60.253	60.070	59.828	59.362	61.465	59.828

Table D5: Mixture Compaction Data for ITLT Tested Specimens

Mixture Type		C2							
Tests Performed		MR, Creep, Strength and Permeability							
Asphalt Content	AC%	5.8	5.8	5.8	5.8	5.8	5.8	5.8	5.8
Maximum Theoretical Density	Gmm	2.3466	2.3466	2.3466	2.3466	2.3466	2.3466	2.3466	2.3466
Asphalt Specific Gravity	Ap. Gr. Asp	1.035	1.035	1.035	1.035	1.035	1.035	1.035	1.035
Bulk Specific Gravity of Compacted Mix	Gmb	2.1833	2.1799	2.1753	2.1743	2.1830	2.1725	2.1833	2.1799
	Pb	5.8	5.8	5.8	5.8	5.8	5.8	5.8	5.8
Specimen Number		**1/t**	**1/b**	**2/t**	**2/b**	**9/t**	**9/b**	**10/t**	**10/b**

Analyzing a Compacted Paving Mixture

A. Bulk Specific Gravity of Aggregates

	Aggregate	S1A	SIB	SCRN	FILLER
Individual % by mass	P	35.35	37.37	25.25	2.05
individual specific Gravity	G	2.4252	2.4509	2.527	2.69

A. Bulk Specific Gravity of Aggregate									
	Gsb	2.465	2.465	2.465	2.465	2.465	2.465	2.465	2.465
B. Effective Specific Gravity of Aggregate									
	Gse	2.545	2.545	2.545	2.545	2.545	2.545	2.545	2.545
C. Maximum Specific Gravity of Mixtures with Different Asphalt Contents									
D. Asphalt Absorption									
	Pba	1.325	1.325	1.325	1.325	1.325	1.325	1.325	1.325
E. Effective Asphalt Content of Mixture									
	Pbe	4.552	4.552	4.552	4.552	4.552	4.552	4.552	4.552
F. Percent VMA in Compacted Mix									
	VMA	16.562	16.692	16.867	16.906	16.573	16.974	16.562	16.692
G. Percent Air Voids in Compacted Mix									
	Va	**6.959**	**7.104**	**7.300**	**7.343**	**6.972**	**7.419**	**6.959**	**7.104**
H. Percent VFA in Compacted Mix									
	VFA	57.981	57.440	56.722	56.568	57.933	56.292	57.981	57.440

Table D6: Mixture Compaction Data for ITLT Tested Specimens

Mixture Type		C3							
Tests Performed		MR, Creep, Strength and Permeability							
Asphalt Content	AC%	5.3	5.3	5.3	5.3	5.3	5.3	5.3	5.3
Maximum Theoretical Density	Gmm	2.3508	2.3508	2.3508	2.3508	2.3508	2.3508	2.3508	2.3508
Asphalt Specific Gravity	Ap. Gr. Asp	1.035	1.035	1.035	1.035	1.035	1.035	1.035	1.035
Bulk Specific Gravity of Compacted Mix	Gmb	2.1886	2.1888	2.1901	2.1863	2.1862	2.1756	2.1927	2.1819
	Pb	5.3	5.3	5.3	5.3	5.3	5.3	5.3	5.3
Specimen Number		**1/t**	**1/b**	**2/t**	**2/t**	**3/t**	**3/b**	**4/t**	**4/b**

Analyzing a Compacted Paving Mixture

A. Bulk Specific Gravity of Aggregates

	Aggregate	S1A	SIB	SCRN	FILLER
Individual % by mass	P	.27	.39	.31	.03
individual specific Gravity	G	2.4252	2.4509	2.527	2.69

A. Bulk Specific Gravity of Aggregate									
	Gsb	2.474	2.474	2.474	2.474	2.474	2.474	2.474	2.474
B. Effective Specific Gravity of Aggregate									
	Gse	2.531	2.531	2.531	2.531	2.531	2.531	2.531	2.531
C. Maximum Specific Gravity of Mixtures with Different Asphalt Contents									
D. Asphalt Absorption									
	Pba	0.948	0.948	0.948	0.948	0.948	0.948	0.948	0.948
E. Effective Asphalt Content of Mixture									
	Pbe	4.402	4.402	4.402	4.402	4.402	4.402	4.402	4.402
F. Percent VMA in Compacted Mix									
	VMA	16.208	16.200	16.151	16.296	16.300	16.706	16.051	16.464
G. Percent Air Voids in Compacted Mix									
	Va	**6.900**	**6.891**	**6.836**	**6.998**	**7.002**	**7.453**	**6.725**	**7.185**
H. Percent VFA in Compacted Mix									
	VFA	57.430	57.462	57.673	57.059	57.043	55.388	58.100	56.362

Table D7: Mixture Compaction Data for ITLT Tested Specimens

Mixture Type		C5							
Tests Performed		MR, Creep, Strength and Permeability							
Asphalt Content	AC%	6.3	6.3	6.3	6.3	6.3	6.3	6.3	6.3
Maximum Theoretical Density	Gmm	2.3418	2.3418	2.3418	2.3418	2.3418	2.3418	2.3418	2.3418
Asphalt Specific Gravity	Ap. Gr. Asp	1.035	1.035	1.035	1.035	1.035	1.035	1.035	1.035
Bulk Specific Gravity of Compacted Mix	Gmb	2.1734	2.1746	2.1693	2.1733	2.1705	2.1698	2.1744	2.1723
	Pb	6.3	6.3	6.3	6.3	6.3	6.3	6.3	6.3
Specimen Number		**1/t**	**1/b**	**2/t**	**2/t**	**3/t**	**3/b**	**4/t**	**4/b**

Analyzing a Compacted Paving Mixture

A. Bulk Specific Gravity of Aggregates

	Aggregate	S1A	SIB	SCRN	FILLER
Individual % by mass	P				
individual specific Gravity	G	2.4252	2.4509	2.527	2.69

A. Bulk Specific Gravity of Aggregate									
	Gsb	2.467	2.467	2.467	2.467	2.467	2.467	2.467	2.467
B. Effective Specific Gravity of Aggregate									
	Gse	2.559	2.559	2.559	2.559	2.559	2.559	2.559	2.559
C. Maximum Specific Gravity of Mixtures with Different Asphalt Contents									
D. Asphalt Absorption									
	Pba	1.509	1.509	1.509	1.509	1.509	1.509	1.509	1.509
E. Effective Asphalt Content of Mixture									
	Pbe	4.886	4.886	4.886	4.886	4.886	4.886	4.886	4.886
F. Percent VMA in Compacted Mix									
	VMA	17.451	17.406	17.607	17.455	17.561	17.588	17.413	17.493
G. Percent Air Voids in Compacted Mix									
	Va	**7.191**	**7.140**	**7.366**	**7.195**	**7.315**	**7.345**	**7.148**	**7.238**
H. Percent VFA in Compacted Mix									
	VFA	58.794	58.980	58.164	58.778	58.347	58.240	58.949	58.624

Table D8: Mixture Compaction Data for ITLT Tested Specimens

Mixture Type		F1							
Tests Performed		MR, Creep, Strength and Permeability							
Asphalt Content	AC%	6.3	6.3	6.3	6.3	6.3	6.3	6.3	6.3
Maximum Theoretical Density	Gmm	2.3378	2.3378	2.3378	2.3378	2.3378	2.3378	2.3378	2.3378
Asphalt Specific Gravity	Ap. Gr. Asp	1.035	1.035	1.035	1.035	1.035	1.035	1.035	1.035
Bulk Specific Gravity of Compacted Mix	Gmb	2.1847	2.1789	2.1774	2.1775	2.1789	2.1826	2.1847	2.1854
	Pb	6.3	6.3	6.3	6.3	6.3	6.3	6.3	6.3
Specimen Number		**1/t**	**1/b**	**2/t**	**2/b**	**5/t**	**5/b**	**6/t**	**6/b**

Analyzing a Compacted Paving Mixture

A. Bulk Specific Gravity of Aggregates

	Aggregate	S1A	SIB	SCRN	FILLER
Individual % by mass	P	20.3004	25.3756	53.2887	1.0353
individual specific Gravity	G	2.4252	2.4509	2.527	2.69

A. Bulk Specific Gravity of Aggregate									
	Gsb	2.488	2.488	2.488	2.488	2.488	2.488	2.488	2.488
B. Effective Specific Gravity of Aggregate									
	Gse	2.554	2.554	2.554	2.554	2.554	2.554	2.554	2.554
C. Maximum Specific Gravity of Mixtures with Different Asphalt Contents									
D. Asphalt Absorption									
	Pba	1.078	1.078	1.078	1.078	1.078	1.078	1.078	1.078
E. Effective Asphalt Content of Mixture									
	Pbe	5.290	5.290	5.290	5.290	5.290	5.290	5.290	5.290
F. Percent VMA in Compacted Mix									
	VMA	17.715	17.933	17.990	17.986	17.933	17.794	17.715	17.688
G. Percent Air Voids in Compacted Mix									
	Va	**6.549**	**6.797**	**6.861**	**6.857**	**6.797**	**6.639**	**6.549**	**6.519**
H. Percent VFA in Compacted Mix									
	VFA	63.031	62.098	61.860	61.876	62.098	62.691	63.031	63.145

Table D9: Mixture Compaction Data for ITLT Tested Specimens

Mixture Type		F2							
Tests Performed		MR, Creep, Strength and Permeability							
Asphalt Content	AC%	5.4	5.4	5.4	5.4	5.4	5.4	5.4	5.4
Maximum Theoretical Density	Gmm	2.3752	2.3752	2.3752	2.3752	2.3752	2.3752	2.3752	2.3752
Asphalt Specific Gravity	Ap. Gr. Asp	1.035	1.035	1.035	1.035	1.035	1.035	1.035	1.035
Bulk Specific Gravity of Compacted Mix	Gmb	2.2008	2.2024	2.2153	2.2148	2.2143	2.2141	2.21148	2.2144
	Pb	5.4	5.4	5.4	5.4	5.4	5.4	5.4	5.4
Specimen Number		**3/t**	**3/b**	**4/t**	**4/b**	**7/t**	**7/b**	**9/t**	**9/b**

Analyzing a Compacted Paving Mixture

A. Bulk Specific Gravity of Aggregates

	Aggregate	S1A	SIB	SCRN	FILLER
Individual % by mass	P	44	0	51	4
individual specific Gravity	G	2.4252	2.4509	2.527	2.69

A. Bulk Specific Gravity of Aggregate									
	Gsb	2.487	2.487	2.487	2.487	2.487	2.487	2.487	2.487
B. Effective Specific Gravity of Aggregate									
	Gse	2.565	2.565	2.565	2.565	2.565	2.565	2.565	2.565
C. Maximum Specific Gravity of Mixtures with Different Asphalt Contents									
D. Asphalt Absorption									
	Pba	1.267	1.267	1.267	1.267	1.267	1.267	1.267	1.267
E. Effective Asphalt Content of Mixture									
	Pbe	4.201	4.201	4.201	4.201	4.201	4.201	4.201	4.201
F. Percent VMA in Compacted Mix									
	VMA	16.276	16.215	15.725	15.744	15.763	15.770	15.870	15.759
G. Percent Air Voids in Compacted Mix									
	Va	**7.343**	**7.275**	**6.732**	**6.753**	**6.774**	**6.783**	**6.893**	**6.770**
H. Percent VFA in Compacted Mix									
	VFA	54.888	55.134	57.188	57.106	57.024	56.991	56.566	57.040

Table D10: Mixture Compaction Data for ITLT Tested Specimens

Mixture Type		C4/F3							
Tests Performed		MR, Creep, Strength and Permeability							
Asphalt Content	AC%	5.6	5.6	5.6	5.6	5.6	5.6	5.6	5.6
Maximum Theoretical Density	Gmm	2.3466	2.3466	2.3466	2.3466	2.3466	2.3466	2.3466	2.3466
Asphalt Specific Gravity	Ap. Gr. Asp	1.035	1.035	1.035	1.035	1.035	1.035	1.035	1.035
Bulk Specific Gravity of Compacted Mix	Gmb	2.1854	2.1710	2.1680	2.1725	2.1792	2.1765	2.1561	2.1567
	Pb	5.6	5.6	5.6	5.6	5.6	5.6	5.6	5.6
Specimen Number		**1/t**	**1/b**	**2/t**	**2/t**	**3/t**	**3/b**	**4/t**	**4/b**

Analyzing a Compacted Paving Mixture

A. Bulk Specific Gravity of Aggregates

	Aggregate	S1A	SIB	SCRN	FILLER
Individual % by mass	P	25.51	35.714	35.714	3.06
individual specific Gravity	G	2.4252	2.4509	2.527	2.69

A. Bulk Specific Gravity of Aggregate									
	Gsb	2.478	2.478	2.478	2.478	2.478	2.478	2.478	2.478
B. Effective Specific Gravity of Aggregate									
	Gse	2.537	2.537	2.537	2.537	2.537	2.537	2.537	2.537
C. Maximum Specific Gravity of Mixtures with Different Asphalt Contents									
D. Asphalt Absorption									
	Pba	0.984	0.984	0.984	0.984	0.984	0.984	0.984	0.984
E. Effective Asphalt Content of Mixture									
	Pbe	4.671	4.671	4.671	4.671	4.671	4.671	4.671	4.671
F. Percent VMA in Compacted Mix									
	VMA	16.733	17.282	17.396	17.224	16.969	17.072	17.849	17.826
G. Percent Air Voids in Compacted Mix									
	Va	**6.870**	**7.483**	**7.611**	**7.419**	**7.134**	**7.249**	**8.118**	**8.093**
H. Percent VFA in Compacted Mix									
	VFA	58.946	56.698	56.248	56.926	57.960	57.540	54.518	54.603

Table D11: Mixture Compaction Data for ITLT Tested Specimens

Mixture Type		F4							
Tests Performed		MR, Creep, Strength and Permeability							
Asphalt Content	AC%	5.7	5.7	5.7	5.7	5.7	5.7	5.7	5.7
Maximum Theoretical Density	Gmm	2.3677	2.3677	2.3677	2.3677	2.3677	2.3677	2.3677	2.3677
Asphalt Specific Gravity	Ap. Gr. Asp	1.035	1.035	1.035	1.035	1.035	1.035	1.035	1.035
Bulk Specific Gravity of Compacted Mix	Gmb	2.1994	2.1986	2.1972	2.1939	2.1949	2.1923	2.1999	2.1985
	Pb	5.7	5.7	5.7	5.7	5.7	5.7	5.7	5.7
Specimen Number		**1/t**	**1/b**	**2/t**	**2/b**	**3/t**	**3/b**	**4/t**	**4/b**

Analyzing a Compacted Paving Mixture

A. Bulk Specific Gravity of Aggregates

	Aggregate	S1A	SIB	SCRN	FILLER
Individual % by mass	P				
individual specific Gravity	G	2.4252	2.4509	2.527	2.69

A. Bulk Specific Gravity of Aggregate									
	Gsb	2.491	2.491	2.491	2.491	2.491	2.491	2.491	2.491
B. Effective Specific Gravity of Aggregate									
	Gse	2.568	2.568	2.568	2.568	2.568	2.568	2.568	2.568
C. Maximum Specific Gravity of Mixtures with Different Asphalt Contents									
D. Asphalt Absorption									
	Pba	1.239	1.239	1.239	1.239	1.239	1.239	1.239	1.239
E. Effective Asphalt Content of Mixture									
	Pbe	4.532	4.532	4.532	4.532	4.532	4.532	4.532	4.532
F. Percent VMA in Compacted Mix									
	VMA	16.739	16.769	16.822	16.947	16.909	17.008	16.720	16.773
G. Percent Air Voids in Compacted Mix									
	Va	**7.108**	**7.142**	**7.201**	**7.340**	**7.298**	**7.408**	**7.087**	**7.146**
H. Percent VFA in Compacted Mix									
	VFA	57.535	57.410	57.193	56.686	56.839	56.443	57.613	57.395

Table D12: Mixture Compaction Data for ITLT Tested Specimens

Mixture Type		F5							
Tests Performed		MR, Creep, Strength and Permeability							
Asphalt Content	AC%	6.7	6.7	6.7	6.7	6.7	6.7	6.7	6.7
Maximum Theoretical Density	Gmm	2.3264	2.3264	2.3264	2.3264	2.3264	2.3264	2.3264	2.3264
Asphalt Specific Gravity	Ap. Gr. Asp	1.035	1.035	1.035	1.035	1.035	1.035	1.035	1.035
Bulk Specific Gravity of Compacted Mix	Gmb	2.1753	2.1591	2.1750	2.1610	2.1614	2.1610	2.1658	2.1625
	Pb	6.7	6.7	6.7	6.7	6.7	6.7	6.7	6.7
Specimen Number		**1/t**	**1/b**	**2/t**	**2/t**	**3/t**	**3/b**	**4/t**	**4/b**

Analyzing a Compacted Paving Mixture

A. Bulk Specific Gravity of Aggregates

	Aggregate	S1A	SIB	SCRN	FILLER
Individual % by mass	P				
individual specific Gravity	G	2.4252	2.4509	2.527	2.69

A. Bulk Specific Gravity of Aggregate									
	Gsb	2.485	2.485	2.485	2.485	2.485	2.485	2.485	2.485
B. Effective Specific Gravity of Aggregate									
	Gse	2.555	2.555	2.555	2.555	2.555	2.555	2.555	2.555
C. Maximum Specific Gravity of Mixtures with Different Asphalt Contents									
D. Asphalt Absorption									
	Pba	1.147	1.147	1.147	1.147	1.147	1.147	1.147	1.147
E. Effective Asphalt Content of Mixture									
	Pbe	5.630	5.630	5.630	5.630	5.630	5.630	5.630	5.630
F. Percent VMA in Compacted Mix =									
	VMA	18.328	18.936	18.339	18.865	18.850	18.865	18.684	18.808
G. Percent Air Voids in Compacted Mix =									
	Va	**6.495**	**7.191**	**6.508**	**7.110**	**7.093**	**7.110**	**6.903**	**7.045**
H. Percent VFA in Compacted Mix									
	VFA	64.562	62.023	64.513	62.312	62.373	62.312	63.053	62.542

Table D13: Mixture Compaction Data for ITLT Tested Specimens

Mixture Type		F6							
Tests Performed		MR, Creep, Strength and Permeability							
Asphalt Content	AC%	6.1	6.1	6.1	6.1	6.1	6.1	6.1	6.1
Maximum Theoretical Density	Gmm	2.3412	2.3412	2.3412	2.3412	2.3412	2.3412	2.3412	2.3412
Asphalt Specific Gravity	Ap. Gr. Asp	1.035	1.035	1.035	1.035	1.035	1.035	1.035	1.035
Bulk Specific Gravity of Compacted Mix	Gmb	2.1819	2.1791	2.188	2.1808	2.1801	2.1769	2.1799	2.1785
	Pb	6.1	6.1	6.1	6.1	6.1	6.1	6.1	6.1
Specimen Number		**1/t**	**1/b**	**2/t**	**2/t**	**3/t**	**3/b**	**4/t**	**4/b**

Analyzing a Compacted Paving Mixture

A. Bulk Specific Gravity of Aggregates

	Aggregate	S1A	SIB	SCRN	FILLER
Individual % by mass	P				
individual specific Gravity	G	2.4252	2.4509	2.527	2.69

A. Bulk Specific Gravity of Aggregate									
	Gsb	2.489	2.489	2.489	2.489	2.489	2.489	2.489	2.489
B. Effective Specific Gravity of Aggregate									
	Gse	2.550	2.550	2.550	2.550	2.550	2.550	2.550	2.550
C. Maximum Specific Gravity of Mixtures with Different Asphalt Contents									
D. Asphalt Absorption									
	Pba	0.999	0.999	0.999	0.999	0.999	0.999	0.999	0.999
E. Effective Asphalt Content of Mixture									
	Pbe	5.162	5.162	5.162	5.162	5.162	5.162	5.162	5.162
F. Percent VMA in Compacted Mix									
	VMA	17.686	17.791	17.456	17.727	17.754	17.874	17.761	17.814
G. Percent Air Voids in Compacted Mix									
	Va	**6.804**	**6.924**	**6.544**	**6.851**	**6.881**	**7.018**	**6.890**	**6.949**
H. Percent VFA in Compacted Mix									
	VFA	61.527	61.083	62.512	61.352	61.241	60.738	61.209	60.989

Table D14: Mixture Compaction Data for ITLT Tested Specimens

Mixture Type		GAC1									
Tests Performed		MR, Creep, Strength and Permeability									
Asphalt Content	AC%	7.1	7.1	7.1	7.1	7.1	7.1	7.1	7.1	7.1	7.1
Maximum Theoretical Density	Gmm	2.4254	2.4254	2.4254	2.4254	2.4254	2.4254	2.4254	2.4254	2.4254	2.4254
Asphalt Specific Gravity	Ap. Gr. Asp	1.035	1.035	1.035	1.035	1.035	1.035	1.035	1.035	1.035	1.035
Bulk Specific Gravity of Compacted Mix	Gmb	2.2588	2.2538	2.2586	2.2540	2.2598	2.2525	2.2580	2.2566	2.2531	2.2543
	Pb	7.1	7.1	7.1	7.1	7.1	7.1	7.1	7.1	7.1	7.1
Specimen Number		**1/1**	**1/2**	**2/1**	**2/2**	**3/1**	**3/2**	**4/1**	**4/2**	**5/1**	**5/2**

Analyzing a Compacted Paving Mixture

A. Bulk Specific Gravity of Aggregates

	Aggregate	#89	Vm10	And. SCR	FILLER
Individual % by mass	P	60	0	40	0
individual specific Gravity	G	2.706	2.7047	2.2352	2.69

A. Bulk Specific Gravity of Aggregate											
	Gsb	2.496	2.496	2.496	2.496	2.496	2.496	2.496	2.496	2.496	2.496
B. Effective Specific Gravity of Aggregate											
	Gse	2.703	2.703	2.703	2.703	2.703	2.703	2.703	2.703	2.703	2.703
C. Maximum Specific Gravity of Mixtures with Different Asphalt Contents											
D. Asphalt Absorption											
	Pba	3.179	3.179	3.179	3.179	3.179	3.179	3.179	3.179	3.179	3.179
E. Effective Asphalt Content of Mixture											
	Pbe	4.147	4.147	4.147	4.147	4.147	4.147	4.147	4.147	4.147	4.147
F. Percent VMA in Compacted Mix											
	VMA	15.919	16.105	15.927	16.098	15.882	16.154	15.949	16.001	16.132	16.087
G. Percent Air Voids in Compacted Mix											
	Va	**6.869**	**7.075**	**6.877**	**7.067**	**6.828**	**7.129**	**6.902**	**6.960**	**7.104**	**7.055**
H. Percent VFA in Compacted Mix											
	VFA	56.852	56.070	56.820	56.101	57.010	55.870	56.725	56.505	55.962	56.147

Table D15: Mixture Compaction Data for ITLT Tested Specimens

Mixture Type		GAC2									
Tests Performed		MR, Creep, Strength and Permeability									
Asphalt Content	AC%	5.7	5.7	5.7	5.7	5.7	5.7	5.7	5.7	5.7	5.7
Maximum Theoretical Density	Gmm	2.5225	2.5225	2.5225	2.5225	2.5225	2.5225	2.5225	2.5225	2.5225	2.5225
Asphalt Specific Gravity	Ap. Gr. Asp	1.035	1.035	1.035	1.035	1.035	1.035	1.035	1.035	1.035	1.035
Bulk Specific Gravity of Compacted Mix	Gmb	2.3482	2.3438	2.3334	2.3393	2.3357	2.3525	2.3395	2.3374	2.3371	2.3467
	Pb	5.7	5.7	5.7	5.7	5.7	5.7	5.7	5.7	5.8	5.8
Specimen Number		**1/1**	**1/2**	**2/1**	**2/2**	**3/1**	**3/2**	**4/1**	**4/2**	**5/1**	**5/2**

Analyzing a Compacted Paving Mixture

A. Bulk Specific Gravity of Aggregates

	Aggregate	#89	WI10	And. SCR	FILLER
Individual % by mass	P	60	40	0	0
individual specific Gravity	G	2.706	2.7047	2.2352	2.69

A. Bulk Specific Gravity of Aggregate											
	Gsb	2.705	2.705	2.705	2.705	2.705	2.705	2.705	2.705	2.705	2.705
B. Effective Specific Gravity of Aggregate											
	Gse	2.762	2.762	2.762	2.762	2.762	2.762	2.762	2.762	2.767	2.767
C. Maximum Specific Gravity of Mixtures with Different Asphalt Contents											
D. Asphalt Absorption											
	Pba	0.789	0.789	0.789	0.789	0.789	0.789	0.796	0.789	0.856	0.856
E. Effective Asphalt Content of Mixture											
	Pbe	4.956	4.956	4.956	4.956	4.956	4.956	4.949	4.956	4.994	4.994
F. Percent VMA in Compacted Mix											
	VMA	18.153	18.306	18.669	18.463	18.589	18.003	18.442	18.529	18.626	18.292
G. Percent Air Voids in Compacted Mix											
	Va	**6.910**	**7.084**	**7.497**	**7.263**	**7.405**	**6.739**	**7.255**	**7.338**	**7.350**	**6.969**
H. Percent VFA in Compacted Mix											
	VFA	61.936	61.302	59.845	60.664	60.162	62.566	60.662	60.398	60.541	61.900

Table D16: Mixture Compaction Data for ITLT Tested Specimens

Mixture Type		GAF1									
Tests Performed		MR, Creep, Strength and Permeability									
Asphalt Content	AC%	7.9	7.9	7.9	6.3	6.3	6.3	6.3	6.3	6.3	6.3
Maximum Theoretical Density	Gmm	2.4134	2.4134	2.4134	2.4134	2.4134	2.4134	2.4134	2.4134	2.4134	2.4134
Asphalt Specific Gravity	Ap. Gr. Asp	1.035	1.035	1.035	1.035	1.035	1.035	1.035	1.035	1.035	1.035
Bulk Specific Gravity of Compacted Mix	Gmb	2.2388	2.2389	2.2515	2.2522	2.2551	2.2528	2.2513	2.2544	2.2548	2.2522
	Pb	7.9	6.3	6.3	6.3	6.3	6.3	6.3	6.3	6.3	6.3
Specimen Number		**1/t**	**1/b**	**2/t**	**2/t**	**3/t**	**3/b**	**4/t**	**4/b**	**5/t**	**5/b**

Analyzing a Compacted Paving Mixture

A. Bulk Specific Gravity of Aggregates

	Aggregate	S1A	S1B	SCRN	FILLER
Individual % by mass	P	20.3004	25.3756	53.2887	1.0353
individual specific Gravity	G	2.4252	2.4509	2.527	2.69

A. Bulk Specific Gravity of Aggregate											
	Gsb	2.488	2.488	2.488	2.488	2.488	2.488	2.488	2.488	2.488	2.488
B. Effective Specific Gravity of Aggregate											
	Gse	2.725	2.651	2.651	2.651	2.651	2.651	2.651	2.651	2.651	2.651
C. Maximum Specific Gravity of Mixtures with Different Asphalt Contents											
D. Asphalt Absorption											
	Pba	3.617	2.558	2.558	2.558	2.558	2.558	2.558	2.558	2.558	2.558
E. Effective Asphalt Content of Mixture											
	Pbe	4.569	3.903	3.903	3.903	3.903	3.903	3.903	3.903	3.903	3.903
F. Percent VMA in Compacted Mix											
	VMA	17.117	15.673	15.199	15.172	15.063	15.150	15.206	15.089	15.074	15.172
G. Percent Air Voids in Compacted Mix											
	Va	**7.235**	**7.230**	**6.708**	**6.679**	**6.559**	**6.655**	**6.717**	**6.588**	**6.572**	**6.679**
H. Percent VFA in Compacted Mix											
	VFA	57.734	53.867	55.862	55.976	56.455	56.075	55.829	56.339	56.405	55.976

APPENDIX E
SUMMARY OF MIXTURE TEST RESULTS

Table E1: Resilient Modulus Data – Coarse whiterock

Mixture Type	Asphalt Content (%)	Testing Temperature (oC)	Cycle	Resilient Modulus (GPa) for STOA			Resilient Modulus (GPa) for STOA		
				Trimmed Mean Value	Average Value (GPa)	Poisson Ratio	Trimmed Mean Value	Average Value (GPa)	Poisson Ratio
C1	6.5	10	1	7.85	7.92	0.42	9.66	9.62	0.27
			2	7.82		0.42	9.78		0.25
			3	8.08		0.39	9.43		0.28
C2	5.8	10	1	7.69	7.73	0.25	11.73	11.78	0.17
			2	7.67		0.26	11.71		0.17
			3	7.83		0.22	11.91		0.17
C3	5.3	10	1	11.44	11.47	0.27	14.69	14.39	0.27
			2	11.44		0.29	14.25		0.29
			3	11.52		0.29	14.24		0.29
C4/F3	5.6	10	1	11.95	12.02	0.32	13.88	13.89	0.31
			2	12.09		0.31	13.95		0.32
			3	12.03		0.32	13.85		0.32
C5	6.3	10	1	9.82	9.73	0.27	11.33	11.39	0.28
			2	9.65		0.28	11.41		0.27
			3	9.71		0.28	11.43		0.27

Table E2: Resilient Modulus Data – Fine Whiterock

Mixture Type	Asphalt Content (%)	Testing Temperature (oC)	Cycle	Resilient Modulus (GPa) for STOA			Resilient Modulus (GPa) for STOA		
				Trimmed Mean Value	Average Value (GPa)	Poisson Ratio	Trimmed Mean Value	Average Value (GPa)	Poisson Ratio
F1	6.3	10	1	9.40	9.49	0.27	9.89	9.93	0.34
			2	9.39		0.28	9.99		0.32
			3	9.68		0.25	9.90		0.32
F2	5.4	10	1	8.62	8.62	0.26	13.23	12.93	0.27
			2	8.74		0.25	12.85		0.28
			3	8.49		0.27	12.72		0.28
F4	5.7	10	1	10.48	10.43	0.33	12.29	12.35	0.27
			2	10.38		0.34	12.37		0.26
			3	10.44		0.33	12.39		0.26
F5	6.7	10	1	8.41	8.32	0.24	9.94	9.81	0.26
			2	8.28		0.25	9.76		0.28
			3	8.28		0.24	9.72		0.28
F6	6.1	10	1	8.09	8.07	0.22	10.59	10.56	0.26
			2	8.11		0.21	10.54		0.27
			3	8.02		0.21	10.54		0.26

Table E3: Resilient Modulus Data – Granite

Mixture Type	Asphalt Content (%)	Testing Temperature (oC)	Cycle	Resilient Modulus (GPa) for STOA			Resilient Modulus (GPa) for STOA		
				Trimmed Mean Value	Average Value (GPa)	Poisson Ratio	Trimmed Mean Value	Average Value (GPa)	Poisson Ratio
GAC1	7.2	10	1	7.41	7.57	0.2	11.06	10.96	0.34
			2	7.67		0.17	11.1		0.34
			3	7.63		0.17	10.73		0.35
GAC2	5.7	10	1	7.08	6.96	0.25	9.21	9.12	0.28
			2	6.9		0.26	9.12		0.28
			3	6.89		0.26	9.03		0.28
GAF1	7.9	10	1	6.98	7.06	0.22	8.05	8.19	0.2
			2	7.11		0.21	8.16		0.2
			3	7.08		0.21	8.36		0.18

Table E4: Tensile Strength Test Data – Coarse Whiterock

Mixture Type	Asphalt Content (%)	Testing Temperature (oC)	Cycle	Tensile Strength (MPa) STOA			Tensile Strength (MPa) LTOA		
				Trimmed Mean Value	Average Value (MPa)	Poisson Ratio	Trimmed Mean Value	Average Value (MPa)	Poisson Ratio
C1	6.5	10	1	1.57	1.61	0.5	2.07	2.10	0.35
			2	1.75			2.16		
			3	1.5			2.08		
C2	5.8	10	1	1.55	1.70	0.37	2.2	2.06	0.3
			2	1.58			2.13		
			3	1.96			1.84		
C3	5.3	10	1	2.11	2.09	0.32	2.47	2.44	0.27
			2	2.14			2.44		
			3	2.02			2.4		
C4/F3	5.6	10	1	1.98	2.02	0.34	2.11	2.16	0.39
			2	2.02			2		
			3	2.07			2.36		
C5	6.3	10	1	1.96	1.80	0.39	1.26	1.79	0.38
			2	1.62			1.99		
			3	1.83			2.12		

Table E5: Tensile Strength Test Data – Fine Whiterock

Mixture Type	Asphalt Content (%)	Testing Temperature (oC)	Cycle	Tensile Strength (MPa) STOA			Tensile Strength (MPa) LTOA		
				Trimmed Mean Value	Average Value (MPa)	Poisson Ratio	Trimmed Mean Value	Average Value (MPa)	Poisson Ratio
F1	6.3	10	1	2.05	2.08	0.46	2.09	2.06	0.39
			2	2.28			1.84		
			3	1.90			2.24		
F2	5.4	10	1	1.98	1.87	0.28	2.62	2.56	0.33
			2	1.82			2.49		
			3	1.82			2.57		
F4	5.7	10	1	1.83	1.92	0.38	1.78	2.14	0.31
			2	1.97			2.40		
			3	1.95			2.24		
F5	6.7	10	1	1.74	1.76	0.29	2.01	1.83	0.39
			2	1.81			1.74		
			3	1.73			1.75		
F6	6.1	10	1	1.59	1.71	0.24	2.00	2.06	0.34
			2	1.84			2.11		
			3	1.70			2.08		

Table E6: Tensile Strength Test Data – Granite

Mixture Type	Asphalt Content (%)	Testing Temperature (oC)	Cycle	Tensile Strength (MPa) STOA			Tensile Strength (MPa) LTOA		
				Trimmed Mean Value	Average Value (MPa)	Poisson Ratio	Trimmed Mean Value	Average Value (MPa)	Poisson Ratio
GAC1	7.2	10	1	1.82	1.75	0.35	1.83	1.84	0.32
			2	1.8			1.78		
			3	1.62			1.91		
GAC2	5.7	10	1	1.59	1.76	0.5	2.04	2.12	0.35
			2	1.97			2.24		
			3	1.73			2.07		
GAF1	7.9	10	1	1.99	1.98	0.34	2.01	2.17	0.34
			2	1.93			2.17		
			3	2.03			2.32		

Table E7: Failure train Test Data – Coarse Whiterock

Mixture Type	Asphalt Content (%)	Testing Temperature (oC)	Cycle	Failure Strain (microstrain) STOA			Failure Strain (microstrain) LTOA		
				Trimmed Mean Value	Average Value (MPa)	Poisson Ratio	Trimmed Mean Value	Average Value (MPa)	Poisson Ratio
C1	6.5	10	1	4629.75	4629.75	0.5	2224.39	2224.39	0.35
			2	4629.75			2224.39		
			3	4629.75			2224.39		
C2	5.8	10	1	3771.26	3771.26	0.37	1896.68	1896.68	0.3
			2	3771.26			1896.68		
			3	3771.26			1896.68		
C3	5.3	10	1	2173.97	2173.97	0.32	1468.29	1468.29	0.27
			2	2173.97			1468.29		
			3	2173.97			1468.29		
C4/F3	5.6	10	1	2355.12	2355.12	0.34	1143.14	1143.14	0.39
			2	2355.12			1143.14		
			3	2355.12			1143.14		
C5	6.3	10	1	1808.41	1808.41	0.39	1413.88	1413.88	0.38
			2	1808.41			1413.88		
			3	1808.41			1413.88		

Table E8: Failure Strain Test Data – Fine Whiterock

Mixture Type	Asphalt Content (%)	Testing Temperature (oC)	Cycle	Failure Strain (microstrain) STOA			Failure Strain (microstrain) LTOA		
				Trimmed Mean Value	Average Value (MPa)	Poisson Ratio	Trimmed Mean Value	Average Value (MPa)	Poisson Ratio
F1	6.3	10	1	2919.62	2919.62	0.46	1833.28	1833.28	0.39
			2	2919.62			1833.28		
			3	2919.62			1833.28		
F2	5.4	10	1	3714.55	3714.55	0.28	1526.15	1526.15	0.33
			2	3714.55			1526.15		
			3	3714.55			1526.15		
F4	5.7	10	1	2235.08	2235.08	0.38	1225.09	1225.09	0.31
			2	2235.08			1225.09		
			3	2235.08			1225.09		
F5	6.7	10	1	2400.07	2400.07	0.29	1626.71	1626.71	0.39
			2	2400.07			1626.71		
			3	2400.07			1626.71		
F6	6.1	10	1	2424.46	2424.46	0.24	1646.78	1646.78	0.34
			2	2424.46			1646.78		
			3	2424.46			1646.78		

Table E9: Failure Train Test Data – Granite

Mixture Type	Asphalt Content (%)	Testing Temperature (oC)	Cycle	Failure Strain (microstrain) STOA			Failure Strain (microstrain) LTOA		
				Trimmed Mean Value	Average Value (MPa)	Poisson Ratio	Trimmed Mean Value	Average Value (MPa)	Poisson Ratio
GAC1	7.2	10	1	2809.97	2809.97	0.35	1875.71	1875.71	0.32
			2	2809.97			1875.71		
			3	2809.97			1875.71		
GAC2	5.7	10	1	4171.69	4171.69	0.5	3402.17	3402.17	0.35
			2	4171.69			3402.17		
			3	4171.69			3402.17		
GAF1	7.9	10	1	5128.47	5128.47	0.34	2685.42	2685.42	0.34
			2	5128.47			2685.42		
			3	5128.47			2685.42		

Table E10: Fracture Energy Test Data – Coarse Whiterock

Mixture Type	Asphalt Content (%)	Testing Temperature (oC)	Cycle	Fracture Energy (kJ/m3) STOA			Fracture Energy (kJ/m3) LTOA		
				Trimmed Mean Value	Average Value (MPa)	Poisson Ratio	Trimmed Mean Value	Average Value (MPa)	Poisson Ratio
C1	6.5	10	1	5.8	5.80	0.5	3.5	3.50	0.35
			2	5.8			3.5		
			3	5.8			3.5		
C2	5.8	10	1	4.8	4.80	0.37	2.9	2.90	0.3
			2	4.8			2.9		
			3	4.8			2.9		
C3	5.3	10	1	3.5	3.50	0.32	2.7	2.70	0.27
			2	3.5			2.7		
			3	3.5			2.7		
C4/F3	5.6	10	1	3.7	3.70	0.34	1.7	1.70	0.39
			2	3.7			1.7		
			3	3.7			1.7		
C5	6.3	10	1	2.5	2.50	0.39	2.1	2.10	0.38
			2	2.5			2.1		
			3	2.5			2.1		

Table E11: Fracture Energy Test Data – Fine Whiterock

Mixture Type	Asphalt Content (%)	Testing Temperature (oC)	Cycle	Fracture Energy (kJ/m3) STOA			Fracture Energy (kJ/m3) LTOA		
				Trimmed Mean Value	Average Value (MPa)	Poisson Ratio	Trimmed Mean Value	Average Value (MPa)	Poisson Ratio
F1	6.3	10	1	4.20	4.20	0.46	2.80	2.80	0.39
			2	4.20			2.80		
			3	4.20			2.80		
F2	5.4	10	1	5.40	5.40	0.28	3.20	3.20	0.33
			2	5.40			3.20		
			3	5.40			3.20		
F4	5.7	10	1	3.10	3.10	0.38	2.00	2.00	0.31
			2	3.10			2.00		
			3	3.10			2.00		
F5	6.7	10	1	3.20	3.20	0.29	2.30	2.30	0.39
			2	3.20			2.30		
			3	3.20			2.30		
F6	6.1	10	1	3.00	3.00	0.24	2.50	2.50	0.34
			2	3.00			2.50		
			3	3.00			2.50		

Table E12: Fracture Energy Test Data – Granite

Mixture Type	Asphalt Content (%)	Testing Temperature (oC)	Cycle	Fracture Energy (kJ/m3) STOA			Fracture Energy (kJ/m3) LTOA		
				Trimmed Mean Value	Average Value (MPa)	Poisson Ratio	Trimmed Mean Value	Average Value (MPa)	Poisson Ratio
GAC1	7.2	10	1	3.9	3.90	0.35	2.6	2.60	0.32
			2	3.9			2.6		
			3	3.9			2.6		
GAC2	5.7	10	1	5.8	5.80	0.5	5.8	5.80	0.35
			2	5.8			5.8		
			3	5.8			5.8		
GAF1	7.9	10	1	8.4	8.40	0.34	4.6	4.60	0.34
			2	8.4			4.6		
			3	8.4			4.6		

Table E13: Creep Test Data – Coarse Whiterock

Mixture Type	Asphalt Content (%)	Testing Temperature (oC)	Creep Compliance (1/GPa) STOA					Creep Compliance (1/GPa) LTOA				
			1 second	10 seconds	100 seconds	1000 seconds	Poisson Ratio	1 second	10 seconds	100 seconds	1000 seconds	Poisson Ratio
C1	6.5	10	0.41	0.85	2.76	13.93	0.5	0.207	0.486	1.42	4.506	0.34
C2	5.8	10	0.38	0.86	3.11	15.09	0.28	0.134	0.289	0.85	2.832	0.26
C3	5.3	10	0.13	0.50	1.98	7.55	0.17	0.148	0.301	0.78	2.178	0.28
C4/F3	5.6	10	0.22	0.57	1.78	6.29	0.33	0.119	0.239	0.59	1.734	0.44
C5	6.3	10	0.17	0.41	1.21	4.09	0.43	0.113	0.201	0.42	1.205	0.5

Table E14: Creep Test Data – Fine Whiterock

Mixture Type	Asphalt Content (%)	Testing Temperature (oC)	Creep Compliance (1/GPa) STOA					Creep Compliance (1/GPa) LTOA				
			1 second	10 seconds	100 seconds	1000 seconds	Poisson Ratio	1 second	10 seconds	100 seconds	1000 seconds	Poisson Ratio
F1	6.3	10	0.25	0.62	1.96	7.89	0.38	0.194	0.453	1.34	4.518	0.39
F2	5.4	10	0.28	0.63	1.93	5.99	0.42	0.125	0.26	0.68	1.896	0.37
F4	5.7	10	0.18	0.44	1.28	4.58	0.38	0.119	0.201	0.38	0.904	0.34
F5	6.7	10	0.25	0.62	1.85	6.00	0.43	0.136	0.259	0.62	2.042	0.42
F6	6.1	10	0.22	0.58	1.93	6.02	0.33	0.147	0.26	0.64	1.988	0.32

Table E15: Creep Test Data – Granite

Mixture Type	Asphalt Content (%)	Testing Temperature (oC)	Creep Compliance (1/GPa) STOA					Creep Compliance (1/GPa) LTOA				
			1 second	10 seconds	100 seconds	1000 seconds	Poisson Ratio	1 second	10 seconds	100 seconds	1000 seconds	Poisson Ratio
GAC1	7.2	10	0.30	0.56	1.78	6.14	0.42	0.142	0.346	1.00	2.964	0.5
GAC2	5.7	10	0.32	0.91	2.62	8.64	0.35	0.263	0.492	1.33	4.174	0.36
GAF1	7.9	10	0.26	0.64	2.05	6.48	0.36	0.169	0.395	0.94	2.764	0.3

Table E16: m-Values for all Mixtures

Mixture	M-Value	
	STOA	LTOA
C1	0.7961	0.5480
C2	0.7729	0.5856
C3	0.6563	0.4977
C5	0.5839	0.5089
F1	0.6560	0.5726
F2	0.5649	0.4955
C4/F3	0.5817	0.5039
F4	0.5773	0.4241
F5	0.5429	0.5677
F6	0.5513	0.5620
GAC1	0.6245	0.5151
GAC11	0.5531	0.5657
GAF1	0.5466	0.4726

APPENDIX F
SUMMARY OF BINDER RESULTS

Table F1: Summary of Penetration Test Results

Mix	**AC-30-1**	**AC-30-2**	**C1S**	**C1L**	**C2S**	**C2L**	**F1S**	**F1L**
Trial 1	63	63	41	38	41	37	35	28
Trial 2	60	60	44	40	40	35	36	29
Trial 3	61	60	41	40	40	37	37	27
Trial 4	60	60	42	39	40	37	35	28
Trial 5	60	60	42	38	41	36	37	29
Av. Pen	**61**	**61**	**42**	**39**	**40**	**36**	**36**	**28**
Mix	**F2S**	**F2L**	**C3S**	**C3L**	**C4/F3S**	**C4/F3L**	**C5S**	**C5L**
Trial 1	35	27	38	31	38	32	39	32
Trial 2	36	26	38	30	38	31	39	34
Trial 3	37	28	37	32	37	32	40	33
Trial 4	36	25	39	32	39	31	40	32
Trial 5	37	25	38	33	38	32	39	32
Av. Pen	**36**	**26**	**38**	**32**	**38**	**32**	**39**	**33**
Mix	**F4S**	**F4L**	**F5S**	**F5L**	**F6S**	**F6L**	**F6S**	**F6L**
Trial 1	35	26	36	28	36	32	36	30
Trial 2	34	25	36	29	37	31	37	29
Trial 3	33	25	36	30	37	33	37	31
Trial 4	33	25	37	29	37	32	37	30
Trial 5	33	26	37	28	36	33	36	31
Av. Pen	**34**	**25**	**36**	**29**	**37**	**32**	**37**	**30**
Mix	**GAC1S**	**GAC1L**	**GAC2S**	**GAC2L**	**GAF1S**	**GAF1S**	**GAF1S**	**GAF1S**
Trial 1	44	38	39	34	39	32	39	32
Trial 2	43	39	38	34	37	34	37	34
Trial 3	45	38	40	35	39	32	39	32
Trial 4	44	39	40	34	39	34	39	34
Trial 5	43	40	38	34	38	32	38	32
Av. Pen	**44**	**39**	**39**	**34**	**38**	**33**	**38**	**33**

Table F2: Summary of DSR Test Results

Mixture		AC30	C1S	C1L	C2S	C2L	C3S	C3L
G*	Trial 1	6.9641E+06	7.5866E+06	8.2483E+06	7.3876E+06	8.0473E+06	6.9239E+06	9.2632E+06
	Trial 2	7.0308E+06	7.5923E+06	8.2593E+06	7.3772E+06	8.0587E+06	8.7615E+06	9.1256E+06
	Trial 3	6.9687E+06	7.5932E+06	8.2649E+06	7.4079E+06	8.0710E+06	7.8895E+06	9.2869E+06
	Average	6.9879E+06	7.5907E+06	8.2575E+06	7.3909E+06	8.0590E+06	7.8583E+06	9.2252E+06
delta	Trial 1	55.8	48.4	46.2	49.9	48.1	47.7	45.7
	Trial 2	55.6	48.5	46.7	49.9	48.3	48.1	45.6
	Trial 3	55.7	48.3	46.5	49.9	47.6	47.9	45.7
	Average	55.7	48.4	46.5	49.9	48.0	47.9	45.7
G*sin(delta)	Trial 1	5.7599E+06	5.6732E+06	5.9533E+06	5.6509E+06	5.9897E+06	5.1211E+06	6.6296E+06
	Trial 2	5.8012E+06	5.6863E+06	6.0109E+06	5.6430E+06	6.0169E+06	6.5213E+06	6.5200E+06
	Trial 3	5.7569E+06	5.6694E+06	5.9952E+06	5.6664E+06	5.9601E+06	5.8538E+06	6.6466E+06
	Average	5.7727E+06	5.6763E+06	5.9864E+06	5.6535E+06	5.9889E+06	5.8321E+06	6.5987E+06
G*cos(delta)	Trial 1	3.9144E+06	5.0369E+06	5.7090E+06	4.7585E+06	5.3742E+06	4.6599E+06	6.4696E+06
	Trial 2	3.9722E+06	5.0308E+06	5.6644E+06	4.7519E+06	5.3609E+06	5.8512E+06	6.3848E+06
	Trial 3	3.9271E+06	5.0512E+06	5.6892E+06	4.7716E+06	5.4423E+06	5.2893E+06	6.4861E+06
	Average	3.9379E+06	5.0397E+06	5.6875E+06	4.7607E+06	5.3925E+06	5.2668E+06	6.4468E+06
G*/sin(delta)	Trial 1	8.4201E+06	1.0145E+07	1.1428E+07	9.6580E+06	1.0812E+07	9.3613E+06	1.2943E+07
	Trial 2	8.5210E+06	1.0137E+07	1.1349E+07	9.6445E+06	1.0793E+07	1.1771E+07	1.2772E+07
	Trial 3	8.4357E+06	1.0170E+07	1.1394E+07	9.6845E+06	1.0930E+07	1.0633E+07	1.2976E+07
	Average	8.4590E+06	1.0151E+07	1.1390E+07	9.6623E+06	1.0845E+07	1.0589E+07	1.2897E+07

Table F3: Summary of DSR Test Results, Continued

Mixture	F1S	F1L	F2S	F2L	C4/F3S	C4/F3L
G*	9.7145E+06	1.1414E+07	9.7898E+06	1.1502E+07	7.7353E+06	9.6385E+06
	9.7319E+06	1.1443E+07	9.7159E+06	1.1473E+07	8.3510E+06	8.9848E+06
	9.7151E+06	1.1415E+07	9.7771E+06	1.1498E+07	7.3020E+06	9.4524E+06
	9.7205E+06	1.1424E+07	9.7609E+06	1.1491E+07	7.7961E+06	9.3586E+06
delta	47.2	45.1	46.3	43.6	47.6	45.7
	47.9	44.8	46.1	43.6	47.8	45.5
	47.5	45.2	46.2	43.6	48.2	45.4
	47.5	45.0	46.2	43.6	47.9	45.5
G*sin(delta)	7.1278E+06	8.0849E+06	7.0777E+06	7.9318E+06	5.7122E+06	6.8982E+06
	7.2208E+06	8.0633E+06	7.0008E+06	7.9119E+06	6.1865E+06	6.4084E+06
	7.1627E+06	8.0997E+06	7.0567E+06	7.9296E+06	5.4435E+06	6.7304E+06
	7.1705E+06	8.0826E+06	7.0451E+06	7.9244E+06	5.7807E+06	6.6790E+06
G*cos(delta)	6.6004E+06	8.0567E+06	6.7636E+06	8.3292E+06	5.2159E+06	6.7317E+06
	6.5245E+06	8.1198E+06	6.7370E+06	8.3083E+06	5.6095E+06	6.2975E+06
	6.5634E+06	8.0433E+06	6.7671E+06	8.3269E+06	4.8670E+06	6.6370E+06
	6.5628E+06	8.0733E+06	6.7559E+06	8.3215E+06	5.2308E+06	6.5554E+06
G*/sin(delta)	1.3240E+07	1.6114E+07	1.3541E+07	1.6678E+07	1.0475E+07	1.3467E+07
	1.3116E+07	1.6240E+07	1.3484E+07	1.6636E+07	1.1273E+07	1.2597E+07
	1.3177E+07	1.6087E+07	1.3546E+07	1.6674E+07	9.7951E+06	1.3275E+07
	1.3178E+07	1.6147E+07	1.3524E+07	1.6663E+07	1.0514E+07	1.3113E+07

Table F4: Summary of DSR Test Results, Continued

Mixture	C5S	C5L	F4S	F4L	F5S	F5L	F6S	F6L
G*	7.7102E+06	9.1216E+06	1.0897E+07	1.2636E+07	9.4883E+06	1.1272E+07	9.3873E+06	1.0921E+07
	7.7356E+06	9.2523E+06	1.0533E+07	1.2755E+07	8.9652E+06	1.1285E+07	9.0610E+06	1.1252E+07
	7.6962E+06	8.9250E+06	1.1357E+07	1.2496E+07	9.9562E+06	1.1252E+07	9.6652E+06	1.0653E+07
	7.7140E+06	9.0996E+06	1.0929E+07	1.2629E+07	9.4699E+06	1.1270E+07	9.3712E+06	1.0942E+07
delta	48.1	44.9	44.9	43.3	46.3	44.1	47.2	44.8
	47.6	44.7	44.9	43.5	46.7	44.9	47.9	45.0
	48.2	44.9	44.7	43.1	45.9	43.7	47.0	44.9
	48.0	44.8	44.8	43.3	46.3	44.2	47.4	44.9
G*sin(delta)	5.7388E+06	6.4387E+06	7.6919E+06	8.6660E+06	6.8597E+06	7.8443E+06	6.8877E+06	7.6955E+06
	5.7124E+06	6.5080E+06	7.4347E+06	8.7799E+06	6.5246E+06	7.9660E+06	6.7230E+06	7.9566E+06
	5.7373E+06	6.2999E+06	7.9884E+06	8.5381E+06	7.1498E+06	7.7740E+06	7.0687E+06	7.5198E+06
	5.7295E+06	6.4155E+06	7.7050E+06	8.6613E+06	6.8447E+06	7.8614E+06	6.8932E+06	7.7240E+06
G*cos(delta)	5.1491E+06	6.4612E+06	7.7188E+06	9.1961E+06	6.5553E+06	8.0947E+06	6.3781E+06	7.7494E+06
	5.2161E+06	6.5765E+06	7.4607E+06	9.2521E+06	6.1485E+06	7.9938E+06	6.0747E+06	7.9566E+06
	5.1298E+06	6.3219E+06	8.0725E+06	9.1240E+06	6.9286E+06	8.1350E+06	6.5917E+06	7.5461E+06
	5.1650E+06	6.4532E+06	7.7506E+06	9.1907E+06	6.5441E+06	8.0745E+06	6.3482E+06	7.7507E+06
G*/sin(delta)	1.0359E+07	1.2922E+07	1.5438E+07	1.8425E+07	1.3124E+07	1.6197E+07	1.2794E+07	1.5499E+07
	1.0475E+07	1.3154E+07	1.4921E+07	1.8530E+07	1.2319E+07	1.5988E+07	1.2212E+07	1.5913E+07
	1.0324E+07	1.2644E+07	1.6146E+07	1.8288E+07	1.3864E+07	1.6287E+07	1.3215E+07	1.5092E+07
	1.0386E+07	1.2907E+07	1.5502E+07	1.8414E+07	1.3102E+07	1.6157E+07	1.2740E+07	1.5502E+07

Table F5: Summary of DSR Test Results, Continued

Mixture		GAC1S	GAC1L	GAC2S	GAC2L	GAF1S	GAF1L
G*	Trial 1	6.2879E+06	8.1394E+06	7.2095E+06	8.9126E+06	7.4320E+06	9.0134E+06
	Trial 2	6.4256E+06	8.0652E+06	7.3526E+06	9.0120E+06	7.4852E+06	9.1336E+06
	Trial 3	6.0125E+06	8.1995E+06	7.3905E+06	8.8996E+06	7.5213E+06	9.0115E+06
	Average	6.2420E+06	8.1347E+06	7.3175E+06	8.9414E+06	7.4795E+06	9.0528E+06
delta	Trial 1	52.4	47.1	50.3	45.2	50.1	45.3
	Trial 2	52.6	47.8	49.9	45.3	50.2	45.6
	Trial 3	52.2	46.2	50.9	45.3	50.1	45.2
	Average	52.4	47.0	50.4	45.3	50.1	45.4
G*sin(delta)	Trial 1	4.9818E+06	5.9625E+06	5.5470E+06	6.3241E+06	5.7016E+06	6.4067E+06
	Trial 2	5.1046E+06	5.9747E+06	5.6242E+06	6.4057E+06	5.7508E+06	6.5257E+06
	Trial 3	4.7508E+06	5.9181E+06	5.7354E+06	6.3258E+06	5.7701E+06	6.3943E+06
	Average	4.9457E+06	5.9518E+06	5.6355E+06	6.3519E+06	5.7408E+06	6.4422E+06
G*cos(delta)	Trial 1	3.8365E+06	5.5407E+06	4.6052E+06	6.2801E+06	4.7673E+06	6.3400E+06
	Trial 2	3.9028E+06	5.4176E+06	4.7360E+06	6.3390E+06	4.7913E+06	6.3904E+06
	Trial 3	3.6851E+06	5.6752E+06	4.6610E+06	6.2599E+06	4.8245E+06	6.3498E+06
	Average	3.8081E+06	5.5445E+06	4.6674E+06	6.2930E+06	4.7944E+06	6.3601E+06
G*/sin(delta)	Trial 1	7.9364E+06	1.1111E+07	9.3703E+06	1.2561E+07	9.6876E+06	1.2681E+07
	Trial 2	8.0885E+06	1.0887E+07	9.6122E+06	1.2679E+07	9.7428E+06	1.2784E+07
	Trial 3	7.6093E+06	1.1360E+07	9.5233E+06	1.2521E+07	9.8040E+06	1.2700E+07
	Average	7.8780E+06	1.1120E+07	9.5019E+06	1.2587E+07	9.7448E+06	1.2721E+07

Table F6: Summary of Viscosity Test Results

	STOA	LTOA	GAIN
Mixture	**Viscosity (Poise)**	**Viscosity (Poise)**	**Viscosity (Poise)**
C1	64348	111069	46721
C2	87063	117500	30437
C3	80636	118598	37963
C5	75204	117376	42172
F1	89653	169535	79882
F2	96500	180482	83982
C4/F3	71391	117212	45821
F4	95063	192043	96980
F5	97689	133069	35380
F6	89263	129216	39953
GAC1	61362	110224	48862
GAC2	88729	121001	32272
GAF1	92063	117813	25750

APPENDIX G
GRAPHS OF MIXTURES AND BINDER STIFFNESSES

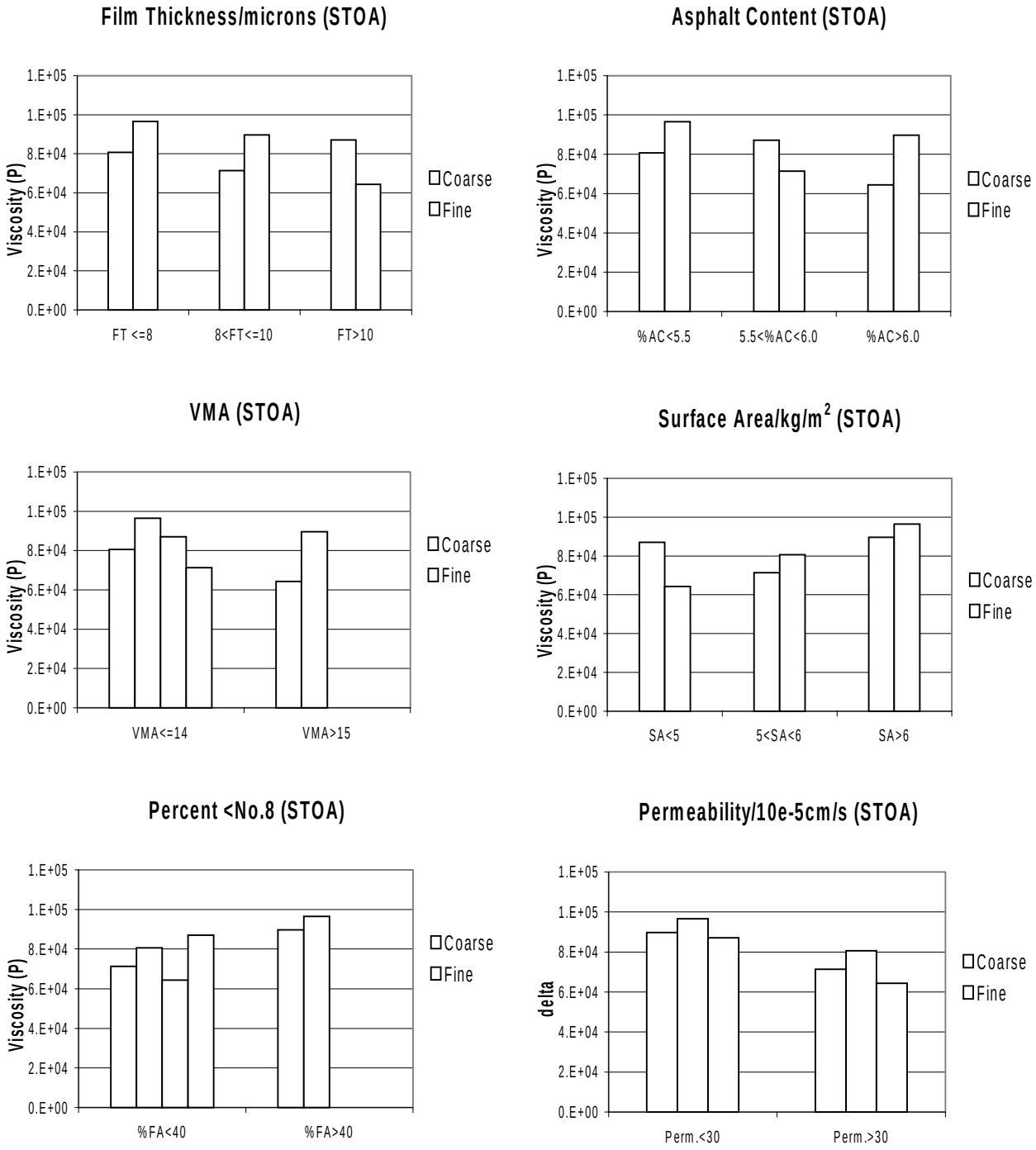

Figure G1: Viscosity after LTOA versus Volumetric Properties and Permeability

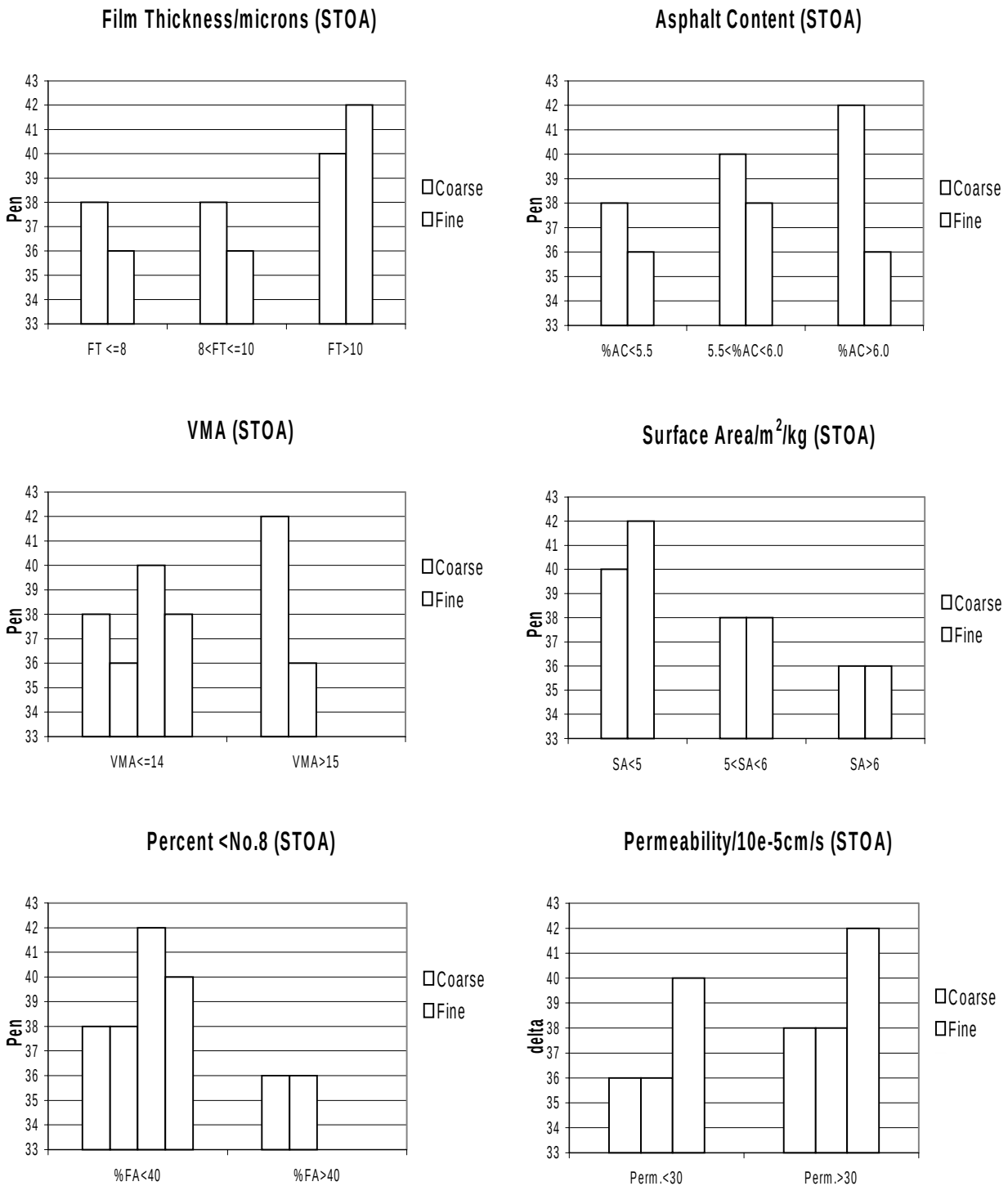

Figure G2: Penetration after LTOA versus Volumetric Properties and Permeability

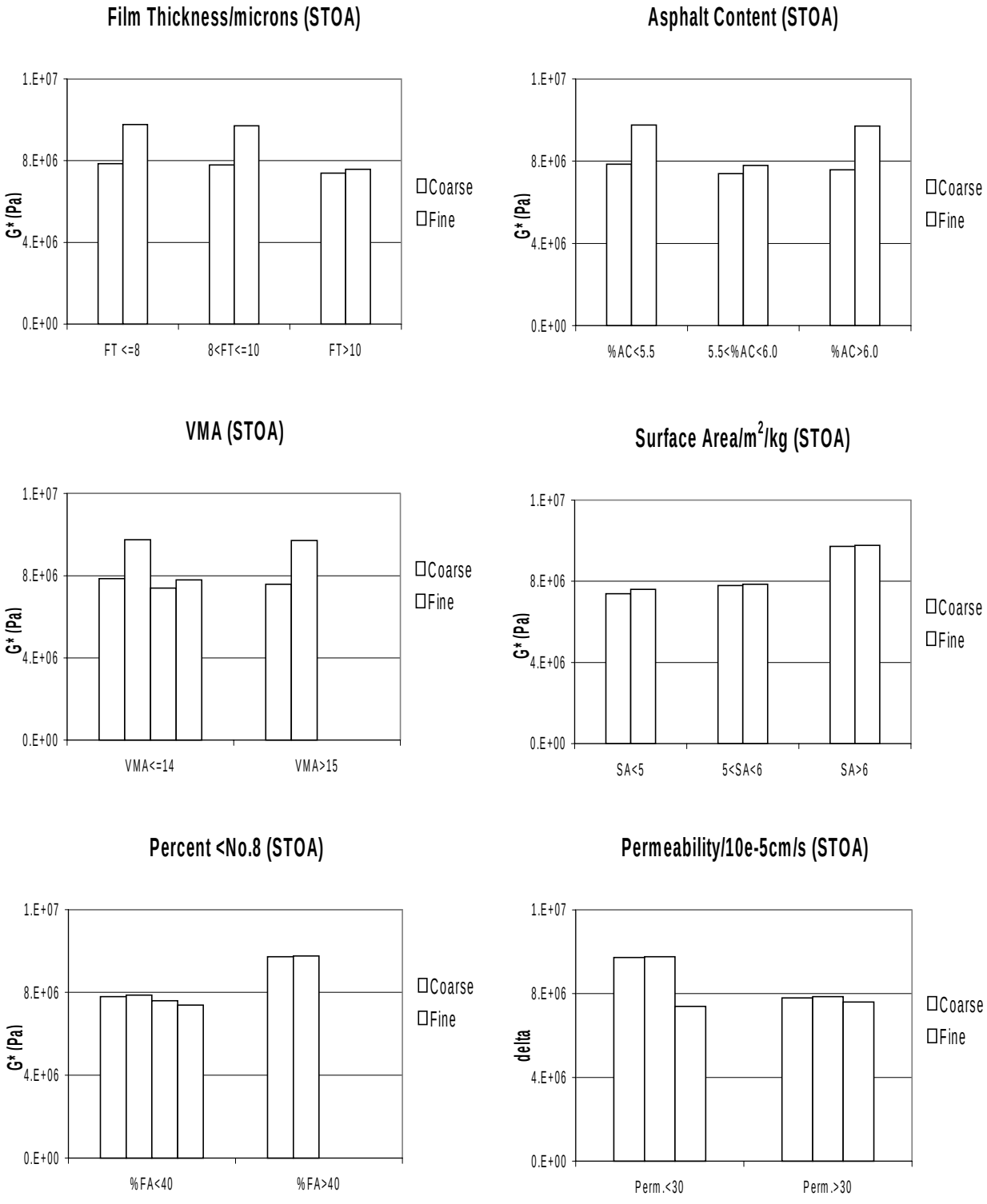

Figure G3: G* after LTOA versus Volumetric Properties and Permeability

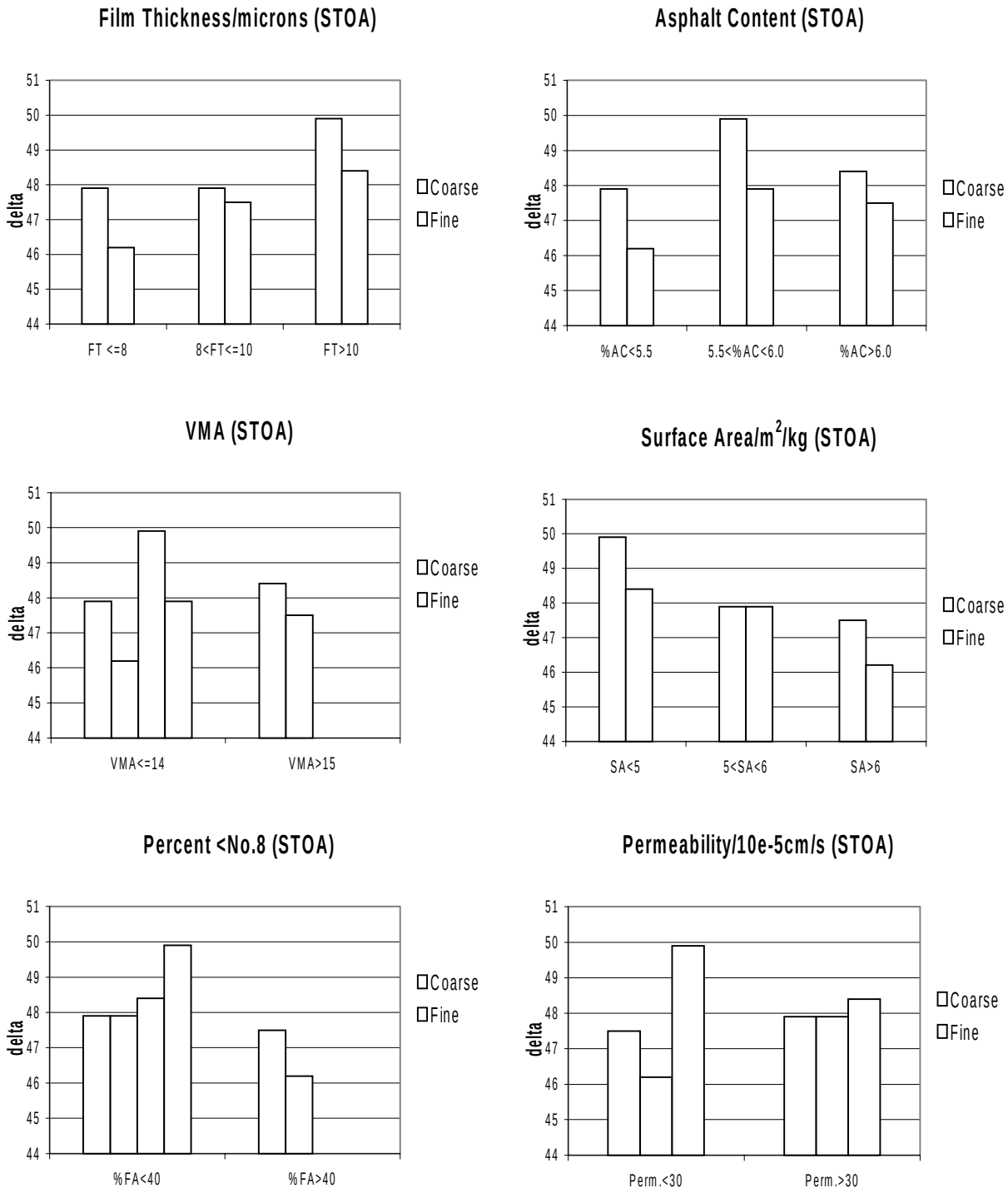

Figure G4: Delta after LTOA versus Volumetric Properties and Permeability

REFERENCES

Anagnos, James N., and Kennedy, Thomas W., "Practical Method of Conducting the Indirect Tensile Test," *Research Report 98-10*, University of Texas, August 1972.

Anderson, R. Michael, and Bahia, Hussein U., "Evaluation and Selection of Aggregate Gradations for Asphalt Mixtures Using Superpave," *Transportation Research Record 1583*, Transportation Research Board (TRB), National Research Council (NRC), Washington, DC, 1997, pp. 91-97.

Aschenbrener, Tim, and MacKean, Charles, "Factors That Affect the Voids in the Mineral Aggregate of Hot-Mix Asphalt," *Transportation Research Record 1469*, TRB, NRC, Washington, DC, 1994, pp. 1-8.

Asphalt Institute, "Research and Development of the Asphalt Institutes Thickness Design Manual (MS-1)," 9th Edition, *Research Report 82-2*, 1986.

Asphalt Institute, *Superpave Mix Design Manual*, Superpave Series No.2 (SP-2), 1995.

Asphalt Institute, "Verification and Performance Testing of Florida DOT Superpave Mixes," *Task K-2-7 Report* for Florida DOT and FHWA by the National Asphalt Training Center, 1998.

Bahia, H. U., and Anderson, D. A., "The SHRP Binder Rheological Parameters: Why Are They Required and How Do They Compare to Conventional Properties?," *Preprint Paper No. 950793*, TRB, January 1995.

Bell, C. A., Felling, M. J., and Wieder, A., "Field Validation of Laboratory Aging Procedures for Asphalt Aggregate Mixtures," *Preprint*, Association of Asphalt Pavement Technologists, Vol. 62, 1994.

Brown, E. R., "Evaluation of Fatigue Properties of Recycled Asphalt Concrete," *Proceedings*, 6th International Conference on Structural Design of Asphalt Pavements, Vol. I, 1987.

Brown, E. R, and Cross, Stephen, "A Study of In-Place Rutting of Asphalt Pavements," *Proceedings*, Association of Asphalt Pavement Technologists, Vol. 58, 1989.

Buttlar, W. G., and Roque, R., "Experimental Development and Evaluation of the New SHRP Measurement and Analysis System for Indirect Tensile Testing at Low Temperatures," *Transportation Research Record 1454*, TRB, NRC, Washington DC, 1994, pp. 163-171.

Campen, J. F., Smith, J. R., Erickson, L. G., and Mertz, L. R., "The Relationships Between Voids, Surface Area, Film Thickness and Stability in Bituminous Paving Mixtures," *Proceedings*, Association of Asphalt Pavement Technologists, Vol. 28, 1959.

Cominsky, R. J., Leahy, R. B., and Harrigan, E. T., "Level 1 Mix Design: Materials Selection, Compaction, and Conditioning," *SHRP Report A-408*, Strategic Highway Research Program, National Research Council, 1994.

Coree, B., and Hislop, W., "The Difficult Nature of Minimum VMA," *Preprint, TRB Paper No. 99-00572*, Transportation Research Board, National Research Council, Washington, DC, 1999.

Dowling, N. E., *Mechanical Behavior of Materials*, Englewood Cliffs, NJ, Prentice Hall, 1993, 773 pp.

Dowling, N. E., and Begley, J. A., "Fatigue Crack Growth During Cross Plasticity and the J Integral," *ASTM STP 590*, American Society of Testing and Materials, Philadelphia, 1976, pp. 82-103.

Dukatz, E. L., "Aggregate Properties Related to Perfor*mance*," *Proceedings*, Association of Asphalt Pavement Technologists, Vol. 58, 1989, pp. 492-501.

Epps, J., and Monismith, C., "Influence of Mixture Variables on the Flexural Fatigue Properties of Asphalt Concrete," *Proceedings*, Association of Asphalt Pavement Technologists, Vol. 38, 1969, pp. 423-456.

Ford, Miller, "Pavement Densification Related to Asphalt Mix Characteristics," Paper Presented at 67th Transportation Research Board, TRB, National Research Council, Washington, DC, 1988.

Foster, Charles R., "The Effects of Voids in Mineral Aggregates on Pavement Performance," *NAPA Information Series 96/86*, 1986.

Haas, R. C. G., "A Method for Designing Asphalt Pavements to Minimize Low-Temperature Shrinkage Cracking," *The Asphalt Institute Research Report 73-1*, January 1973.

Hadley, William O., Hudson, W. Ronald, and Kennedy, Thomas, "An Evaluation of Factors Affecting the Tensile Properties of Asphalt-Treated Materials," *Research Report 98-2*, University of Texas, August 1972.

Hadley, William O., Hudson, W. Ronald, and Kennedy, Thomas, "A Method of Estimating Tensile Properties of Materials Tested in Indirect Tension," *Research Report 98-7*, Center for Highway Research, University of Texas, August 1970.

Harm, E. E., and Hughes, C. S., "Paving Specifications and Inspection Related to Pavement Performance," *Proceedings*, Association of Asphalt Pavement Technologists, Vol. 58, 1989, pp. 595-607.

Harvey, J., and Tsai, B. W., "Effect of Asphalt Content and Air Void Content on Mix Fatigue and Stiffness," *Transportation Research Record 1543*, TRB, NRC, Washington, DC, 1996, pp. 38-45.

Hinrichsen, John A., and Heggen, John, "Minimum Voids in Mineral Aggregate in Hot-Mix Asphalt Based on Gradation and Volumetric Properties," *Transportation Research Record 1545*, TRB, NRC, Washington, DC, 1996, pp. 75-79.

Huber, G. A., and Heiman, G. H., "Effect of Asphalt Concrete Parameters on Rutting Performance: A Field Investigation," *Proceedings*, Association of Asphalt Pavement Technologists, Vol. 56, 1987.

Hudson, S. B., and Davis, R. L., "Relationship of Aggregate Voidage to Gradation," *Proceedings*, Association of Asphalt Pavement Technologists, Vol. 34, 1965.

Hveem, F. N., "Gradation of Mineral Aggregates for Dense-Graded Bituminous Mixtures," *Proceedings*, Association of Asphalt Pavement Technologists, Vol. 11, 1940.

Hveem, F. N., "Use of the Centrifuge Kerosene Equivalent as Applied to Determine the Required Oil Content for Dense-Graded Bituminous Mixtures," *Proceedings*, Association of Asphalt Pavement Technologists, Vol. 13, 1942.

Jacobs, M. M. J., Hopman, P. C., and Molenaar, A. A. A., "Application of Fracture Mechanics Principles to Analyze Cracking in Asphalt Concrete," *Proceedings*, Association of Asphalt Pavement Technologists, Vol. 65, 1996, pp. 1-39.

Jimenez, R. A., "Flow Rate as an Index of Shape and Texture of Sands," *Transportation Research Record No. 1259*, TRB, NRC, 1990, pp. 120-31.

Kandhal, Prithvi S., and Chakraborty, S., "Evaluation of Voids in the Mineral Aggregates," *NCAT Report No. 96-4*, National Center for Asphalt Technology, March 1996.

Kandhal, Prithvi S., Foo, Kee Y., and Mallick, Rajib B., "Critical Review of VMA requirements in Superpave," *NCAT Report No. 98-1*, National Center for Asphalt Technology, January 1998.

Kandhal, Prithvi S., Khatri, M. A., and Motter, J. B., "Evaluation of Particle Shape and Texture of Mineral Aggregates and Their Blends," *Asphalt Paving Technology*, Vol. 62, 1992.

Kandhal, Prithvi S., and Koehler, W. S., "Marshall Mix Design Method: Current Practices," *Proceedings*, Association of Asphalt Pavement Technologists, Vol. 54, 1985.

Kandhal, Prithvi S., Parker, Jr., Frazier., and Mallick, R. B., "Aggregate Test for Hot Mix Asphalt: State of the Practice," *TRB Paper No. 97-0736*, TRB, NRC, Washington, DC, 1997.

Kim, Y. R., Lee, D. L., and Little, D. N., "Fatigue Characterization of Asphalt Concrete Using Viscoelasticity and Continuum Damage Theory," *Journal of the Association of Asphalt Paving Technologists*, Vol. 59, 1997, pp. 520-569.

Lefebvre, J., "Recent Investigations of the Design of Asphalt Paving Mixtures," *Proceedings*, Association of Asphalt Pavement Technologists, Vol. 26, 1957.

Majidzadeh, K., Kaufmann, E. M., Ramsamooj, D. V., "Application of Fracture Mechanics in the Analysis of Pavement Fatigue," *Proceedings*, Association of Asphalt Pavement Technologists, Vol. 40, 1971, pp. 227-246.

Marshall Consulting and Testing Laboratory, *The Marshall Method for the Design and Control of Bituminous Paving Mixtures*, 3rd rev., Jackson, MS, 1949.

McFadden, Gayle, and Ricketts, Walter G., "Design and Field Control of Asphalt Pavements for Military Installations," *Proceedings*, Association of Asphalt Pavement Technologists, Vol. 17, 1948.

McLeod, N. W., "Design of Dense Graded Asphalt Concrete Pavements," *Proceedings*, Canadian Technical Asphalt Association, Vol. 32, 1987.

McLeod, N. W., "Designing Standard Asphalt Paving Mixtures for Greater Durability," *Proceedings*, Canadian Technical Asphalt Association, Vol. 16, 1971.

McLeod, N. W., "Discussion on J. H. Dillard's Paper: Comparison of Density of Marshall Specimens and Pavement Cores," *Proceedings*, Association of Asphalt Pavement Technologists, Vol. 24, 1955.

McLeod, N. W., "Relationships Between Density, Bitumen Content and Voids Properties of Compacted Bituminous Paving Mixtures," *Proceedings*, Highway Research Board, vol. 35, 1956.

McLeod, N. W., "Selecting the Aggregate Specify Gravity for Bituminous Paving Mixtures," *Proceedings*, Association of Asphalt Pavement Technologists, Vol. 36, 1957.

McLeod, N. W., "Voids Requirements for Dense-Graded Bituminous Paving Mixtures," *Special Technical Publication 252*, ASTM, 1959.

Monismith, C., "Fatigue Characteristics of Asphalt Paving Mixtures and their use in Pavement Design," *Proceedings*, 18th Paving Conference, Lansing, MI, 1985.

National Center for Asphalt Technology (NCAT*), Hot Mix Asphalt Materials, Mixture Design and Construction*, NAPA Research Foundation, 1996.

Papazian, H. S., "The Response of Linear Visco*ela*stic Materials in the Frequency Domain with Emphasis on Asphaltic Concrete," *Proceedings*, International Conference on the Structural Design of Asphalt Pavements, University of Michigan, 1962.

Read, J. M., and Collop, A. C., "Practical Fatigue Characteristics of Bituminous Paving Mixtures," *Journal of the Association of Asphalt Paving Technologists*, vol. 66, 1997, pp. 74-108.

Rex, H. M., and Robert, A. P., "A laboratory Test to Evaluate the shape and Surface Texture of Fine Aggregate Particles," *Public Roads*, Vol. 29, No.5 December 1956, pp. 118-120.

Richardson, Clifford, *The Modern Asphalt Pavement*, John Wiley and Sons, First Edition, 1905.

Roque, R., and Buttlar, W. G., "The Development of a Measurement and Analysis System to Accurately Determine Asphalt Concrete Properties Using the Indirect Tensile Mode," *Journal of the Association of Asphalt Pavement Technologists*, Vol. 61, 1992, pp. 304-332.

Roque, R., Buttlar, W. G., Ruth, B. E., Tia, M., Dickison, S. W., and Reid, B., "Evaluation of SHRP Indirect Tension Tester to Mitigate Cracking in Asphalt Pavements and Overlays," *Final Report* of the Florida Department of Transportation, University of Florida, Gainesville, August 1997.

Roque, R., Hiltunen, D.R., Buttlar, W. G., and Farwanna, T., "Development of the SHRP Superpave Mixture Specification Test Method to Control Thermal Cracking Performance of Pavements," *ASTM STP 1265*, Symposium on Engineering Properties of Asphalt Mixtures and Relation to Performance, G. A. Huber and D. S. Decker, Eds., American Society for Testing and Materials, Philadelphia, PA, 1994.

Ruth, B. E., and Birgisson, B., "An Overview of Operational Aspects Relating to Volumetric Design and Construction of Asphalt Paving Mixtures," *Proceedings*, Canadian Technical Asphalt Association, 1999, pp. 345-368.

Santucci, L. E., Allen, D. D., and Coats, R. L., "The Effects of Moisture and compaction on Quality of Asphalt Pavements," *Proceedings*, Association of Asphalt Pavement Technologists, Vol. 54, 1985.

Schapery, R. A., "A Theory of Crack Growth in Visco-Elastic Media," *Report MM 2764-73-1*, Mechanics and Materials Research Center, Texas A & M University, College Station, TX, 1973.

Schapery, R. A., "A Theory of Crack Initiation and Growth in Visco-Elastic Media, I: Theoretical Development, II: Approximate Methods of Analysis and III: Analysis of Continuous Growth," *International Journal of Fracture*, Vol. 11: No. 1, pp. 141-159; No. 3, pp. 369-388; No. 4, 1975, pp. 549-592.

Schapery, R. A., "Corresponding Principles and a Generalized J Integral for Large Deformation and Fracture Analysis of Visco-Elastic Media," *International Journal of Fracture*, Vol. 25, No. 1, 1984, pp. 195-223.

Sedwick, S. C., "Effect of Asphalt Mixture Properties and Characteristics on Surface Initiated Longitudinal Wheel Path Cracking," *Master's Thesis*, University of Florida, Gainesville, 1998.

Seed, H. C., Chan, C. K., and Lee, C. E., "Resilient Characteristics of Subgrade Soils and their Relation to Fatigue Failures in Asphalt Pavements," *Proceedings*, International Conference on the Structural Design of Asphalt Pavements, University of Michigan, 1962.

Shell Pavement Design Manual, SHELL International Petroleum, Co. Ltd., London, 1978.

Strategic Highway Research Program (SHRP), "Binder Characterization and Evaluation," *SHRP Report No. SHRP-A-368*, National Research Council, 1993.

Tayebali, A. A., and Malpas, Glen A., and Khosla, N. Paul, "Effect of Mineral Filler Type and Amount on the Design and Performance of Asphalt Concrete Mixtures," *Transportation Research Record 1545*, TRB, NRC, Washington, DC, 1998, pp. 75-79.

Tayebali, A. A., Rowe, G., and Sousa, J., "Fatigue Damage Properties of Asphaltic Concrete Pavements," *Proceedings*, Association of Asphalt Pavement Technologists, Vol. 61, 1992, pp. 333-353.

Thompson, M. R., and Cation, K., "A Proposed Full-Depth Asphalt Concrete Thickness Design Procedure," *Transportation Engineering Series No. 45*, Civil Engineer Studies, University of Illinois at Urbana-Champaign, 1986.

Tseng, K., and Lytton, R. L., "Fatigue Damage Properties of Asphaltic Concrete Pavements," the 69th Annual Meeting of the Transportation Research Board, 1990, pp. 43.

Van der Poel, C., "A General System Describing the Viscoelastic Properties of Bitumens and Its Relation to Routine Test Data," *Journal of Applied Chemistry*, Vol. 4, 1954.

van Dijk, W., "Practical Fatigue Characterization of Bituminous Mixes," *Proceedings*, Association of Asphalt Pavement Technologists, Vol. 46, 1975, pp. 38-75.

van Dijk, W., and Visser, W., "The Energy Approach to Fatigue for Pavement Design," *Journal of Association of Asphalt Pavement Technologists*, Vol. 46, 1977, pp. 1-38.

Zhang, Z., "Identification of Suitable Crack Growth Law for Asphalt Mixtures Using the Superpave Indirect Tensile Test (IDT)," *Doctoral Dissertation*, University of Florida, Gainesville, 2000.

Zube, Ernst, "Compaction Studies of Asphalt Concrete Pavement as Related to Water Permeability Test," Paper presented at the Annual Meeting of the Highway Research Board, 1962.